DOCTOR OF PHILOSOPHY

Investigation of macroalgal polyphenols and peptides with potential antioxidant and antihypertensive activities.

Tierney, Michelle

Award date:
2014

Awarding institution:
Bangor University

Investigation of macroalgal polyphenols and peptides with potential antioxidant and antihypertensive activities.

Michelle Tierney

A thesis submitted in partial fulfilment of the requirements for the degree of

Doctor of Philosophy

School of Chemistry, Bangor University • Food Biosciences Department, Teagasc

Acknowledgements

Firstly, I would like to particularly thank Dr. Nigel Brunton for his supervision, guidance and support, which is greatly-appreciated.

I also would like to gratefully thank Dr. Anna Croft for her supervision, direction and valued advice with regard to the computational chemistry work.

I especially want to thank Dr. Thomas Smyth for his continual patience, perseverance and highly-regarded advice in all aspects of the experimental work.

I would like to thank Dr. Maria Hayes for her supervision and assistance, and for giving me the opportunity to undertake this PhD.

I would like to gratefully acknowledge Dr. Dilip Rai for his supervision and respected guidance and advice with regard to the mass spectrometry work.

I want to thank Dr Padraig McLoughlin for his assistance in carrying out the NMR analysis. I want to acknowledge Paula O'Connor for carrying out the peptide synthesis work. My thanks go to Anna Soler-Vila for supplying the array of macroalgal species required for this project.

I also want to extend my sincere gratitude to the staff and students of Teagasc Food Research Centre for all their help and support. I especially want to thank Natalie Heffernan for being a great friend and always willing to lend a helping hand.

I would also like to appreciatively acknowledge Wilma Groenewald for her help and assistance with the computational chemistry work and during my time in Bangor.

I would like to thank the staff of the School of Chemistry in Bangor University for always being very helpful and patient.

I would like to gratefully acknowledge The Walsh Fellowship Programme and Nutramara, the Marine Functional Foods Research Initiative, for providing me with the funding to carry out this project.

Very special thanks go to my parents, John and Siobhan, for their unconditional support, and to Sean for his extraordinary patience and support.

Table of Contents

Abstract

Macroalgal phlorotannins and peptides are increasingly being investigated for their health-promoting properties; however in-depth research into the occurrence, bioactivity, profiling and molecular properties of these components in Irish species is limited.

The process by which bioactives are extracted and purified from their original biomass must be efficient and food-friendly to be applicable to the food industry. Two different extraction methods, solid-liquid extraction (SLE) and pressurised liquid extraction (PLE), were compared for the extraction of polyphenols from three brown macroalgae, *Ascophyllum nodosum*, *Pelvetia canaliculata* and *Fucus spiralis*, and a green macroalga, *Ulva intestinalis*. SLE was deemed to be a more industrially relevant technique for generating food-friendly antioxidant extracts than PLE as it requires less capital investment, is food-safe, and can be scaled up.

Molecular weight cut-off (MWCO) fractionation and reverse-phase flash chromatography techniques were employed to enrich the polyphenol content of brown macroalgal SLE extracts by removing predominantly sugars from the extracts. Furthermore, the use of bioassay-guided fractionation indicated that the observed antioxidant activities of the extracts could be attributed to the polar, medium-to-high molecular weight phlorotannins.

The analytical quality control and standardisation of naturally-sourced functional extracts has become a requirement for their use in the food industry. In this work, a rapid ultra-performance liquid chromatography® (UPLC®) method was presented for the profiling of low molecular weight phlorotannin isomers for polymers up to 16 monomers in length from the three brown species. The predominant size ranges of the phlorotannins found in *A. nodosum*, *P. canaliculata* and *F. spiralis* were 6-11, 6-13 and 4-6 monomers, respectively.

The identification of bioactive peptides has been largely unexplored. In this work, various peptides were isolated from a trypsin-digested *Ascophyllum nodosum* protein extract. A selection of peptides were synthesised and their in vitro antioxidant and antihypertensive activities assayed. The polypeptide EKTGLLNVVETAEKFL displayed the highest renin enzyme inhibition of 56.12 ± 2.66 % and this is the first report of renin inhibitory peptides identified from brown macroalgae

Computational chemistry may act as a support to natural products experiment, through the provision of data on the molecular properties of individual components and also on potential binding interactions between mixtures of bioactive components. Density functional theory was employed to theoretically determine the radical scavenging potential of various 7-phloroeckol conformers through the calculation of their O-H bond dissociation enthalpies. Furthermore, a molecular dynamics simulation approach was proposed for the investigation of binding interactions between a selected macroalgal phlorotannin and a bioactive peptide from *A. nodosum*.

List of Original Publications

This thesis is partially based on the following co-authored publications that are cited in the text by their Roman numerals. Papers **I-V** are attached in the Original Publications section. I declare as first author of these publications that I was the principal contributor to these publications in terms of the experimental work carried out, paper drafting and addressing reviewer comments. The thesis text also includes unpublished material.

I

Tierney, M. S.; Croft, A. K.; Hayes, M., A review of antihypertensive and antioxidant activities in macroalgae. *Botanica Marina*, **2010**, 53, 387-408.

II

Tierney, M.S.; Soler-Vila, A.; Croft, A.K.; Hayes, M., Antioxidant activity of the brown macroalga *Fucus spiralis* Linnaeus harvested from the west coast of Ireland. *Current Research Journal of Biological Sciences,* **2013**, 5, 81-90

III

Tierney, M.S.; Smyth, T.J.; Hayes, M.; Soler-Vila, A.; Croft, A.K.; Brunton, N., Influence of pressurized liquid extraction and solid-liquid extraction methods on the phenolic content and antioxidant activities of Irish macroalgae. *International Journal of Food Science and Technology*, **2013**, 48, 860–869

IV

Tierney, M.S.; Smyth, T.J.; Rai, D.K.; Soler-Vila, A.; Croft, A.K.; Brunton, N., Enrichment of polyphenol contents and antioxidant activities of Irish brown macroalgae using food-friendly techniques based on polarity and molecular size. *Food Chemistry*, **2013**, 139, 753-761

V

Tierney, M.S.; Soler-Vila, A.; Rai, D.K.; Croft, A.K.; Brunton, N.; Smyth, T.J. UPLC-MS profiling of low molecular weight phlorotannin polymers in *Ascophyllum nodosum*, *Pelvetia canaliculata* and *Fucus spiralis*. *Metabolomics*, **2014**, 10, 524-535.

List of Tables

Page no.

List of Figures

Page no.

Abbreviations

ACE-I	Angiotensin-converting enzyme I
AM1	Austin model 1
ARP	Antiradical power
ASE®	Accelerated solvent extraction®
B3LYP	Becke 3-parameter Lee-Yang-Parr
BDE	Bond dissociation enthalpy
BP	Bioactive peptide
CAM	Coulomb-attenuating method
DFT	Density functional theory
DP	Degrees of polymerisation
DPPH	2,2-diphenyl-1-picrylhydrazyl
EAE	Enzyme-assisted extraction
EIC	Extracted ion chromatogram
ESI	Electrospray ionization
FIC	Ferrous-ion chelating
FRAP	Ferric reducing antioxidant power
GAFF	General amber force-field
GGA	Generalized gradient approximation
GRAS	Generally recognized as safe
HAT	Hydrogen-atom transfer
HF	Hartree-Fock
HMW	High molecular weight
HOMO	Highest-occupied molecular orbital
HPC	High performance computing
HPLC	High performance liquid chromatography
IC_{50}	Half maximal inhibitory concentration
K	Kelvin
kDa	Kilo dalton
LC	Long-range corrected
LDBS	Local dense basis set
LMW	Low molecular weight
MD	Molecular dynamics
Mm	Millimolar
MM	Molecular mechanics
MP2	Second-order Møller-Plesset
MRM	Multiple reaction monitoring
MS	Mass spectrometry
MWCO	Molecular weight cut-off
NMR	Nuclear magnetic resonance
NP	Normal-phase
NPT	Normal pressure and temperature
OPLS	Optimized potential for liquid simulations
ORAC	Oxygen radical absorbance capacity
PA	Proton affinity
PGU	Phloroglucinol units
PLE	Pressurised liquid extraction

PME	Particle mesh ewald
QM	Quantum mechanics
Q-Tof	Quadrupole time-of-flight
RAS	Renin-angiotensin system
RO	Restricted open-shell
ROS	Reactive oxygen species
RP	Reverse-phase
RSA	Radical scavenging activities
SEC	Size exclusion chromatography
SET-PT	Single electron transfer followed by proton transfer
SHRSP	Stroke-prone spontaneously hypertensive rats
SIE	Self-interaction error
SLE	Solid-liquid extraction
SPLET	Sequential proton loss electron transfer
TIC	Total ion chromatogram
TPC	Total phenolic content
UHPLC	Ultra high performance liquid chromatography
UPLC-MS	Ultra performance liquid chromatography-mass spectrometry
XC	Exchange correlation

1. Introduction

Macroalgae are classified into three higher taxa, brown (Class Phaeophyceae), red (Phylum Rhodophyta) and green (Phylum Chlorophyta), based predominantly on their pigmentation,[1] but also on their biopolymer products.[2] The variation in pigmentation is due to their respective divergent habitats and, therefore, different requirements of light for photosynthesis.[2] Macroalgae are required to adapt to extreme and diverse ecological conditions consisting of varying salt concentrations, varying temperatures, grazing stresses and low nutrient availability.[3-5] As a reflection of their changeable habitats, macroalgae contain a diverse array of secondary metabolites that are either often not found, or found only in low quantities, in terrestrial plants.[4, 6] The array of bioactive metabolites produced by macroalgae include polyphenols, phycobiliproteins, mycosporine-like amino acids, peptides, polysaccharides, sterol esters and polyunsaturated fatty acids, which are all discussed further in Paper I.[7] The relative quantities of these metabolites in macroalgae are dependent on species, seasonality, macroalgal maturity, geographical location and environmental variables. These metabolites provide protective effects to macroalgae in the form of UV radiation protection, limiting oxidation and deterring grazing.[8-10]

With the increased occurrence globally of chronic conditions, including heart disease, stroke, cancer, chronic respiratory diseases, obesity and diabetes,[11] there is an emerging trend towards the development of alternative, effective means of treatment that can be incorporated into daily diets,[12] as opposed to traditional medication. To date, macroalgal components have been proven to possess antioxidant,[13] antidiabetic,[14] anti-inflammatory,[15] antihypertensive[16] and antiobesity properties.[17] Paper I provides tabulated summaries of angiotensin converting enzyme I (ACE-I)-inhibitory (antihypertensive) activities and antioxidant activities found from the various macroalgal classes.[7] Owing to their diverse bioactive components and the abundance of this resource, macroalgae have the potential to be valuable components for the pharmaceutical and functional food industries.[4] Functional foods are defined as foods that beneficially affect "one or more target functions in the body, beyond adequate nutritional effects, in a way that is relevant to either an improved state of

health and well-being and/or reduction of disease risk''.[18] Consumer preferences generally favour functional ingredients that are naturally sourced rather than synthetically produced.[19] Macroalgal components have been incorporated into countless traditional and modern foods,[20-21] and are the central ingredient in many Asian dishes.[7]

Polyphenols have been extensively investigated experimentally for their potential bioactivities. However, thus far the uptake of polyphenols into therapeutic and functional products appears to be relatively low. This may be due either to the lack of knowledge regarding either the identification of specific target sites of bioactive polyphenols or the nature of the interactions involved between the polyphenols and receptors/proteins. Knowledge-gaps such as these can impede the progression of natural product "hits" from the bioactive discovery phase onto a stage where a health claim can be submitted. The employment of computer-aided molecular modelling (CAMM) makes it possible for these gaps to be narrowed. CAMM involves the use of high performance computing resources to obtain information about the chemical and biological aspects of ligands and/or targets to aid with the optimisation of new drugs.[22] The use of various types of CAMM tools; such as molecular docking, reverse-docking, pharmacophore-based screening, quantum mechanics and molecular dynamics, for the structure-activity prediction of polyphenols can complement existing experimental data.[23] Also, with the recent widespread availability of grid-computing and cloud-computing, the use of computationally intensive applications has been facilitated by the provision of remote access to supercomputers.[24]

Paper I reviews areas relevant this thesis; such as the bioactive components found in macroalgae; previously reported ACE-I-inhibitory and antioxidant activities of macroalgae; types of assays employed to assess bioactivity; some of the method used to extract bioactive components; the characterisation of compounds; and the potential use of macroalgal bioactive in functional foods. Some of these areas, along with additional topics of relevance, are discussed in more detail in the sections that follow.

1.1 Irish macroalgae: Uses and potential exploitability

The Irish macroalgal biomass predominantly consists of *Laminaria*, *Saccharina*, *Sacchorhiza*, *Fucus*, *Pelvetia*, *Ascophyllum*, *Ulva*, *Palmaria*, *Chondrus*, *Mastocarpus Phymatolithon* and *Lithothamnion* species.[25] Traditionally, Irish macroalgae have been used in foods, as agricultural fertiliser, and as a source of alginate for the food industry.[26-27] At present, the commercialisation of macroalgae in Ireland consists of several sectors; including biopolymers, agriculture/horticulture, cosmeceuticals, and human consumption.[28] The most commonly employed Irish species involved in these industries include *Phymatolithon calcareum*, *Lithothamnion corallioides* (agriculture, horticulture), *Ascophyllum nodosum* (alginate extraction, agriculture, cosmetics), *Palmaria palmata* (human consumption), and *Chondrus crispus* (medicinal use).[25] The future development of the macroalgal industry in Ireland is largely dependent on the extent to which the macroalgal resources can be sustained.[29] Currently, there are three main sources of macroalgae that could be exploited, namely the natural macroalgal stocks, the use of drift macroalgae, and the cultivation of seaweed at either coastal sites or using offshore infrastructure.[29] In relation to natural stocks, presently the only existing harvest of significance is of *Ascophyllum nodosum* and, according to a survey by the Irish Seaweed Industry Organisation (ISIO), less than half of the stock that could be potentially sustainably harvested annually is being currently exploited.[30]

Macroalgae represent a food group that is not normally ingested in its unprocessed form to any great extent in Western cultures. However, in recent years, increased attention has been given to Irish macroalgae as a plentiful and valuable source of nutritional and bioactive components.[31-33] The world-wide macroalgal industry is estimated to be worth US$ 5.5–6 billion annually, with US$ 5 billion being generated from products for human consumption, with the remainder being generated from hydrocolloids and other varied products.[34] It has been predicted that with the aid of aquaculture the Irish macroalgal industry may be worth up to €30 million per annum in 2020. The bulk (~ 99 %) of the Irish macroalgal production goes into general agricultural products to yield 70 % of the revenue generated within this industry.[34] However, interestingly, only a small percentage (~ 1 %) of the national

production goes into the cosmetics and therapies, but these yield disproportionately high revenue of 30 %.[34] The latter figure reflects how the existing consumer demand for macroalgal health and well-being products can be profitable and this demand bodes well for the potential development of Irish functional foods with macroalgal ingredients.

1.2 Oxidative Stress and Antioxidants

The health of cells in the human body under normal physiological conditions is maintained through a subtle balance of antioxidative-oxidative reactions. Reactive oxygen species (ROS), also known as free radicals, are produced as a result of oxygen metabolism and possess the potential to cause oxidative damage to lipids, proteins and DNA in the body.[35] Equally, the presence of ROS is necessary for the normal functioning of various intracellular signalling and regulatory pathways that maintain cell function.[36-37] During the physiological state, ROS are produced at low concentrations acting as signalling molecules regulating vascular smooth muscle cell contractions and relaxation.[38-39] However, excess ROS are thought to be produced as a result of the aging process,[40] pollutant exposure,[41] endurance exercise[42] and high fat diets/excess caloric intake.[43] Oxidative stress can cause irreversible deterioration of biological systems and is thought to be a contributory factor in the development of some cardiovascular diseases, such as hypertension and hyperlipidaemia, by facilitating the occurrence of vascular damage and inflammation.[44] The principal reactive radical intermediates formed during oxidative reactions are hydroxyl (HO·), alkoxyl (RO·) and peroxyl (ROO·) radicals.[45] Antioxidants are endogenous and exogenous metabolites that have the ability to donate electrons and hydrogens, chelate transition metals and break down peroxidation compounds and, therefore, have the potential to prevent oxidative stress by altering ROS to produce stable radicals, that are either too unreactive for further reactions or form non-radical products.[46] Antioxidant compounds scavenge free radicals, reducing the potential damage they may cause, via three known mechanisms; hydrogen-atom transfer (HAT), single-electron transfer followed by proton transfer (SET-PT) and sequential proton loss electron transfer (SPLET).[47] These three mechanisms may co-exist, and their level of involvement in oxidative reactions depends on solvent properties and characteristics

of individual radicals.[48] The HAT mechanism involves the transfer of a hydrogen atom (proton together with the one of its two bonding electrons) from an antioxidant species such as a phenolic compound (ArOH) to a free radical:

$$ArOH \rightarrow ArO^{\bullet} + H^{\bullet} \quad (1)$$

The HAT mechanism can be characterised by the homolytic bond dissociation enthalpy (BDE) of the hydroxyl group, where the lower the BDE value the greater the ability of an antioxidant to donate a hydrogen atom from the hydroxyl group; therefore resulting in an easier free radical scavenging reaction.[48] The SET-PT mechanism involves two steps;[48] firstly electron transfer phase (2a), which is characterised by the ionisation potential (IP), and secondly the deprotonating phase (2b):

$$ArOH \rightarrow ArOH^{+\bullet} + e^{-} \quad (2a)$$

$$ArOH^{+\bullet} \rightarrow ArO^{\bullet} + H^{+} \quad (2b)$$

The more recently confirmed SPLET mechanism also involves two steps;[49] the initial deprotonation of the phenolic molecule (3a), which results in the formation of a phenoxide anion, followed by electron transfer from the phenoxide anion (3b):

$$ArOH \rightarrow ArO^{-} + H^{+} \quad (3a)$$

$$ArO^{-} \rightarrow ArO^{\bullet} + e^{-} \quad (3b)$$

The latter two mechanisms are preferred for radicals with high electron affinity.[48]

Endogenous antioxidants, such as glutathione peroxidase, superoxide dismutase, catalase,[50] and exogenous metabolites, such as vitamin C,[51] α-tocopherol,[52] epigallocatechin gallate,[53] lycopene[54] and anthocyanins, possess the capability to prevent or slow down the oxidation of other molecules by transforming ROS into non-radicals either via electron or hydrogen donation, the transition metal chelation and/or decomposition of peroxidation compounds.[55] It is widely recognised that phenolic compounds act as chain-breaking antioxidants through their electron/hydrogen-donating ability and as chelators of redox-active metal ions that are capable of catalysing lipid peroxidation.[56] Phenolic antioxidants have the ability to

inhibit oxidation at a rate considerably faster than that of chain propagation, resulting in a non-radical product that cannot propagate the chain reaction.[57]

Arising from the link between oxidative stress and many disease states there has been an interest in measuring the oxidative status of biological systems. However, a standardised process for assaying total antioxidant capacity within biological systems does not exist, due to the fact that antioxidants are isolated from variety of sources and can include enzymes (e.g. superoxide dismutase), large molecules (e.g. ferritin), small molecules (e.g. phenols) and hormones (e.g. oestrogen). Additionally, there are numerous free radical oxidant sources and antioxidants may respond in a different manner to a different radical or oxidant source.[58] Paper I reviews various types of in vitro antioxidant assays; including the oxygen radical absorbance capacity (ORAC) assay, the 2,2-diphenyl-1-picrylhydrazyl (DPPH·) radical scavenging ability assay, the ferric reducing antioxidant power (FRAP) assay, microsomal lipid peroxidation (MLP) assay and the ferrous-ion chelating (FIC) capability assay, available for determining the antioxidant potential of extracts, fractions and compounds from natural sources.[7] Generally, multiple assays are employed to investigate potential antioxidant activities due to the variability between antioxidant assays, which is attributed to inconsistent experimental conditions and the differences in the physicochemical properties of oxidants employed.[59]

Synthetic antioxidants have traditionally been used as food additives and preservatives for the prevention of free radical-initiated lipid oxidation; however, at high doses they are associated with toxic and carcinogenic effects.[60-61] As a result, research in this area has become more focused on finding alternative natural sources of antioxidants that not only have the potential to be used as food preservatives,[62-63] but also as bioactive agents in functional foods.[64-65]

1.3 Hypertension and renin-angiotensin system (RAS)

Hypertension is a global chronic disease that affects 20-30 % of adults globally and carries a high risk factor for the development of atherosclerosis, stroke and myocardial infarction.[66] Essential hypertension, where the specific cause is unidentified, accounts for more than 90% of cases of hypertension. Many

pathophysiologic factors have been implicated in triggering essential hypertension; such as increased sympathetic nervous system activity, overproduction of sodium-retaining hormones and vasoconstrictors; long-term high sodium intake; increased renin-angiotensin sytem (RAS) stimulation; alterations in expression of the kallikrein-kinin system; increased activity of vascular growth factors; alterations in adrenergic and altered cellular ion transport.[67] In the RAS the conversion of angiotensinogen to the decapeptide angiotensin I is catalysed by the enzyme renin and the conversion of angiotensin I to the vasoconstrictor octapeptide angiotensin II is catalysed by the dipeptide-liberating exopeptidase ACE-I resulting in an increase in blood pressure.[68] In addition, ACE-I also catalyses the degradation of the vasodilator bradykinin, further promoting an increase in blood pressure.[69] A graphical outline of the RAS pathway is available in Paper I (Figure 6).[7] Therefore, the RAS renin and ACE-I enzymes, as well as free radicals involved in altering normal nitric oxide (NO) function,[70] present viable targets for the development of potential antihypertensive components.

The development of captopril initiated the widespread use of ACE-I inhibitors for the treatment of hypertension and related cardiovascular complications, such as acute myocardial infarction and congestive heart failure.[71-73] RAS inhibitors possess advantages over other antihypertensive agents, such as diuretics, beta-adrenergic blockers and calcium antagonists, due to their improved tolerability, relatively fewer side effects and favourable metabolic profile.[74] Although, some tolerability issues, including taste alterations, cough and skin rashes,[75] are still present with the administration of synthetic RAS. Therefore, increased focus has been given to finding naturally-sourced components with RAS inhibitory activity, particularly for the treatment of mild-to-high blood pressure where antihypertensive drugs may not be necessary.[66, 76-77] In particular, much research had been carried out in the area of ACE-I inhibitory components from marine sources,[78-80] and the potential commercial opportunities from the large-scale isolation of natural RAS inhibitory agents is evident from current approved products.[54, 81-82]

1.4 Relationship between oxidative stress and hypertension

It is widely accepted that there is a link between the increase of oxidative stress and incidence of hypertension, however, there are conflicting opinions as to whether oxidative stress is a contributory factor toward the development of hypertension or a product of hypertension.[83] Many sources of ROS exist in cardiovascular diseases, including nitric oxide synthases, xanthine oxidase, NADPH oxidase, myeloperoxidase, lipoxygenases and mitochondrial respiratory chain.[84] It has been suggested that the over-production of ROS leads to endothelial dysfunction, decreased nitric oxide bioavailability, endothelial cell damage and the generation of vasoconstrictor lipid peroxidation products, therefore increasing vascular contraction and inflammation.[83, 85-86] It has also been shown that ROS production is increased in cases of hypertension in stroke-prone spontaneously hypertensive rats (SHRSP) and that antioxidant treatment with vitamin C and vitamin E may prevent progression of hypertension by improving endothelium-dependent vasodilation, decreasing vascular oxidative stress, decreasing NADPH oxidase activation and increasing activity of superoxide dismutase.[87] Furthermore, it has been demonstrated that the release of angiotensin requires a conformational change in its precursor angiotensinogen to allow access, followed by the complementary binding, to renin. The conformational change is facilitated by an oxidative switch resulting in the transition of a labile disulphide bridge to a more active oxidised form.[88] Whether oxidative stress is a cause or a product of hypertension, the isolation of bioactive agents exhibiting both antioxidant and RAS inhibitory capabilities would be promising in terms of their development as functional antihypertensive agents.

1.5 Phlorotannins

Phlorotannins are dehydro-oligomers ($\leq$ 10 units) or -polymers ($>$ 10 units) of phloroglucinol (1,3,5-trihydroxybenzene) monomers and consist up to 25-30 % of the dry weight of brown macroalgae.[89] Phlorotannins are thought to be biosynthesised via the polyketide pathway and located in membrane-bound vesicles called physodes, linked to cell wall components, such as alginic acid, and/or free in the cytoplasm.[90-92] While polysaccharides play primary roles, including the formation of the macroalgal cell wall, phlorotannins have been suggested to play secondary roles such as minimizing oxidative stress in response to changes in UV radiation and nutrient

availability.[93] It has also been reported that phlorotannins are produced to deter herbivore grazing of macroalgae; however, this view has become distorted with more recent reports implying that other compounds, such as galactolipids, are responsible for the deterrent activity.[94-95] Phlorotannins are classified into four main categories according to the type of linkage between the phloroglucinol units and/or the presence of additional hydroxyl groups;[96] phlorotannins with ether linkages (fuhalols and phlorethols), with phenyl linkages (fucols), with ether and phenyl linkages (fucophlorethols) and those with a dibenzodioxin linkage (eckols) (Examples in Figure 4 of Paper I and Figure of Paper V).[97] The level of phlorotannins in macroalgae also varies greatly depending on the genus, location and time of year.[98] Although it has been reported that these molecules can range in molecular weights from 200 Da to 650 kDa,[99] they are more commonly reported in the 10-100 kDa range.[100-103]

Apart from the level, the composition of the phlorotannin pool within certain macroalgal species can vary depending on the genus, seasonality, geo-morphological features and depth of collection site.[104] For example, Le Lann and colleagues reported that the phenolic content of a 5-12/14 kDa molecular weight cut-off (MWCO) fraction increased significantly with increased depth in *Sargassum* species, but not in *Turbinaria* species. In the same study, it was observed that low molecular weight phenolic compounds (less than 2 kDa) decreased in *Sargassum* and *Turbinaria* species as depth of the macroalgal collection increased, which suggests that small macroalgal phenolics possess a photo-protective role within the macroalgae.[104] It has been reported that species of the Fucales order exhibit maximum phlorotannin contents during the summer period.[104]

1.5.1 Antioxidant activity of phlorotannins

As noted above, macroalgae synthesize phlorotannins to minimise oxidative stress and damage from exposure to UV radiation.[105] Phlorotannins are effective radical scavengers due predominantly to their aromatic polyphenolic structures, which allow them to accept and stabilise free electrons of radicals and, therefore, reduce their potential damage. Phlorotannins have regularly been reported as possessing eight or more phenol rings in their structure and, hence, are expected to be more potent

antioxidants than terrestrial polyphenols.[106] For example, phlorotannins isolated from *Eisenia bicyclis*, *Ecklonia cava* and *Ecklonia kurome* have been shown to possess antioxidant activity 2-10 times higher than catechin, α-tocopherol and ascorbic acid.[106] Furthermore, it has been suggested that increased polymerization of phloroglucinol is correlated to increased bioactivity.[107] Brown macroalgal species in general display considerably higher in vitro antioxidant activity relative to green and red macroalgal species,[108] which has been attributed to higher levels of phlorotannins in the brown species. Macroalgal genera, such as *Sargassum*, *Ecklonia*, *Fucus*, and *Ascophyllum*, have been widely reported as possessing in vitro antioxidant activity linked with their high phenolic content.[103, 109-111] The radical scavenging abilities of various phlorotannins against both peroxynitrite and ROS have been investigated, and promising activities have been observed.[106,112] It has been shown that the phlorotannins phlorofucofuroeckol A, dieckol and dioxinodehydroeckol isolated from the Korean brown macroalga *Ecklonia stolonifera* have exhibited strong DPPH· radical scavenging activity, following bioactivity-guided fractionation.[15]

In order to assess the physiological significance of the above in vitro studies it is important to understand the various metabolic processes that phlorotannins may encounter following ingestion. The antioxidant benefits potentially gained from phlorotannins is largely dependent on their absorption, distribution, metabolism and excretion (ADME) characteristics.[113] Some polyphenols are absorbed in the stomach, others reach the duodenum and are affected by the neutral to alkaline duodenal juice. These digestive fluids influence the amount and structural characteristics of the polyphenols reaching the small and large intestine. Following this, polyphenols will continue to be influenced by the pH, microbiota and enzymatic activities of the digestive tract prior to absorption or excretion.[114] As with other polyphenols, the level of phlorotannin absorption will also be determined by many physico-chemical factors such as their molecular size, lipophilicity, solubility and pKa values as well as biological factors such as membrane permeability and lumen/surface pH.[113, 115] In general, polyphenols in their aglycone form can be absorbed from the small intestine; however most polyphenols are present in food in the form of esters, glycosides or polymers that cannot be absorbed in native form.[116] Although, these barriers may prevent phlorotannins from being absorbed systemically in their active form,

phlorotannins may also act locally in the GI tract. For example, pure polyphenols and polyphenolic extracts have shown in vivo to be capable of lowering the severity of colitis.[117] The form or food matrix in which phlorotannins are administered will also affect their bioavailability. The antioxidant power of a complex of crude phlorotannins and soybean protein has been determined in order to evaluate the potential application of phlorotannins as functional food ingredients. A phlorotannin pentamer and phlorotannin hexamers showed pronounced affinity for soybean protein and the DPPH· radical scavenging activity of the complex was approximately four times stronger than soybean protein extract used alone.[106]

The successful absorption of an antioxidant phlorotannins may have beneficial effects of various chronic diseases, such as hypertension, where oxidative stress is thought to play a detrimental role. For instance, ROS production leads to endothelial dysfunction, enhanced contractility of vascular smooth muscle cells, lipid peroxidation and inflammation. Therefore, phlorotannins may be employed to target these markers of systemic oxidative stress, which have been shown to be increased in both experimental and human hypertension.[118-119] For example, the observed positive effects of dark chocolate flavanols in hypertension has been attributed to multiple mechanisms.[120] Flavanols modulate oxidative stress and the cell redox state, which in turn defines NO availability and NO-synthase activity.[121] It has also been proposed that their antihypertensive properties may occur through the inhibition of ACE-I.[122]

1.5.2 RAS-inhibitory activity of phlorotannins

The ability of phlorotannins to inhibit RAS activity may be attributed to their protein-binding abilities.[123] It has been reported that phlorotannin molecular size influences their ability to interact with certain enzymes, with pentamers and hexamers of phloroglucinol showing stronger inhibition.[124] The phlorotannins phloroglucinol, triphlorethol A, eckol, dieckol and eckstolonol isolated from an ethanol extract of *Ecklonia cava* all displayed ACE-I-inhibitory activity, with dieckol being the most potent with an IC_{50} value of 1.47 mM.[125] It has also been suggested that their ACE-I-inhibitory activity may be exerted through the sequestration of the enzyme metal factor, Zn^{2+} ion.[126] However, in biological systems the efficiency of phlorotannins RAS-inhibitory activity, as with its antioxidant activity, depends largely on their

bioavailability and integrity, therefore, the encapsulation of phlorotannnins may facilitate their transport to target organs where they can exert their RAS-inhibitory activity, and potentially antihypertensive capabilities.[127]

1.6 Bioactive Peptides

Bioactive peptides (BPs) possess beneficial pharmacological properties beyond normal and adequate nutrition that are available either directly through their presence in intact food, or after their release from their respective host proteins by hydrolysis in vivo or in vitro.[128] Various types of BPs have been sourced from marine sources, such as fish,[129] squid,[130] and macroalgae.[16] Udenigwe and Aluko identified two key factors that should be considered when sourcing BPs from food protein, namely; the 'pursuit of value-added use of abundant under-utilized proteins or protein-rich food industry by-products' and the 'utilization of proteins containing specific peptide sequences or amino acid residues of particular pharmacological interest'.[131] The development of BPs is dependent on the employment of efficient bio-transformation processes.

1.6.1 Processing for bioactive peptides

Peptide production and processing based on structure-function parameters can lead to the production of BPs with potent bioactivities. The use of enzymatic hydrolysis is advantageous as it mimics what occurs in the human digestion of proteins and, therefore, yields information about the potential peptides that may be produced in vivo.[132] The properties of BPs can be affected in various ways depending on the enzyme used for hydrolysis, the processing settings and the peptide size. Following the hydrolysis of food protein to yield peptides, further processing is often necessary in order to enhance the BP concentration, thereby boosting bioactivity and facilitating characterisation. Peptides, therefore, are regularly fractionated based on their size, charge or hydrophobic nature, or a combination of these. Membrane-ultrafiltration, dialysis and size-exclusion chromatography are some of the techniques employed to separate hydrolysate into different molecular weight fractions. For example, membrane ultrafiltration was employed to fractionate peptides, into < 1, 1-3, 3-5 and 5-10 kDa fractions, which were digested from purple sea urchin using the

proteases neutrase, trypsin, papain and pepsin. The study found that all samples possessed antioxidant activity in the in vitro DPPH· radical scavenging and FRAP assays, however the activities of the < 1 kDa fractions were superior.[133] More recently, the combination of separation techniques based on different physico-chemical characteristics have been introduced, such as electrodialysis-ultrafiltration (EDUF) which separates cationic, anionic and neutral peptides of defined molecular sizes.[134] These techniques may aid in the purification of macroalgal peptides in the future.

The isolation of BPs of lower molecular weights is more favourable than that of BPs possessing higher molecular weights, as they can better persist under conditions of further in vivo proteolytic digestion and, consequently, are more likely to reach the target tissue with bioactivity intact.[131] Where the potential to utilize food-derived BPs exists commercially, for instance as functional food ingredients, it is important to consider that the peptide processing methods employed must be food-grade. The potential scale-up of peptide processing for potential industrial food applications, while at the same time preserving the peptide profiles and bioactivity of resultant peptides, has also been effectively demonstrated.[135] However, for the successful introduction of BPs into functional foods, it is necessary to identify the optimum form in which bioactive peptides can be incorporated into food matrices. Crude or semi-purified peptide fractions may be more economically feasible than pure peptide compounds. The high cost associated with the production of purified peptides may also mitigate their use in foods. Furthermore, the potential for synergistic activity occurring, where several peptides are present, may result in heightened bioactivities.[136]

1.6.2 Antioxidant activity of Bioactive Peptides (BPs)

Antioxidant peptides can act as radical scavengers, proton donors and metal-ion chelators.[137-138] Hydrolysates of most plant and animal proteins contain antioxidant peptides however, the composition, number and order of amino acids found in peptides determines overall antioxidant potential.[139] For that reason, the type of hydrolytic enzyme used and the hydrolysis conditions can affect the type and efficiency of antioxidant peptides generated.[139-140] Radical scavenging activity of

peptides has been suggested to significantly correlate to the presence of specific amino acids, such as histidine, tyrosine, tryptophan, methionine, cysteine and proline.[141-142] Reactive aromatic amino acids can give up protons easily to electron deficient radicals whilst maintaining radical stability via resonance structures.[143] Peptides containing hydrophobic amino acids can possess enhanced antioxidant properties in lipid-rich environments, as they have the ability target the hydrophobic polyunsaturated chain of fatty acids of biological membranes.[144] In cells, transition metal ions act as initiators for the production of radical and non-radical oxygen species. The ability of metal pro-oxidants to produce radicals can be inhibited by peptides through sequestration and chelation. The ability of histidine to chelate metals is a major contributor to its antioxidant activity.[143] In terms of their potential use as either components in functional foods or agents to inhibit lipid oxidation-mediated off-flavour and colour deterioration, antioxidant protein hydrolysates and peptides are, unfortunately, generally associated with a bitter taste.[145] The encapsulation of peptides or spray drying of hydrolysates with mixtures of gelatin and soy protein isolates may afford an approach to overcome these organoleptic issues.[146-147]

1.6.3 RAS-inhibitory activity of bioactive peptides (BPs)

Food derived BPs have the potential to prevent ACE-I through various modes of inhibition, such as competitive, non-competitive or uncompetitive, with replacement of single amino acids affecting the nature of the interactions between ACE-I and various BPs.[16] The intensity of peptide RAS inhibition is largely dependent on the peptide structure. ACE-I substrates with hydrophobic amino acid residues at the three C-terminal sites are favourable for interaction. Additionally, lysine or arginine, which have a positive charge on the ε-amino group at the c-terminal site, are also likely to aid ACE-I inhibition.[148] Furthermore, food BPs have the potential to lower hypertension via routes outside the of the RAS pathway, such as by promoting the production of the vaso-relaxant nitric oxide.[149] It is important to consider that the extent of pharmacological application of bioactive peptides is dependent on the absorption and bioavailability of them as intact forms in target tissues, and, as discussed earlier, encapsulation may facilitate this. For the most part, the identification of individual peptides from macroalgae exhibiting RAS-inhibitory activity has been restricted to *Undaria pinnafidia* and *Palmaria palmata*.[16, 80, 150]

1.7 Extraction, separation and characterisation of bioactive components from macroalgae

1.7.1 Extraction techniques

There is an array of techniques available for the extraction of bioactive components from macroalgae.[7] However, extra consideration needs to be given to the use of appropriate, selective, cost-effective, and environmentally-friendly extraction procedures that comply with the legal requirements regarding the use of food-grade solvents and processes in order to obtain bioactives suitable for functional foods.[151]

Solid-liquid extraction (SLE) is one of the more conventional extraction techniques and one of the most long-standing, efficient methods employed for natural product extraction and is a common practice in many industrial processes.[152] The efficiency of SLE can depend on many factors, such as solvent composition, length of extraction, temperature, solid-to-liquid ratio and particle size.[153-154] SLE is relatively inexpensive in terms of capital costs, and requires less state-of-the-art knowledge and optimisation compared to some of the more modern methods, such as pressurised liquid extraction (PLE). SLE is also one of the most commonly employed and researched methods for the extraction of antioxidant phenolic compounds from natural sources.[155-156] The extraction of particular compounds of interest can be simplified by the employment of suitable extraction solvents. For example, the advantage of using solvents of different polarities is that the chemical complexity of the biomass is simplified, as components will be extracted based on their solubility in a particular solvent.[157] Soxhlet extraction, maceration, percolation, turbo-extraction and sonication are all considered to be SLE techniques.[158]

Of late, a trend towards the development of "green" extraction, which aims to minimise the use of harmful solvents, has emerged. The challenges associated with green techniques are maintaining process intensification and the cost-effective production of high quality extracts achieved with other conventionally used methods.[159] Ethanol is one of the most common "green" solvents, and, even though it is flammable, ethanol is used on a large scale due to its availability in high purity, its low price and biodegradability. Water is also an obvious choice for use in green extraction due to its highly polar nature and lack of toxicity.[159]

PLE, also known as pressurised hot water extraction (PHWE) or accelerated solvent extraction® (ASE®), is an automated technique for extracting solid and semi-solid samples with liquid, organic or aqueous solvents. Pressure is applied to allow the use of liquids at temperatures higher than their normal boiling point.[151] Samples are placed in sample cells to which solvent is added and the sample is then extracted statically under raised temperature and pressure conditions for short periods (5–10 minutes).[160] Through the combination of high pressures and temperatures, faster extraction that requires smaller amounts of solvents is achieved. Higher analyte solubility is promoted by increasing the extraction temperature, and also high temperatures decrease the viscosity and the surface tension of the solvents, helping to reach areas of the matrices more easily, thus improving the extraction rate.[151] Zaibunnisa *et al.*[161] compared the efficiency of PLE to other extraction methods and found that PLE had shorter extraction times, less use of solvents and lower overall costs. Furthermore, PLE is usually carried out in an oxygen and light-free environment, which is ideal when working with potential bioactive compounds, and is also considered a more environmentally-friendly option for extraction.[162] Following its development, PLE was largely used initially for investigating environmental samples,[163-164] however, in recent times, the extraction of phenolic compounds from macroalgae, such as *Stypocaulon scoparium*,[165] *Porphyra tenera*, and *Undaria pinnatifida*[166] has been carried out using PLE.

An alternative 'green' method is supercritical fluid extraction (SFE), which is based on the use of solvents at temperatures and pressures above their critical points. Under these conditions, various properties of the fluid are placed between those of a gas and those of a liquid.[19] The advantage of this technique over conventional methods is that supercritical fluids have better transport properties than liquids and, therefore, can diffuse easily through solid materials and provide faster extraction yields.[19] In general, carbon dioxide is used as the solvent in SFE to extract bioactive compounds from natural sources, as it is cost efficient, its critical conditions are easily attainable and it is generally recognized as safe (GRAS) for use in the food industry.[167]

The use of pulsed electric fields has also been introduced in order to further maximise the extraction potential of bioactives by reducing the number of steps

involved in an extraction process and the extraction time, and thus the energy consumption.[159] Ultrasound assisted extraction (UAE) uses acoustic cavitation to disrupt plant cell walls, reduce biomass particle size, and enhance the level of contact between the solvent and the target compounds.[168] UAE also exerts a mechanical effect, which allows greater infiltration of the solvent into the sample matrix, increasing the contact surface area between the solid and liquid phases.[169] Microwave-assisted extraction (MAE) uses microwave radiation that causes motion of polar molecules and rotation of dipoles to heat solvents and to promote transfer of target compounds from the sample matrix into the solvent.[151] In general the chosen solvent possesses a high dielectric constant and, therefore, strongly absorbs microwave energy.[158] A significant advantage of this technique in terms of bioactive extraction is that, in some instances, the matrix itself can interact with microwaves resulting in the surrounding solvent possessing a low dielectric constant and thus remaining cold and, thus, reducing potential damage to thermally labile compounds.[158]

While the previously discussed methods are generally efficient for the extraction of bioactives, such as polyphenols and carotenoids, they are less efficient for other bioactives, such as peptides and polysaccharides, that often form complexes with other plant components. For example, peptides and proteins often form complexes with other metabolites making them more difficult to extract and purify.[170-171] In enzyme-assisted extraction (EAE) various enzymes, such as proteases and carbohydrases, which are often employed to disrupt the structural integrity of the plant cell wall thereby enhancing the extraction of bioactives from plants, have shown faster extraction, higher recovery, reduced solvent usage and lower energy consumption when compared to non-enzymatic methods.[172] Thus, EAE may serve as a potential alternative to conventional solvent-based extraction methods as this 'green' technique functions efficiently under mild processing conditions in aqueous solutions.[173] Enzymatic hydrolysis methods can be tailored to mimic, to some degree, the varying enzymatic and pH environment of the human digestive system and, therefore, may give insight into how particular bioactives may be treated in vivo.[174] EAE has been proposed as a promising technique for the food-friendly extraction of bioactives such as polyphenols, peptides and polysaccharide from macroalgae.[175] Although many of the new 'greener' extraction processes appear to be efficient at

analytical scale, their capabilities at industrial scale have yet to be monitored only then can realistic comparisons to the more conventional techniques be made with regards cost and efficiency.

1.7.2 Fractionation and purification techniques

Opportunities exist for the inclusion of macroalgal extracts into food and cosmetic products without specific considerations. However, in order to improve their consistency and bioactivity and, thus, their effectiveness as potential functional ingredients, food preservatives, nutraceuticals and/or cosmeceuticals.[97, 176-177] Further refinement of extracts using various fractionation and purification techniques is required. In particular, the exploitation of macroalgal phlorotannin polymers is dependent on the development of suitable purification and analytical methods capable of analysing the metabolite profile. With the exception of *Fucus vesiculosus*[178] and *Ecklonia cava* species,[179] the complexity of phlorotannins has meant that relatively few of these molecules have been purified from macroalgal species. The difficulty in phlorotannin purification is attributed to their similar chemical properties and the polymeric nature of their production.

Mannitol, the major low molecular weight carbohydrate present in brown seaweed,[180-181] is often co-extracted with bioactive components of interest and, therefore, must be eliminated to improve the bioactives purification process. Although the removal of mannitol from smaller molecular weight fractions has proven to be difficult, the use of chromatography on silica columns has been shown to successfully remove most of the mannitol present in higher molecular weight portions.[103] Fractionation methods for the purification of macroalgal bioactive compounds often involve a combination of techniques based on polarity and/or molecular size. Solvent partitioning is recognised as one of the simpler separation techniques and involves the partitioning of the analytes of interest into one of two immiscible solvents. This is considered a soft fractionation technique that relies on the solubility of the bioactive of interest and not on physical interaction with another medium.[157]

Reverse-phased column chromatography using Sephadex LH-20, a beaded hydroxypropylated cross-linked dextran, is widely applied in the fractionation of polyphenols.[178] Both polar and non-polar bioactive compounds can be fractionated

using this technique according to two types of mechanisms; size and polarity.[157] Macroalgal phlorotannins can be separated on Sephadex LH-20 based on adsorption partition, whereby small phlorotannins adsorb with low affinity and tend to be washed out first, larger phlorotannins, such as hexamers and octamers, are eluted next, and last to elute are phlorotannin polymers.[182] A recognised procedure for the separation of tannins from non-tannin phenolics involves sorption to Sephadex LH-20 in ethanol and selective de-binding with aqueous acetone.[14] In particular, Sephadex LH-20 open column chromatography seems to be the method of choice for the separation of high molecular weight procyanidins.[183-184] It has also shown to be useful for smaller molecular weight phlorotannins as Heo and Jeon *et al.* employed silica gel and Sephadex LH-20 column chromatography for the purification of the low molecular weight diphlorethohydroxycarmalol, which exhibited radical scavenging activity and a protective effect against H_2O_2-induced cell damage, from *Ishige okamurae*.[185]

Flash chromatography, also known as medium pressure chromatography, was introduced as an alternative to the conventional slow, gravity-fed column chromatography.[186] Flash chromatography is different from the conventional technique in that pressure is used to force the solvent through the column of stationary phase resulting in faster and higher resolution chromatography.[187] It employs pre-packed cartridge columns, which contain the sorbent, and a compression module into which the cartridges are introduced and pressurised. With this separation system void spaces on the column head are minimized and, depending on the column sized employed, milligrams to grams can be separated.[157] The advantages associated with flash chromatography include the ease-of-use of pre-packed columns, the containment of harmful sorbent in cartridges, the ability to re-use columns and high resolution.[157] Flash chromatography has shown to be useful for the separation of both peptides and polyphenols of natural sources.[188-189] Furthermore, flash chromatography has proven to be useful for the separation of various metabolites from macroalgae. Kubanek *et al.* separated and isolated an antimicrobial, polycyclic macrolide, lobophorolide, from *Lobophora variegata* with the aid of gradient reversed-phase flash column chromatography.[190] Anti-foulant diterpenes of *Canistrocarpus cervicornis* were isolated from a crude dichloromethane extract using silica gel flash column chromatography.[191] Normal-phase flash chromatography carried out on a silica gel

column was employed for the separation of numerous phlorotannins in macroalgae *Sargassum spinuligerum*, *Carpophyllum maschalocarpum*, *Carpophyllum angustifolium* and *Scytothamnus australis*.[192]

High-performance liquid chromatography (HPLC) traditionally has been the method of choice for natural product separation and is generally employed in conjunction with reverse-phase stationary phases.[157] The use of HPLC for the separtion of phlorotannins is favourable, as it allows for the large-scale isolation of individual compounds.[147, 162] Both reverse-phase and normal-phase HPLC have been assessed for the appropriate separation of phlorotannins from macroalgae, to aid the potential use of mass spectrometry (MS) analysis to identify individual phlorotannin compounds.[193] There are some disadvantages with using normal-phase HPLC such as the requirement to use chlorinated solvents and also the poor solubility of hydrophilic analytes in normal-phase eluents, which can result in adsorption onto the silica stationary phase.[194] Koivikko *et al.* (2007) assessed normal-phase and reverse-phase HPLC methods for the separation of phlorotannins from *F. vesiculosus*.[193] The reverse-phase method displayed limited retention of the phlorotannins, however, the normal-phase HPLC method appeared to be more effective method and there was good separation of the oligomers, however, the phlorotannin polymers were not separated as well.[193] More recently, Wang *et al.* (2012) also employed a reverse-phase HPLC method in an attempt to further purify *F. vesiculosus* fractions generated from size exclusion chromatography (SEC).[178] Once again, this method worked well for the separation of the initial fractions containing phlorotannin oligomers; however, for the latter fractions containing polymers, good separation was not observed. Although, several previous studies have shown the efficiency of HPLC for low molecular weight phlorotannins,[96, 178, 193] the HPLC technique lacks the ability to separate high molecular weight phlorotannins and, as a result, other techniques, such as size exclusion chromatography, must be employed to ensure efficient separation takes place.[178]

1.7.3 Metabolite profiling and characterisation

Due to the lack of commercial standards for phlorotannins, with the exception of the monomer phloroglucinol, the characterisation and quantification of purified

phlorotannins can be a lengthy and difficult process. Ultra high-performance liquid chromatography-mass spectrometry (UHPLC-MS) has recently been used to profile phlorotannins from various species of brown macroalgae.[195] UHPLC, commercially known as UPLC®, has been developed to endure much higher system back-pressures than in conventional HPLC, allowing the use of columns with much smaller particle sizes and, therefore improving its speed, sensitivity and resolution.[196] UHPLC operating in hydrophilic interaction liquid chromatography (HILIC) mode has been combined with high resolution MS (HRMS) to analyse phlorotannin enriched fractions from the brown macroalgae *Fucus spiralis*, *Fucus vesiculosus*, *Pelvetia canaliculata* and *Ascophyllum nodosum*.[194] HILIC has been deemed to be a 'mixed-mode' separation system with selectivity based on electrostatic interactions, dipole-dipole interactions, cation/anion exchange and hydrogen bonding.[197-198] The UHPLC-HRMS method was optimised for an extract of *Fucus vesiculosus*, whereby separation of lower molecular weight phlorotannins was achieved in 15 minutes.[194] The molecular weights of the phlorotannins detected using HRMS were small relative to those detected by size exclusion chromatography previously,[199] however they were large compared to those previously detected by MS.

The separation of phlorotannins is a highly laborious process. However, the current advances in analytical techniques allow the extensive qualitative analysis of impure phlorotannin extracts and fractions to be carried out. Hence, metabolic profiling and fingerprinting of crude macroalgal extracts and fractions has become more accessible. This in turn facilitates the standardisation of bioactive composition within macroalgal samples, which is a necessary requirement if these components are to be commercialised as functional ingredients.

1.8 Quantum mechanics (QM) and molecular dynamics (MD) methods for investigating structure-activity relationships (SARs) of polyphenols

1.8.1 Electronic properties of antioxidant polyphenols

Polyphenolic compounds have the ability to scavenge free radicals *via* three main reaction mechanisms that are discussed in section 1.2 ; HAT, SET-PT and the more recently discovered SPLET.[49, 200] The equilibrium between these mechanisms is dependent on both the environment and the reactants.[201-202] Enthalpies associated with

each of these mechanisms are quantifiable using theoretical quantum mechanics (QM) and, therefore, the extent of the antioxidant capability a polyphenolic compound possesses can be investigated. The bond dissociation enthalpy (BDE) of the O-H bond, ionisation potential (IP) and proton affinity (PA) are the measurable reaction enthalpies that direct the HAT, SET-PT and SPLET mechanisms, respectively, and can be calculated using QM.[47] BDE is a measure of the bond strength and the lower the BDE of an O-H bond of a molecule, the more likely it will exhibit antioxidant behaviour. The IP describes the process of single electron donation by the antioxidant and a lower IP is preferred to increase electron-transfer reactivity.[200, 203] PA is used to assess the proton loss and a lower PA indicates that the heterolytic bond cleavage is more likely. The planarity of polyphenols is also of particular interest when studying their antioxidant activity and can be investigated using geometry optimisation. This is because a free radical can be more easily delocalised by a more planar polyphenol.[47] A QM study has shown how the antioxidant ability of quercetin is related to the planar conformation of the radical that allows extended electronic delocalization between adjacent rings.[204] The planar structure of flavonoids allows the conjugated π-system of the AC-ring and the B-ring to efficiently interact, therefore distributing the electron donating effect of the OH groups over the whole molecule.[205-206] A QM study comparing the flavanol catechin to its planar derivative found that planar configuration of catechin can mainly affect the BDE for hydroxyl groups on ring B, however no effect is obtained for the hydroxyls on ring A.[207]

1.8.2 Quantum Mechanics and Density Functional Theory (DFT)

Various QM techniques have been compared in terms of their ability to describe the electronic structure of polyphenols reliably and can assist in the selection of the most suitable method for the measurement of the antioxidant parameters of interest. QM techniques can be broadly classified into three groups; ab initio methods, semi-empirical methods and density functional theory (DFT) methods. High level ab initio methods are highly accurate and computationally intensive. They can give an energy and wavefunction for a molecule by solving the Schrödinger equation. The wavefunction is then used to calculate the electron distribution of the molecule. Semi-empirical methods are also based on the Schrödinger equation, but are much faster than ab initio methods because they are parameterised. These methods involve

drawing on elements of theory and experimental values to calculate the electronic descriptors of a molecule. Density functional theory is similar to ab initio and semi-empirical calculations in that it is based on the Schrödinger equation, however, unlike those methods, DFT derives the electron distribution directly rather than calculating a wavefunction.[208] In DFT there is no systematic way of improving the exchange-correlation energy functional, whereas in wavefunction theory improvements can be made by using perturbation theory or configuration interaction treatments of electron correlation.[208] Hybrid DFT methods consist of different amounts of the Hartree-Fock (HF) non-local exchange operator and DFT exchange-correlation functionals, and have shown to be effective in acquiring accurate molecular structures, vibrational frequencies, and bond energies.[209] The hybrid Becke, 3-parameter, Lee-Yang-Parr (B3LYP) functional is currently one of the most widely used DFT methods for QM calculations.[209] It employs three empirical parameters to combine the exact exchange, gradient-corrected exchange and local spin-density (LSD) exchange with a correlation term based on the LSD approximation.[210] The initial gain from the development of this correlation-exchange was that the HF method frequently produces errors opposite to those found at DFT level, which leads to an almost systematic cancelling of errors.[211] It is generally considered that DFT methods predict van der Waals forces, such as hydrogen bonding, quite well; however they are limited for the accurate prediction of dispersion interactions.[212] The type of dispersion, in this case, is the attractive interaction created by the response of electrons in one region to instantaneous charge density fluctuations in another. The standard hybrid exchange-correlation DFT functionals are not capable of describing dispersion because they do not consider instantaneous density fluctuations and they only consider local properties to calculate the exchange-correlation energy.[213] Of late, attempts to develop dispersion corrected and long-range corrected-DFT methods that accurately account for dispersion interactions have increased.[211, 214]

1.8.3 Investigating the electronic properties of polyphenols using quantum mechanics

Computational expense and accuracy are the two main factors that influence which of these methods are to be chosen for QM calculations and a summary of some of the methods used for investigating the electronic structure of phenolic compounds are provided in table 1.

Many of the QM calculations that have been performed on polyphenols to date focus on flavonoids and deciphering what role the B-ring of flavonoids plays in their potential antioxidant activity.[215-216] The molecular structures of luteolin (**1**) and apigenin (**2**), and their mono-deprotonated forms, were characterised using the ab initio second-order Møller-Plesset perturbation method (MP2), and the DFT B3LYP and Generalized Gradient Approximation (GGA) Perdew, Burke and Ernzerhof (PBE) exchange-correlation (XC) functionals in solvent and in vacuum.[217] The basis sets 6-31+G(d) and 6-31G(d,p) were employed for all methods and also 6-311++G(d,p) was used with B3LYP. Calculations in water were carried out using the conductor-like polarisable continuum model (CPCM). In terms of geometry optimisation of the polyphenols, the B3LYP and PBE exchange correlation functionals produced parameters very similar to each other, and both were also comparable to the MP2 method. However, the dihedral torsion angle between ring B and C of both structure calculations differed between the DFT and MP2 methods, with the MP2-calculated angle approximately twice as large as that obtained by the DFT methods for both compounds in vacuo and in solvent. In this case, it was suggested that the DFT functionals overestimated the π-conjugation, resulting in a smaller calculated dihedral angle and a more planar structure compared to the MP2 method. To investigate this further, the potential energy curves around the dihedral angle were also obtained in steps of 5° using both the B3LYP and MP2 methods. The planar structures for both polyphenolic molecules represent saddle points, and the potential is almost flat at the angles observed for the MP2 and B3LYP methods in the earlier calculation. Large discrepancies between the calculated barrier heights of the two methods, however, reinforced how the π-conjugation is described differently between them.

QM calculations have become progressively more useful for investigating how the location the polyphenolic hydroxyl groups contribute to their antioxidant capacities and for validating existing experimental data in this area.[218] Pahari *et al.* (2012) carried out QM calculations on five mono- and poly-hydroxyflavones (**3-7**) to observe how varying the position at which O-H detachment occurs affects their BDEs.[215] BDE is an indicator of the likelihood of a polyphenol to transfer a hydrogen atom and, therefore, is a good measure of radical scavenging activity. The five flavonoid structures were firstly optimized using the MM+ molecular mechanics

force-field, an extension of the MM2 force-field, in vacuo and then were fully optimised using the Austin model 1 (AM1) semi-empirical method within the restricted Hartree-Fock (RHF) formalism. The flavonoid radical equivalents were optimized using the AM1 method, combined with unrestricted Hartree-Fock (UHF) calculations. Pahari and colleagues found that hydrogen atom-transfer from the 4'–OH and 3'–OH groups on the B-ring requires less energy than the transfer from OH groups on the A-ring and these findings support those found experimentally.[215] It was also found that, for the flavonoids fisetin (**6**) and robinetin (**7**), the corresponding 4'–OH radicals were more stable structures than the other possible 3'–OH and 5'–OH radical structures. This may be because, following geometry optimisation of the radical after hydrogen transfer from the 4'–OH site, the structure changes to a planar structure from the initial non-planar form of the parent structure. As a result of this structural change, expansive delocalization of this radical occurs and, furthermore, the residual spin and electron density is lower at this 4'-OH site compared to radicals formed at the other sites. The free radical-scavenging activity of polyphenols can also be related to the distribution of the frontier orbital energy, or highest-occupied-molecular orbital (HOMO), and it is an alternative parameter to assess the electron-donating ability of antioxidants. Molecules with higher HOMO energy values have stronger electron-donating abilities.[219] The DFT B3LYP method with the 6-31G(d) basis set was employed to calculate the HOMO energies of the flavonoids **3-7**. It was found that the presence of the hydroxyl groups in the B-ring increases the HOMO energy, i.e. the molecule is a good electron donor; and, therefore, highlights the significant contribution of the hydroxyl groups on this ring to the compounds' antioxidant activity.

The suitability of a particular basis set for the structure being analysed is also an important consideration. Pople's extended basis sets are widely used for polyphenol DFT studies.[203, 220] The Pople's basis sets have split valence descriptions and can be enlarged with d-type polarization functions on heavy atoms only or on all atoms, with p-functions on the hydrogens.[221] Polarisation functions are important for reproducing chemical bonding. Diffuse functions can also be added to these basis sets (usually of s-type or p-type) to represent very broad electron distributions.[221] Lucarini *et al.* (2004) carried out DFT calculations on isomers of catechol (**8**) and the parent

semi-quinone radical (**9**) using B3LYP and the couple-cluster method with single and double excitation (CCSD) to assess the effect of different levels of Pople's basis sets on the BDE values (table 1).[222] They found that the use of the 6-31+G(d) basis set, which adds diffuse functions on oxygen, with B3LYP significantly increased the BDE of catechol. However, little further effect on the BDE was observed when the valence double-zeta 6-31++G(d,p), with polarisation and diffuse functions on hydrogen, or when the enlarged valence triple-zeta 6-311++G(d,p) basis sets were employed. Therefore, even with the use of a moderately large basis set B3LYP still underestimated the BDE of catechol with respect to the experimental value. When the *ab initio* CCSD method was used the addition of diffuse and polarisation functions also had little effect on the BDE. However, the use of the CCSD method increased the catechol BDE by approximately 2 kcal mol^{-1}, which meant the resulting BDE correlated well with the experimental value, making CCSD the more reliable method for the calculation of catechol BDE than B3LYP.[222]

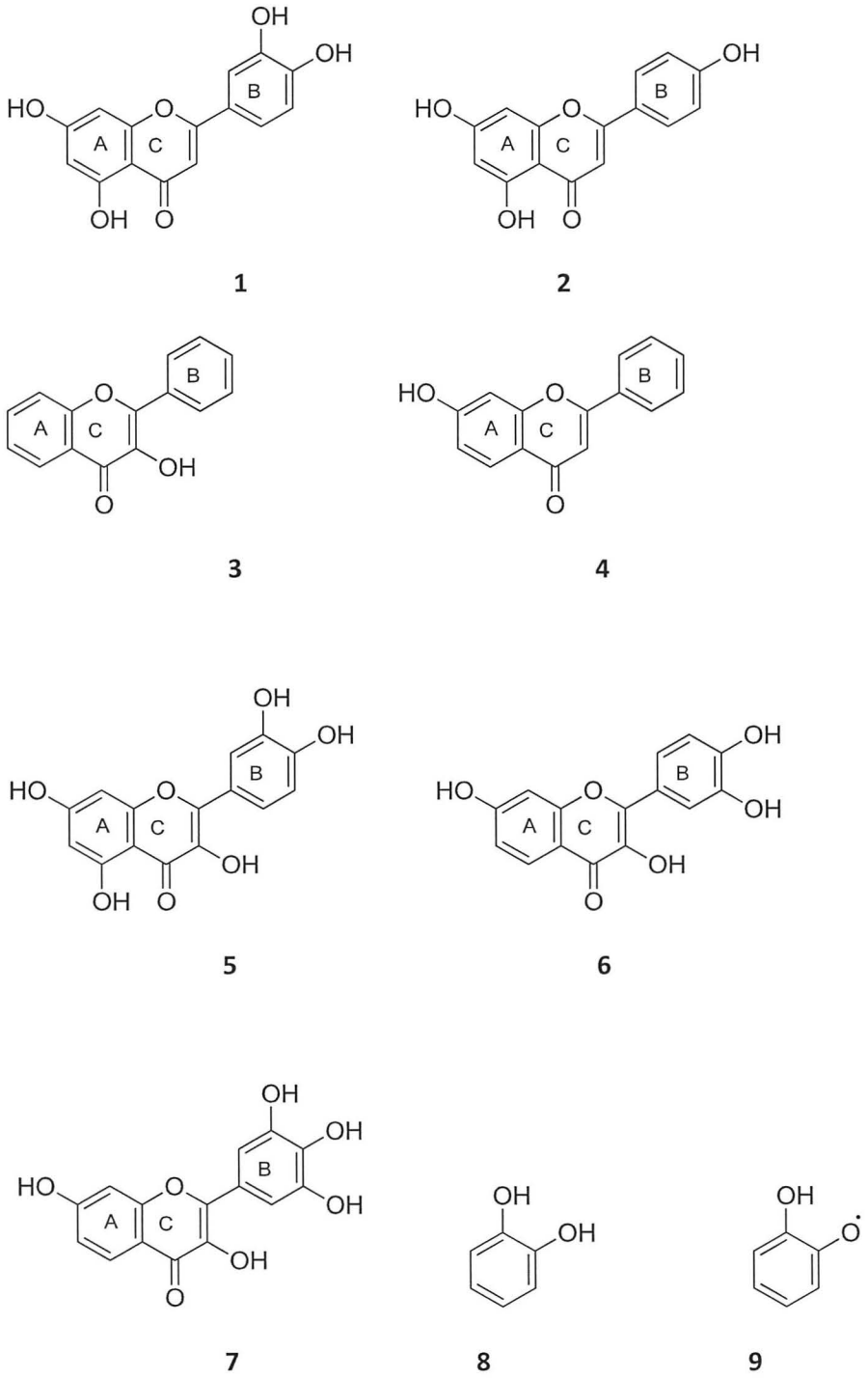

Figure 1: Polyphenol structures, luteolin (**1**), apigenin (**2**), 3-hydroxyflavone (**3**), 7-hydroxyflavone (**4**), quercetin (**5**), fisetin (**6**), robinetin (**7**), catechol (**8**) and parent semi-quinone radical (**9**), investigated in QM and/or MD studies.

Table 1: Summary of selected quantum mechanics methods used for investigating the electronic structure of phenolic compounds

QM Method(s)	Polyphenols	Description	Ref
MP2, B3LYP and PBE functionals Basis sets: 6-31+G(d) and 6-31G(d,p) were employed for all methods. 6-311++G(d,p) was used with B3LYP	Luteolin (**1**) and apigenin (**2**) & their mono-deprotonated forms	Geometry optimisation. Investigated changes in potential energy curves as a function of dihedral angle between ring B and C.	217
(a) AM1 method with the RHF formalism for neutral structures and UHF formalism for radicals (b) B3LYP with the 6-31G(d) basis set	3-hydroxyflavone (**3**), 7-hydroxyflavone (**4**), quercetin (**5**), fisetin (**6**) & robinetin (**7**).	(a) Investigated how varying the position at which O-H detachment occurs affects their bond dissociation energies (BDEs). (b) Assessed the electron-donating capabilities.	215
CCSD and B3LYP Basis sets: 6-31G(d), 6-31G(d,p), 6-31+G(d), 6-31++G(d,p), (B3LYP only) 6-311++G(d,p)	Catechol (**8**) & parent semi-quinone radical (**9**) isomers	Assessed the effect of different levels of Pople's basis sets on the BDE values.	222
Semi-empirical modified neglect differential overlap (MNDO), AM1, RM1, PM3 and PM6.	Quercetin (**5**) & myricetin (**10**).	Calculated the H-abstraction from various hydroxyl sites of both flavonoids.	223
PM6 method and DFT functional M05-2X	Morin (**11**)	Investigated the conformational space of morin as a function of the torsion angle between the B and C rings.	48
(a) MP2 and B3LYP, Basis sets: 6-31G(d), 6-31+G(d), 6-31G(d,p), 6-31+G(d,p), 6-311G(d,p), 6-311+G(d,p), 6-311++G(d,p) & aug-cc-pVTZ	Trans-resveratrol (**12**) and trans-piceatannol (**13**)	(a) Geometry analyses. (b) To examine the dependence of stacking interactions amid two planar trans-resveratrol compounds on optimised vertical distance values.	220

(b) MP2, B3LYP and HF; aug-cc-pVTZ		between the molecules.	
MP2, MP3, MP4 and B3LYP	37 ortho-, para- and meta-substituted phenols	Evaluated the suitability of the different methods in representing variations in BDE and IPs as a result of substituent changes.	[203]
ONIOM approach: (RO)B3LYP/6-311++G(2df,2p) with the PM6 method	Different conformations of curcumin (**14**) and epicatechin (EC) (**15**), epigallocatechin (EGC) (**16**), epicatechin gallate (ECG) (**17**) and epigallocatechin gallate (EGCG) (**18**)	Calculated the BDEs of large polyphenols.	[224]

Justino and Vieira (2010) carried out five types of semi-empirical molecular orbital calculations using the following Hamiltonians; modified neglect differential overlap (MNDO), AM1, Recife model 1 (RM1), parameterized model 3 (PM3) and parameterized model 6 (PM6), in both the gas phase and water phase, to compare these methods in their evaluation of the antioxidant mechanisms of the flavonoids myricetin (**10**) and quercetin (**5**).[223] The methods were consistent in leading to the 4′-site as being the most acidic hydroxyl group in both the gas phase and water phase, and that in the gas phase the hydrogen atom at this site is more easily removed from quercetin. However, in the water phase, all approaches, with the exception of the AM1 method, indicate that the removal of the hydrogens at the 3'-OH and 4'-OH sites require less energy than for the other hydroxyl sites. In relation to myricetin, although it was anticipated that the 4'-OH site would be the easiest hydrogen abstraction site, the MNDO, AM1 and RM1 methods indicated that the 3-OH site would be where the hydrogen would be removed. From these outcomes, the PM6 method, and to a lesser extent the PM3 method, were considered to be most in agreement with the previous literature in the description of the acidic OH groups in these flavonoids. The paper also compared the PM6 method to previously calculated BDEs and PAs of myricetin using DFT at different basis set levels (B3LYP/6-311++G(d,p), B3LYP/6-31G(d), B3LYP/6-311G(2d,p)). When compared to the DFT methods, the semi-empirical methods are inclined to over-estimate the energetics of the flavonoid anions and under-estimate the energetics of the radicals, suggesting that in general the PM6 method may only be suitable for semi-quantitative analysis of flavonoid structures.

Marković *et al.* (2012) also compared a semi-empirical PM6 method to a DFT functional, M05-2X, for the assessment of free radical scavenging activity of morin (**11**).[48] M05-2X is a recently-developed hybrid meta exchange-correlation functional and it claims to yield generally good performance for the main-group thermochemistry and thermochemical kinetics, and organic and non-covalent interactions.[225] In order to establish the preferred positions of the B- and C-rings relative to each other, an investigation into the conformational space of morin, as a function of the torsion angle, between the rings was carried out. Both the M05-2X DFT functional with 6-311++G(d,p) basis set and the PM6 method gave the stable

conformation as being non-planar. Although, after the removal of the torsion angle constraint, the PM6 method gives smaller values for the dihedral angle, the local minimum and inter-conversion barrier than those calculated for the DFT method. Following the calculation of PA values in gas-phase and solvent of all present OH groups, DFT suggested that proton transfer from the 3-OH group was more likely, as opposed to the other four possible OH sites, as found previously.[226-227] However, the PM6 result differed in that it found the 7-OH group to be more reactive in gas-phase and benzene, and that these differences may be due to the inability of this method to sufficiently describe ions. Nonetheless, where DMSO or water were employed, both M05-2X and PM6 were considered to be useful for the study of free radical scavenging reactions. [48] This outcome supports an earlier study that also found that DFT results can be well reproduced by the semi-empirical PM6 method.[228]

Geometry analyses of the stilbenes *trans*-resveratrol (**12**) and *trans*-piceatannol (**13**) were recently carried out using MP2 and B3LYP methods.[220] using the following basis sets; 6-31G(d), 6-31+G(d), 6-31G(d,p), 6-31+G(d,p), 6-311G(d,p), 6-311+G(d,p) and 6-311++G(d,p). MP2 calculations using these basis sets suggested that the geometries of *trans*-resveratrol and *trans*-piceatannol are not planar structures; in contrast the DFT calculations of *trans*-piceatannol implied that these structure types are planar. Furthermore, both methods were also performed using the more computationally expensive Dunning's correlation consistent polarized valence triple zeta basis set (aug-cc-pVTZ) and, in this case, both the MP2 calculations for *trans*-resveratrol and *trans*-piceatannol and the DFT calculation for *trans*-piceatannol indicated that these structures are in fact planar. Therefore, the use of B3LYP in conjunction with Pople's basis sets for the geometry analysis of the flavonoids was validated. The dependence of the stacking interactions between two planar *trans*-resveratrol compounds on optimised vertical distance values between the molecules was also examined at the MP2 (full)/aug-cc-pVTZ, B3LYP/aug-cc-pVTZ and HF/aug-cc-pVTZ levels. It was observed from the MP2 curve that the minimum occurs at a distance that is in good agreement with the crystal structure; however, the B3LYP and HF curves deviate largely from the MP2. This is explained by the fact that the interaction energy in the long-range interaction region and repulsive effects at short-range are described accurately by the MP2 curve, whereas the B3LYP and HF

methods neglect long-range attractive dispersion interactions. Long-range-corrected (LC) DFT methods developed to deal with this issue are discussed below.

Klein *et al.* (2006) assessed the accuracy of various *ab initio* methods (MP2, MP3 and MP4), and B3LYP method for the calculation of the BDEs and IPs of 37 *ortho*-, *para*- and *meta*-substituted phenols. The suitability of the different methods in representing variations in BDE and IPs as a result of substituent changes are evaluated by comparing data to experimental values. Initially, various basis sets; namely 6-31G(d), 6-311G(d,p), 6-311++G(d,p), 6-311++G(2d,2p) and 6-311++G(3df,3pd), were assessed for the determination of phenol BDE and IP in conjunction with the B3LYP, MP(*n*), CCSD(T) and HF methods. In all cases, as a higher order of basis set is employed, the BDE value for phenol also rises. The MP(*n*) BDEs were found to oscillate, where MP2 and MP3 represented the upper and lower limits for the BDEs, respectively, with the MP4 BDEs in-between. Experimental BDEs of the substituted phenol were obtained using four different methods; an electrochemical method (EC), a thermodynamic cycle method (TDC), pulse radiolysis (PR) and a parabolic model (PM). The MP2 method was found to overestimate BDEs for strong electron-donating groups, although the experimental data of EC and TDC were correlated to MP2 for electron-withdrawing groups. On the other hand, MP3 significantly underestimated BDEs for electron-withdrawing groups. When the B3LYP results were compared to EC experimental data they were found to be consistent; and the average deviation of B3LYP BDEs from EC and TDC data were deemed comparable to the standard deviation of the experimental values. Further investigation of the Hammett constants for substituent in *meta*- and *para*-positions resulting from the different methods found that MP2 was unable to differentiate between effects caused by groups at either position. Overall, B3LYP seemed to be more reliable for the calculation of the phenols BDEs compared to the MP(*n*) methods, and it is also the more favourable option as it requires less computational resources. In terms of calculating the IPs, the HF method correlated well with the experimental values, while B3LYP was found to underestimate them. However, after the addition of an empirical correction to the B3LYP calculated IPs, the deviation from the experimental values dropped considerably. The study concluded that phenol substitution in the *para*-position results in more effective antioxidant potentials, compared to the *meta*-position.[203]

As the overview of QM techniques above indicates, many of studies involving polyphenols focus on method comparisons for terrestrially-sourced molecules; however, there is also a need to assess the electronic structure of marine-origin polyphenols, which have displayed antioxidant activity, and for which such studies are lacking.[110] The evidence suggests that the DFT method B3LYP appears to be a reliable option for flavonoids and stilbenes and, therefore, it potentially would be the most suitable option for investigating marine polyphenols. However, it has been suggested that self-interaction error (SIE) is a problem in many traditionally used DFT methods and, therefore, long-range corrected (LC) functionals have been introduced in an attempt to partially remove the self-interaction errors by incorporating a long-range Hartree-Fock exchange.[229] One such LC functional, CAM-B3LYP, combines the hybrid qualities of B3LYP and the long-range correction presented by Tawada and colleagues.[230] The CAM-B3LYP functional comprises of 19 % HF plus 81 % Becke 1988 (B88) exchange interaction at short-range, and 65 % HF plus 35 % B88 at long-range.[231] Another recently introduced LC hybrid density functional ωB97XD includes empirical atom–atom dispersion corrections.[232] When compared to existing dispersion-corrected DFT functionals (B97-D, B3LYP-D and BLYP-D[233]) and previous LC hybrid functionals (ωB97X and ωB97) for calculations on a set of data including atomization energies, reaction energies, non-covalent interaction energies, equilibrium geometries, and a charge-transfer excited state, ωB97XD was on the whole better in overall performance, however, this functional does have the drawback of suffering from some self-interaction error at short-range.[229]

Another important consideration is that some marine polyphenols, such as phlorotannins, exist naturally as oligomers and polymers. In such cases traditional DFT methods may not have the resources to deal with such a large system. Wright *et al.* (2001) introduced a local dense basis set (LDBS) partitioning system, based on DFT, to enable the BDEs of larger phenolic antioxidants to be accurately determined.[234] With the LDBS procedure the molecule is partitioned according to pre-defined criteria.[235] For example, in the case of the B3LYP/LDBS procedure being applied to p-aminophenol single point calculations, the region where the O-H bond breakage occurs is considered primary and, therefore, is assigned the large 6-311+G(2d,2p) basis set.[234] The benzene ring, and the attached hydrogen atoms, is

considered secondary as it is directly conjugated to the primary region. The secondary region is assigned the intermediate 6-311+G(d) basis set, where the number of polarization functions on each carbon is reduced to a single d-function. The amino group, or in other cases the substituent group, is considered to be tertiary and assigned the small 6-31G(d) basis set. The same procedure is adhered to for the corresponding radical, i.e. oxygen is primary, benzene is secondary and substituent group is tertiary. Exceptions to this LDBS partitioning scheme exists when there are several OH groups that are hydrogen bonded. In these cases, it has been advised that OH groups adjacent to the OH group of interest should be considered primary.[234] The B3LYP/LDBS procedure was compared to the use of a traditional full basis set B3LYP method, where the 6-311+G(2d,2p) basis set was applied to the whole molecule, for a number of mono-substituted phenols. The LDBS method agreed well with the full-basis method and also, for the most part, with accurate experimental data.[234] The LDBS procedure was also demonstrated with a number of commercial antioxidants. The advantage of the LDBS procedure is evident when the calculation of the BDE for large polyphenols, such as EGCG (**18**), is made possible. The tri-hydroxy region of EGCG was deemed primary, the attached benzene secondary, and the remainder of the molecule tertiary. Wright *et al.* (2001) showed that EGCG was a better antioxidant compared to other tea catechins, but indicated that the number of OH groups in EGCG (**18**) is largely irrelevant, and that it is the location of these groups that dictates antioxidant activity.[234] Wright (2002) also used the LDBS process to obtain BDE data of various forms of curcumin (**14**), and concluded that the phenolic OH bond was the weakest in all the curcumin structures and, therefore, was the region responsible for their antioxidant activity.[236] Overall, the B3LYP/LDBS partitioning system has shown to be comparable to traditional full basis set B3LYP for the calculation of phenol BDEs with the added advantage of requiring less computational resource.

Alternatively, the use of ONIOM methods, which can involve DFT in conjunction with either ab initio[237] or semi-empirical methods[224] may be employed to overcome the issue of dealing with larger polyphenolic systems, while retaining the accuracy for the site of interest. The use of systematic ONIOM methods allows the chemically important region to be treated with an accurate high level QM method and the rest is treated with computationally less exhaustive lower level methods.[238] Nam

et al. (2013) amalgamated a (RO)B3LYP/6-311++G(2df,2p) method with the PM6 method, resulting in an ONIOM procedure that was found to produce reasonably accurate BDE(O–H)s of substituted phenolic compounds with less consumption of computer time. This method was then used to calculate the O-H BDEs of curcumin (**14**) conformations and four catechin derivatives (**15-18**) flavonoids.

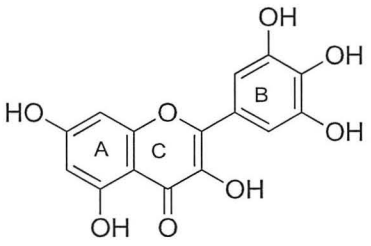

10

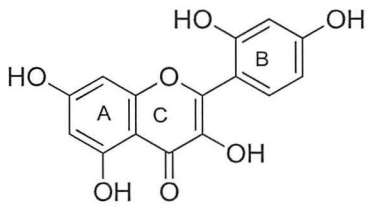

11

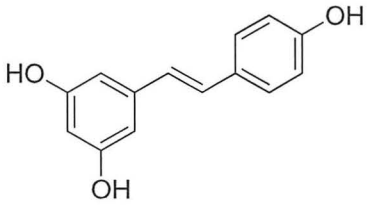

12

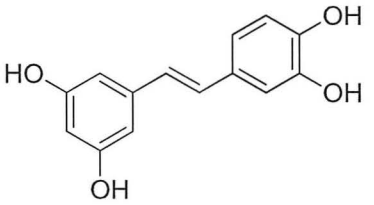

13

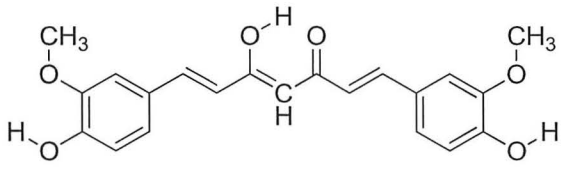

14

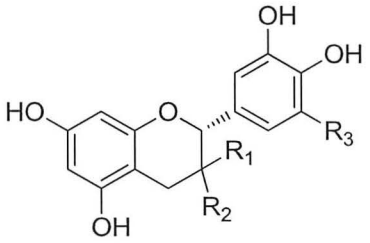

15 R1=OH, R2=H, R3=H

16 R1=OH, R2=H, R3=OH

17 R1=H, R2=OH, R3=H

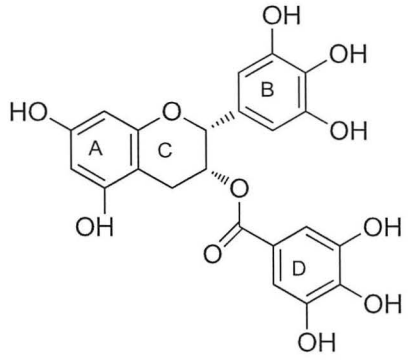

18

Figure 2: Polyphenol structures, myricetin (**10**), morin (**11**), trans-resveratrol (**12**), trans-piceatannol (**13**), curcumin (**14**), epicatechin (**15**), epigallocatechin (**16**), epicatechin gallate (**17**) and epigallocatechin gallate (**18**), investigated in QM and/or MD studies.

1.9 Molecular dynamics (MD) simulations of polyphenols with proteins

Molecular dynamics (MD) simulations employ approximations based on Newton's laws of motion in order to simulate the movements of atoms in complex molecular systems. Simulations cover wide spatial and temporal ranges, and can involve thousands to millions of individual atoms.[239] The availability of molecular dynamics has largely reduced the amount of time and expense involved in describing the movements and chemical interactions of molecular systems by offering an alternative to the traditional crystallographic studies used for this purpose.[240] As a result, MD studies have become very valuable in observing how complex systems operate; but there are still particular areas that require improvement, such as the conformational sampling methods and suitability of force-fields.[240] Despite these pitfalls, it has been anticipated that the increased use of MD in drug discovery, through the facilitation of improved drug design, will greatly lower the cost and resources involved in the lead optimisation stages.[239] The interaction of polyphenols with proteins/peptides is pertinent to various areas of research such as chemistry, food science, and nutraceuticals. Many in vitro and in vivo experimental studies have indicated that polyphenols are highly bioactive compounds as a result of interactions with either proteins/peptides or nucleic acids. However, in order to facilitate the application of polyphenols at the therapeutic level an understanding of the location of specific biological targets, the polyphenol binding site and type of binding interfaces is required.[239] This information is not easily obtained by experiment alone and with the improved speed and access to high performance computing (HPC) resources, CAMM methods, such as molecular dynamics and molecular mechanics, can be used to make such knowledge more accessible. A summary of some of these methods used to model polyphenolic compounds are provided in table 2.

1.9.1 Molecular Mechanics

Molecular mechanics (MM) can be applied alone to carry out conformational analysis or as part of a more comprehensive MD simulation study for the molecule(s) of interest. The principle behind molecular mechanics is the expression of molecular energy as a function of its resistance toward bond stretching, bond bending, and atom

crowding. This energy equation is then employed to find bond lengths, angles, and dihedrals that equate to the various possible potential energy surface minima. The form of a mathematical expression for the energy, and the parameters in it define a force-field, and MM methods are sometimes called force-field methods.[208] Conformational analysis using MM of the ellagitannin diastereosiomers vescalagin (**19**) and castalagin (**20**) has been carried out to investigate the nature of their experimental physicochemical differences despite their small structural variances.[239] In this MM study, modified MM2* or MM3* force-fields were employed to locate the conformational minima of the phenolic compounds. MM2* and MM3* differ from their parent force-fields, MM2 and MM3, by using distance-dependent dielectric electrostatics instead of the standard dipole-dipole electrostatics, and, as a result, employ the point-charge Coulomb potential to describe the electronic electrostatic interactions.[240] They include partial charge electrostatics and explicit parameterisation of conjugated systems.[241] These force-fields have been found to perform well for the optimisation of stacked complexes, which commonly occur with polyphenols.[241] Each conformer was fully minimised with the MM3* force-field. The Monte Carlo method employed resulted in 19 and 15 conformers for vescalagin and castalagin, respectively, and a cluster analysis on these structures was performed. A critical distance-clustering method was employed to classify the conformers into groups based on the conformational space available. The two cluster groups found for vescalagin and castalagin were almost identical and corresponded to two conformations of a hexahydroxytriphenic entity. The conformational analysis established that vescalagin was more hydrophilic and more reactive to electrophilic reagents compared to castalagin, which supported the experimental findings that vescalagin was indeed more polar, oxidizable and thermally labile. This study successfully demonstrated how theory and experiments can be employed in order to find correlations between the physicochemical and conformational aspects of polyphenols.

1.9.2 Molecular dynamics force-fields

As the bioactive basis of many naturally-occurring polyphenols is as a result of interaction with endogenous and exogenous proteins/peptides, it is necessary that during MD studies the atomic forces of both are properly described. Force-fields are a

set of parameters representing bonded and non-bonded inter-atomic forces and they are applied in MD to calculate the forces on each atom of a molecular system, therefore allowing the atomic position and velocity to be renewed at each simulation time-step.[242] On the whole, force-fields have been created with the intention that they would be used with macromolecules such as proteins and, therefore, it is necessary that force-fields that translate well for use with smaller molecules are used to study polyphenols and peptides. The General Amber Force-Field (GAFF) force-field has been extensively used on polyphenols to assess their interactions with protein/peptides. This force-field contains parameters for most organic and pharmaceutical molecules that consist of H, C, N, O, S, P, and halogens, and it incorporates both empirical and heuristic models to estimate force constants and partial atomic charges.[243] London dispersion forces or van der Waals terms between hydrogen atoms have shown to be significant in protein-polyphenol interactions and must be described accurately. In the majority of the following MD studies discussed, the electrostatic interactions are described using the Particle Mesh Ewald (PME) method, which calculates direct-space interactions within a finite distance using a modification of Coulomb's Law.[244]

Table 2: Summary of selected molecular mechanics and molecular dynamics methods used for modelling polyphenolic structures

MM/MD Method(s)	Polyphenols	Description	Ref
MM2* or MM3* force-fields Monte Carlo method	Vescalagin (**19**) and castalagin (**20**)	Conformational analysis to investigate the nature ofexperimental physicochemical differences despite their small structural variances.	239
Force-field parameters for polyphenol were generated using the GAFF force-field GNNQQNY modelled using all-atom Amber force-field Amber 99SB force-field and igb5 implicit solvent model used for MD	Myricetin (**10**)	To investigate the disaggregation effect of the flavonoid on GNNQQNY oligomers, which have the ability to form amyloid fibrils, using MD.	245
Force-field parameters for polyphenol were generated using the GAFF force-field. AMBER 1999 force-field (parm99) was used for modelling the protein Cornell force-field and TIP3P explicit solvent model used for MD	Dimer (**21**), trimer (**22**) and tetramer procyanidin (**23**)	To investigate the inhibition caused by dietary tannins on porcine pancreatic elastase (PPE) digestive activity and their potential to be used as a target for obesity control.	246
The non-bonded and internal parameters of the polyphenol were simulated using the GAFF force-field Amber ff99SB force field parameters were used	Quercetin (**5**)	To gain information on the molecular mechanisms involved in inhibition effect of quercetin on matrix metalloproteinase 9 activity, a potential target for flavonoid cardio-protective activity.	247

GROMOS96 53A6 and GROMOS 53A6OXY force-field parameter sets were for EGCG Simulation was carried out with the GROMOS96 53A6 force-field single point charge (SPC) water model	(−)-Epigallocatechin-3-gallate (EGCG) (**19**)	To investigate the inhibition effect of EGCG on the conformational transition of the amyloid β-peptide42 (Aβ42).	248
The polyphenol was parameterized using the Dundee PRODRG2 server GROMOS96 force field (G43a1) and SPC water model were used for MD simulation	Procyanidin dimer B3 (catechin-(4β→8)-catechin) (**24**)	To study the effect and level of binding of a procyanidin dimer B3 with porcine protease trypsin as reduced trypsin activity is considered harmful due to its ability to reduce absorption of nutrients in the body.	249
Atomic partial charges of polyphenol were derived using the R.E.D. III package. Other bonded and non-bonded parameters were taken from the OPLS-all-atom force-field OPLS-AA force-field used for temperature swapping REMD simulation solvated with SPC water model	Resveratrol (**11**)	An extensive REMD simulation was carried out to study the early aggregation of a human islet amyloid polypeptide segment in the presence and absence of the polyphenolic inhibitor.	250
QM/MM hybrid modeling method employing M06-2X/6-31+G* for the polyphenol and a couple of protein side-chains, and OPLS-AA for main protein structure	Quercetagetin (**25**)	To model and predict the π-stacking interactions between the flavonoid and glycogen phosphorylase, a target to control hyperglycemia in type 2 diabetes, using QM/MM-PBSA.	251

Berhanu and Masunov[245] investigated the disaggregation effect of the flavonoid myricetin (**10**) on oligomers of the peptide GNNQQNY using MD. These oligomers have the capability to form amyloid fibrils, which have been connected with many fatal diseases, including Alzheimer's disease. Initially, various implicit solvent models (igb1, igb2, igb5, igb7) along with different Amber force-fields (ff96, ff99, ff99SB, ff03) were screened for their ability to keep a decamer of GNNQQNY aggregated, and the combination of the 99SB force-field and the igb5 solvent model was chosen. There is a disadvantage of implicit solvent models in that they do not use periodic boundary conditions and, therefore, the potential for a large separation to occur between the ligand and protein is greater than in explicit solvent systems. As such, in this study a harmonic constant was applied to prevent the sampling of a large area that doesn't represent any significant interaction between the polyphenol and aggregate.[245] Before carrying out MD simulations, the force-field parameters for myricetin were generated using the GAFF force-field.[243] In order to validate the force-field parameters of myricetin, a 2 ns simulation with the implicit solvent was performed. The bond lengths and bond angles were well maintained in the MD simulations in agreement with the HF/6-31G(d) structure.[245] The structure of GNNQQNY consisted of two beta-sheets stabilised by hydrogen bonds between polar side chains and was modelled using the all-atom amber force-field. The simulation was performed using generalised Born approximation at constant temperature (300 K) using the Langevin system. The simulations were run for 10 ns and, in the presence of myricetin, disaggregation of the decamer was observed within the first 1 ns, while in it absence disaggregation occurred after 5 ns. When the polyphenol is present within the first ns total dissociation of one of the beta-sheets, increased curvature of the beta-sheet and increased separation of the beta-sheets are observed. After analysis of hydrogen-bonding it was found that the number of hydrogen bonds between the beta sheets is greater than in the presence of the polyphenol. This occurs as a result of myricetin forming hydrogen bonds with both the peptide backbone NH group and side chain NH groups, therefore weakening the backbone to backbone bonds between the two strands of the beta sheet that it is closest to. In addition, side-chain to side-chain hydrogen bonding is also diminished. Both of these situations have been observed previously.[252] Finally, it was observed that the reduction of intermolecular van der Waals interactions contributes to the destabilisation effect of the bilayer.[245]

The elastase inhibition caused by dietary tannins on digestive enzymes' activity has been theoretically investigated.[246] Bras and colleagues studied the interactions between dimer (**21**), trimer (**22**) and tetramer procyanidin (**23**) structures and porcine pancreatic elastase (PPE) using MD simulations. MD simulations were performed with the accepted parameterisation using the AMBER 1999 force-field (parm99) for the protein and the GAFF for the polyphenols.[246] An explicit TIP3P solvent model was employed and 5 ns time-step MD simulations were carried out on optimised structures in the isothermal-isobaric normal pressure temperature (NPT) ensemble with periodic boundary conditions using the Cornell force-field.[253] The binding free energies of all complexes were calculated using Molecular Mechanics-Poisson–Boltzmann Surface Area (MM-PBSA). MM-PBSA is a post-processing, end-state method used to calculate free energies of molecules in solution.[254] It was found that the procyanidin tetramer structure had the highest affinity for PPE, as it had created more contact points with more of the amino acids present at the active site. This finding is in line with what has been observed experimentally, where a lower binding affinity of the lower polymerised trimer was found. The interaction was predominantly directed by short hydrogen bonds and van der Waals interactions between the tetramer and the side chains of the active site residues.[246] The inhibition of elastase is thought to contribute to the reduction of protein proteolysis and, therefore, this study indicates that certain procyanidins may be used as a target for obesity control in the future.

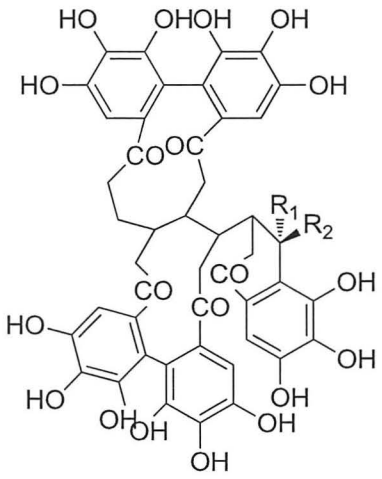

19 R_1=H R_2=OH

20 R_1=OH R_2=H

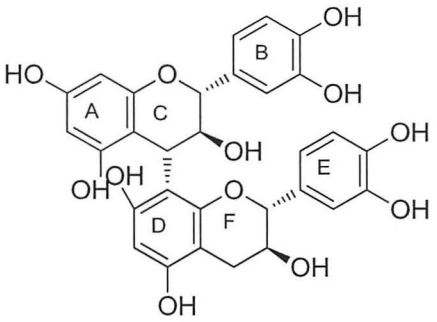

21

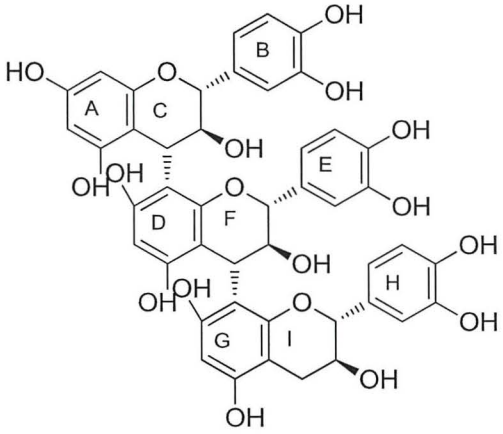

22

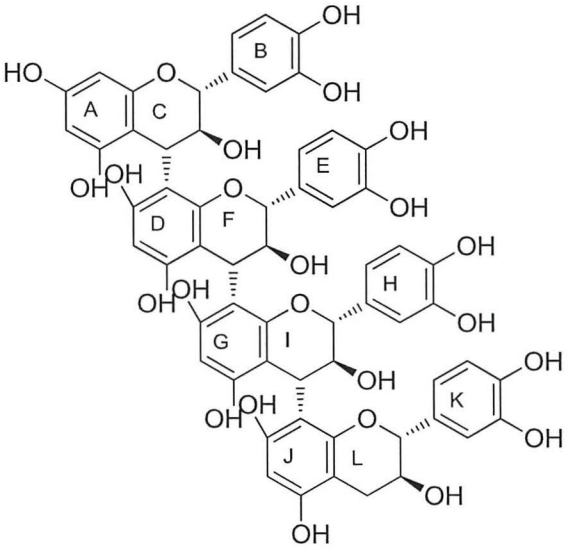

23

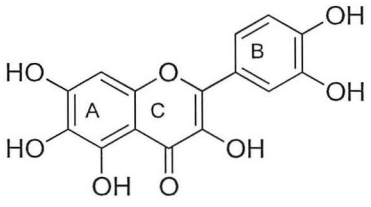

24

Figure 3: Polyphenol structures; vescalagin (**19**); castalagin (**20**); dimer (**21**), trimer (**22**) and tetramer (**23**) of procyanidin; procyanidin (**24**), investigated in MM and/or MD studies.

MD simulations have been carried out to gain information on the molecular mechanisms involved in inhibition effect of quercetin (**5**) on matrix metalloproteinase 9 (MMP-9) activity, a potential target for flavonoid cardio-protective activity.[247] The starting structures, corresponding to free MMP-9 or flavonoid–MMP-9 complexes were obtained from a previous docking simulation and were added to a TIP3P explicit solvent model. The Berendsen barostat and thermostat were used with periodic boundary conditions. Long-range electrostatic interactions with a 10 Å cut-off were treated with Ewald summation. The Amber ff99SB force-field parameters were used for all protein residues, and for quercetin the non-bonded and internal parameters were simulated using the GAFF force-field.[255] As in the previous study, 5 ns time-step simulations were carried out and MM-PBSA was used to calculate the binding free energies. From the simulation the two most favourable binding modes of quercetin with the MMP-9 catalytic domain were obtained, i.e. those that were at least two-fold smaller than the other possible interaction modes. In both of the complexes identified, quercetin was observed to interact in the same sub-site (S1') of the MMP-9 active site. This outcome is in agreement with previous reports that found synthetic MMP inhibitors bind to the same sub-site and, subsequently, this site has been deemed to be the most significant in terms of substrate and inhibitor specificity.[256] The main differences between the two quercetin complexes were their energy values corresponding to the energy contributions of the electrostatic and van der Waals interactions. In both complexes, the hydroxyl groups of quercetin involved in the hydrogen bond interaction with the MMP-9 catalytic domain were $R^{3'}$-OH and $R^{4'}$-OH of the B-ring. However, the chromone ring hydroxyl group involved in the hydrogen bond interactions was R^{5}-OH in one complex and R^{3}-OH in the other. Generally, the study showed how the number and localization of hydroxyl substitutions in quercetin influence its interaction with the MMP-9 catalytic domain.

GROMOS force-fields are also applied quite often in MD studies of polyphenols and proteins, and offer an advantage over some other methods in that they are based on the united-atom approach to parameterisation.[248, 257] As a result, non-polar hydrogen atoms are not explicitly represented and this considerably speeds up simulations.[258] The molecular mechanism of the (−)-epigallocatechin-3-gallate (EGCG) (**18**) inhibition effect on the conformational transition of the amyloid β-

peptide$_{42}$ ($A\beta_{42}$) has been studied.[248] The GROMOS96 53A6 force-field parameter set was used to assign the atomic charges and charge groups of EGCG.[259] Charges of aromatic hydroxyl groups were assigned based on the tyrosine phenol group in the same force-field. The charges of ether and ester groups, which do not exist in the force-field, were taken from the GROMOS 53A6OXY force-field parameter set. This recently developed parameter set combines reoptimized parameters for oxygen-containing chemical functions (alcohols, ethers, aldehydes, ketones, carboxylic acids, and esters) with the current biomolecular force-field version (53A6) for all other functional groups.[260] Prior to the MD simulation, EGCG molecules were located and oriented randomly around the $A\beta_{42}$ peptide in a cubic box with periodic boundary conditions. The simulation was carried out with the GROMOS96 53A6 force-field with 2 fs time-steps and the single point charge (SPC) water model. The temperature (300 or 330 K) and pressure (1 atm) of the simulation were controlled by the Nosé–Hoover thermostat and Parrinello–Rahman barostat, respectively. Three MD simulations of 300 ns were conducted for each system under different initial conditions by assigning different initial velocities on each atom of the simulation systems. Binding free energies were calculated again using MM-PBSA.[248] Entropy contributions occurring from changes in the degrees of freedom of the peptide were not included in the free energy calculation due to its high computational demand. A time evolution of the secondary structure of $A\beta_{42}$ at different EGCG concentrations was carried out, and showed that EGCG inhibition of the peptide conformational transition was did not occur in 0.04 mol L^{-1} of the polyphenol solution, but did at 0.08 mol L^{-1}, with the initial α-helical structure still well preserved after the entire 300 ns simulation. It was found that both nonpolar and polar interactions are favourable for the binding of EGCG, but that the majority were due to non-polar interactions described by the van der Waals term. The nonpolar energies mainly originated from the side-chains of the residues and the main chains of some non-hydrophobic residues. Overall, EGCG was found to prevent the formation of peptide β-sheet structure and, therefore, it was suggested that it may be an effective agent to prevent the onset of Alzheimer's disease.

The effect and level of binding of a procyanidin dimer B3 (catechin-(4β→8)-catechin) (**24**) with porcine protease trypsin, a serine protease, was studied using the

GROMOS96 force-field (G43a1).[249] Reduced trypsin activity is considered harmful because it can contribute to a reduced absorption of nutrients in the body. The procyanidin molecule was parameterized using the Dundee PRODRG2 server web site version 2.5 (beta) (http://davapc1.bioch.dundee.ac.uk/prodrg/). It should be noted that this server has come under some scrutiny with regards its inconsistencies; in particular it has been found that the server does not reproduce topologies for many well-characterized species in the GROMOS force field due to conflicting charges and charge groups and potential alternative have been developed.[258, 261] The 2 ns time-step MD runs were performed in a SPC water model at constant temperature (300 K) and pressure (P = 1 bar) with a Berendsen coupling. Nine different simulations were run with six below the tannin–critical micellar concentration (CMC), in order to mimic a low-concentration of B3 and avoid any auto-association, and three around or above the tannin–CMC. In the runs carried out below the tannin-CMC of B3, the molecule interacts with trypsin as a free molecule, displaying specificity. The observed interactions were attributed to hydrogen bonds between the polyphenolic hydroxyl groups and the amide and carbonyl group of the protein backbone. However, in the more concentrated cases, self-aggregation of tannins was observed before any tannin–trypsin interaction, so that interacting entities are no longer unique procyanidin B3 molecules. This study concluded that the level of binding between procyanidin B3 and porcine protease is largely dependent on the concentration of procyanidin involved, which is a similar outcome to previous experimental work.[262]

The optimized potential for liquid simulations (OPLS) force-field has also recently emerged as a viable option for the parameterisation of polyphenols and carrying out MD simulations involving phenolic interactions with proteins[263] and other biomolecules.[264-265] The parameters for both torsional and non-bonded energetics of this force-field have been derived, while the bond stretching and angle bending parameters have been adopted predominantly from the AMBER all-atom force-field.[266] An extensive replica-exchange molecular dynamics (REMD) simulation has been carried out to study the early aggregation of a human islet amyloid polypeptide segment in the presence and absence of the polyphenolic inhibitor resveratrol (**11**).[250] As was discussed earlier, the formation of such amyloid fibrils plays a significant role in the development of Alzeihemers. The geometry

optimization of resveratrol was initially carried out at the HF/6-31G(d) level and the atomic partial charges were derived using the R.E.D. III package.[267] Other bonded and non-bonded parameters of resveratrol were taken from the OPLS all-atom (OPLS-AA) force-field. A section of an amyloid polypeptide was employed for the simulation. The initial conformation for the simulations consisted of a parallel β-sheet, consisting of four strands (preformed β-peptides) centered in a dodecahedron box, surrounded by three monomers (added peptide monomers). A temperature-swapping REMD simulation system was performed with the OPLS-AA force-field with 32 replicas. REMD is used to improve sampling relative to the standard MD studies by allowing systems of similar potential energies to sample conformations at different temperatures, therefore increasing the probability that the barriers on the potential energy surface (PES) will be overcome, and allowing for the exploration of new conformational space.[244] The inhibitory mechanism was studied by adding twelve resveratrol molecules randomly to the system. The peptide/polyphenol mixture was solvated with SPC water. The binding free energies of resveratrol on peptide segments were calculated using the molecular mechanics generalized Born/surface area (MM-GBSA) method. The formation of the β-secondary structure in the absence and presence of the polyphenol was observed in order to monitor the possible assembly of peptide segments. It appeared that in the presence of resveratrol the preformed β-structure was preserved, but prevented the added peptide monomers from forming new β-structure with the present preformed β-structure. Following this finding, possible different inhibitory effects of resveratrol on the preformed β-structure and added peptide monomers were further analysed. A significant aspect of this inhibition was that the ordered hydrophobic matching patterns demonstrated in the double-layered oligomer species were greatly reduced in the presence of the polyphenol. Previous experiments have found that the characteristic fibrils do not form when the full-length amyloid poly-peptide is in the presence of resveratrol.[268] Therefore, if resveratrol acts on the full-length poly-peptide with the same mechanism as was observed in the MD study, resveratrol may be used as an inhibitor of amyloid fibril formations.

Many polyphenolic bioactivities are thought to be governed by non-covalent cation-π and π-π stacking interactions with aromatic amino acids within proteins.[269-

[270] However, it has been suggested that the shortcomings of some currently used molecular mechanics force-fields may not allow for accurate descriptions of such unique interactions to be achieved and that the use of more complex and realistic "Class 3" force-fields, as MM4, may be more suitable for this purpose for future studies.[242]

1.9.3 Quantum mechanics in molecular dynamics

As seen earlier, MM force-fields, often in conjunction with continuum models such as PBSA and GBSA, are also widely employed for determining binding free energies of small ligands. However, it has been observed that there may be an inadequacy of MM to allow for charge variations in-line with environmental changes, such that these methods do not allow for reliable quantitative comparison with environmental data.[271] For this reason, and with increasing availability of computational resources, a trend toward the use of QM, which provides molecular descriptors of electrostatic potential; local hardness and softness; frontier orbital analysis; and density of states, in conjunction with MM force-fields for calculating binding free energies has emerged. Hybrid methods such as QM/MM allow MM force-fields to be applied to the receptor/protein molecule, while QM potentials are used for the ligand/core molecules.[272] Of late, the increased use of accurate DFT for this purpose means QM can be quite time-consuming and, therefore, to further improve these methods QM/MM-PBSA methods have been introduced.[273] It has been recently demonstrated that a QM/MM-PBSA method employing M06-2X/6-31+G* to model the π-stacking interactions between the flavonoid quercetagetin (**24**) and glycogen phosphorylase correctly reproduced related experimental results.[251]

1.10 Rationale and Objectives

Paper I explored the potential use of macroalgal species, and their secondary metabolites, as bioactive ingredients that could be incorporated into functional foods for use in the prevention and/or treatment of hypertension and oxidative stress-related diseases. An extended literature review in this area revealed that while research into phlorotannins and macroalgal peptides is widespread, the level of knowledge in relation to these components in Irish species is limited. Furthermore, from the literature view it is clear that there is the opportunity to combine information gathered

from experimental bioactivity studies involving marine components with computational chemistry data to gain more information surrounding the molecular descriptors involved in a components bioactivity. On this basis, an aim of this thesis was to firstly assess potential methods that could be employed to efficiently and safely extract macroalgal phlorotannins from macroalgal biomass. Furthermore, as it is well understood that co-extractants may interfere with the bioactivity of plant polyphenols, it was envisaged that steps to remove these from the extracts and, therefore, enrich the phlorotannin content would have to be taken. The emergence of new EU regulations for functional foods highlights the need for procedures that can ensure the standardisation of extracts and naturally-sourced ingredients from various plant sources can be monitored. Therefore, it was the intention of this work to develop an efficient analytical method for the profiling of polymerised phlorotannins (DP $\leq$ 16 monomers) in brown macroalgal species, as studies in this area to date have largely concentrated only in the profiling of dimers, trimers and oligomers (up to 10 monomers). Most studies investigating the isolation of bioactive peptides from macroalgae have focused on the red species, thus one of the aims of this thesis was to investigate the presence of peptides in a brown macroalgal species and determine their potential bioactivity. As discussed earlier, computational chemistry tools may act as support to natural products experiment through the provision of data on the molecular properties of individual components, and also on potential binding interactions between mixtures of bioactive components. Density functional theory (DFT) was employed to theoretically determine the radical scavenging potential of various 7-phloroeckol conformers through the calculation of their O-H bond dissociation enthalpies. Furthermore, a molecular dynamics simulation approach was proposed for investigating of binding interactions between a selected macroalgal phlorotannin and a bioactive peptide from *A. nodosum*.

2. Chapter 2 – Extraction of macroalgal antioxidants and enrichment of brown algal polyphenols

2.1 Summary

This chapter is based on the works published in Papers II, III and IV. The potential uptake of macroalgal extracts for use as polyphenol blends by functional food and cosmeceutical industries is dependent on many factors. The type of extraction method and solvents used, along with the amount of time and capital cost involved are all variables that affect the quality, safety, effectiveness and value of an extract. Therefore, much consideration needs to be given to these areas to optimise the production of bioactive extracts. There are a multitude of extraction techniques available, each providing their own benefits, for the extraction of bioactive compounds from macroalgae, such as soxhlet extraction, supercritical fluid extraction, microwave-assisted extraction, ultra-sound assisted extraction, pressurised-liquid extraction, enzyme-assisted extraction and solid-liquid extraction.[274-276]

Papers II and III and predominantly focuses on assessing different extraction methods and extraction solvents for the generation of antioxidant extracts from *Ascophyllum nodosum* (Linnaeus) Le Jolis (*A. nodosum*), *Pelvetia canaliculata* (Linnaeus) Decaisne & Thuret (*P. canaliculata*), *Fucus spiralis* Linnaeus (*F. spiralis*) and *Ulva intestinalis* Linnaeus (*U. intestinalis*). At the outset, pressurised liquid extraction (PLE) was compared to an enzyme-assisted extraction (EAE), using the carbohydrase Viscozyme, for antioxidant extraction from *F. spiralis* (Paper II). Enzyme-assisted extraction (EAE) of macroalgae was introduced in an attempt to improve antioxidant extraction efficiency without using organic solvents.[175] The use of individual or combinations of carbohydrases and proteases to detach macroalgal polyphenols from cell wall polysaccharides and peptides, respectively, has increased in recent years.[274, 277] Pressurised-liquid extraction (PLE), also known as accelerated solvent extraction (ASE), involves the use of high temperatures and pressures in order to enhance the potential bioactive yield compared to that achieved by other commonly used methods.[278] It has been proven to be a useful technique for the production of macroalgal extracts with antioxidant activities, with the added advantage of being a fast, automated and targeted technique.[162, 279-280]

Following the initial methods comparison it was concluded that PLE was superior to a Viscozyme EAE for the generation of antioxidant extracts. Consequently, the PLE method was then compared to solid-liquid extraction (SLE) (Paper III). Until recently, SLE was considered the method of choice for the extraction of bioactives from natural sources.[276, 281-282] However, with the emergence of various technically-enhanced methods that claim to improve the extraction process with regards to the extraction yield, speed, efficiency, eco-friendliness and/or solvent consumption, SLE is no longer the method of choice for bioactive extraction among researchers.[275] For that reason, the aim of Paper III was to compare the technical advances of the recently developed PLE method against SLE to monitor which method was more efficient at generating antioxidant extracts from the four species of macroalgae examined.

As well as a suitable extraction method, the appropriate consideration must also be given as to how the extract should be processed further in order to maximise the concentration of the polyphenols and, therefore, enhance bioactivity. This is generally achieved by excluding components that may have been co-extracted alongside the polyphenols, thus enriching the content of the target species. Enrichment usually involves excluding unwanted co-extracted material on the basis of polarity or molecular weight. A diverse range of techniques and instrumentation is available for this purpose, however, if the ultimate goal is to enrich extracts with polyphenols at a large scale for potential use as ingredients in food (as opposed to use as a pharmaceutical), the enrichment method should be low cost, efficient and food-friendly.

Solvent partitioning is widely used in research as a method for the enrichment of some polyphenolic compounds, as they are known to be selectively soluble in polar organic solvents.[178] However if potentially harmful solvents are used in this process, then the enriched extract may not be safe for use as a food additive. In addition, partitioning is a solvent-intensive method, thus making it an expensive process when performed on a large scale. The removal of interfering compounds based on size is also a popular means of polyphenol enrichment. This consists of the use of either pressure-driven membrane processes, such as ultrafiltration[283] and nanofiltration[284], or concentration gradient driven techniques such as molecular weight cut-off (MWCO)

dialysis. MWCO dialysis has the advantage of being a simple, food-friendly technique that performs similarly to many of the commercial pressure-driven membrane processes, but without the excess instrumentation. In the work contained in Paper IV, MWCO fractionation was employed to separate phlorotannin-containing crude extracts into low molecular weight (LMW) and high molecular weight (HMW) fractions. Flash chromatography was employed to further purify the LMW fraction and to investigate what effect this technique would have on phlorotannin enrichment. Flash chromatography, using both reverse-phase and normal-phase mode, has been utilised for the successful separation of phlorotannins.[285,110] However in the present study, a simple reverse-phase (RP) method was used, initially eluting with water to elute polar LMW impurities such as sugars, followed by methanol to elute a predominantly polyphenolic fraction. The resulting polyphenolic fractions had phenolic contents comparable to or significantly greater than the HMW fractions and the presence of phlorotannins in these fractions was confirmed by Q-Tof-MS.

2.2 Discussion

From the comparison of PLE and EAE (in Paper II) in terms of their capabilities in producing phenolic and antioxidant extracts from *F. spiralis* it was found that the total phenolic content (TPC) was significantly higher ($p < 0.05$) in the PLE extracts of *F. spiralis* than the carbohydrase Viscozyme hydrolysate and control. Furthermore, the TPC of the hydrolysate was not enhanced when compared to the control water extract suggesting that Viscozyme was not effective for liberating bound polyphenols from this species. This may be due to an incompatibility between this particular enzyme and *F. spiralis*, as it has been shown previously that EAE can be useful for extracting polyphenols from certain species of macroalgae, but its success appears to depend on species/enzyme pairings.[286] The antioxidant activity of the hydrolysate, tested by the DPPH, FRAP and ORAC assays, also did not improve relative to the control without the enzyme. Furthermore, for these antioxidant assays, one or more of the PLE extracts had higher antioxidant activity than the enzyme-treated extract. The data suggested that the use of aqueous organic solvents under high pressures and temperatures is more effective for the extraction of antioxidant polyphenols from *F. spiralis* than EAE using Viscozyme. As a consequence of the these findings, a comparative study (Paper III) of PLE and SLE was then carried out

to assess whether the high temperatures and pressures of PLE are necessary to produce antioxidant extracts from macroalgae (*A. nodosum*, *P. canaliculata*, *F. spiralis* (Phaeophyceae) and *U. intestinalis* (Chlorophyceae)) when comparing methods that both use organic solvents. It was found that the application of PLE using acetone/water (80:20) consistently produced higher TPC for each species being assessed when compared with SLE extraction using the same solvent mixture. However, when the food-friendly solvents of water and ethanol/water (80:20) were used, the three brown macroalgae consistently exhibited higher TPCs when extracted using SLE rather than PLE. On the whole, when the antiradical power (ARP), assessed using the DPPH assay, FRAP and ferrous ion chelating (FIC) ability of the extracts were determined it was found that the SLE extracts had higher antioxidant activities than their PLE equivalents, particularly when either water or ethanol/water were used as the solvents. This information is particularly useful for extracts that are intended for incorporation into foods as ethanol and water can be used in a food-friendly manner. The data in Paper III concludes that the high temperatures and high pressures involved in PLE is not warranted for producing antioxidant extracts from macroalgae and, when considering the large-scale production of extracts from macroalgae, the efficiency and relative cost savings of SLE would be far greater. This chapter provides vital information regarding the different techniques that can be employed to generate antioxidant extracts from macroalgae. Taking both bodies of work into consideration it can be concluded that SLE should be the method of choice as it is simple, requires less capital investment, is food-safe, and can be easily scaled up.

In addition to investigating differences in antioxidant extraction efficiency between the PLE and SLE methods, the differences between the green macroalgal species and the brown macroalgal species were also highlighted. Consistently *U. intestinalis* was found to have much lower TPC and antioxidant activity, as determined in DPPH and FRAP assays, than the brown macroalgal equivalent extracts. This finding is in agreement with previous studies,[32] and it is assumed to be due to the high levels of phlorotannins and carotenoids present in brown macroalgae.[99]

In this work of Paper IV the aim was to enrich phlorotannins from cold water (CW), hot water (HW) and ethanol/water (EW) crude extracts of *A. nodosum*, *P. canaliculata* and *F. spiralis*, based on size and polarity separation using MWCO dialysis and reverse-phase flash chromatography, respectively (Paper IV). Following MWCO dialysis the phenolic content and antioxidant activity of the HMW fractions of 3.5-100 kDa and/or greater than 100 kDa were significantly enhanced for all species in comparison to crude extracts. In general, the largest enrichment of TPC was observed in the 3.5-100 kDa fractions, with the exception of cold water *A. nodosum* and ethanol/water *A. nodosum* extracts, where the greater than 100 kDa fractions had a higher value. Since phlorotannins are the major polyphenolic species present in macroalgae, the relative distribution of polyphenols between different MWCO fractions potentially gives an insight into the molecular weight distribution of these species. The level of TPC enrichment of the 3.5-100 kDa fractions was considerably lower in HW extracts when compared with the CW and EW extracts and, therefore, we did not proceed with purification of this extract any further. The free radical scavenging activities (RSA), assessed by the DPPH and FRAP assays, for the most part correlated with the trend observed in the TPC assay. However, metal chelating activity of the fractions did not follow the same trend, with the less than 3.5 kDa and/or 3.5-100 kDa fractions showing the highest level of ferrous ion inhibition. This activity may attributed to the presence of small molecules other than polyphenols, such as bioactive peptides,[287] in these fractions that possess FIC ability that are not in the HMW fractions.

Due to the lack of significant enhancement in the TPC of the LMW fraction (< 3.5 kDa) from the majority of the crude extracts, further refinement of this fraction using a RP flash chromatography technique was carried out. The flash chromatograms for all species and extracts showed that small molecule polar impurities were eluted by water. Polar and less polar polyphenols eluted afterwards with methanol. (See appendices, appendix 1 (a) – (f)). This was confirmed by the TPC assay, which showed that the third methanol fractions for the extracts, with the exception of *P. canaliculata* CW extract, and the second aqueous fractions, in the case of *P. canaliculata* and *F. spiralis* CW extracts, were significantly enriched relative to the

initial aqueous fraction. RSAs were highly correlated with the TPC of the fractions ($r = 0.895, p < 0.05$).

This work demonstrates how a MWCO dialysis procedure is very effective for the phlorotannin enrichment of water and ethanol/water extracts of macroalgae. The use of water makes this process inexpensive and food-safe and, therefore, a reliable enrichment procedure in terms of potential scaling up for use in the functional food and nutraceutical industries. The use of Q-Tof-MS validated the assumption that phlorotannins were present in the polyphenol-enriched flash fraction of all three species and it also gave an insight into the degree of polymerisation occurring in these fractions. The number of phloroglucinol units (PGU) ranged from 4 to 20 PGU, 7 to 48 PGU and 4 to 24 PGU for *A. nodosum* EW, *P. canaliculata* EW and *F. spiralis* EW, respectively. Chapter 3 will deal with the in-depth profiling analysis of the flash fractions from *F. spiralis*, *A. nodosum* and *P. canaliculata* using MS and NMR to give a more complete description of the polymerisation and isomerisation levels within each species and their extracts, and further systematic separation of phlorotannins will be described.

Chapter 3 – Separation and profiling of low molecular weight (LMW) phlorotannins in brown macroalgae

3.1 Summary

The previous chapter primarily dealt with the extraction of polyphenols and generation of fractions, with enriched phlorotannin content, from crude extracts. Such enrichment processes are practical in that they can yield fractions with increased bioactivity relative to the crude extract. Nevertheless, if such fractions are to be applied as functional ingredients, food preservatives, nutraceuticals and/or cosmeceuticals,[97, 176-177] it is necessary that the consistency of the fractions, in terms of the relative levels of components and level of structural isomerisation, can be monitored.[288] In relation to the monitoring of phlorotannin contents, this involves the application of additional separation steps, such as normal phase chromatography and size exclusion chromatography, and advanced analysis techniques, such as MS and NMR, to generate metabolite profiles of appropriate quality.

This chapter, initially, assesses normal phase (NP) flash chromatography as a tool for the further separation of the RP phlorotannin-enriched flash fractions from *A. nodosum*, *P. canaliculata* and *F. spiralis* that were generated in the previous chapter. NP chromatography has been successfully used previously for the separation of polyphenols from various natural sources.[57, 289] NP chromatography has an advantage over RP chromatography in that generally highly polar impurities, such as sugars (which are likely to be major components of the enriched macroalgal fractions), are retained on the NP silica column allowing for the separation of the polyphenolic compounds. In addition, although RP chromatography may be efficient for the separation of oligomer polyphenols, it is not as effective for the separation of polymers that are present on brown macroalgae.[57] Koivikko *et al.* (2007) compared the NP and RP HPLC methods for the separation of phlorotannins from *Fucus vesiculosus*.[193] The NP method displayed improved separation of phlorotannins relative to the RP method, as with the latter the phlorotannin samples eluted directly with the solvent. This is due to the RP column material being non-polar and, therefore, does not form linkages with the polar polyphenolic compounds.[193] The

aforementioned study examined the effect of various flash chromatography conditions such as mobile phase composition, flow rate and run time, on the separation of phlorotannins from *A. nodosum*, *P. canaliculata* and *F. spiralis*.

In Paper V a study profiling the phlorotannin molecular size ranges and isomers of the phlorotannin-enriched fractions (generated in chapter 2) using ultra performance liquid chromatography-mass spectrometry (UPLC-MS) analysis is outlined. However, in cases where the purity of the samples was not adequate for MS analysis, NP flash chromatography or solid-phase extraction (SPE) was employed to further refine the fractions. UPLC-MS, utilising tandem mass spectrometry (multiple reaction monitoring (MRM) mode), was employed specifically to increase sensitivity and overcome the potential problems with chromatographic resolution of different molecular weight phlorotannins and their isomers.

Following the profiling study it was evident that the phlorotannin-enriched fractions of all three species were still very complex, containing phlorotannins of various degrees of polymerisation (DP) and, furthermore, numerous isomers were present for most individual molecular ions. In an attempt to extensively separate the profiled samples into less complex fractions, and propose the structural characteristics of phlorotannins responsible for the antioxidant and angiotensin converting enzyme I (ACE-I) activities observed, Sephadex LH-20 column chromatography was employed. Column chromatography, in conjunction with elution using aqueous alcohol or aqueous acetone solvents, has commonly been proven to be effective for the separation of polymeric proanthocyanidins from plant extracts.[290-291] Column chromatography using Sephadex LH-20 has been employed previously for the separation of phlorotannins from *F. vesiculosus*,[178] however, in this chapter an attempt was made to improve on this method by comprehensively separating the highly polymeric compounds, in addition to the smaller oligomers, from *A. nodosum*, *P. canaliculata* and *F. spiralis*.

3.2 Experimental

3.2.1 Reagents and materials

All chemicals used were of reagent-grade. All solvents used were of HPLC-grade. 2,2-diphenyl-1-picrylhydrazyl (DPPH·), 6-hydroxy-2,5,7,8-tetramethylchroman-2-carboxylic acid (Trolox) and Sephadex LH-20 were obtained from Sigma–Aldrich Chemical Co. (St. Louis, MO, USA). The SuperFlash™ SF10-8g Si 50 column was obtained from Apex Scientific, Maynooth, Co. Kildare. Angiotensin-converting enzyme assay kit was obtained from NBS Biologicals Ltd., Cambridgeshire, England, PE29 7DT.

3.2.2 Normal-phase (NP) flash chromatography

Normal-phase (NP) flash chromatography runs were carried out on the LMW polyphenol-enriched (RP) flash fractions from the brown macroalgae that were discussed in Chapter 2. Custom gradients were designed for each LMW fraction to ensure maximum purity of the flash fractions isolated. In all cases a NP SuperFlash™ SF10-8g Si 50 column, 90.4 x 14.2 mm, was used.

(a) *P. canaliculata* ethanol/water (80:20) (EW)

The fraction (150 mg) was dissolved in a minimum volume of methanol, mixed with a small amount of silica and then dried on the rotary evaporator. The silica-sample mixture was added to a DASi sample loader module attached to the NP column. A gradient elution of mobile phase A (ethyl acetate) and B (methanol) was used for the separation. The step-wise gradient used was as follows: 0 % B, 0–2 min; 10 % B, 2–4 min; 20 % B, 4–6 min; 30 % B, 6–8 min; 40 % B, 8–10 min; 50 % B, 10–12 min; 60 % B, 12–14 min; 70 % B, 14–16 min; 80 % B, 16-18 min; 90 % B, 18-20 min; 100 % B, 20-24 min. The flow rate was 12 mL min^{-1} and 12 fractions were collected.

(b) *F. spiralis* EW

NP chromatographic run was carried out on the enriched-polyphenolic flash sample from *F. spiralis* EW. The fraction (121 mg) was prepared as described as above and a gradient elution of mobile phase A (ethyl acetate) and B (methanol) was as follows:

0% B, 0–2 min; 5 % B, 2–4 min; 10 % B, 4–6 min; 15 % B, 6–8 min; 20 % B, 8–10 min; 25 % B, 10–12 min; 30 % B, 12–14 min; 35 % B, 14–16 min; 40 % B, 16-18 min; 45 % B, 18-20 min; 50 % B, 20-22 min; 55 % B, 22-24 min; 60 % B, 24-26 min; 65 % B, 26-28min; 70 % B, 28-30 min; 75 % B 30-32 min; 80 % B 32-40 min. Twenty fractions were collected.

(c) *A. nodosum* EW

A similar NP chromatographic run to *P. canaliculata* was carried out for the *A. nodosum* EW phlorotannin-enriched flash fraction (160 mg) with the only modification being that the flow rate was 18 mL min^{-1}. Twenty four fractions were collected.

A second NP chromatographic run was carried out on the enriched-polyphenolic RP flash fraction from *A. nodosum* to observe if the use of chloroform as the mobile phase A rather than ethyl acetate improved fraction separation. The fraction (40 mg) was prepared as above and a gradient elution of mobile phase A (chloroform) and B (methanol) was as follows: 0% B, 0–2 min; 5 % B, 2–4 min; 10 % B, 4–6 min; 15 % B, 6–8 min; 20 % B, 8–10 min; 25 % B, 10–12 min; 30 % B, 12–14 min; 35 % B, 14–16 min; 40 % B, 16-18 min; 45 % B, 18-20 min; 50 % B, 20-22 min; 55 % B, 22-24 min; 60 % B, 24-30 min; 65 % B, 30-32 min; 70 % B, 32-34 min. In all cases the chromatograms were viewed at 210, 225 and 230 nm and selected fractions from each run were analysed by UPLC-MS.

3.2.3 Sephadex LH-20 column chromatography

Sephadex LH-20 column chromatography of *F. spiralis* (0.909 g) and *A. nodosum* (1.537 g) phlorotannin-enriched RP flash fractions was carried out using a method similar to that used by Wang *et al.* (2012), with some alterations. Sephadex LH-20 was swelled with 50:50 methanol/acetone.[178] The flash fractions were dissolved in 50:50 methanol/water. The column was equilibrated with at least three volumes of 50:50 methanol/water. The sample was added and following adsorption of the sample to the column sample elution was initiated. The fraction was eluted with the following solvents of decreasing polarity; 1:1 methanol/water, 3:1 methanol/water,

100% methanol, 5:1 methanol/acetone, 3:1 methanol/acetone, 1:1 methanol/acetone. All fractions (30) were concentrated on rotary evaporator at 40 °C and freeze-dried.

3.2.4 UPLC-MS analysis

UPLC-MS analysis of the fractions eluted from the NP flash chromatography and column chromatography was conducted using an Acquity™ UPLC® System (Waters Corporation, Micromass MS Technologies, Manchester, UK), consisting of a binary pump solvent manager capable of generating pressures up to 15000 psi, coupled with an Acquity™ TQD-MS (Waters Corp.). A Waters Acquity™ HSS PFP column (100Å, 1.8 µm particle size, 2.1 mm x 100 mm) maintained at 40 °C was used for separation. Mobile phases consisted of 0.1% formic acid aqueous solution (A) and acetonitrile with 0.1% formic acid (B). The flow rate was 0.5 mL min^{-1} and injection volume was 5 µl. Elution was performed as follows for the analysis of the NP flash fractions; 0.5 % B from 0-6.5 min; 15 % B from 6.5-7.0 min; 50 % B from 7.0-8.5 min and 0.5 % B from 8.5-10.0 min. Elution was performed as follows for the analysis of the Sephadex fractions; 0.5 % B from 0-10 min, 0.5-30 % B from 10-26 min, 30-90 % B from 26-28 min and 0.5 % B from 28-30 min.

The MS was operated in electrospray negative ion mode with multiple reaction monitoring (MRM). The MRM method was developed and optimised with phlorotannin mixtures using the IntelliStart™ software (Waters Corp.) according to molecular masses of phlorotannins containing 3 to 16 (maximum permitted with TQD) units of phloroglucinol. The following were the parameters for the MS; capillary voltage, 2.8 kV; source temperature, 350 °C; desolvation temperature, 50 °C; desolvation gas, 800 L hr^{-1}; core gas, 50 L hr^{-1}.

3.2.5 In vitro antioxidant activity

The antioxidant capabilities of the *F. spiralis* and *A. nodosum* Sephadex fractions were assessed by the DPPH· radical scavenging ability (RSA) assay. The DPPH· RSA was determined using a method similar to that reported by (Goupy and co-workers), though modified to be carried out in a microplate. The assay DPPH· solution (0.048 mg mL^{-1}) was prepared by making a 1 in 5 dilution, with methanol, of the methanolic DPPH· stock solution (2.38 mg mL^{-1}). Prior to analysis, dilutions of the *F.*

spiralis and *A. nodosum* stock samples (200 μg mL^{-1}) were prepared at concentrations of 100, 50, 25, 12.5 and 6.25 μg mL^{-1}. A standard curve of trolox, using standard concentrations of 0.01 mM-0.05 mM, was used as a reference. The standard/diluted sample (100 μl) and DPPH· solution (100 μl) were added to a 96-well microplate. The microplate was left in the dark for 30 minutes at room temperature. The absorbance was then measured in triplicate against methanol (blank solution) at 515 nm on an automated FLUOstar Omega microplate reader system. The decrease in absorbance of the sample extract was calculated by comparison to a control (100 μl methanol and solvent and 100 μl DPPH· solution). The relative decrease in absorbance (PI) was calculated as follows:

$$PI\ (\%) = [1 - (A_e/A_b)] \times 100,$$

where A_e = absorbance of sample extract and A_b = absorbance of control. The PIs used to calculate the related antioxidant activity were superior (PI_1) and inferior (PI_2) to the value estimated at the 50 % decrease of DPPH· absorbance.[292] Antioxidant activity was expressed as Antiradical Power (ARP), which is the reciprocal of the IC_{50} (mg mL^{-1}). The IC_{50} is defined as the concentration of sample extract that produces a 50 % reduction of the DPPH· radical absorbance.[292] The higher the ARP value the stronger the radical scavenging activity of a sample.[293]

3.2.6 Angiotensin converting enzyme I (ACE-I) inhibitory activity

Angiotensin converting enzyme I (ACE-I) inhibition was determined using an ACE kit that uses 3-hydroxybutylyl-gly-gly-gly (3H-GGG) as the ACE substrate. The assay was carried out according to the suppliers' protocol.[294] The enzyme working solution and indicator working solution were was prepared as outlined by supplier protocol. Reagent blank wells, full activity wells and positive control inhibitor wells were tested in triplicate. Captopril tested at 0.02 and 0.005 μM was used as a positive control. *F. spiralis* flash fraction wells were tested in duplicate at 250 μg mL^{-1} concentrations. The reagent blank wells consisted of 40 μl deionised water and 20 μl substrate buffer. The full activity wells consisted of 20 μl deionised water, 20 μl substrate buffer and 20 μl enzyme working solution. The inhibitor wells contained 20 μl positive control/sample, 20 μl substrate buffer and 20 μl enzyme working solution. The plate was incubated at 37 °C for an hour. Then 200 μl indicator solution was

added to each well and incubated again at room temperature for ten minutes. The absorbance of the wells was read at 450 nm with a microplate reader. The percentage ACE-I inhibition was calculated using the following formula:

$$\left(\frac{A_{\text{Full enzyme activity}} - A_{\text{Inhibitor}}}{A_{\text{Full enzyme activity}} - A_{\text{Reagent blank}}} \right) \times 100$$

3.2.5 ^{1}H Nuclear magnetic resonance (^{1}H NMR)

^{1}H NMR spectroscopy data of the RP flash phlorotannin-enriched fractions for *A. nodosum*, *P. canaliculata* and *F. spiralis* EW were recorded using a Bruker Avance III 500 Mhz spectrometer (Bruker, Coventry, U.K.). The *A. nodosum* fraction was further purified using SPE to improve the observed NMR spectrum. Samples were dissolved in deuterated methanol (MeOD). Spectra were obtained using a water suppression method due to residual water in the samples. Water suppression using 3-9-19 pulse sequence with gradients, gradient ratio 20% with a sinusoidal gradient was used for these experiments with 64 scans, a sweep width of 8012.820 Hz. Processing was carried out using Topspin 2.1.1 software and a line broadening of 0.3 Hz was applied during processing. NMR samples were ran and analysed by Dr. Padraig McLoughlin (Teagasc Food Research Centre, Ashtown, Dublin 15).

3.3 Results and Discussion

3.3.1 Separation of phlorotannins using normal-phase (NP) flash chromatography

The successful profiling and characterisation of phlorotannins is highly dependent on the purity of the sample. Various NP runs were carried out to first establish if an initial NP run using mobile phases of ethyl acetate and methanol would be suitable for phlorotannin separation and generating fractions of sufficient purity for UPLC-MS analysis from all three species. The effect of using chloroform, rather than ethyl acetate, as the less polar mobile phase A and the effect of different run times and flow rates were also investigated.

The NP flash run of *A. nodosum* EW which involved eluting fractions with the mobile phases ethyl acetate (A) and methanol (B). The amount of methanol was increased from 0-100 % B in 10 % increments. From the chromatogram (figure 4(a)) an initial large peak is observed before any methanol is present in the mobile phase. Following this relatively small increases in absorbance are observed for each increment up to 40 % methanol and then the absorbance slowly decreases. A fraction from *P. canaliculata* EW was eluted under the same conditions. From the chromatogram (figure 4(b)) it was seen again that an initial peak elutes when no methanol is present. However, unlike the *A. nodosum* run larger absorbances, relative to the initial peak, are evident from between 20 % and 50 % B.

A similar method was used for the elution of the *F. spiralis* RP flash fraction; however, it was modified so that the mobile phase B increased in 5 % increments ending when 80 % B was reached. A chromatographic profile (figure 4(c)) similar to that observed for *P. canaliculata* was observed. An initial peak was observed at 5 % methanol and, again, a large increase in the absorbances relative to the first peak was observed from between 15 % and 35 % methanol before slowly decreasing. From these NP flash runs it appears increasing the gradient in steps of either 5% or 10 % is suitable for the separation of the macroalgal fractions.

A NP run employing a different mobile phase system of chloroform (A) and methanol (B) was also attempted with *A. nodosum* EW fraction going from 0-70 % B

in 5 % increments. From the chromatogram (figure 4(d)) it appears that this system does not separate the eluting compounds as effectively as the initial system. The absorbance remains quite low for the duration of the run, with a small increase at 60 % B.

UPLC-MS was employed to screen the individual fractions that eluted from the NP flash runs. For the fractions eluting from the run with *A. nodosum* using ethyl acetate and methanol the fractions with the strongest signal (AU) were for fractions 1-5 and signals sharply decreased following this (figure 5). Fractions 1 and 2 correspond to the sharp peak observed at the start of the chromatogram for this sample (figure 4(a)) and exhibit the strongest signals of all the fractions. In fractions 1-4 the dominant molecular ion was at *m/z* 1241 which corresponds to a degree of polymerisation of phloroglucinol (DP) of 10. The peak for the molecular ion at *m/z* 1117, which corresponds to a phlorotannin with a DP of 9, was also prominent in fractions 3-5. These molecular ions are the same ones that were prominent for this species following separation through a Sephadex LH-20 column by Nwosu *et al.* (2011)[14] and subsequent to molecular weight-based enrichment study featured in chapter 2.[295]

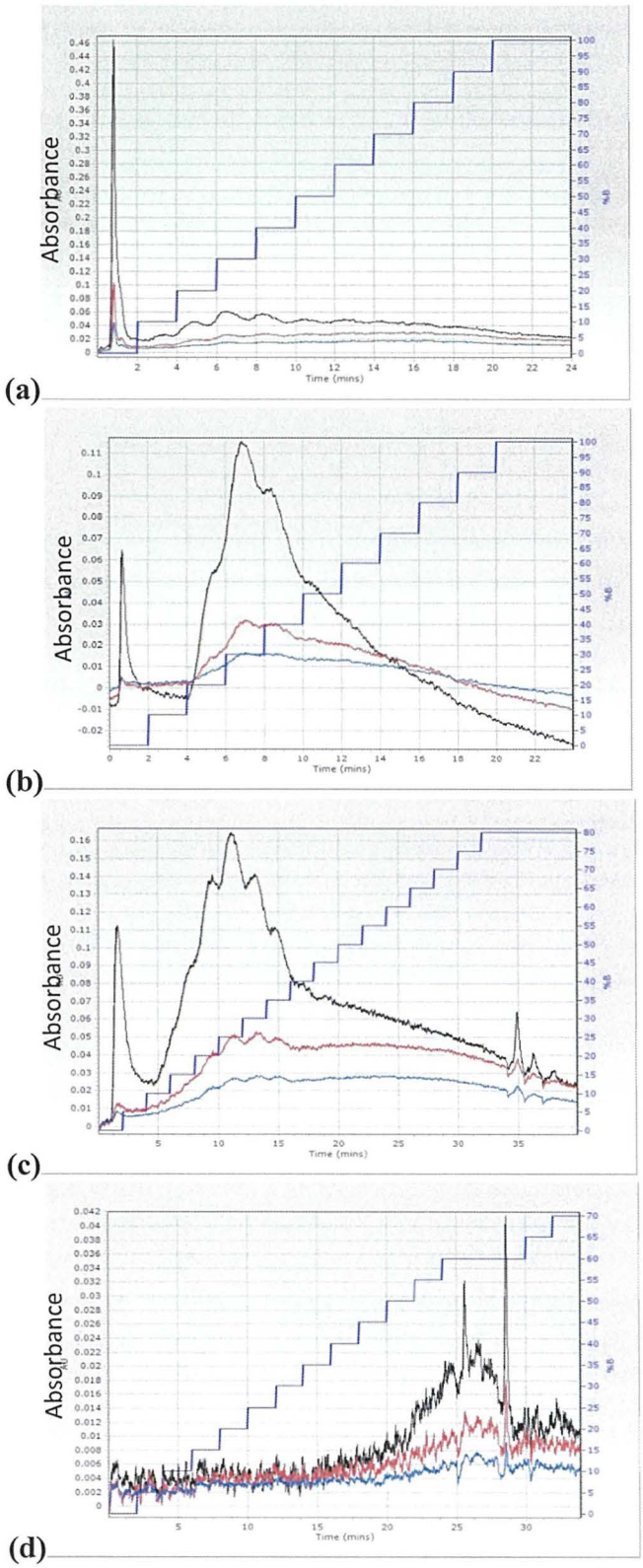

Figure 4: Chromatograms of normal-phase flash runs of (a) *A. nodosum* (b) *F. spiralis* and (c) *P. canaliculata* using ethyl acetate/methanol and (d) *A. nodosum* using chloroform/methanol.

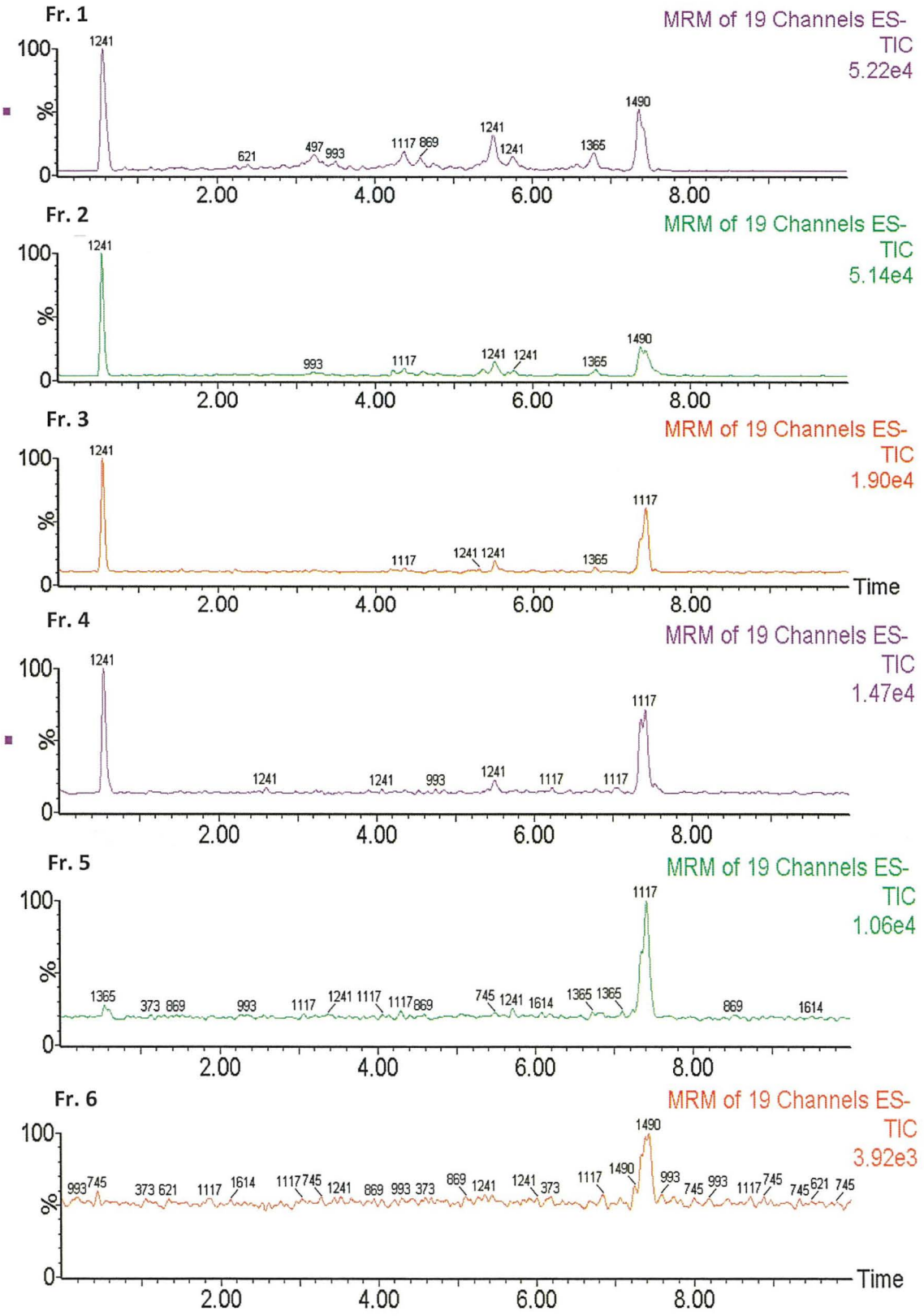

Figure 5: UPLC-TQD-MS spectra of *Ascophyllum nodosum* EW normal phase (NP) flash chromatography fractions 1-6 eluted with ethyl acetate/methanol.

A similar situation to *A. nodosum* was observed also for *P. canaliculata* in that the strongest signals observed following UPLC-MS analysis were the fractions that eluted early on; fractions 1-3 (figure 6). Fraction 1 corresponds to the initial sharp peak seen in the chromatogram for this sample (figure 4(b)), however, even though the absorbances for some of the fractions after 6 minutes are higher, the signals observed after UPLC-MS analysis do not imitate this. The only peak of note in fractions 1 and 2 was for the molecular ion at 1490 *m/z*, equivalent to a phlorotannin with a DP of 12. In fraction 3 the only significant molecular ion was at *m/z* 1241, corresponding to a DP of 10. These molecular ions were also found to be significant for this species in the earlier enrichment study included in chapter 2.[295]

The analysis of the *F. spiralis* NP fractions again revealed that the earlier fractions of 1-5 exhibited the strongest signals (figure 7). Fraction 1 and 2 are linked to the initial peak seen in the chromatogram (figure 4(c)), and similar to *P. canaliculata*, after 8 minutes the absorbances for a number of the fractions are higher. Whereas the initial fractions from *A. nodosum* and *P. canaliculata* displayed one or two dominant peaks many of the initial fractions from *F. spiralis* had a number of significant molecular ions present. The molecular ion at *m/z* 993 is prominent in fraction 1, however peaks for ions at *m/z* 497 (DP of 4) and 621 (DP of 5) are also significant, which is in line with what was observed in the previous enrichment work outlined in chapter 2 for this species.[295] The molecular ion at *m/z* 1117 is prominent in fraction 2, but again numerous smaller peaks are also present. The most significant peak in fractions 3-5 is *at m/z* 869.

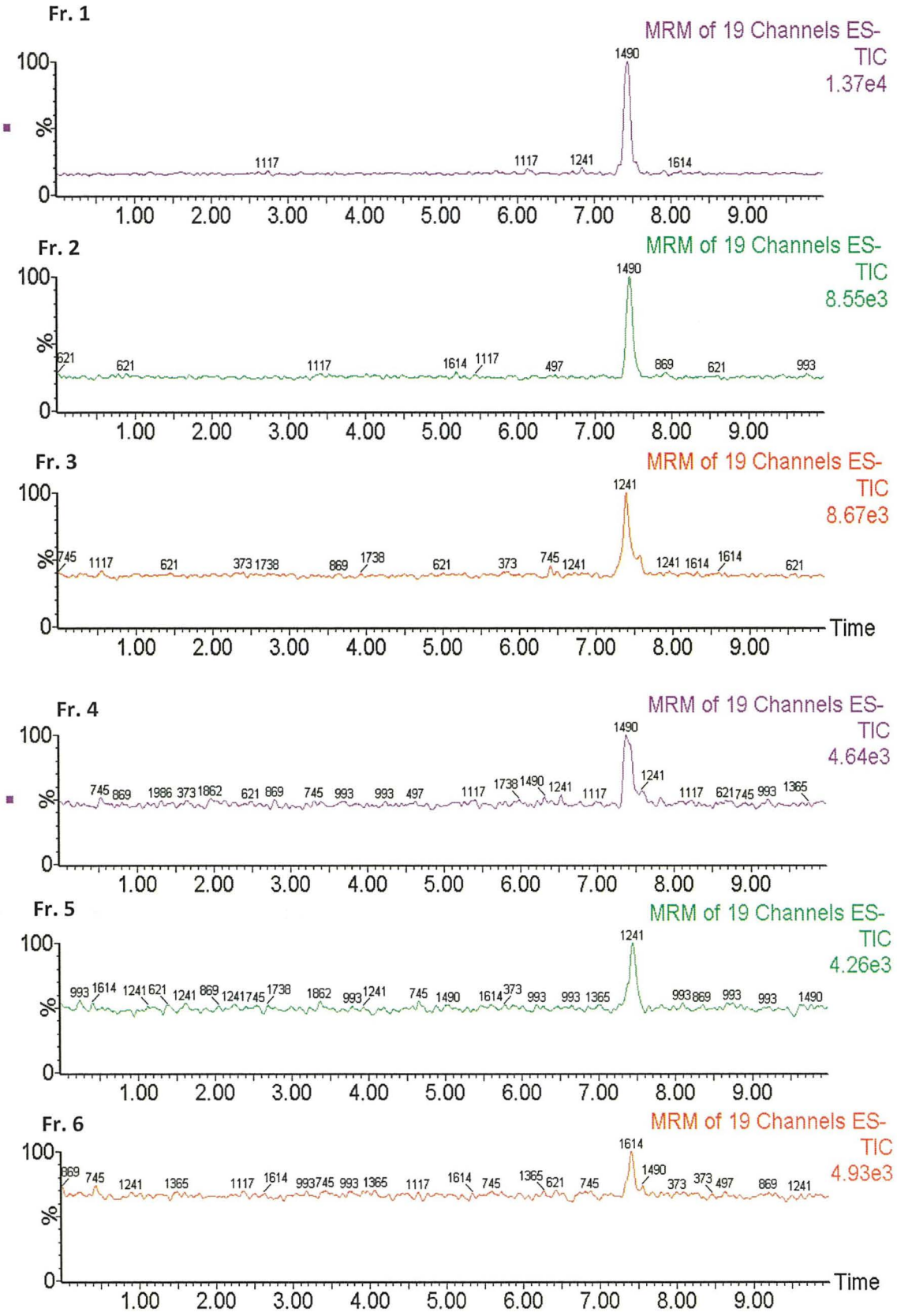

Figure 6: UPLC-TQD-MS spectra of *Pelvetia canaliculata* EW normal phase (NP) flash chromatography fractions 1-6 eluted with ethyl acetate/methanol.

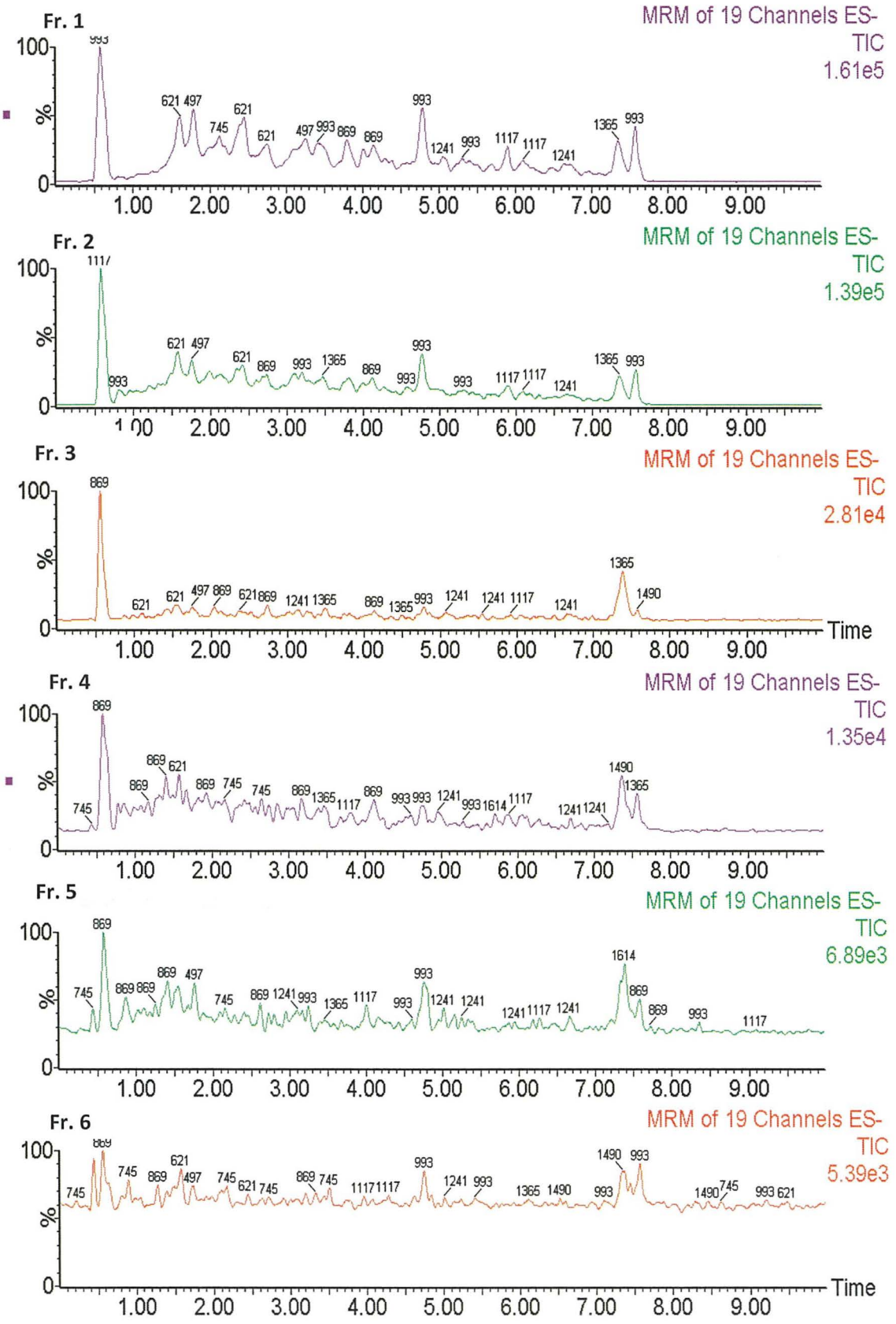

Figure 7: UPLC-TQD-MS spectra of *Fucus spiralis* EW normal phase (NP) flash chromatography fractions 1-6 eluted with ethyl acetate/methanol.

Although it appeared from the flash chromatogram for the *A. nodosum* NP run involving chloroform as mobile phase A that good separation did not occur the fractions were still analysed by UPLC-MS. Due to the small amount of fraction loaded onto the NP column in this run, it was assumed that the flash instrument may not have been sensitive enough to detect the separation. From the flash chromatogram, it appears the stronger fractions eluted at a higher percentage of the polar solvent near the end of the run, and indeed the fractions 22-25 give the strongest signals (AU) in the UPLC-MS spectra (figure 8). The prominent peak observed in the fraction 22 was at *m/z* 1241, which was also observed in the fractions of the earlier NP run for *A. nodosum*, however, peaks at 1490 and 1738 *m/z* were dominant in fractions 23-25, which were not significant in the earlier NP run nor in the enrichment work in paper IV.[295]

From the evaluation of the NP runs, it was concluded that a NP flash method using ethyl acetate/methanol, rather than chloroform/methanol, as the mobile phases was the better option due to the better separation observed, and that the run time (24 min or 40 min) and flow rate (12 or 18 mL min^{-1}) with this system did not significantly affect the elution of phlorotannin fractions (see figure 4(b) and 4(c)). It's also apparent that this method is more suitable for the separation of the phlorotannins from *A. nodosum* and *P. canaliculata*, as from the UPLC-MS spectra (Figures 5 and 6) it can be seen that some of the fractions contain only one or two dominant molecular ions, whereas for *F. spiralis* (Figure 7) the spectra are far more complex. This may suggest that although NP chromatography is efficient for the separation of larger phlorotannin polymers it is not as useful for the separation of oligomers and small polymers that are known to be present in abundance in *F. spiralis*. (Paper V)

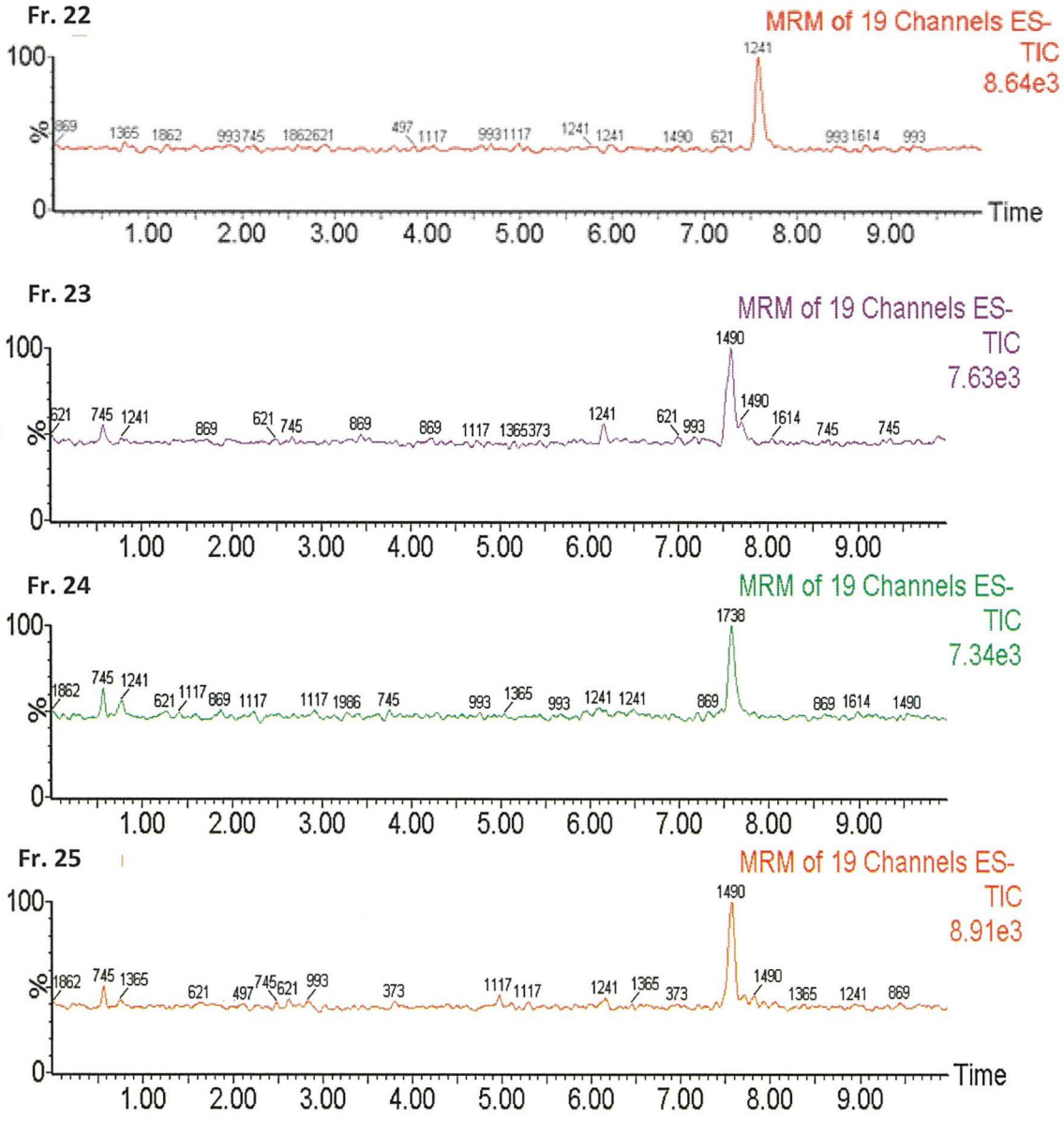

Figure 8: UPLC-TQD-MS spectra of *Ascophyllum nodosum* normal phase (NP) flash chromatography fractions 22 -25 eluted with chloroform/methanol.

3.3.2 UPLC-MS profiling of LMW phlorotannin polymers (Paper V)

A study to profile the phlorotannin composition and level of isomerisation present in *A. nodosum*, *P. canaliculata* and *F. spiralis* using UPLC-MS was carried out and is outlined in detail in paper V. Phlorotannin-enriched fractions from macroalgal water (CW) and aqueous ethanol (EW) extracts, discussed in paper IV, were analysed by UPLC-MS performed in multiple reaction monitoring mode (MRM) to detect molecular ions consistent with the molecular weights of phlorotannins. Further separation of some of the phlorotannin-enriched fractions (*A. nodosum* CW and EW, and *P. canaliculata* CW) generated by RP flash chromatography was necessary to yield UPLC-MS signals of appropriate strength. Due to the assessment of the various NP flash chromatography runs, the method with ethyl acetate and methanol as mobile phases A and B, respectively, was employed to purify samples of inadequate purity for *A. nodosum*. Solid phase extraction (SPE) was used for *P. canaliculata* CW as the UPLC-MS signals for the NP fractions for this sample were still insufficient for analysis.

Total ion chromatograms (TICs) highlighted the differences in the phlorotannin profiles among the different species and, also, among different extracts of the same species. For the first time, the use of a penta-fluoro-phenyl (PFP) column facilitated the detection and separation of polymeric (10-16 monomers) phlorotannins. The PFP column employs a combination of different separation/retention mechanisms including polar interactions (hydrogen bonding), π-π interactions and dipole-dipole interactions, which is ideal when attempting to separate highly polar, aromatic phlorotannin polymers.[296] The ranges of LMW phlorotannins found in *A. nodosum*, *P. canaliculata* and *F. spiralis* were 6-11, 6-13 and 4-6 monomers, respectively. Analysis of the extracted ion chromatograms (EICs) of individual negative molecular ions ($[M-H]^-$) allowed for the identification in most cases of multiple peaks corresponding to isomers for the molecular weights of phlorotannin corresponding to DPs of 3-16. The maximum number of detected isomers was 90 found in *P. canaliculata* CW extract, for the molecular ion equivalent to a DP of 8. Through the profiling of phlorotannin isomers for polymers up to a DP of 16 units in length in the three species, it was evident that even when only LMW phlorotannins are being

analysed these samples are extremely complex and that further advanced purification is necessary in order to attempt characterisation.

3.3.3 Separation and profiling of phlorotannins using Sephadex LH-20

Column gel chromatography using Sephadex LH-20 gel, in conjunction with a range of solvents, was employed for the further separation of phlorotannins based predominantly on polarity. The degree of hydrogen bonding between hydroxyl groups of the phenolic compounds and the ether oxygen atoms within the cross-linking chain of the gel directs the separation.[178] Therefore, it would be expected that larger phlorotannins, which have more phenolic hydrogens, would be retained for longer due to stronger hydrogen bonding with the gel. The method employed to elute the phlorotannin fractions was a stepwise system using solvents of decreasing polarity and similar to the Sephadex LH-20 elution method employed by Wang (2012),[178] however, in present study we collected29 fractions, based on volume, whereas Wang and colleagues collected only 6 fractions. The use of solvent systems that gradually move from polar to less polar in nature further assists in the separation of smaller oligomers from larger polymers. The displacement of complex polymeric phlorotannins is achieved by increasing the amount of acetone in the solvent systems, as this solvent contains carbonyl oxygen, which can act as a strong hydrogen bond acceptor.[183] Similar elution systems containing high percentages of acetone have been used to recover large molecular weight procyanidins.[297]

In order to profile the size ranges of the individual Sephadex fractions from both *A. nodosum* and *F. spiralis* the samples were analysed using UPLC-MS. By individually tuning for theoretical molecular weights of phlorotannins and utilising the IntelliStart™ software suitable MRM fragments for each phlorotannin up to 16 PGUs in negative mode ionisation could be determined. From *A. nodosum* Sephadex fractions 14-17 it is evident that the oligomers, with molecular ions at *m/z* 373, 497 and 621 (corresponding to a DP of 3, 4 and 5), are the dominant peaks visible in these spectra (Figure 8). From fractions 18-25 it is evident that the phlorotannins that are eluting at these stages are larger oligomers with the dominant peaks observed possessing *m/z* of 745, 869, 1117 and 1365 (corresponding to a DP of 6, 7, 9 and 11). There is also a noticeable shift throughout the individual spectra from left to right

showing the polar nature of the fractions containing the oligomers and the less polar nature of the polymers.

From *F. spiralis* Sephadex fractions 8-17 it is evident that oligomers are present, as peaks with ions at *m/z* 497, 621 and 869 (equivalent to a DP of 4, 5 and 7), are the dominant peaks visible in these spectra (Figure 10). From fractions 18-22 onwards the larger phlorotannins seem to be the most prominent with the major peaks observed being at *m/z* 993, 1117 and 1241 (relating to a DP of 8, 9 and 10). The spectra for fractions 22-25 become quiet complex with a large number of significant peaks being observed for ions between *m/z* 1117 and1490 (corresponding DPs of between 9 and 12).

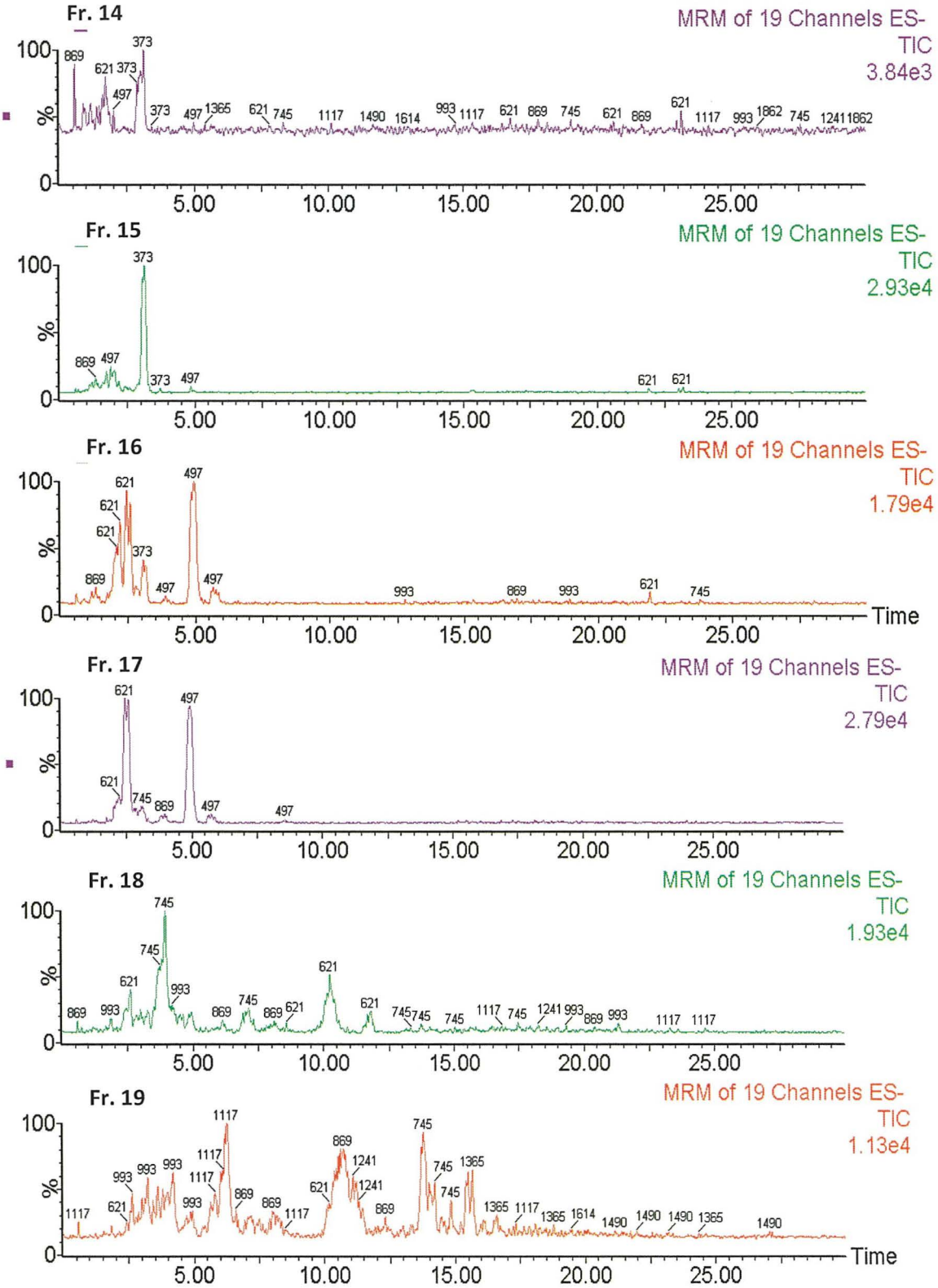

Figure 9: TQD-MS spectra of *Ascophyllum nodosum* EW Sephadex fractions 14-25.

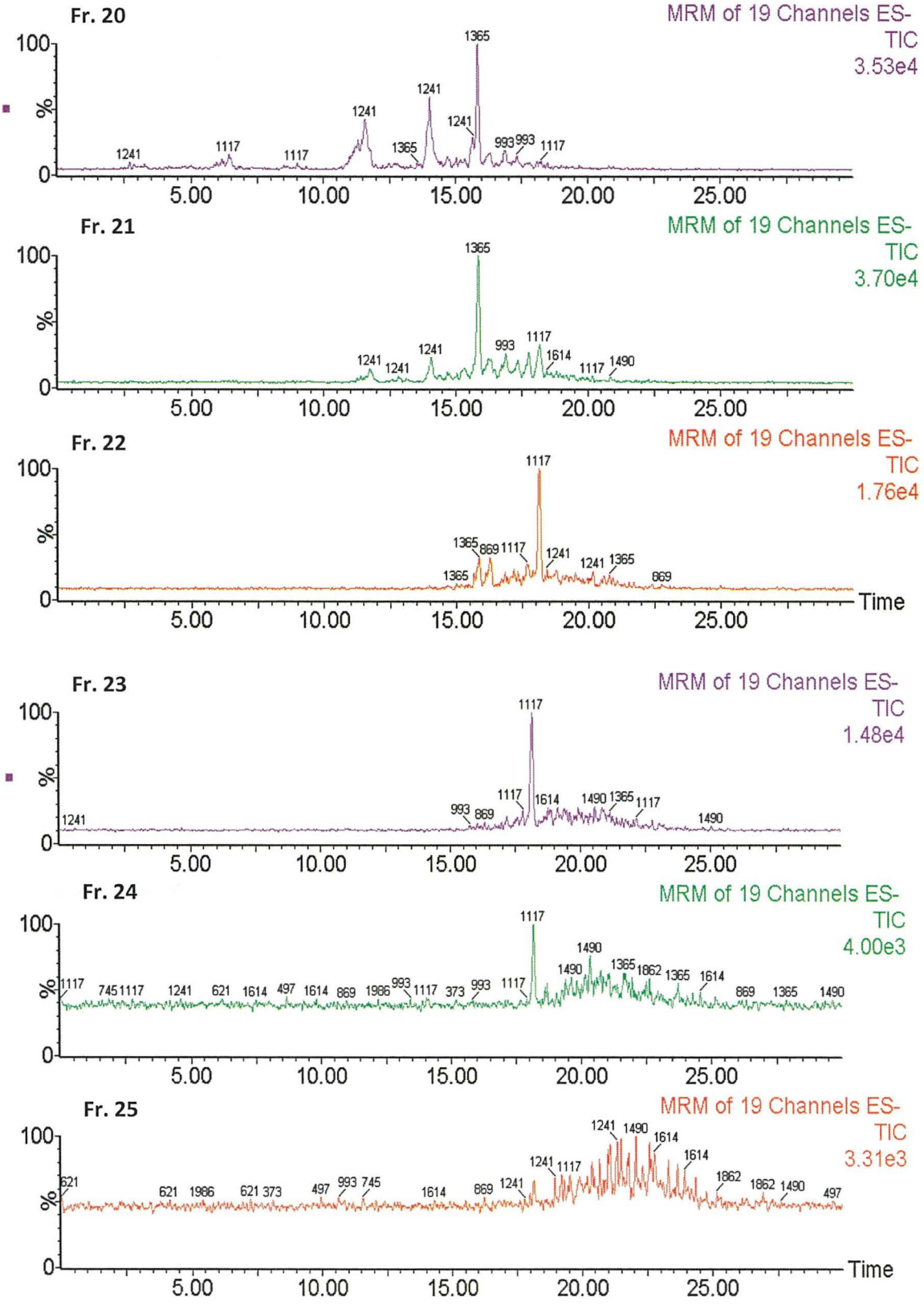

Figure 9: TQD-MS spectra of *Ascophyllum nodosum* EW Sephadex fractions 14-25.

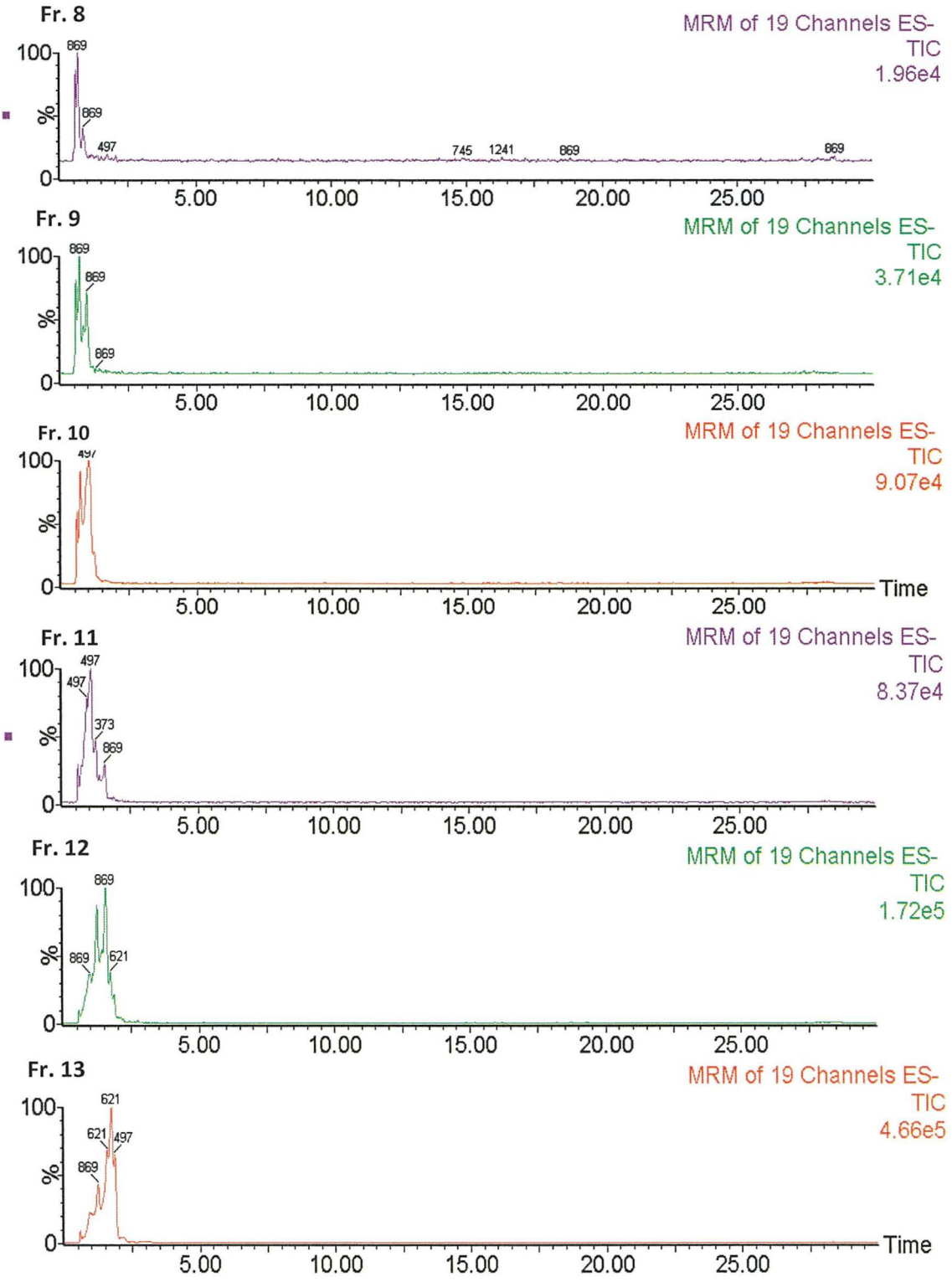

Figure 10: UPLC-TQD-MS spectra of *Fucus spiralis* water ethanol Sephadex fractions 8-25.

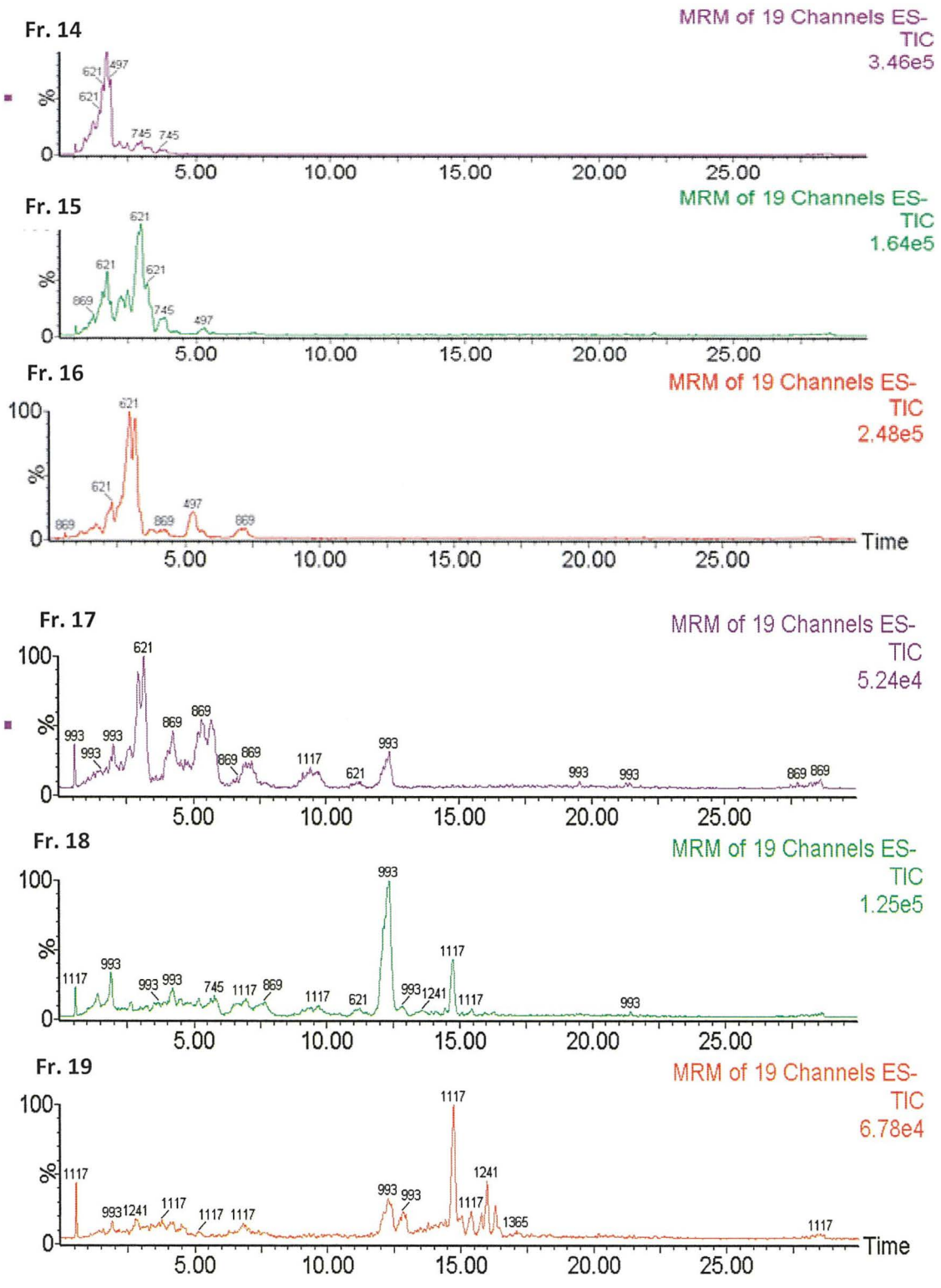

Figure 10: UPLC-TQD-MS spectra of *Fucus spiralis* water ethanol Sephadex fractions 8-25.

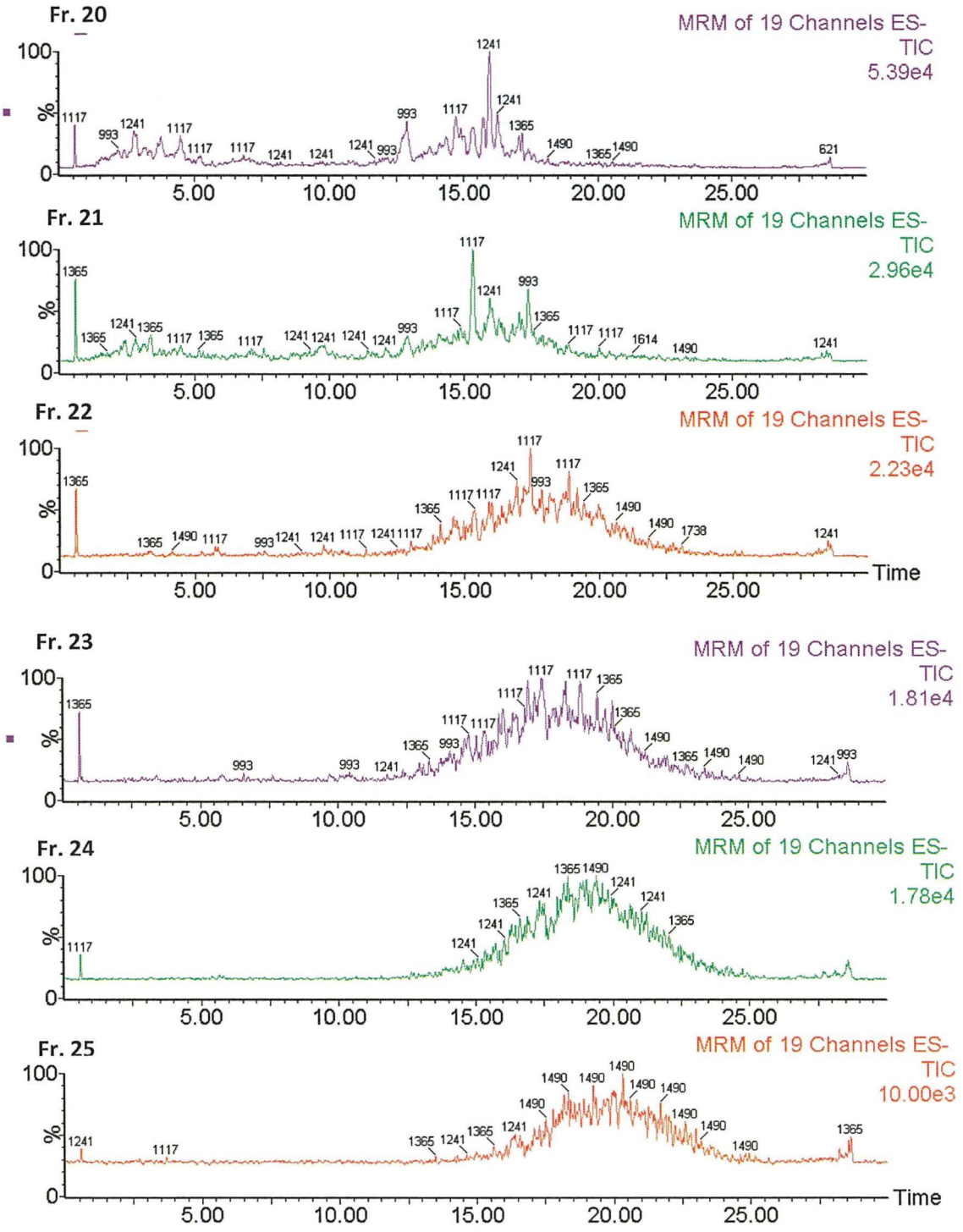

Figure 10: UPLC-TQD-MS spectra of *Fucus spiralis* water ethanol Sephadex fractions 8-25.

Analysis of the EICs of individual negative molecular ions ([M-H]$^-$) from the Sephadex fractions spectra allowed for the identification of multiple peaks corresponding to isomers for the following molecular weights of phlorotannin; 374 (DP of 3), 498 (DP of 4), 622 (DP of 5), 746 (DP of 6), 870 (DP of 7), 994 (DP of 8), 1118 (DP of 9), 1242 (DP of 10), 1366 (DP of 11), 1490 (DP of 12), 1615 (DP of 13), 1739 (DP of 14), 1863 (DP of 15) and 1987 Da (DP of 16). From the Figure 11(a) containing the percentage peak intensities for the *A. nodosum* Sephadex fractions, it can observed that for fractions 9-17 small phlorotannin oligomers of six or less monomers are dominant. In the case of fractions 14-17 oligomers of six or less units account for 90% of the peak intensities. From fraction 18 onwards polymers of seven or more monomers account for the majority of the peak intensity and in the case of fraction 22-25 phlorotannins of eleven or more monomers account for 50-80% of the peak intensity. The highest number of isomers detected at one particular molecular ion was 62 in fraction 18 at m/z 869, followed by 49 at *m/z* 1117 also in fraction 18.

Figure 11(b) shows the percentage peak intensities for the *F. spiralis* Sephadex fractions. For fractions 8-16 small phlorotannin oligomers of six or less monomers are most abundant. From fraction 17 onwards, similar to what was observed in *A. nodosum*, polymers of seven or more monomers are responsible for the majority of the peak intensities. In fractions 22 and 24-26 phlorotannins of eleven or more monomers account for 50-80% of the peak intensity, which matches what was found for the same group of fractions in *A. nodosum*. The highest number of isomers of 81 and 71 were detected in fraction 22 at the molecular ions of *m/z* 1614 and 1365 (equivalent to DP of 13 and 11, respectively). Seventy one isomers were also detected for a peak at *m/z* of 1614 in fraction 23.

This is the first report of the use of Sephadex LH-20 for the separation of phlorotannins from *F. spiralis* and, although Sephadex has been reported to have been used for *A. nodosum* previously a much simpler method where only two fractions (bound and unbound) were collected was employed.[14] The procedure employed in this study was an adaptation of a previous method used by Wang *et al.* (2012) to purify phlorotannins from *F. vesiculosus*.[178] The most noteworthy modification made was to increase the number of fractions collected due to the fact that *F. vesiculosus* is known to contain phlorotannins of much smaller size ranges than those found in *F. spiralis*

and *A. nodosum*,[298] and that more fractions would need to be collected to reduce their potential complexity and aid in the MS profiling. Although it is evident that Sephadex LH-20 was effective at separating phlorotannins based on molecular weight, the complexity within individual fractions remains high due to the high level of isomerisation (Figures 11(a) and 11(b)) in both species. Despite the fact such a meticulous and time-consuming Sephadex separation procedure was employed even the simplest fraction, for example fraction 9 in *A. nodosum* (Figure 9(a)), still contain numerous phlorotannins of different molecular weights.

(a)

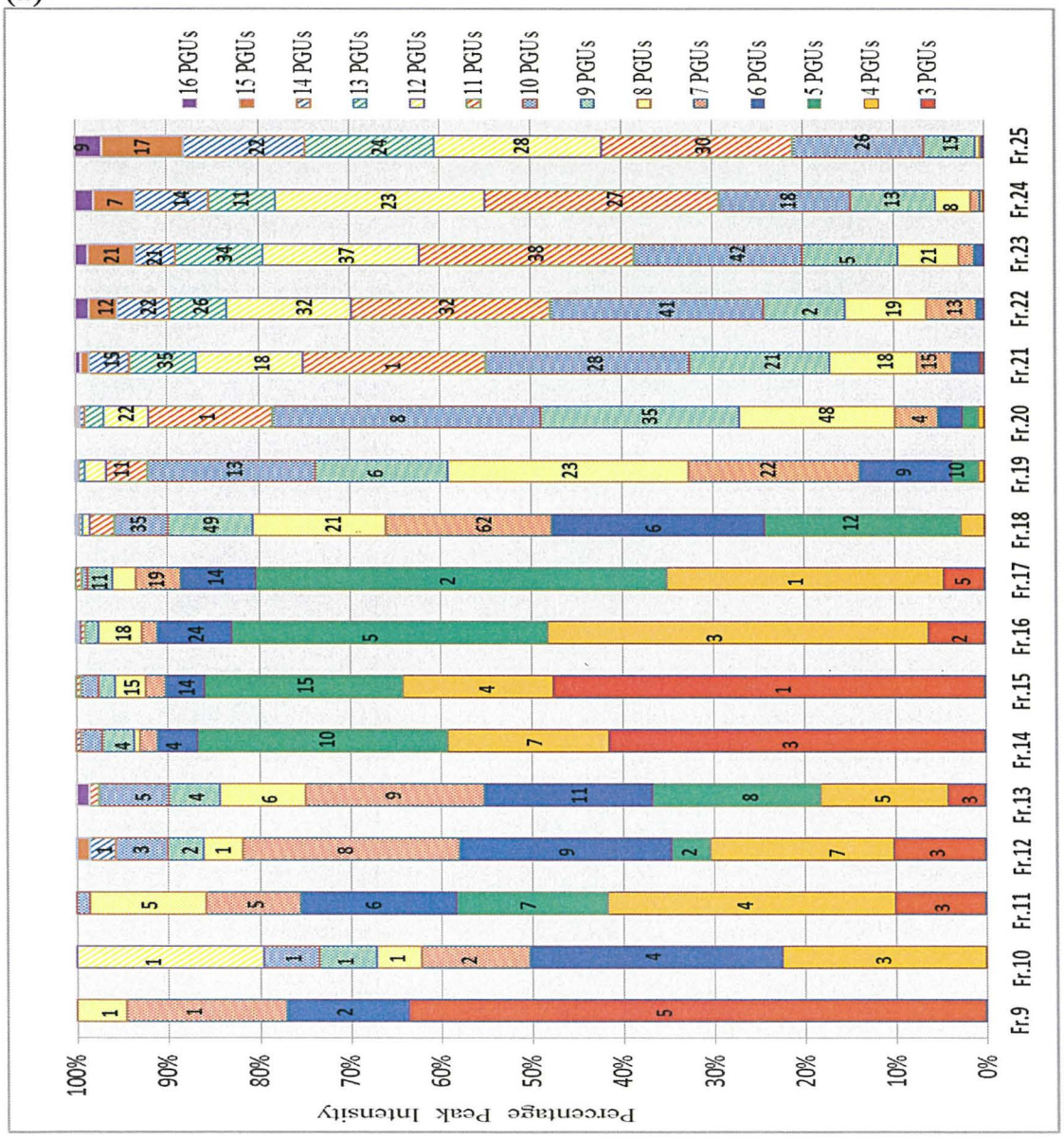

(b)

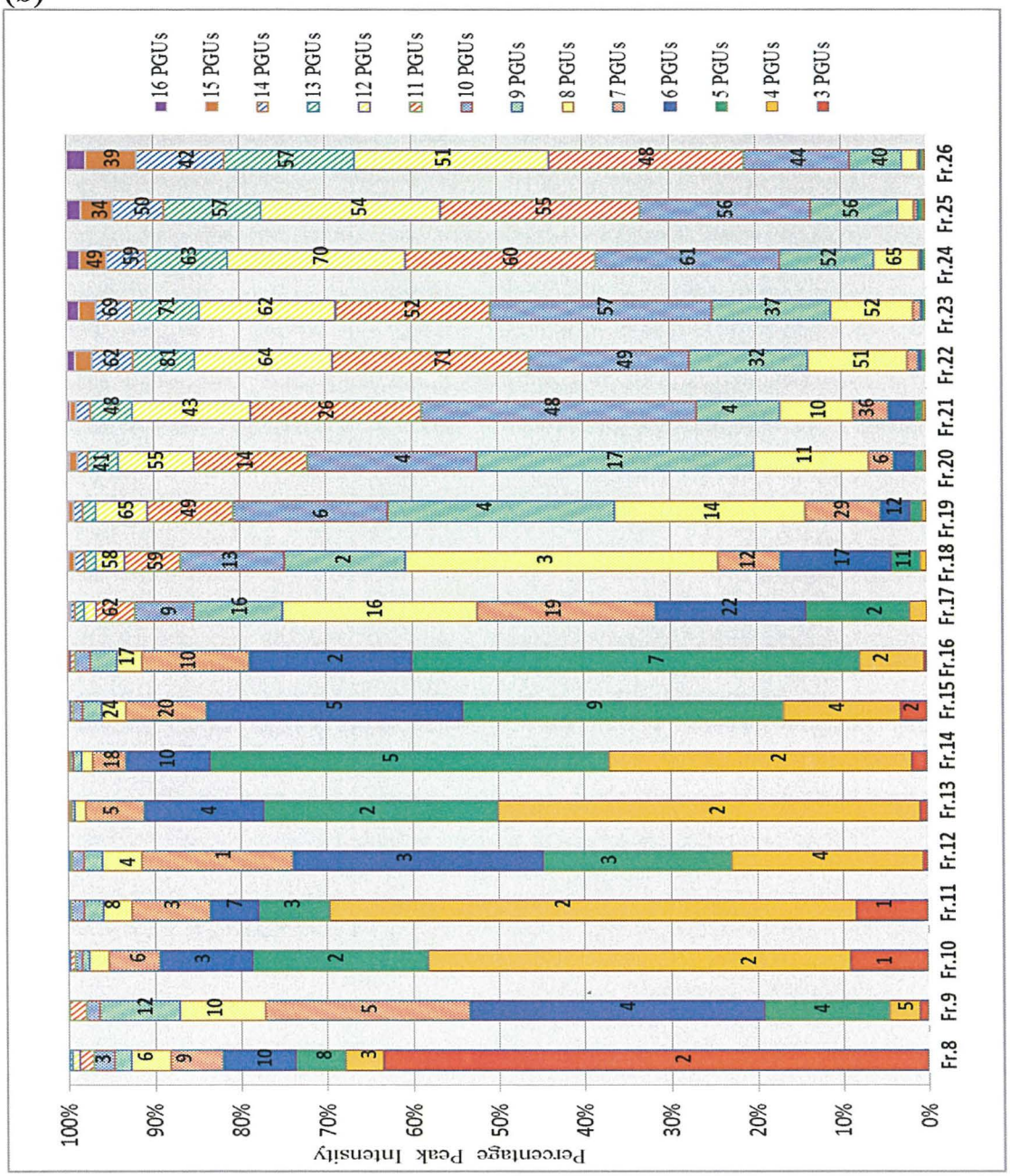

Figure 11: Bar chart showing the UPLC-MS percentage peak intensity for individual molecular ions (colour-coded) corresponding to phlorotannins of between 3 and 16 phloroglucinol units (PGUs) for the Sephadex fractions from (a) *A. nodosum* and (b) *F. spiralis* EW phlorotannin-enriched flash fractions. Isomers detected for each molecular weight are highlighted with bold numbers.

3.3.4 Radical scavenging activity of algal Sephadex LH-20 fractions

There are conflicting reports with regards the relationship between phlorotannin molecular size and antioxidant activity. Some reports suggest that antioxidant activity increases with increasing degrees of polyphenol polymerisation,[111] however, many have shown that there is no correlation between the DP and antioxidant activity.[110, 178, 299] In fact, there is evidence to suggest that the number of hydroxyl groups and ether linkages present, rather than DP, are the determining factors related to high antioxidant activity.[110]

The radical scavenging activities (RSAs) of the *A. nodosum* and *F. spiralis* EW Sephadex fractions against the DPPH· radical were determined. The fractions that exhibited UPLC-MS peaks corresponding to phlorotannins were assessed for their RSA. For *A. nodosum* fractions 7-29 were assayed for their antioxidant activity (Figure 12(a)). The antiradical powers (ARPs) for fractions 7-17 ranged between 10.00 and 21.57 ± 2.08, with a mean ARP of 15.67. On the other hand, fractions from 18-28 display a mean ARP of 30.12; the highest ARP observed being 36.43 ± 2.95 from fraction 22. In fraction 22 the most prominent peak is at *m/z* 1117, corresponding to a DP of 9. The ARP then dropped down to 13.27 ± 1.06 for the final fraction 29. When the antioxidant activity is compared with the molecular ions detected by UPLC-MS for each fraction, it would appear that the antioxidant activity is related to the molecular size of the phlorotannins present. However, the increased RSA may also be due to increased numbers of hydroxyl groups in the latter fractions and, if some of the *A. nodosum* phlorotannins are of the phlorethol class, increased number of ether linkages.[110]

For *F. spiralis* fractions 4-29 were assayed for their antioxidant activity (Figure 12(b)). The mean ARP of fraction 4-14 was 31.73, whereas fraction 6 which had an ARP of 52.64 ± 4.53. Fractions 15-28 displayed a mean ARP of 47.54, with the highest ARP observed being 64.50 ± 4.61 from fraction 23, where the most dominant peak was at *m/z* 1117. Again, the ARP then dropped down to 17.62 ± 1.15 for the final fraction 29. The *F. spiralis* Sephadex fraction again generally appear to follow the trend that the fractions with high molecular weight phlorotannins tend to have better RSAs. Conversely, it should be noted that Sephadex fraction 16, for which

the prominent peak detected was at *m/z* at 621 (equivalent to an oligomer of 5 monomers) displayed the second highest ARP. This finding supports the previous suggestions that antioxidant activity for phlorotannins is not directly related to molecular size.[110, 299] At least seven different phlorotannins possessing a molecular weight of 622.5 Da have been characterised from brown macroalgae, varying in their number of hydroxyl groups, number of ether linkages and/or structural conformation.[300-303] In addition to this, from Figure 11(b) it is visible that 22 isomers were detected for this molecular weight in Sephadex fraction 17 of *F. spiralis*. So it could proposed that the phlorotannins of 622.5 Da in fraction 16 may have a higher number of hydroxyl groups and/or ether bonds, or may differ in its structural conformation,[110] from phlorotannin isomers of the same molecular weight in earlier fractions. These potential differences may then be responsible for the increase in RSA observed for that fraction.

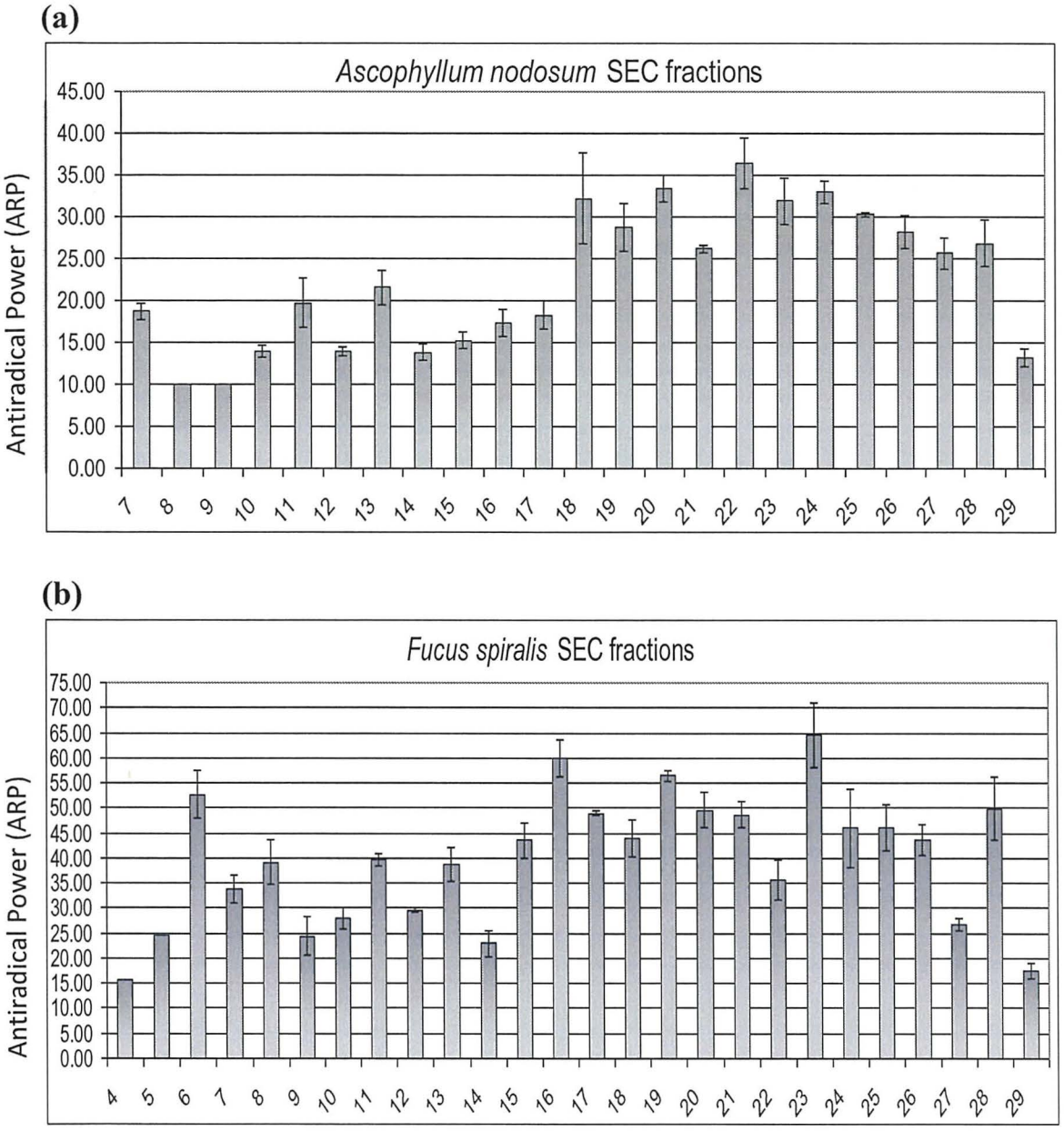

Figure 12: DPPH· radical scavenging activity (RSA) of the Sephadex fractions from (a) *Ascophyllum nodosum* and (b) *Fucus spiralis* ethanol water phlorotannin-enriched flash fractions, expressed as antiradical powers (ARPs) ± standard deviation (n=3).

3.3.5 Angiotensin converting enzyme I (ACE-I) inhibitory activity of algal Sephadex fractions

Brown algal phlorotannins have also been reported to have angiotensin converting enzyme I (ACE-I) inhibitory properties,[112, 125] in addition to antioxidant activity. Both of these bioactivities could provide evidence for the development of potential antihypertensive therapeutic agents. Research into the SAR of phlorotannins and ACE inhibition is limited, however, it has been suggested that a closed-ring dibenzodioxin moiety and/or a dibenzofuran ring may be crucial to the ACE-inhibitory activity.[112]

Captopril, a potent synthetic ACE inhibitor, was used as a positive control as it is a widely used ACE-inhibitor,[304] and in this work the percentage ACE inhibition of this compound was 90.09 ± 2.3 % at 0.0043 μg mL^{-1}. The IC_{50} for captopril was found to be 0.0015 μg mL^{-1} which is consisted with what has been found previously.[305] The percentage inhibitions of the *F. spiralis* Sephadex fractions at 250 μg mL^{-1} ranged from 7.18 ± 3.44 % to 61.31 ± 4.23 %, with fraction 25 (250 μg mL^{-1}) displaying the highest ACE inhibition (Figure 13). The inhibition of fraction 25 is good relative to what has been reported previously for some pure phlorotannins isolated from the *Ecklonia* species. For example Jung *et al.* (2006) tested phlorotannin compounds of varying DP from *Ecklonia stolonifera* for their ACE inhibitory activity with a method where N-[3-(2-Furyl)acryloyl]-Phe-Gly-Gly (FAPGG) was employed as the ACE substrate. Eckstolonol (DP of 2), eckol (DP of 3), phlorofucofuroeckol A (DP of 4), dieckol (DP of 5) and triphlorethol-A (DP of 6) displayed IC_{50}s of 410.12 ± 63.07 μM (151 μg mL^{-1}), 70.82 ± 0.25 μM (26 μg mL^{-1}), 12.74 ± 0.15 μM (7.7 μg mL^{-1}), 34.25 ± 3.56 μM (25 μg mL^{-1}), and 700.9 ± 132.2 μM (262.1 μg mL^{-1}), respectively.[112] The phlorotannins with the highest inhibition, eckol, dieckol and phlorofucofuroeckol A possess dibenzodioxin links and the latter also contains a dibenzofuran ring.

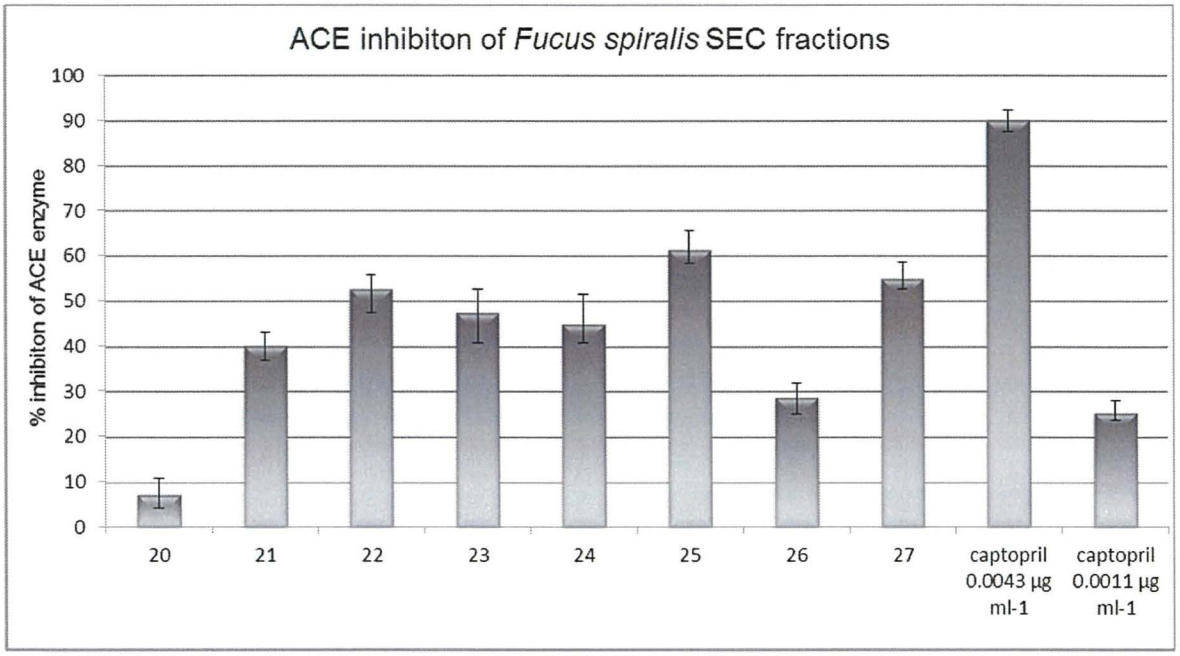

Figure 13: Angiotensin converting enzyme (ACE) inhibition by the Sephadex fractions 20-27 from *Fucus spiralis* ethanol water phlorotannin-enriched flash fractions (n=2) and the positive control captopril (n=3) at 0.0043 and 0.0011 µg mL^{-1}, expressed as percentage inhibition ± standard error.

Eckstolonol, triphlorethol, eckol and dieckol, along with phloroglucinol, isolated from *Ecklonia cava* were also assayed for their ACE inhibition where HHL was used as the ACE substrate and they gave IC_{50}s of 2.95 mM (1.09 mg mL^{-1}), 2.01 mM (0.75 mg mL^{-1}/mL), 2.27 mM (0.84 mg mL^{-1}), 1.47mM (1.09 mg mL^{-1}) and 2.57 mM (0.32 mg mL^{-1}), respectively.[125] These values are much higher than the values reported by Jung *et al.* (2012) and this may be due to the differences in the methods employed.

This is the first report of ACE inhibitory bioactivity from *F. spiralis* and although previous reports in this area seem to have dealt with predominantly small oligomers, the fractions that show inhibition of 50% or more (fraction 22, 25 and 27) in this study contain 9 and 12 monomers. If feasible it would be necessary to further purify these fractions to isolate the individual phlorotannins from the complex mixtures and observe if the ACE inhibitory activity can be further improved. Fraction 25 also displayed relatively good RSA activity which is highly favourable as it is widely believed that compounds possessing both antioxidant and ACE-inhibitory activity have improved potential of becoming antihypertensive therapeutics.[76]

3.3.6 ^{1}H Nuclear Magnetic Resonance (NMR)

Throughout this chapter UPLC-MS has been the method of choice to confirm the presence of phlorotannins by the consistent detection of molecular ions that correlate to particular phlorotannins. NMR was employed to emphasise the presence of the aromatic regions in each of the three brown macroalgae. The NMR spectra for *A. nodosum*, *P. canaliculata* and *F. spiralis* can be viewed in Figure 12 and they all show signals between the 5.7-6.5 ppm region characteristic for phlorotannins.[111] *A. nodosum* (Figure 14(a)) and *P. canaliculata* (Figure 14(b)) display very similar NMR profiles with the main aromatic region showing between 5.9 and 6.4 ppm. Parys *et al.* (2009) reported ^{1}H NMR signals for *A. nodosum* phlorotannins between 6.0 and 6.3 ppm.[306] The *F. spiralis* profile (Figure 14(c)) also has an aromatic region between 5.9 and 6.4 ppm, however, the profile appears to be different to the other two species and it also contains an extra aromatic region between 7.2 and 7.4 ppm. Full NMR profiles are provided in Appendix 2. NMR, in addition to MS, may be a useful tool for the metabolite profiling of macroalgal extracts and fractions, as it has been shown before that *F. spiralis* fractions separated from an extract with different solvents give very different ^{1}H NMR profiles.[111]

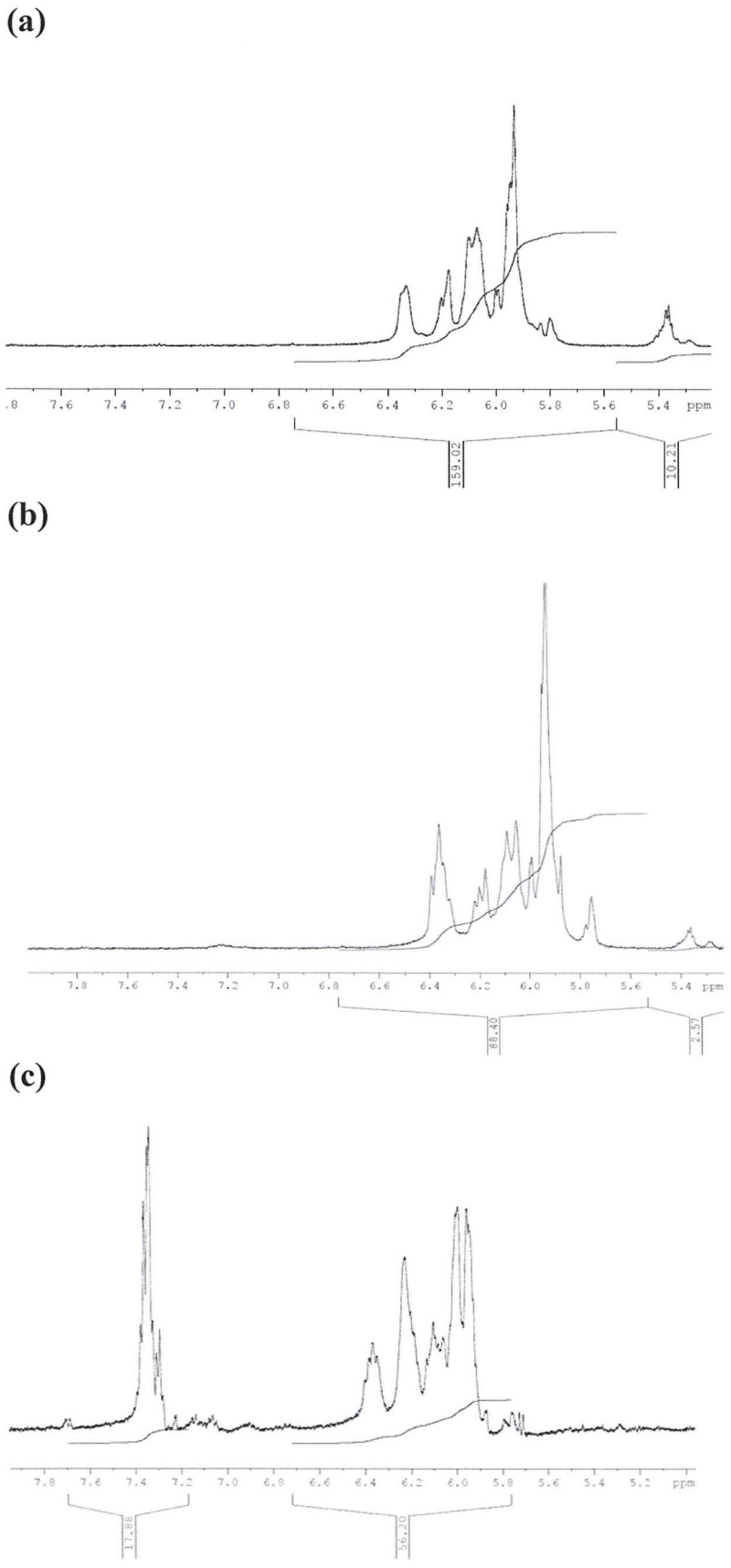

Figure 14: ^{1}H NMR spectra for phlorotannin-enriched reverse-phase flash fractions from (a) *A. nodosum*, (b) *P. canaliculata* and (c) *F. spiralis*.

Chapter 4 – Extraction, separation and detection of antihypertensive peptides from *Ascophyllum nodosum*.

4.1 Introduction

The previous chapters have dealt predominantly with the extraction, separation and profiling of phlorotannins that occur in abundance in brown macroalgal species. Macroalgae have also been identified as good sources of bioactive peptides,[307-308] although studies pertaining to the purification of peptides from brown species are sparse and, to date, have been predominantly limited to *Undaria pinnatifida*.[16, 80] Therefore, the focus of this chapter was to extract, purify and identify peptides from the brown macroalga *A. nodosum* with antihypertensive and antioxidant properties.

Hypertension is the most common chronic health problem and currently affects 20-30 % of all adults.[66] The renin-angiotensin system (RAS) plays a pivotal role in the pathogenesis of hypertension.[7] In this pathway the conversion of angiotensinogen to angiotensin I is catalysed by the enzyme renin and the conversion of angiotensin I to the vasoconstrictor angiotensin II is catalysed by the angiotensin-converting enzyme I (ACE-I) resulting in an increase in blood pressure.[68] Furthermore ACE-I is involved in the inactivation of the vasodilator bradykinin and, therefore, this also contributes to an increase in blood pressure.[309] Therefore, both the renin enzyme and ACE present good targets for anti-hypertensive agents. In addition, it is widely believed that oxidative stress may be a cause or product of hypertension and,[310] therefore, the isolation of agents with antihypertensive and antioxidant properties would be beneficial. Bioactive peptides (BP) derived from many sources have demonstrated the ability to inhibit both renin and ACE and are, therefore, good candidates as potential anti-hypertensive agents.[78-79, 311]

Various types of marine-derived protein hydrolysates and peptides have been shown to exhibit antihypertensive[148, 308] and antioxidant activities.[312] The amino acid composition of marine proteins differs to that of terrestrial-based proteins due to their varying ecological environments, consequently, marine proteins potentially contain novel BPs.[313] The protein content found within macroalga exists in a diverse range of forms and cellular locations and can vary widely depending on species, season and nutrient availability.[314] The protein content of brown macroalgae has previously

reported to generally range between 6 and 13 % dry weight,[315-316] but some specific brown species, such as *Undaria pinnatifida,* have reported to have higher contents.[317] However, the protein content of brown macroalgae tends to be lower in comparison to the contents found in green and red macroalgae.[318] Due to their relatively high protein content the extraction and isolation of protein and BPs from red macroalgae has been extensively investigated,[150, 307, 319] however, studies relating to the extraction of BPs from brown macroalgae are not as widespread, with *Undaria pinnatifida* being the species of focus in this group.[16, 80]

Enzymatic hydrolysis has become the method of choice for the release of BPs from protein as it is environmentally safe and allows for targeted peptide production.[313] The biological properties of BPs extracted by enzymatic hydrolysis can be affected in various ways depending on a number of factors including; the type of enzyme used for hydrolysis, the processing settings and the size and the composition of the amino acids present in the parent protein. This technique has also been shown to have the potential for scale-up for industrial applications, whilst preserving peptide profiles and bioactivity of resultant peptides.[135]

BPs possess beneficial pharmacological properties beyond normal and adequate nutrition that can be available either directly through their presence in the intact food itself or after their release from the respective host proteins by hydrolysis in vivo or in vitro.[128] They usually contain 3–20 amino acids and the type and level of bioactivity they possess generally depends their amino acid composition and sequence.[320] BPs exhibiting varying bioactivities have been extracted from a range of marine sources such as salmon,[129] shark meat,[321] squid[130] and macroalgae,[322] and some have been incorporated into functional foods.

The objective of the present chapter was to examine an under-exploited potential source of BP's (*A. nodosum*) and to identify food-friendly scaleable techniques to isolate and purify them from their natural sources.

4.2 Experimental

4.2.1 Reagents and Materials

All solvents used were HPLC-grade. Ferric chloride, 2,4,6-tris(2-pyridyl)-s-triazine (TPTZ), 6-hydroxy-2,5,7,8-tetramethylchroman-2-carboxylic acid (Trolox), captopril, QuantiPro™ BCA Assay Kit and Amicon Ultra-15 Centrifugal Filter Units with 10kDa cut off were obtained from Sigma-Aldrich Chemical Co. (St. Louis, MO, USA). BioDesignDialysis Tubing™ with 3.5 kDa cut-off was acquired from Fisher Scientific. Renin inhibition screening assay kits were acquired from Cayman Chemical Company (Ann Arbor, MI 48108). The renin inhibitor Z-Arg-Arg-Pro-Phe-His-Sta-Ile-His-Lys(Boc)-OMe was obtained from Bachem (4416 Bubendorf, Switzerland). ACE inhibition kits – WST were obtained from NBS Biologicals Ltd. (Cambridgeshire, England, PE29 7DT). Agilent SuperFlash™ SF25-55g C18 columns were obtained from Apex scientific (Maynooth, Ireland).

Ascophyllum nodosum used in this study was harvested in Spiddal, Co. Galway, Ireland in November 2011.

4.2.2 Extraction and recovery of macroalgal protein concentrates

The harvested macroalgal material was washed to remove sand and epiphytes. The material was then freeze-dried and ground into a fine powder using a Waring® blender (New Hartford, CT, USA) and stored in vacuum packed bags at -80 °C prior to extraction. The extraction of protein from *A. nodosum* was carried out according to a previously described method,[323] with some modifications.

Macroalgal powder (40 g) was suspended in HPLC-grade water (800 mLs) (1:20 w/v). The suspension was sonicated for 1 hour in an ultrasonic bath, in order to enhance protein release by causing structural disruption of the macroalgal powder,[324] and then shaken overnight in a water bath set to 35 °C. The macroalgal mixture was clarified by centrifugation at 4 °C and 10,000 g for 40 minutes. The pellets were combined and suspended in 400 mL of HPLC-water and subjected to a second extraction procedure as described above. The supernatants from both extractions were pooled and protein precipitation was carried out at 4 °C. The precipitation involved

bringing the supernatant to 80 % ammonium sulfate saturation, stirring for an hour and then leaving to stand for another hour. The mixture was then centrifuged using the conditions described above. The protein rich pellet was suspended in a minimal volume of distilled water and dialyzed overnight with a 3.5 kDa membrane. The retentate, containing the protein concentrate, was freeze-dried.

4.2.3 Reduction, alkylation and trypsin digestion of protein concentrates

Reduction and alkylation of the *A. nodosum* protein was carried out to destabilise cysteine linkages present.[325] The reduction and alkylation of the *A. nodosum* protein concentrate were carried using a method similar to one described previously,[326] with some modifications. The protein concentrate was dissolved in minimal water. The dissolved algal sample, aqueous ammonium bicarbonate (1M), dithiothreitol (DTT) (100 mM) (reduction step), acetonitrile, iodoacetamide (200 mM) (alkylation step) and 1 % formic acid were combined at a ratio of 12:1:1:12:1.2:5. The mixture was incubated at room temperature in the dark for 20 minutes prior to the addition of the 1 % formic acid. The reduced samples were centrifuged in 10 kDa cut-off filter units to almost dryness. The retentate was rinsed twice with water and re-centrifuged to remove solvents. The greater than 10 kDa retentate was freeze-dried.

Digestion of the reduced macroalgal sample was carried out by first dissolving it in 50 mM sodium phosphate buffer and then digesting it the using bovine trypsin at a pH of 8.0 and 37 °C.[327] The substrate: trypsin enzyme ratio was 50:1 w/w.[328-329] The pH of the mixture was altered to its optimal pH value prior to enzymatic hydrolysis. The enzymatic reaction was carried out for 8 hours at 37 °C in a shaking water-bath. The digests were boiled at 99 °C for 10 minutes to denature the trypsin enzyme and centrifuged with 10 kDa cut-off tubes. The less than 10 kDa digested sample was freeze-dried

4.2.5 Separation of A. nodosum digest by C18 flash chromatography

Reverse-phase C18 flash chromatography was carried out on the less than 10 kDa digest fraction. The fraction was first dissolved in a minimum (approx. 5-10 mLs) volume of water containing 0.1 % trifluoroacetic acid (mobile phase A) and loaded onto a SuperFlash™ SF25-55g C18 column. The flash chromatography run-

time was 30 min and was performed using a gradient of 0–100 % mobile phase B (acetonitrile containing 0.1 % trifluoroacetic acid) as follows; 0 % B, 0–2 min; 0-10 % B, 2–4 min; 10-20 % B, 4–6 min; 20-50 % B, 6–21 min; 80 % B, 21–25 min; 100 % B, 25–30 min. The flow rate was 30 mL min^{-1} and fractions were collected every minute.

4.2.6 Liquid Chromatography-Tandem Mass Spectrometry (LC-MS/MS) conditions

The analysis of the *A. nodosum* digest flash fractions was carried out on a nanoACQUITY UltraPerformance LC® coupled to an electrospray ionization quadrupole time-of-flight (ESI-QTof) Premier mass spectrometer (Waters Corporation, Manchester, UK). Selected flash fractions were dissolved in deionised water containing 0.1% formic acid (mobile phase A) and loaded onto a Symmetry® C18 nanoAcquity Trap (100Å, 5 µm, 180 µm X 20 mm) followed by an Acquity BEH300 PST C18 column (300Å, 1.7 µm, 1 mm X 100 mm) on the LC system with an injection volume of 2 µL and flow rate of 300 nL min^{-1}. The LC separation run-time was 80 min and was performed using gradient of 0–100 % mobile phase B (acetonitrile containing 0.1% formic acid) with the following gradient; 5 % B, 0–2 min; 5-15 % B, 2–5 min; 15-20 % B, 5–20 min; 20-30 % B, 20–60 min; 30-70 % B, 60–63 min; 70-2 % B, 63–65 min; 2 % B, 65–80 min. The elution from the LC was analysed in positive ES mode with the following parameters; capillary voltage, 1.4 kV; sampling cone voltage, 45 kV; desolvation gas, 400 L hr^{-1}; source temperature, 120 °C; desolvation temperature, 350 °C; nanoflow gas pressure, 0.5 bar. Initial nano-LC-MS/MS data were recorded using the data directed analysis (DDA) mode and later MS/MS were performed by manual selection of the molecular ions. The collision energy ranged from 150 eV TO 60 eV where the lowest energy was applied for low molecular weight species and the higher collision energy for the larger molecules. De novo sequencing of the peptides was achieved with the aid of Waters PepSeq software and was carried out by Dr. Dilip Rai (Teagasc Food Research Centre, Ashtown, Dublin 15). Peptide sequences obtained from the de novo sequencing were searched using the BLAST facility on the online database UniProt (http://www.uniprot.org) in an attempt to identify the protein origin.

4.2.7 Synthesis of identified A. nodosum peptides

This work was carried out by Paula O'Connor (Teagasc Food Research Centre, Moorepark, Fermoy, Co. Cork). Peptides were synthesised on Fmoc-amino acid Wang resins (Matrix Innovation, Quebec, Canada) using Microwave-assisted Solid Phase Peptide Synthesis (MW-SPPS) performed on a Liberty^{TM} CEM microwave peptide synthesiser. Synthetic peptides were purified using RP-HPLC on a C18 Vydac (10 u, 300A) column (Vydac, California, USA) and peptides were eluted using peptide specific acetonitrile 0.1 % TFA gradients run over 40 minutes. Fractions containing the desired molecular mass were identified using MALDI-TOF mass spectrometry and were pooled and lyophilised on a Genevac HT 4X (Genevac Ltd. Ipswitch, UK) lyophiliser.

4.2.7 Protein content determination

The protein content of the *A. nodosum* digest flash fractions was determined using the QuantiPro^{TM} bicinchoninic acid (BCA) assay kit and carried out in accordance to the manufacturers' protocol. The BCA colorimetric assay is similar to the Lowry protein assay in principle,[330] as both assays rely on the formation of a Cu^{2+}-protein complex under alkaline conditions, followed by reduction of the Cu^{2+} to Cu^{1+}.[331] The level of Cu^{2+} reduction is proportional to the protein present. The assay involves mixing 1 part of a test sample with 1 part of prepared QuantiPro working reagent. The QuantiPro working reagent is a mixture of reagent QA, reagent QB and reagent QC (copper (II) sulphate) in a ratio of 25:25:1, respectively. The test sample refers to a blank sample, a protein standard (bovine serum albumin (BSA)) or an unknown *A. nodosum* fraction. BSA protein standards were prepared ranging from 0.5-30 μg mL^{-1}.

A test sample (150 μL) and QuantiPro working reagent (150 μL) were added to individual wells of a 96-well microplate. The microplate was incubated at 60 °C for minutes. The absorbance was read at 562 nm on the plate reader. The protein concentration of the *A. nodosum* fractions, expressed as μg BSA equivalents mL^{-1}, was calculated from the BSA standard curve.

4.2.8 Measurement of the antioxidant activity of C18 flash peptide fractions

Ferric reducing antioxidant power (FRAP)

The ferric reducing antioxidant power (FRAP) of each of the macroalgal C18 flash fractions, at a concentration of 250 μg mL^{-1}, was assayed in triplicate according to a previously described method with slight modifications.[332] The oxidant in the FRAP assay consisted of a reagent mixture that was prepared prior to use by mixing acetate buffer (pH 3.6), ferric chloride solution (20 mM) and TPTZ solution (10 mM TPTZ in 40 mM HCl) in the ratio of 10:1:1, respectively. The FRAP reagent was heated, while protected from light, until it had reached a temperature of 37 °C. A trolox standard curve, using standard concentrations of 0.1 mM-0.5 mM, and two-fold dilutions of the macroalgal stock samples (1.5 mg mL^{-1}) were prepared. The assay mixture contained 20 μL of MeOH (blank), diluted sample or standard and 180 μL of FRAP reagent in a microplate. The absorbances were measured at 593 nm after 50 minutes on an automated FLUOstar Omega microplate reader system (BMG LABTECH GmbH, Germany). The trolox standard curve was used to calculate the antioxidant activity of the samples and was expressed as microgram trolox equivalents (TE) per milligram of sample (μg TE mg^{-1}).

4.2.9 Measurement of renin inhibitory activity of C18 flash peptide fractions

The assay was carried out according to the suppliers' protocol. A 50 mM Tris-HCL buffer (pH 8.0, containing 100 mM NaCl) was prepared. A supplied solution of human recombinant renin enzyme was diluted 1:20 with the assay buffer. The renin substrate Arg-Glu(EDANS)-Ile-His-Pro-Phe-His-Leu-Val-Ile-His-Thr-Lys(Dabcyl)-Arg in DMSO was supplied in a ready to use form. The assay buffer was pre-warmed to 37 °C before assaying. Background wells, full activity wells and positive control inhibitor wells were tested in triplicate. Z-Arg-Arg-Pro-Phe-His-Sta-Ile-His-Lys(Boc)-OMe at 1 μM (1.5 μg mL^{-1}) was used as the positive control. *A. nodosum* flash fraction wells were tested in duplicate at 250 μg mL^{-1} concentrations. The background wells consisted of 20 μL substrate, 160 μL assay buffer and 10 μL methanol. The full activity wells consisted of 20 μL substrate, 150 μL assay buffer, 10 μL methanol. The inhibitor wells contained 20 μL substrate, 160 μL assay buffer and 10 μL of sample. The reaction was initiated 10 μL of renin to the full activity well and

inhibitor wells. The plate was covered and incubated at 37 °C for 15 minutes. The fluorescence of the wells was read using the FLUOstar Omega microplate reader system at the excitation wavelength of 340 nm and emission wavelength of 500 nm. The percentage renin inhibition was calculated using the following formula:

$$\left(\frac{A_{\text{Full enzyme activity}} - A_{\text{Inhibitor}}}{A_{\text{Full enzyme activity}}} \right) \times 100$$

4.2.10 Measurement of angiotensin converting enzyme I (ACE-I) inhibitory activity of C18 flash peptide fractions

The assay was carried out according to the suppliers' protocol. The enzyme working solution and indicator working solution were was prepared as outlined by supplier protocol. Reagent blank wells, full activity wells and positive control inhibitor wells were tested in triplicate. Captopril at 0.02 μM (0.004 μg mL^{-1}) was used as a positive control. *A. nodosum* flash fraction wells were tested in duplicate at 250 μg mL^{-1} concentrations. The reagent blank wells consisted of 40 μL deionised water and 20 μL substrate buffer. The full activity wells consisted of 20 μL deionised water, 20 μL substrate buffer and 20 μL enzyme working solution. The inhibitor wells contained 20 μL positive control/sample, 20 μL substrate buffer and 20 μL enzyme working solution. The plate was incubated at 37 °C for an hour. Then 200 μL indicator solution was added to each well and incubated again at room temperature for ten minutes. The absorbance of the wells was read at 450 nm with a microplate reader. The percentage ACE-I inhibition was calculated using the following formula:

$$\left(\frac{A_{\text{Full enzyme activity}} - A_{\text{Inhibitor}}}{A_{\text{Full enzyme activity}} - A_{\text{Reagent blank}}} \right) \times 100$$

4.3 Results and Discussion

4.3.1 Extraction and separation of A. nodosum peptide-enriched samples

Following the protein extraction of the *A. nodosum* sample we obtained a yield of 2.2-4.7 %. This range is low in comparison to what has been found before where *A. nodosum* has reported protein contents of 3.4-6 %,[333] 6.1 %,[334] 5-10 %,[335] 6.8-11 %,[336] and 5-12 %.[27] The low protein content may be related to fact that the macroalgal material was harvested in the winter season (November) when habitat temperatures were low. Variation in macroalgal protein content can depend on changes in temperature, salinity concentrations and nutrients. For example, Marinho-Soriano *et al.* (2006) found that, following the observation of the protein content of the brown macroalga *Sargassum vulgare* over a year, that protein content significantly varied ($p < 0.01$) and that there was a negative correlation between protein content with temperature and salinity.[337]

The use of enzymatic hydrolysis is advantageous for generating peptides as it mimics to some degree what occurs in the human digestion of proteins and, therefore, yields information about the potential peptides that may be produced *in vivo*.[174] The use of exogenous enzymes, as opposed to the use of endogenous enzymes under controlled conditions of temperature and pH, results in reduced hydrolysis times and more predictability in terms of the sites of peptide cleavage and peptide composition.[136] Protein hydrolysates of many plant and animal proteins contain bioactive peptides however, the composition, number and order of amino acids found in peptides determines what bioactivity they possess and the strength of the activity.[139] For that reason, the type of hydrolytic enzyme used and the hydrolysis conditions can affect the type and efficiency of antioxidant peptides generated.[139-140] Proteases such as alcalase, protamex, pepsin, trypsin, α-chymotypsin, neutrase and papain have all been employed for the generation of antioxidant peptides from various marine sources.[136] Autolysis, using the endogenous enzymes of the food source to produce peptides, is also sometimes useful; however, it is a much slower process in comparison to hydrolysis by specific enzymes and generates more random peptides.[136, 338]

The occurrence of disulfide bonds created by cysteine residues allows proteins to fold and can make difficult for digestion enzymes to reach target bonds. Therefore, the reduction and alkylation of the *A. nodosum* protein was carried out to destabilise cysteine linkages present and to improve the degree of protein digestion by trypsin.[325]

Following the hydrolysis of food proteins to yield peptides, often further processing is necessary in order to enhance the BPs concentration and, therefore, boost bioactivity and facilitate characterisation. Hence, peptides are often fractionated based on their size, charge or hydrophobic nature, or a combination of these properties.[339] In this chapter, the trypsin digest was purified using a 10 kDa membrane cut-off and the less than 10 kDa fraction was further purified using reverse phase flash chromatography. Lower molecular weight BP's were targeted in the present study as they tend to be more resistant to further in vivo proteolytic digestion and, consequently, are more likely to reach the target tissue with bioactivity intact then their high molecular weight counterparts.[131] Membrane cut-off ultrafiltration has been employed in other studies to fractionate peptides, into < 1, 1-3, 3-5 and 5-10 kDa fractions, derived from purple sea urchin using the proteases neutrase, trypsin, papain and pepsin.[133] The study found that all samples possessed antioxidant activity in the in vitro DPPH· radical scavenging and FRAP assays, however the less than 1kDa fractions had the highest activities.[133] Where the potential to utilize food-derived BPs commercially exists, such as their use as functional food ingredients,[128] it is important to consider that the peptide processing methods employed must be industrially relevant. In this study, both the protein precipitation and enzymatic digestion are food-friendly processes and have the potential to be suitably scaled up for industry.

Flash chromatography was employed to purify the trypsin digest further by removing any sugars still present and to generate fractions enriched with *A. nodosum* peptides. Sugars are polar compounds and, therefore, a reverse-phase chromatography run was employed as it was expected that the sugar compounds would elute initially with the polar water solvent and the elution of the peptides would follow. The percentage of the summed dry weight of all the flash fractions for each eluted fraction is presented in Table 3. The majority (93.34 %) of the dry weight is contained within the first 7 fractions, which presumably contains mostly polar components, being predominantly sugars. For that reason, the protein content of only the eluted *A.*

nodosum flash fractions from 8-27 were determined using the BCA protein assay. Figure 15 shows the protein content of fractions 8-27, expressed as microgram BSA equivalents mg^{-1} fraction (μg BSA mg^{-1}). Fractions 8-12 showed to have a much higher protein content range (340.54 ±7.87 to 424.86 ± 16.45 μg BSA mg^{-1}) than the fractions 13-27 following this (20.35 ± 1.54 to 257.12 ± 37.64 μg BSA mg^{-1}). Fractions 10 and 12 had the highest exhibited the highest protein content with 418.72 ± 9.96 and 424.86 ± 16.45 μg BSA mg^{-1}, respectively. This may be due to the fact that the elution of these particular fractions, 8-12, occurs following an increase in the less polar mobile phase B promoting the initial elution of protein.

Table 3: The percentage of the eluted C18 flash chromatography *A. nodosum* digest sample in each fraction

Fraction	% of eluted sample
1	1.03
2	46.17
3	3.46
4	17.24
5	12.98
6	8.49
7	3.97
8	1.73
9	1.03
10	0.59
11	0.51
12	0.40
13	0.29
14	0.18
15	0.11
16	0.15
17	0.18
18	0.29
19	0.15
20	0.22
21	0.22
22	0.15
23	0.11
24	0.15
25	0.07
26	0.07
27	0.07

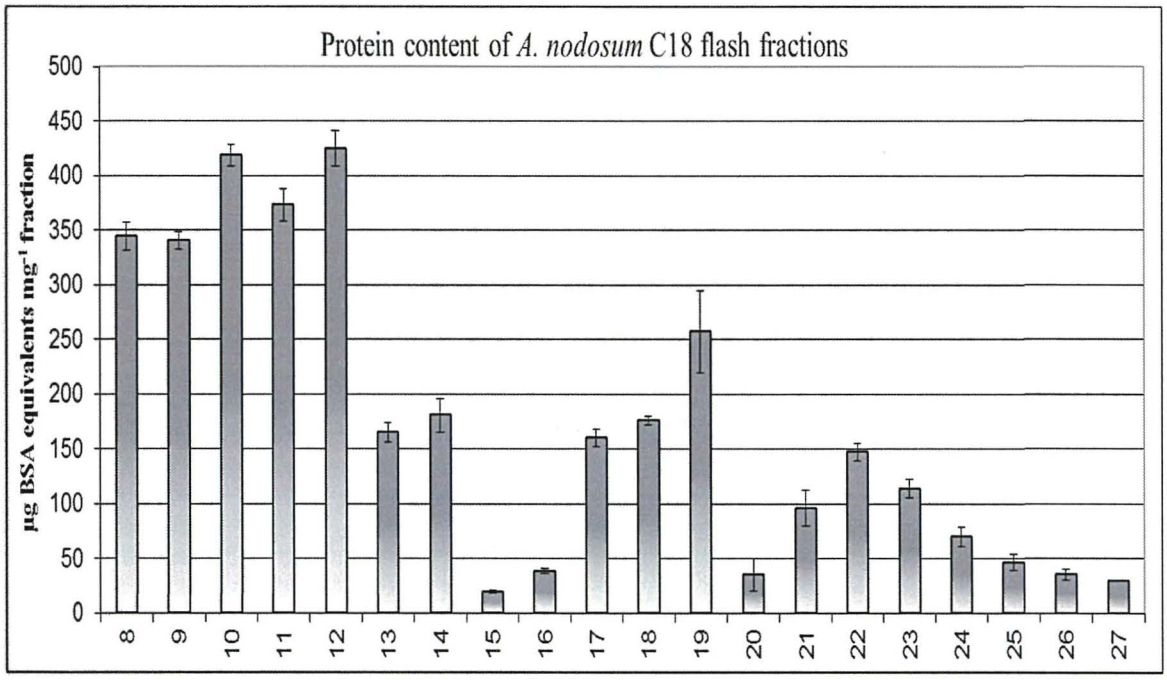

Figure 15: Protein content, expressed as µg BSA mg^{-1} fraction, of *A. nodosum* digest C18 flash fractions 8-27. Values are means ± S.D., n= 3.

4.3.2 LC-MS analysis of reverse phase flash fractions from A. nodosum

The LC-MS chromatograms for selected *A. nodosum* flash fractions are shown in Figure 16 with the retention times and molecular ion of the most abundant peaks annotated. A shift in elution of the major components from left to right is observed representing the change from more polar to less polar components. Figure 17 shows spectra for the de novo sequencing of selected peptides. The protease trypsin was used for the *A. nodosum* digestion due to its cleavage site specificity at lysine and arginine residues. The occurrence of basic residues, such as lysine and arginine, at the C-terminal of a peptide is ideal as they give strong doubly charged ions in ESI-MS and it favours the formation of a stable y-ion series for peptide sequencing. However, several peptides sequenced were generated by non-tryptic cleavages, possibly due to autolysis. The peptides identified by de novo sequencing were searched in the online database Uniprot for an associated parent protein, but no hits were found. To the best of the authors' knowledge this is the first report involving the detection of peptides, with potential antihypertensive properties, in *A. nodosum*. This may be because it is generally believed that brown macroalgae have a relatively low protein content.[142, 315]

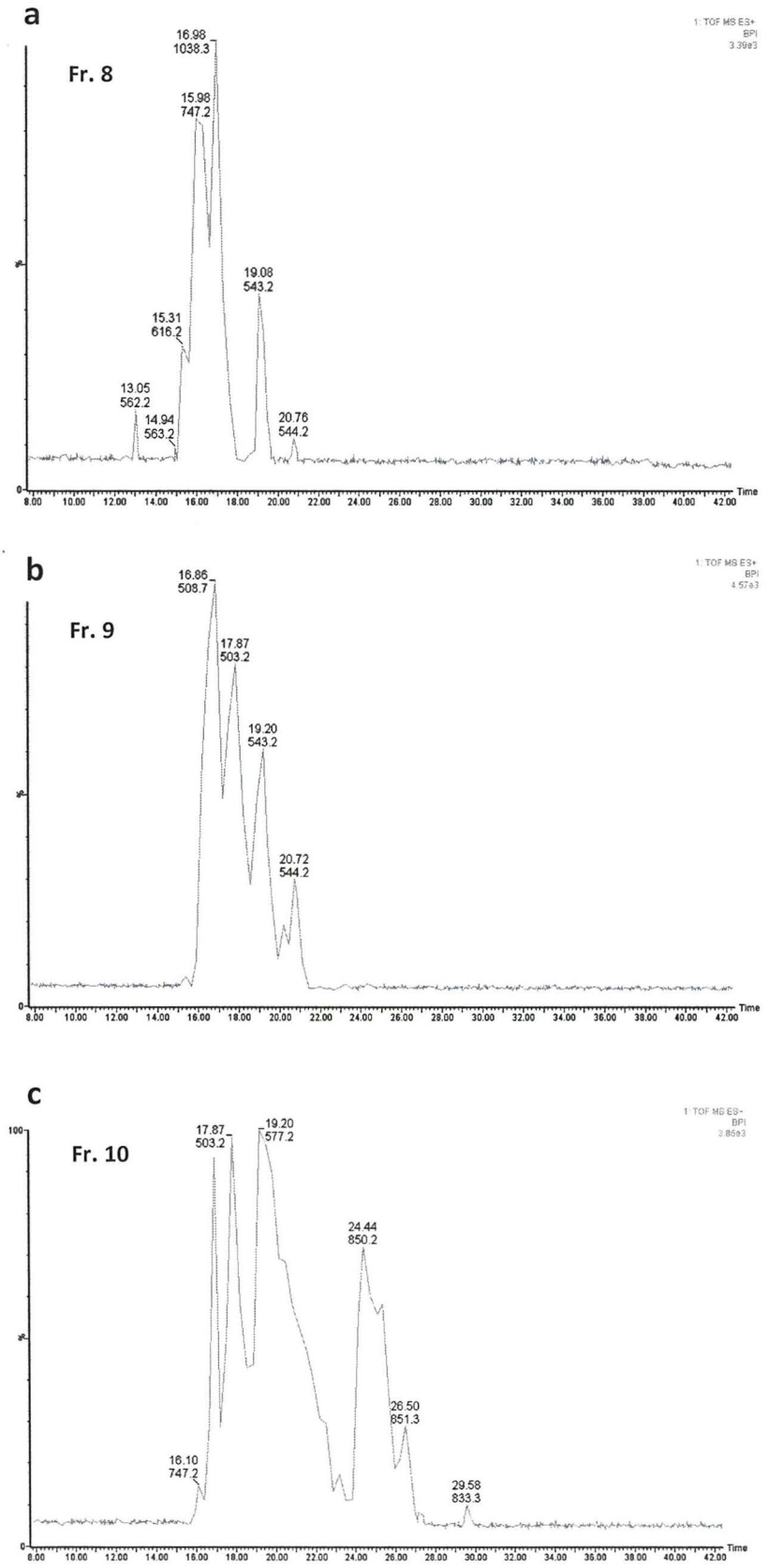

Figure 16: LC-MS chromatograms of selected *A. nodosum* digest C18 flash fractions (8-16, 19-22) showing most abundant ion.

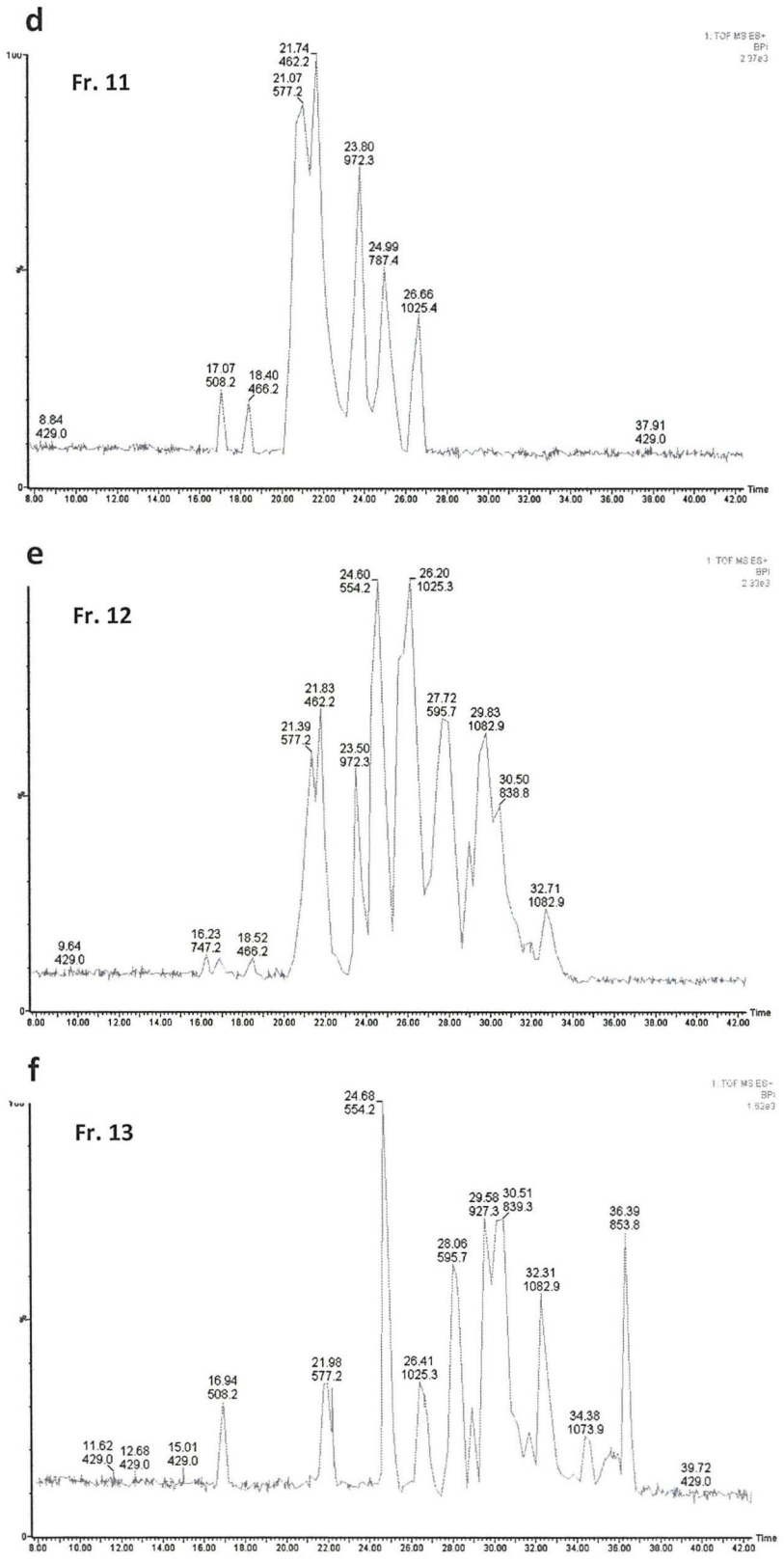

Figure 16: LC-MS chromatograms of selected *A. nodosum* digest C18 flash fractions (8-16, 19-22) showing most abundant ions.

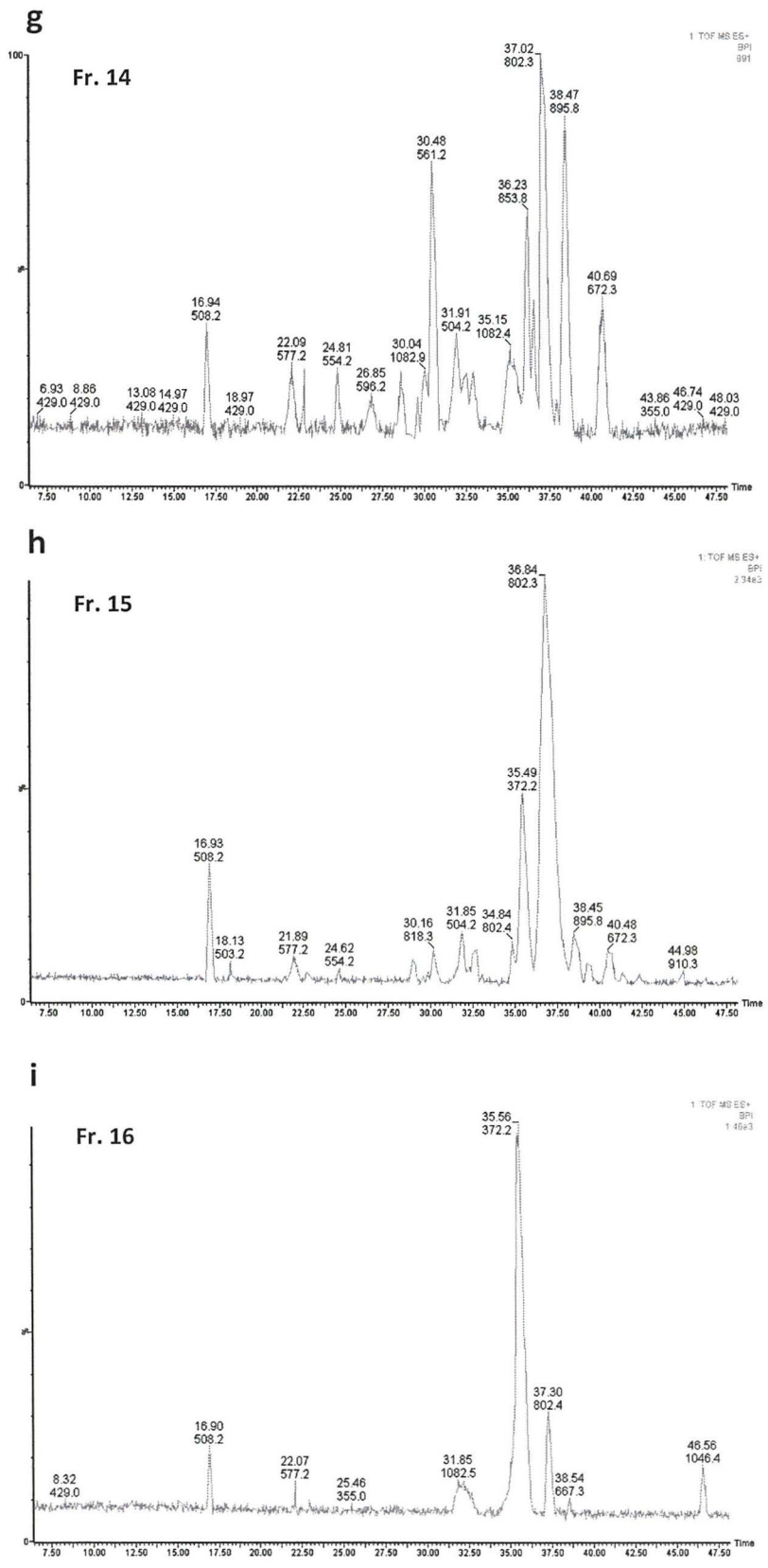

Figure 16: LC-MS chromatograms of selected *A. nodosum* digest C18 flash fractions (8-16, 19-22) showing most abundant ions.

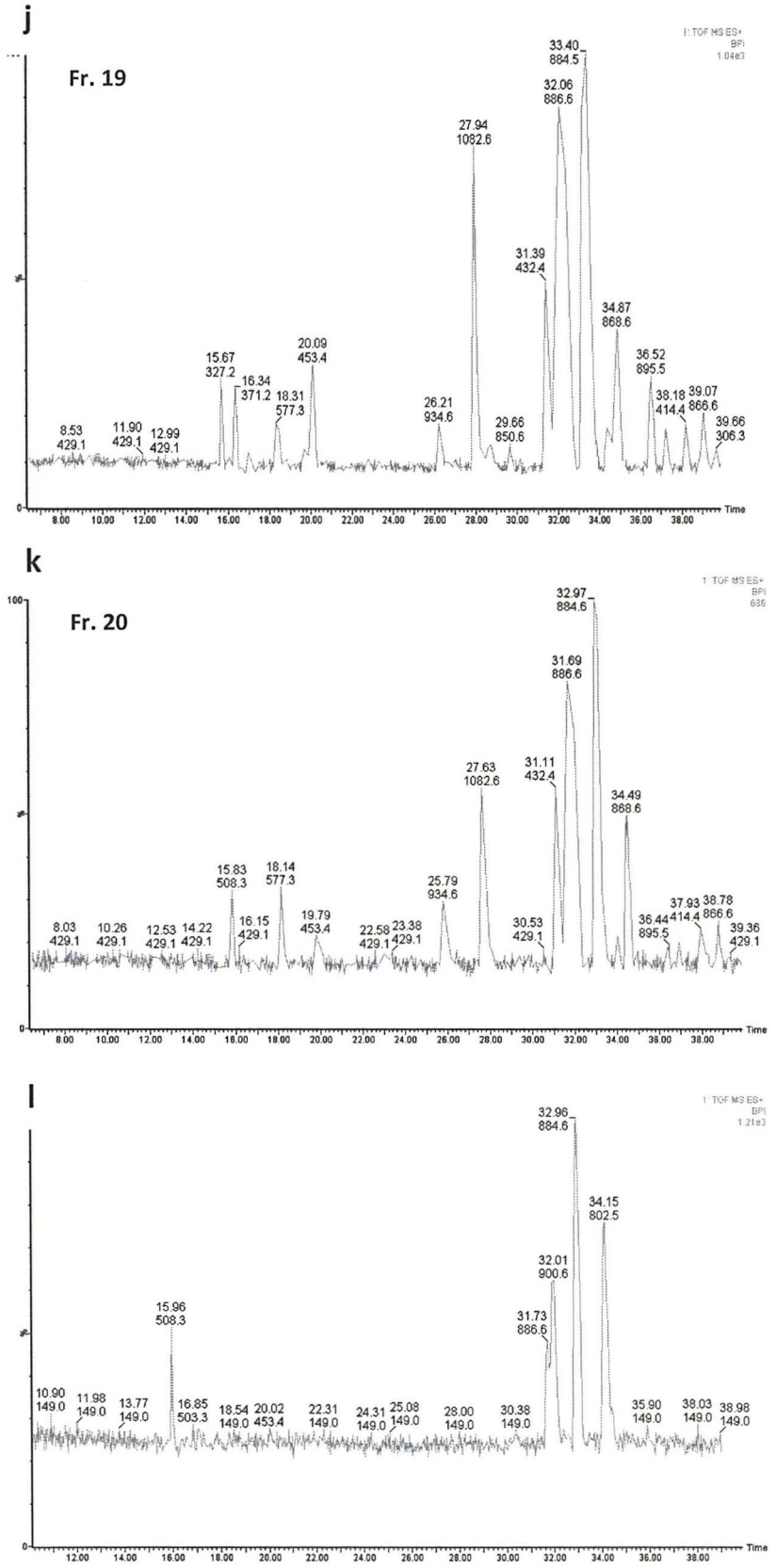

Figure 16: LC-MS chromatograms of selected *A. nodosum* digest C18 flash fractions (8-16, 19-22) showing most abundant ions.

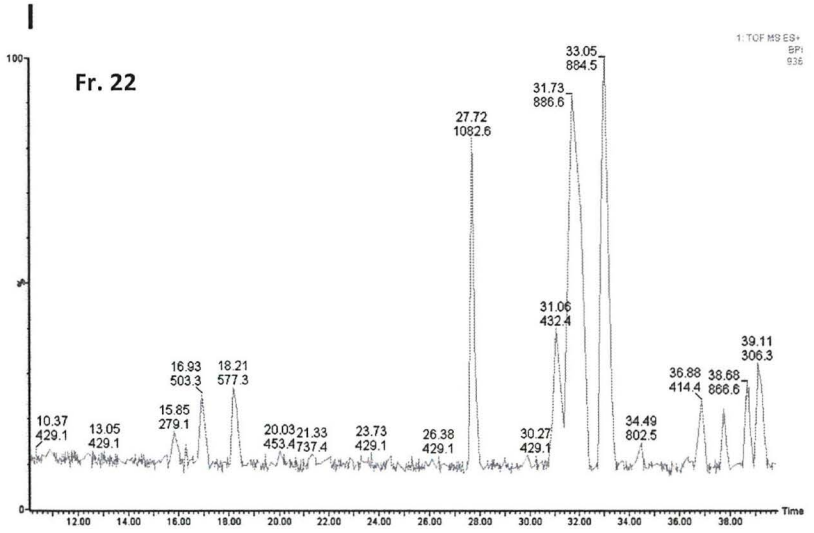

Figure 16: LC-MS chromatograms of selected *A. nodosum* digest C18 flash fractions (8-16, 19-22) showing most abundant ions.

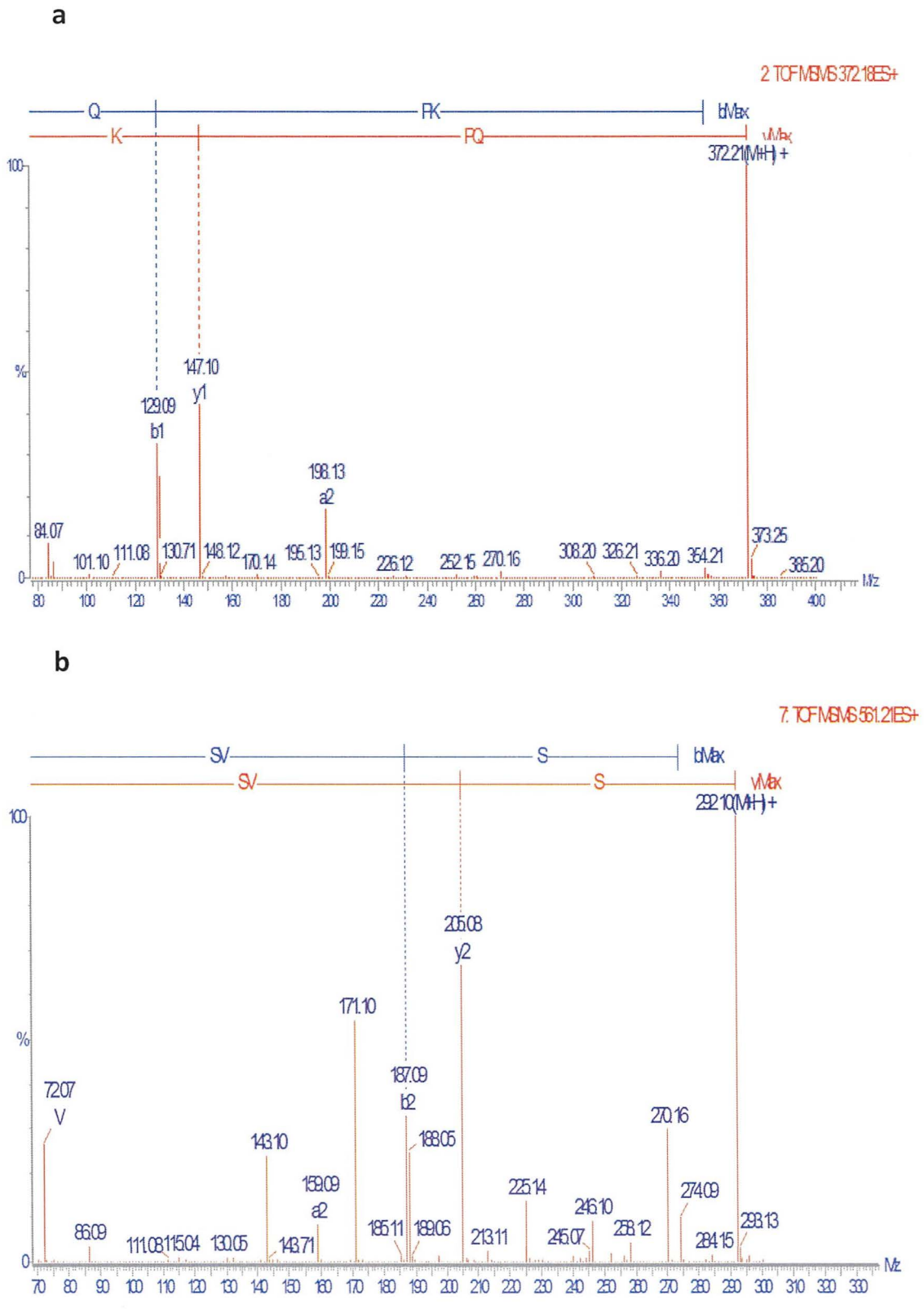

Figure 17: Examples of de novo sequencing for *A. nodosum* peptides (a) QPK, (b) SVS, (c) LVGGY, (d) MYGAHNAN, (e) NNDVDLMNK and (f) QSPCPENVAHEGSGSPGCFDK.

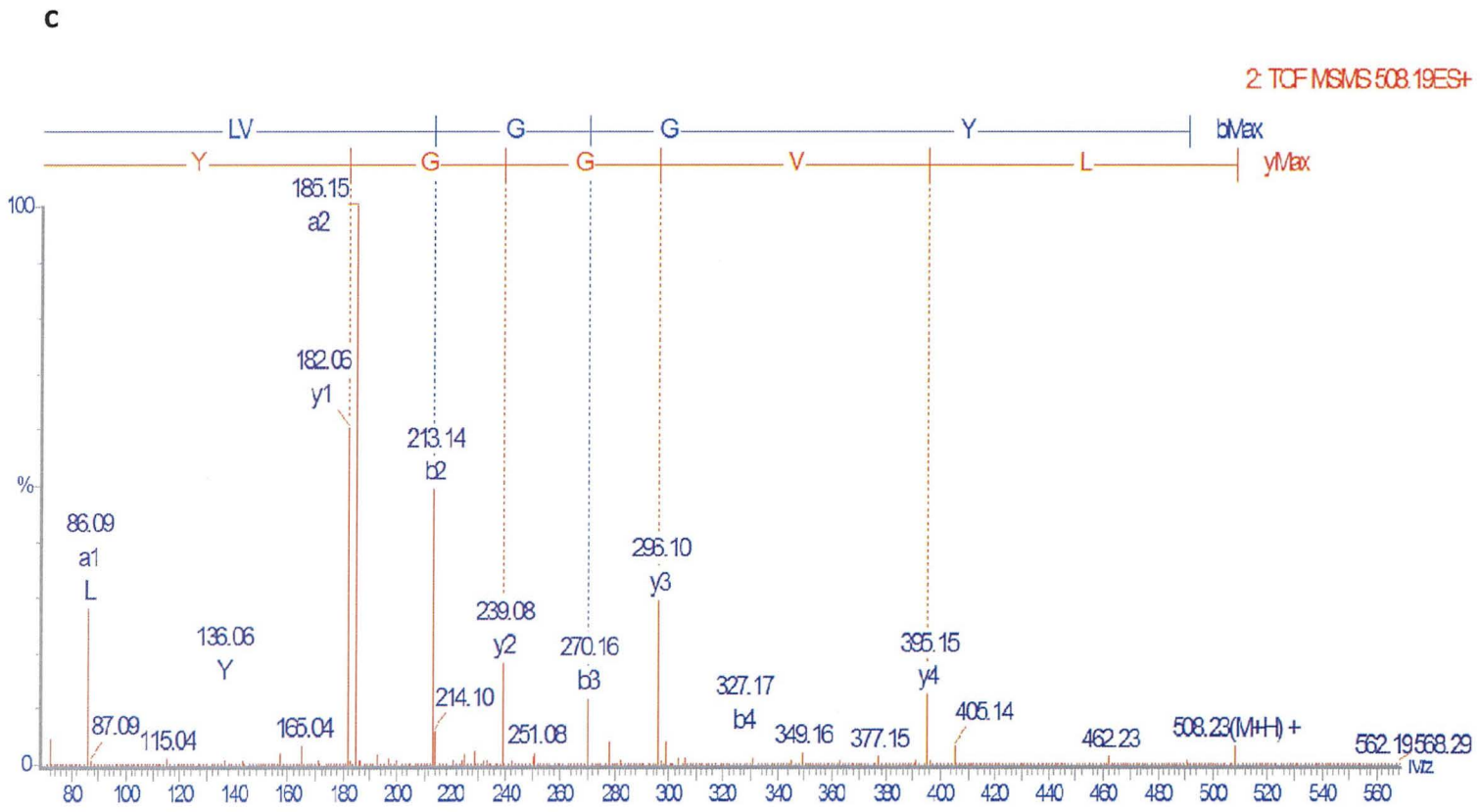

Figure 17: Examples of de novo sequencing for *A. nodosum* peptides (a) QPK, (b) SVS, (c) LVGGY, (d) MYGAHNAN, (e) NNDVDLMNK and (f) QSPCPENVAHEGSGSPGCFDK.

d

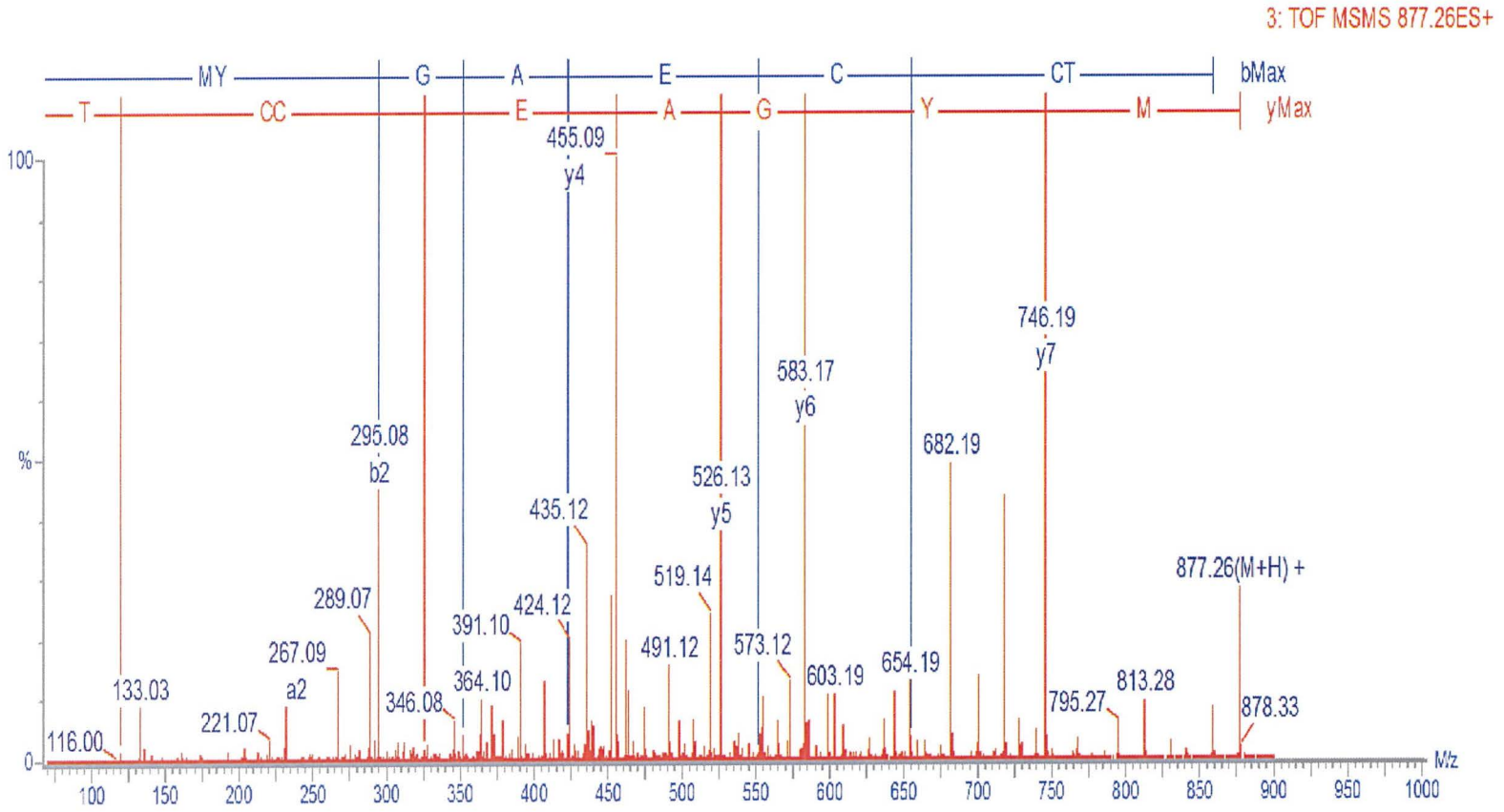

Figure 17: Examples of de novo sequencing for *A. nodosum* peptides (a) QPK, (b) SVS, (c) LVGGY, (d) MYGAHNAN, (e) NNDVDLMNK and (f) QSPCPENVAHEGSGSPGCFDK.

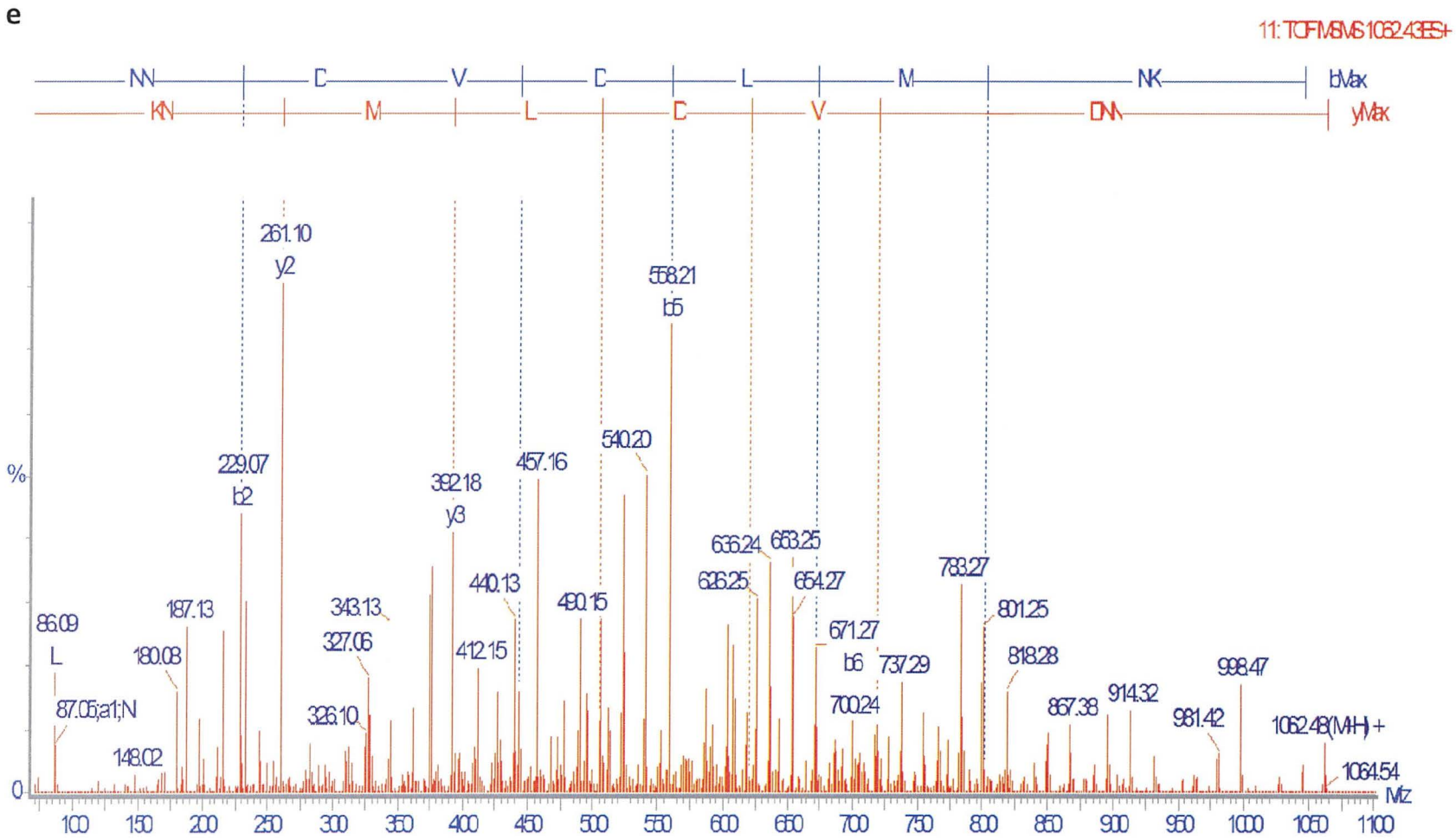

Figure 17: Examples of de novo sequencing for *A. nodosum* peptides (a) QPK, (b) SVS, (c) LVGGY, (d) MYGAHNAN, (e) NNDVDLMNK and (f) QSPCPENVAHEGSGSPGCFDK.

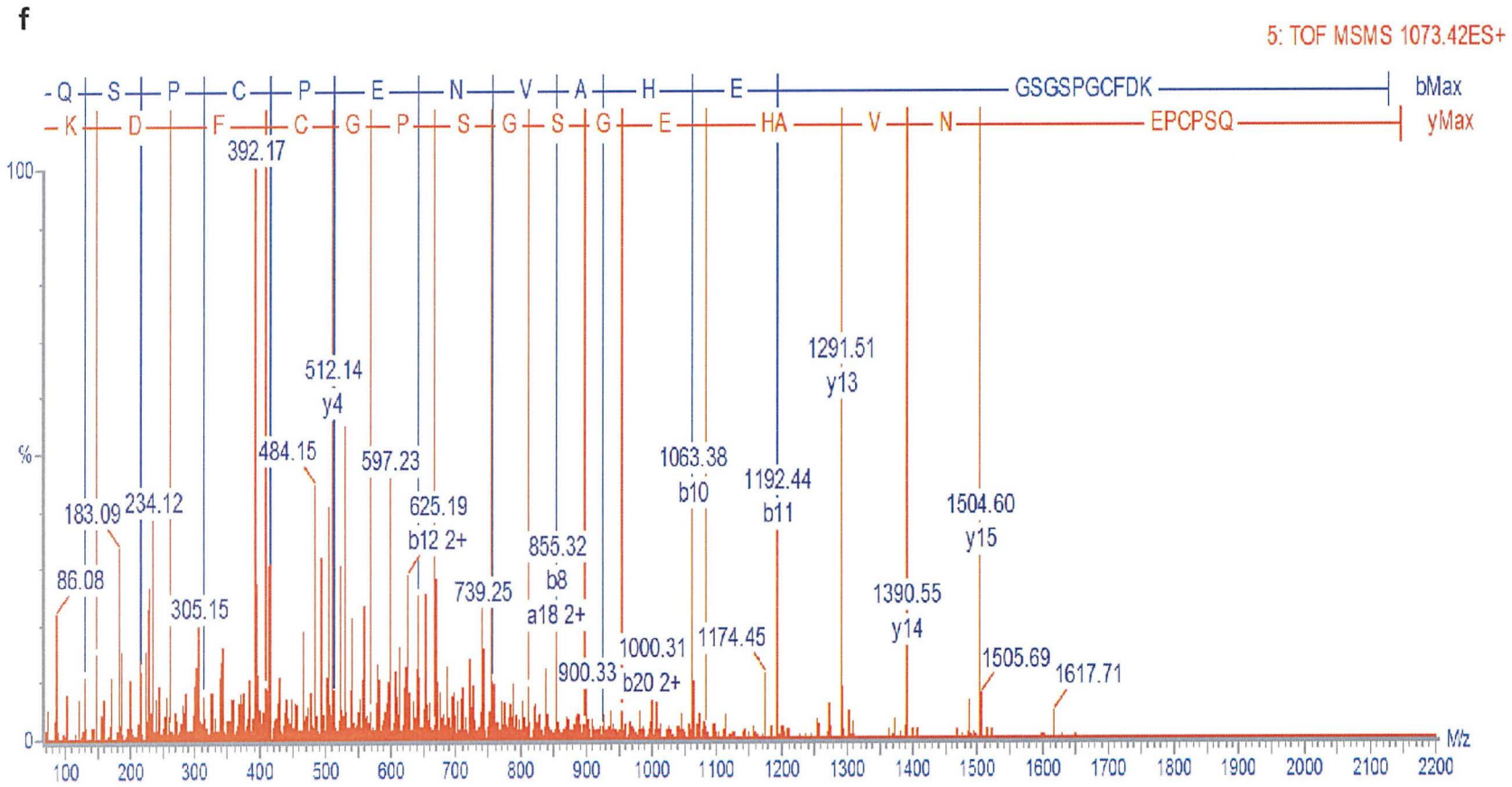

Figure 17: Examples of de novo sequencing for *A. nodosum* peptides (a) QPK, (b) SVS, (c) LVGGY, (d) MYGAHNAN, (e) NNDVDLMNK and (f) QSPCPENVAHEGSGSPGCFDK.

4.3.3 Antioxidant activity of A. nodosum C18 peptide-enriched fractions

The antioxidant activity of the *A. nodosum* flash fractions was assessed using the FRAP assay. Fractions 8-12 and 15-16 showed high antioxidant activity, with fractions 10, 12 and 16 displaying the highest values of 90.66 ± 1.07, 87.52 ± 6.58 and 89.40 ± 5.53 microgram trolox equivalents (TE) mg^{-1} values (μg TE mg^{-1}), respectively (Figure 18). The FRAP activity for fractions 13-14 and 17-21 are all very low with values of less than 30 μg TE mg^{-1}. It appears, from comparing Figure 13 and 14, that an association between protein content and in vitro antioxidant activity of fractions 8-14 is present and, indeed, a strong correlation was calculated for these fractions ($r = 0.967$, $p < 0.01$)

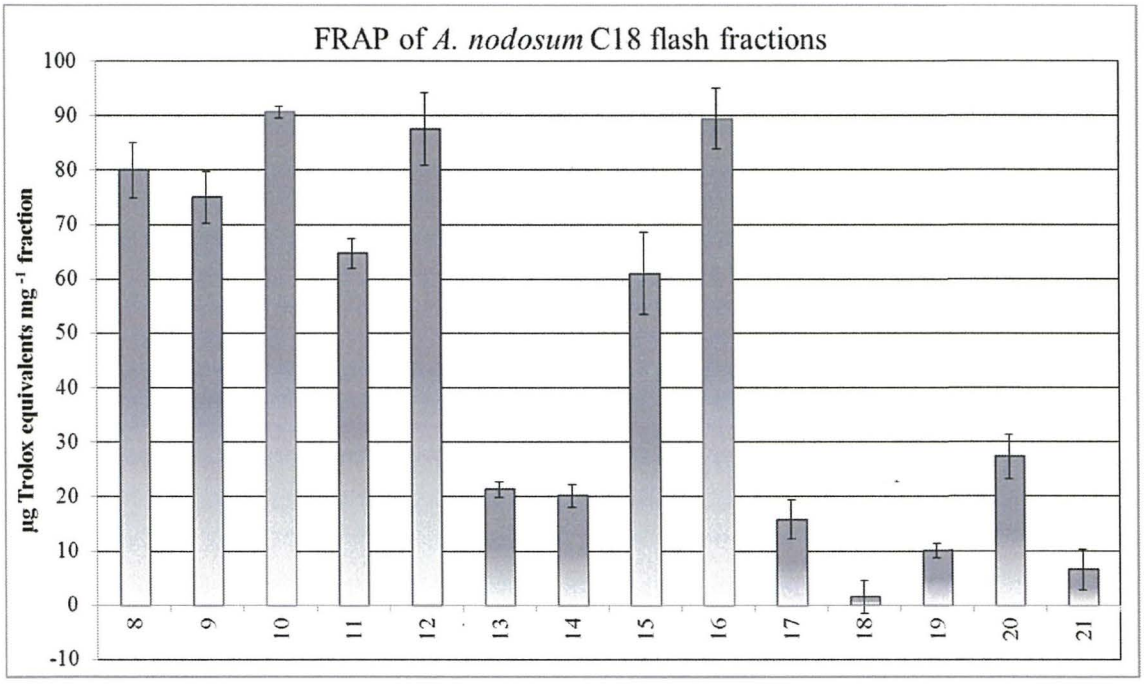

Figure 18: Ferric reducing antioxidant power (FRAP), expressed as μg trolox equivalents (TE) mg^{-1} fraction, of *A. nodosum* digest C18 flash fractions 8-21 at 250 μg mL^{-1}. Values are means ± S.E., n=3.

The proposed mode of action for antioxidant peptides includes metal ion chelation, free radical scavenging and aldehyde adduction.[340-341] The ability of metal pro-oxidants to produce radicals can be inhibited through sequestration and chelation.[144] Antioxidant peptides identified to date have been found to generally have molecular weights of between 500 and 1800 Da. Radical scavenging capabilities of peptides has been suggested to significantly correlate to the presence of particular amino acids, such as histidine, tyrosine, tryptophan, methionine, cysteine and proline

in the amino acid sequence.[141-142] Aromatic amino acids, such as phenylalanine, histidine, tyrosine and tryptophan, can give up protons easily to electron deficient radicals whilst maintaining their stability via resonance structures.[143] Histidine-containing peptides are also thought to possess antioxidant activity due to their hydrogen-donating ability, lipid peroxyradical trapping, and/or the metal ion chelating ability of the imidazole group.[342] Peptides containing hydrophobic amino acids, such as valine and leucine, can possess enhanced antioxidant properties as they have the ability target the hydrophobic polyunsaturated chain of fatty acids of biological membranes.

QTof-MS was employed in this study to elucidate the amino acid sequence of *A. nodosum* derived flash fractions displaying antioxidant activity. The list of the peptides, their retention times and the fractions in which they feature are summarised in Table 4. Fraction 9 (Figure 16b), which has a FRAP activity of 75.00 ± 4.80 μg TE mg^{-1}, showed abundant ions for m/z 503 and 508 which are associated with peptides SGLQV and LVGGY, respectively. Both of these peptides contain leucine and valine, with LVGGY also containing tyrosine, which are all amino acids identified as possessing antioxidant activity. One of the major ions in fraction 10 (Figure 16c), which exhibited the highest antioxidant activity of 90.66 ± 1.07 μg TE mg^{-1}, was also detected at m/z of 508. The most significant ion in fraction 11 (Figure 16d) is 462 which corresponds to the peptide LSGAD, which contains the antioxidant leucine at its N-terminal. The principal ions observed in fraction 12 (Figure 16e) are at m/z 554 and 1025, which correspond to the peptides YVSW and MNSSYPDVL, respectively (Table 4). YVSW contains the known antioxidant amino acids tyrosine, valine and tryptophan, while MNSSYPDVL contains tyrosine, valine and leucine. The predominant ion in fraction 16, which displayed the second highest antioxidant activity, is at m/z 373.2 (Figure 16i), which corresponds to the tri-peptide QPK (Table 4). It is important to note that peptide abundance alone is not a determining factor for the initiation of antioxidant activity and, it may be that the less abundant peptides within these fractions possess the structures that are conducive to free radical scavenging. Although only one peptide has been identified in fraction 10, numerous peptides have been identified in fractions 12 and 16 and, therefore, less abundant peptides with more amino acids favourable to radical scavenging action may be

responsible for the activities observed in these fractions or possibly there may be synergism among peptides occurring.[343]

It may be possible that the identified peptides may not have the capacity to pass the intestinal wall due to their size, however, such peptides would have the potential to exert antioxidant activities within the gut lumen or via intestinal wall receptors or may be digested further within the gastro-intestinal tract generating small absorbable peptides. One concern relating to the in vitro antioxidant activity measurement of peptides is that many of these assays have been developed predominantly for use with small molecule antioxidants such as polyphenols and have not been validated for the measurement of peptides.[136] Therefore, it is important that when considering how to apply antioxidant peptides for either food or biological uses that assay(s) that yield information relevant to their mechanism(s) of action and target sites are employed.

Table 4: Amino acid sequence, collision energy, calculated mass and fractions of *A. nodosum* peptides detected by LC-ESI-MS.

Retention time (min)	*m/z* Ion for MS/MS (charge)	Calculated mass (Da)	Collision energy (eV)	Peptide Sequence	Fractions
15.85	279.16 (1)	278.13	15	PY	19, 20, 21, 22
16.01	371.27 (1)	370.16	15	THN	19, 20, 21, 22
16.85	503.41 (1)	502.32	23	SGLQV	21, 22
16.88	539.19 (2)	1076.48	25	APLLSDSSGCK	12
16.94	508.19 (1)	507.27	20	LVGGY	10, 11, 13, 14, 15, 16, 17
21.60	972.62	971.60	40	TKTLGLAAVV	19, 20, 21, 22
21.83	462.15 (1)	461.21	30	LSGAD	11, 12
24.68	554.18 (1)	553.25	20	YVSW	12, 13, 14
26.20	1025.34 (1)	1024.45	38	MNSSYPDVL	12, 13
26.61	596.23 (2)	1190.54	23	TLNDDLFLLK	12, 13, 14
28.93	877.26 (1)	876.28	30	MYGAHNAN	12, 13, 14, 15
29.59	927.30 (1)	926.36	35	YNSGDVSW	13, 14
30.48	292.10 (1)	291.14	15	SVS	14, 15, 19, 20, 21, 22
30.51	561.21 (1)	560.29	23	LGVSW	13, 14, 15
31.91	1081.92 (2)	2161.98	30	DSPDNLNVVETAEQFLSASK	12, 13, 14, 15, 16, 17
32.93	588.24 (2)	1174.58	25	VDNGSDNLTLK	13, 14, 15
33.61	838.76 (2)	1675.65	30	QDGDPENVPMGNEACT	13
34.15	802.54 (1)	801.50	40	LQGLVSSV	19, 21, 22
34.38	1073.42 (2)	2144.85	30	QSPCPENVAHEGSGSPGCFDK	12, 13, 14, 15, 16
35.56	372.18 (1)	371.22	15	QPK	15, 16, 17
36.12	895.49	1789.98	30	EKTGLLNVVETAEKFL	19, 20, 21, 22
37.02	802.34 (1)	801.44	40	LQGLVSW	14, 15, 16, 17
38.59	895.33 (2)	1788.78	30	MFQEGNEVVNLHMNK	13, 14
38.85	1062.43 (1)	1061.48	45	NNDVDLMNK	13, 14, 15, 16
40.69	672.24 (1)	671.33	30	SPPVSW	14, 15
46.56	1046.48 (1)	1045.47	50	MLLMTLPDL	15, 16

4.3.4 In vitro antihypertensive activity of A. nodosum C18 peptide-enriched fractions

Food derived BPs have the potential to prevent ACE and renin enzymes of the RAS pathway acting via various modes of inhibition, such as competitive, non-competitive or uncompetitive, with replacement of single amino acids sometimes affecting the nature of the interactions between the RAS enzymes and various food-derived BPs.[16]

A selection of the *A. nodosum* C18 flash fractions were tested for both renin (Figure 19, fractions 8-25) and ACE inhibition (Figure 20, fractions 18-27) at a concentration of 250 μg mL^{-1}. The renin inhibition ability of the fractions ranged from 12.75 ± 0.50 to 73.14 ± 5.41 %. The positive control Z-Arg-Arg-Pro-Phe-His-Sta-Ile-His-Lys(Boc)-OMe displayed 100 % renin inhibition at a concentration of 1.5 μg mL^{-1}. In contrast to what was observed for the antioxidant activity of the fractions, the fractions with the highest renin enzyme inhibition were the later eluting ones specifically from fractions 18-25. The highest percentage inhibition was observed for fractions 23, 24 and 25 with 70.60 ± 1.0, 72.37 ± 0.31 and 73.14 ± 5.41 %, respectively. Fractions 19-21 also gave percentage inhibitions of greater than 60 %. These activities are good considering the fractions are not pure and, as such, may contain a mixture of different peptides, some of which may not possess renin inhibition activity. It is also possible that non-peptidic compounds are present and may be masking the BPs full bioactive potential. For example, the most abundant peaks in fractions 19 onwards were *m/z* 884 and/or 886 (Figure 16); however fragmentation of these ions produce very limited product ions and, thus, did not reflect typical peptide origin.

Far more attention has been given to investigating the SAR of ACE-I inhibitory peptides than renin inhibitory peptides, however it has been suggested that peptides with a leucine residue in close proximity to a hydrophobic region is important for renin inhibition, but not necessarily leucine alone.[344] Several peptides were identified in fractions 19-21 as seen in table 4, of which one or many may be responsible for the renin inhibition observed in these fractions.

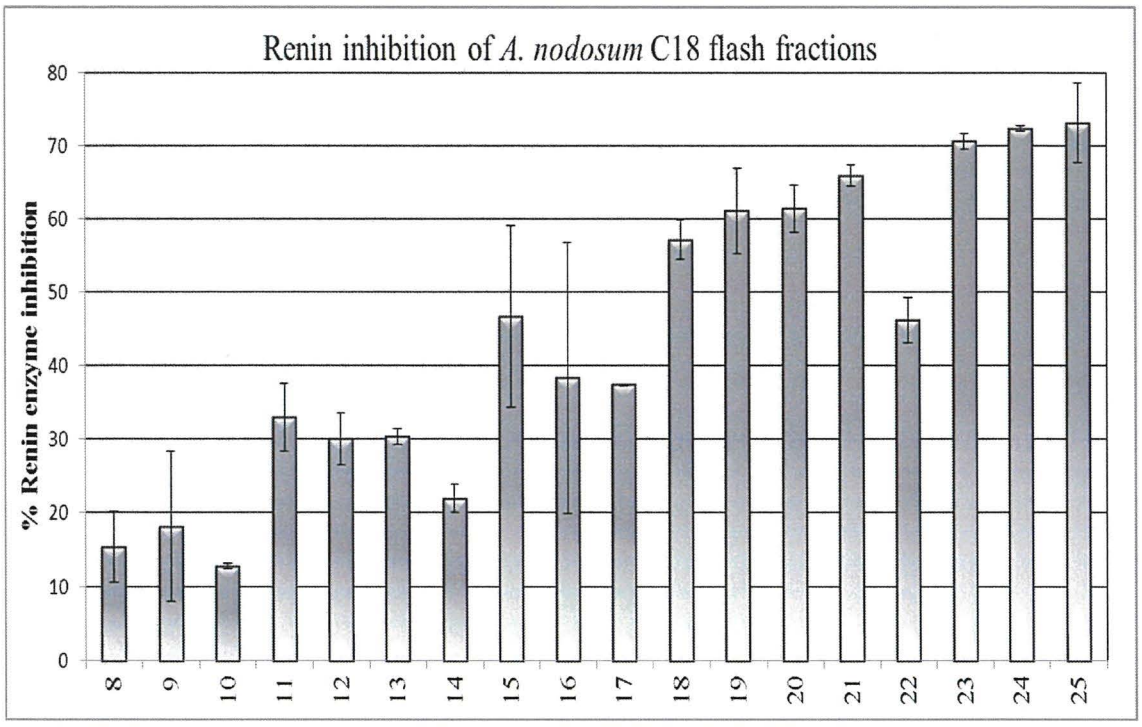

Figure 19: Percentage renin enzyme inhibition of *A. nodosum* digest C18 flash fractions 8-25 at 250 μg mL^{-1}. The positive control Z-Arg-Arg-Pro-Phe-His-Sta-Ile-His-Lys(Boc)-OMe displayed 100 % inhibition at 1.5 μg mL^{-1}. Values are means ± S.E., n=2.

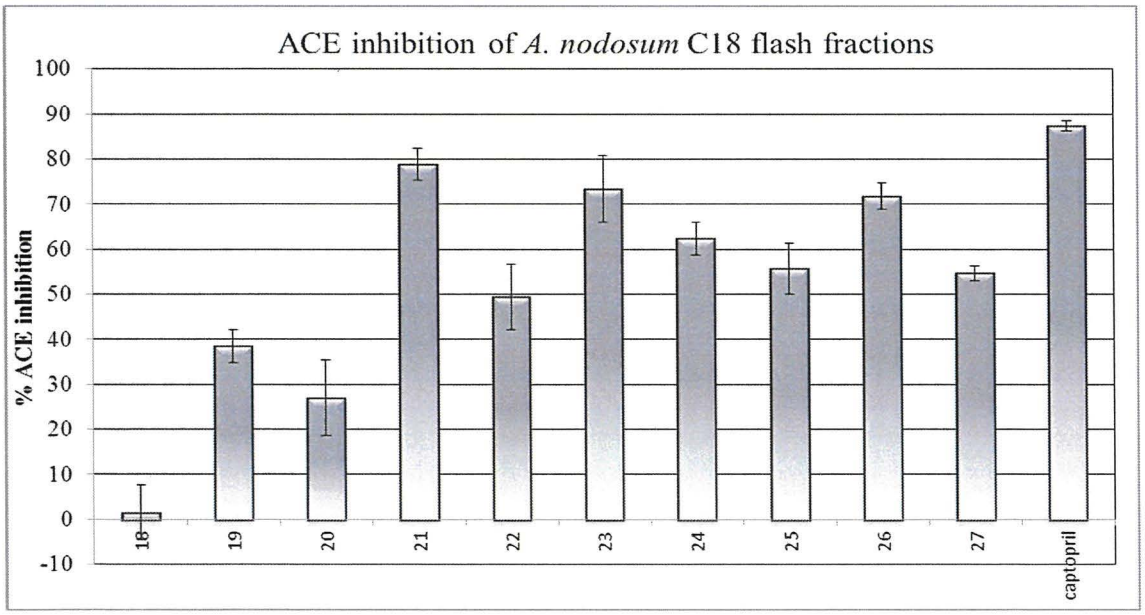

Figure 20: Percentage angiotensin converting-enzyme I (ACE-I) inhibition of *A. nodosum* digest C18 flash fractions 18-27 at 250 μg mL^{-1}. The ACE inhibition of the positive control captopril was measured at 0.004 μg mL^{-1}. Values are means ± S.E., n=2

A *Palmaria palmata* protein HPLC fraction, tested at 1 mg mL^{-1}, and a purified peptide IRLIIVLMPILM from that fraction, tested at 3.34 mM (5 mg mL^{-1}), displayed renin inhibitions of 60 % and 50 %, respectively.[150] This is a situation where an unpurified fraction has stronger bioactivity than a purified peptide, and possible synergism between peptides or between peptides and other active components contributes to the bioactivity. In another study ten HPLC fractions from rapeseed protein were assessed for renin inhibition at 100 μg mL^{-1} concentrations and displayed activity ranges of 29–70 %.[345] A fraction purified from flaxseed protein, using RP HPLC, exhibited renin inhibition of 94.6 %, which is higher than the maximum of 73.14 ± 5.41 % observed in this study, although the flaxseed fraction was assayed at 1 mg mL^{-1}.[346] In addition African yam bean seed protein hydrolysate HPLC fractions at a concentration of 1 mg mL^{-1} have been reported to have a maximum renin inhibition was activity of 55.49 %.[347] Overall, taking into consideration that the *A. nodosum* fractions in this study were assayed at 250 μg mL^{-1} the renin inhibition observed seems promising in comparison to the previous reports in this area.

The ACE inhibitory activities of fraction 18-27 (250 μg mL^{-1}) ranged from 1.52 ± 6.09 to 78.88 ± 3.5 % (Figure 20). The positive control displayed an ACE inhibition of 87.41 ± 1.07 % at 0.004 μg mL^{-1}. Fractions 21, 23 and 26, at 250 μg mL^{-1}, showed the greatest inhibition of the enzyme with percentage inhibitions of 78.88 ± 3.50, 73.40 ± 7.46 and 74.77 ± 2.97 %, respectively. The intensity of peptide ACE inhibitory bioactivity is largely dependent on the peptide structure. To date, a definitive SAR of marine-sourced ACE-inhibitory peptides has not been recognised. ACE substrates with hydrophobic amino acid residues at the three c-terminal sites are thought to be favourable for ACE interaction. Additionally, lysine or arginine, which have a positive charge on the ε-amino group at the C-terminal site, are also likely to aid ACE inhibition.[148] It's also apparent that di or tri-peptides containing tryptophan, phenylalanine, tyrosine or proline at their C-terminal, and a branched aliphatic amino acid terminal display good ACE inhibitory activity.[348] Kobayashi *et al.* (2008) have suggested that tryptophan in the C-terminal position is very important for ACE inhibitory activity, along with a positively charged amino acid next to an aromatic one.[349] In contrast to many studies that focus on the importance of the final three C-terminal residues, it has been reported that for peptides greater than 5 residues in

length the C-terminal tetra-peptide are more influential on activity. Wu *et al.* (2006) used Quantitative Structure-Activity Relationship (QSAR) modeling to determine that collectively the most favourable amino acid residues for ACE-inhibitory activity of these peptides were tyrosine or cysteine for the first position on the C-terminal side, histidine, tryptophan or methionine for the second position with isoleucine, leucine, valine or methionine for the third position, and tryptophan for the fourth position.[350] The peptides detected in this study did not contain these criteria.

Fraction 21, which displayed both good renin (65.87 ± 1.46 %) and ACE (78.88 ± 3.5 %) inhibition, was found to contain many peptides as observed in table 4, but in particular contained the peptide LQGLVSSV in relatively good abundance. The amino acid leucine has been deemed to be important also for both antioxidant and ACE-inhibitory activity by Alemán *et al.* (2011).[130] A number of peptides detected in some of the ACE-inhibitory fractions contain one or more leucine residues, such as SGLQV (fractions 21 and 22), LQGLVSSV (fractions 19, 21 and 22), TKTLGLAAVV (fractions 19, 20, 21 and 22) and EKTGLLNVVETAEKFL (fractions 19, 20, 21 and 22).

Gu and colleagues (2011) hydrolysed salmon skin using alcalase and papain to generate a salmon skin collagen peptides hydrolysate. The salmon peptide mixture was subjected to RP HPLC and eleven fractions were collected. The fractions were assessed for their ACE-I inhibitory activity at 1 mg mL^{-1} and inhibitions of 91.10 ± 1.34% and 80.51 ± 1.32% were observed for two of the fractions. Considering in the present study that *A. nodosum* fractions were tested at a concentration four-fold lower than Gu *et al.* (2011), the observed inhibitions of greater than 70 % are promising.

Suetsuna and Nakano (2000) isolated four tetra-peptides, AIYK, YKYY, KFYK and YNKL, from the brown macroalga *Undaria pinnatifida* with ACE inhibitory IC_{50}s of 213 μM (105.14 μg mL^{-1}), 64.2 μM (40.81 μg mL^{-1}), 90.5 μM (46.48 μg mL^{-1}) and 21 μM (11.27 μg mL^{-1}), respectively.[322] These activities are superior in comparison to the ACE inhibitory activity of the *A. nodosum* fractions. However, it must be taken into consideration that in this case pure compounds are being compared to less pure fractions. Therefore, further purification of *A. nodosum* fractions could result in improved activity. All of these peptides (AIYK, YKYY, KFYK and YNKL) have tyrosine and lysine residues which may indicate that they are

central to their ACE-inhibitory activity. Therefore, in terms of the *A. nodosum* ACE-inhibitory fractions the presence lysine in LQGLVSSV and TKTLGLAAVV and the tyrosine in PY may be potentially be contributing to the ACE activity of these peptides present in the active fractions. PY in particular may be the key peptide contributing to the high ACE activity of fraction 21, and to a lesser extent fraction 22, as it has been reported in various studies that di-peptides with C-terminal tyrosine residues exhibit good ACE-inhibition.[321, 351-353] The peptide YP has previously shown to have both *in vitro* and *in vivo* ACE-inhibitory activity.[354] Gu and colleagues (2011) identified various ACE-I inhibitory peptides from salmon skin and two, AP and VR, were analysed further based the presence of a C-terminal proline residue and N-terminal valine residue. These di-peptides were synthesised and IC_{50}s against ACE of 0.060 ± 0.001 mg mL^{-1} (60 μg mL^{-1}) and 0.332 ± 0.005 mg mL^{-1} (332 μg mL^{-1}) were found.[129] In comparison to the latter inhibition value, the activities of the *A. nodosum* fractions 21, 23 and 26 seem impressive. It is important to consider that the extent of pharmacological application of bioactive peptides is dependent on the absorption and bioavailability of them as intact forms in target tissues. The probability of a peptide being adsorbed intact after digestion and, therefore possibly, exerting an ACE inhibitory effect is increased when peptides contain only two or three amino acids and C-terminal proline or hydroxyproline residues.[148, 355]

In the present study BP's with both *in vitro* antihypertensive and antioxidant properties have been isolated and characterised from the same source and it is widely believed that hypertension and oxidative stress are co-dependent.[310] However, reports in this area are in conflict as to whether the onset of hypertension causes oxidative stress or is caused by oxidative stress.[356-358] Zhou et. al. (2010) have suggested that a redox switch in angiotensinogen can control angiotensin release.[88] They found that when the reduced and oxidised forms of angiotensinogen were incubated with renin a four-fold increase in renin-binding affinity and, therefore, four-fold increase in the catalytic release of angiotensin was observed in the presence of the oxidised form of angiotensinogen.[88] Studies involving genetic models of hypertension, such as spontaneously hypertensive rats (SHR) and stroke-prone SHR (SHRSP), have shown increased superoxide radical generation in resistance arteries, aorta and kidneys.[87, 359] Furthermore, it has been shown that lifelong treatment with antioxidants can prevent the development of hypertension in SHR. Either way, whether oxidative stress is a

cause or a product of hypertension, the isolation of bioactive agents exhibiting both antioxidant activity and renin/ACE inhibition would be promising in terms of their development as functional anti-hypertensive agents.

4.3.5 Antioxidant and renin-inhibitory activity of synthesised A. nodosum peptides

Nine of the identified peptides; namely YVSW, TLNQMPNDMK, NNDVDLMNK, QPK, LSGAD, LKGLVSSV, SGLKV, TKTLGLAAVV and EKTGLLNVVETAEKFL, were chosen for chemical synthesis due to their presence in the most active antioxidant and antihypertensive fractions. The antioxidant activity of the synthesised peptides was assessed at 250 μg mL^{-1} using the FRAP assay. The FRAP activities ranged from 8.59 ± 1.42, for SGLKV, to 297.11 ± 9.39, for QPK, μg trolox equivalents mg^{-1} (Figure 21). QPK was more than five times more active than any other peptide assayed. Furthermore, QPK was found earlier to be the most predominant ion in the second most antioxidant *A. nodosum* peptide fraction. Figure 22 shows the structure of QPK. The amino acid glutamine (Q) has shown to alleviate alleviated oxidative stress, normalize superoxide dismutase activity, increase levels of total glutathione and block nitric oxide overproduction as well as the formation of peroxynitrite.[360] The amino acid proline (P) has also shown to strongly correlate with both DPPH radical scavenging activity and FRAP.[361]

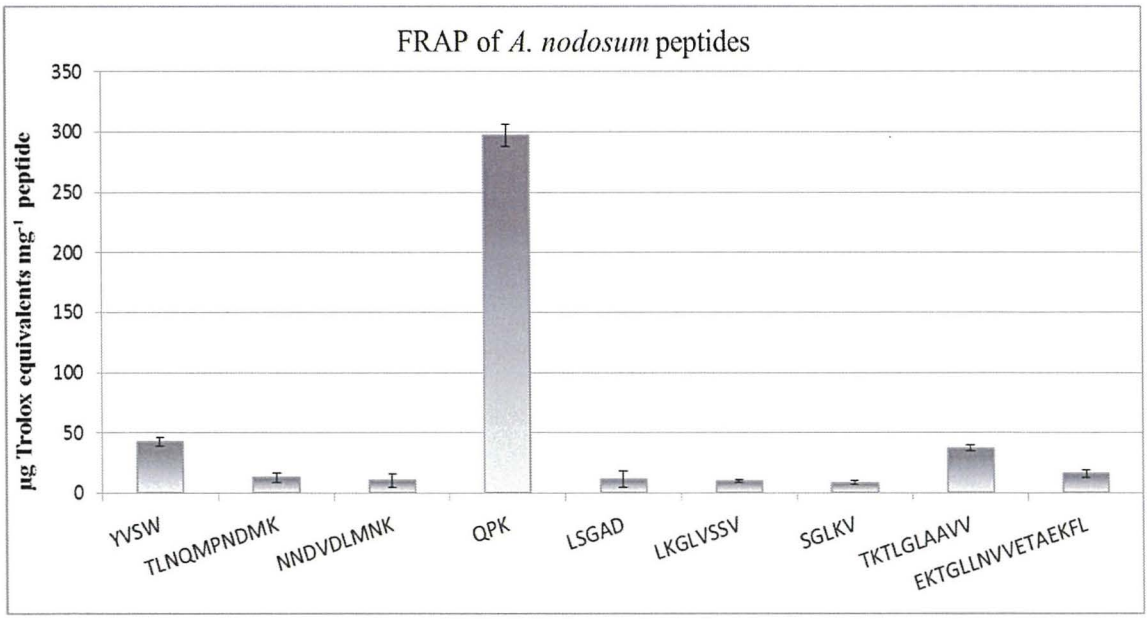

Figure 21: FRAP, expressed as μg TE mg^{-1} peptide, of *A. nodosum* peptides at a concentration 250 μg mL^{-1}. Values are means ± S.D., n=3.

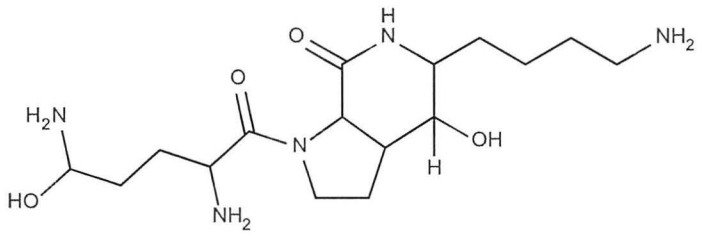

Figure 22: Structure of *A. nodosum* peptide QPK.

The percentage renin enzyme inhibition of the nine peptides assayed at 250 μg mL^{-1} ranged from 9.59 ± 0.06 % for QPK to 56.12 ± 2.66 % for EKTGLLNVVETAEKFL (Figure 22). EKTGLLNVVETAEKFL was identified in a number of *A. nodosum* fractions that exhibit both renin and ACE-inhibitory activity which may be attributed to this polypeptide. YVSW also exhibited good renin inhibitory activity of 49.78 ± 9.78 %, which was also previously identified as the synthesised peptide with the second highest antioxidant activity. In general, reports of antihypertensive peptides identified from brown macroalgae are scarce,[318] with no reports to date of renin inhibitory peptides identified from brown macroalgae.

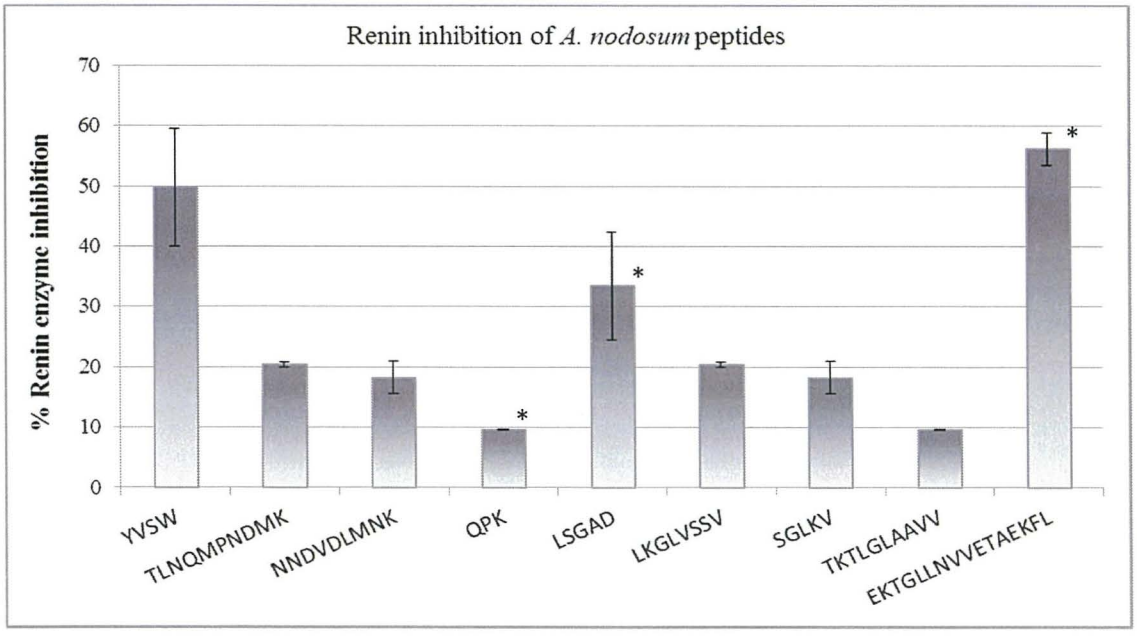

Figure 23: Percentage renin enzyme inhibition of *A. nodosum* peptides at 250 μg mL^{-1}. Values are means ± S.D., n=2 or n=3*.

When attempting to identify a promising source of BP's from foods two key factors that should be considered; (1) value-added use of abundant under-utilized proteins or protein-rich food industry by-products, and the (2) utilization of proteins containing specific peptide sequences or amino acid residues of particular pharmacological interest.[131] In terms of the first key aspect, the protein content of the *A. nodosum* species used in this study was relatively low, however, this may have been due to the winter season harvesting and the protein content may be maximised by harvesting during the summer. Furthermore, *A. nodosum* is predominantly used industrially as a source of alginate and, therefore, by-product material from this extraction process may be an enriched source of BPs.[362] With respect to the latter factor, *A. nodosum* digest fractions in the present study had *in vitro* antihypertensive activities comparable to previously reported for pure BPs from other sources. Therefore, de-novo synthesis of a selection of peptides present in the active fractions seemed worthwhile in order to reveal which peptides are responsible for the antioxidant and/or antihypertensive activities observed. From the nine peptides synthesised, one peptide, QPK, displayed impressive FRAP antioxidant activity, while two, peptides EKTGLLNVVETAEKFL and YVSW, displayed good renin enzyme inhibition.

Extensive research has been carried out in the area of BPs from milk and meat, and multiple studies have shown the benefits of these on hypertension. Seppo and colleagues found that a *Lactobacillus helveticus* fermented milk high in bioactive peptides, such as VPP and IPP, had a blood pressure–lowering effect in hypertensive subjects and thus may be useful as a dietary treatment.[70] A meta-analysis of randomized controlled trials concerned with observing the effect of food-derived BPs on blood pressure revealed that BPs may lead to significantly reduced blood pressure and suggested they may be used as a supplement or alternative to pharmaceutical treatment for mild hypertension.[363]

This chapter has revealed the existence of bioactive peptides in *A. nodosum* and, thus, there may be the potential for brown algal peptides to be used as antihypertensive ingredients in functional food, if their effectiveness can be supported by intervention studies.[128] However, in order to achieve sufficient protein yield from brown macroalgae for digestion and separation processes, local species with inherently high protein contents need to be identified and harvested at an optimal time

of the year to maximise BP yields. In addition, in vitro bioactivity data needs to be validated by the determination of the antihypertensive activity of orally administered brown algal peptides on SHR.

Furthermore, the nature of the interaction between marine-derived BPs and target enzymes/ free radical species is still unclear and, therefore, their mode of action is unknown. However through the use of computational resources such as in silico digestion, QSAR and molecular dynamics to investigate the combination of residues of most relevance for antihypertensive activities could be employed so that BP production can be streamlined to produce those that are most active.[354, 364-365] In terms of their potential use as functional food components it would also be worthwhile to determine what effect the presence other active constituents, such as polyphenols, may have on the structure and functionality of BPs and this is area addressed in the following chapter with the use of molecular dynamics

Chapter 5 - Calculating the OH-bond dissociation enthalpies of small phenolics and 7-phloroeckol with long-range-corrected density functional theory

5.1 Introduction

Computational chemistry comprises the array of *in silico* techniques that are available for investigating chemistry-based systems. Computational techniques are used to gain information in areas relating to molecular geometries and energies, physical properties, chemical reactivity and enzyme/substrate interactions.[208] The most commonly employed *in silico* techniques involve those based on molecular mechanics, ab initio calculations, semi-empirical calculations, density functional theory (DFT) calculations and molecular dynamics.[208] The area of antioxidants in particular is regularly the focus of computational chemistry studies, in which attempts to decipher the SARs of naturally-derived antioxidants, such as polyphenols, are often made.[366-368] To date, numerous characteristics of polyphenols have been suggested as indicators of potential antioxidant activity; (a) the occurrence of multiple hydroxyl groups attached to aromatic rings; (b) the arrangement of hydroxyl groups in the *ortho*-dihydroxy conformation; (c) the planar structure of phenolics allowing conjugation and electron delocalisation; and (d) the presence of additional functional groups.[369]

Many phenolic compounds have the ability to exert antioxidant effects via the transfer of hydrogen from a hydroxyl group to the chain carrying peroxyl radicals of the oxidizable substrate. The rate of this reaction is affected by several parameters, of which bond dissociation enthalpy (BDE), i.e. the strength needed to break the phenolic OH bond, is one of the most important.[370-371] The BDE of phenolic OH bonds is widely considered as a reliable indicator of antioxidant activity since phenols donate the hydrogen atom to free radicals in order to neutralise them and, therefore, the lower a compound's BDE, the more likely it will act as an efficient antioxidant.[369] Other antioxidant parameters include adiabatic ionisation potential (AIP), OH proton dissociation enthalpy (PDE), proton affinity (PA) and electron transfer enthalpy (ETE).[372] BDE has shown to strongly correlate with experimental free radical scavenging capacity regardless of the antioxidant mode of action, namely HAT, SET-PT or SPLET.[373] Furthermore, it has been shown previously that HAT, which can be theoretically predicted by a compound's BDE, is the most important mechanism in the free

radical scavenging activity of polyphenols.[372] Theoretical quantum mechanics (QM) calculations are widely employed to rapidly determine accurate O-H BDEs. Additionally, a theoretical approach, as opposed to an experimental one, can help to interpret observed substituent and/or conformer effects on the BDEs of novel phenolic structures, as well as on known phenolics.[374]

To date, many of the QM studies investigating the thermodynamic characteristics of antioxidant polyphenols have focused on flavonoid structures.[204-205, 223] As is evident from chapters 1-3, macroalgal phlorotannins are progressively gaining research interest in terms of their antioxidant capacities, however, until this current work no study had carried out a QM study dealing with the calculation of phlorotannin BDEs. 7-Phloroeckol is a polyphenolic phlorotannin identified in various brown macroalgae, such as *Ecklonia cava*,[110, 375] *Eisenia bicyclis*,[376] and *Ecklonia stolonifera*.[377] 7-Phloroeckol has previously been reported as having good *in vitro* radical scavenging activity, exhibiting IC_{50} values of 18.6, 39.6, 21.9 and 22.7 μM against the DPPH·, hydroxyl, superoxide and peroxyl radicals, respectively.[110] To gain a more informed understanding of a polyphenol's potential to inhibit free radicals, various forms of data must be generated, such as the dynamic competition (K_s) between polyphenols-free radicals under the simulation of an oxidative stress, the reactivity properties of the polyphenols in polar and non-polar media, solubility in water, and their ability to donate hydrogen atoms or electrons by means of thermochemical properties.[378] This can be achieved by combining suitable experimental techniques with computational methods, of which DFT is considered one of the most resourceful.

Quantum chemical DFT calculations are employed for calculations of BDEs, in addition to other thermochemical data. Similarly to other QM methods, such as *ab initio* and semi-empirical calculations, DFT calculations are based on the Schrödinger equation, however, unlike those methods, DFT derives the electron distribution directly rather than calculating a wavefunction.[379] DFT calculations are based on the Hohenberg-Kohn theorem, according to which, the electron density can be used to determine all properties of a system under consideration.[380] DFT methods include the effects of electron correlation and, thus, provide the benefits of some more computationally expensive *ab initio* methods.[381] Many versions of DFT have been developed, such as local-density approximation (LDA) and gradient-corrected functionals, however, to date, the best results have been observed with hybrid functionals.[208] Hybrid functionals include some contribution from Hartree-Fock (HF)-type exchange, the most popular of which is the local spin-density approximation (LSDA)

gradient-corrected techniques, which employ the Becke-three parameter Lee-Yang-Parr (B3LYP) functional.[208] The B3LYP DFT functional employs three empirical parameters to combine the exact exchange, gradient-corrected exchange and LSD exchange with a correlation term based on the LSDA.[210] The initial gain from the development of this correlation-exchange was that the HF method frequently produces errors opposite to those found at DFT level, which leads to an almost systematic cancelling of errors.[211] Of late, renewed focus has been given to improving conventionally employed DFT methods particularly for the treatment of dispersive interactions and long-range correlation found in non-covalent interactions between/within biomolecules.[211, 233, 382-383] Self-interaction error is a problem in many conventional DFT methods and, therefore, long-range-corrected (LC) functionals attempt to partially remove the self-interaction errors. LC functionals, also known as range-separated functionals, are based on the separation of the Coulomb operator into long- and short-range parts using a standard error function. Only the short-range portion is retained, while the long-range part is replaced with an exact orbital expression using HF exchange integrals.[384] One such LC functional, the coulomb attenuated method (CAM)-B3LYP, combines the hybrid qualities of B3LYP and the long-range correction presented by Tawada and colleagues.[230] The CAM-B3LYP functional comprises of 0.19 HF plus 0.81 Becke 1988 (B88) exchange interaction at short-range, and 0.65 HF plus 0.35 B88 at long-range.[231]

The recently introduced ωB97XD functional is a LC hybrid density functional that includes empirical atom–atom dispersion corrections.[229] This functional was developed in an attempt to improve on the existing LC functionals, which tended to be substandard to the best hybrids for calculating thermochemistry properties, without adding computational cost.[229] It consists of 100% long-range exact exchange, approximately 22% of short-range exact exchange, a modified B97 exchange density functional for short-range interaction, the B97 correlation density functional[385] and additional empirical dispersion correction.[229] The ωB97XD showed notable improvement on the previous ωB97X functional only for non-covalent interactions. In relation to existing dispersion-corrected DFT functionals (DFT-D) (B97-D, B3LYP-D and BLYP-D[233]) and previous LC hybrid functionals (ωB97X and ωB97) for calculations on a set of data including atomization energies, reaction energies, non-covalent interaction energies, equilibrium geometries, and a charge-transfer excited state, ωB97XD was in general better in overall performance.[229] However, this functional does have the drawback of suffering from some self-interaction at short-range. [229]

Chapter 5 initially deals with comparing the performance of the two LC DFT functionals, CAM-B3LYP and ωB97XD, in combination with different Pople basis sets for the calculation of the BDEs for a group of small phenolics that were previously investigated using the locally dense basis set (LDBS) B3LYP/6-311+G(2d,2p) method.[234] Secondly, the intention of this work was to employ one of the LC DFT functionals, that showed an improvement over the non-LC methods for the calculation of the small phenolic BDE values, to assess the conformational and H-abstraction site effects on the BDE of 7-phloroeckol.

5.2 Experimental

All calculations were performed using the Gaussian 09 (revision B.01) program package.[386]

5.2.1 Calculation of small phenolic BDEs using two long-range-corrected DFT functionals

For this work, the performances of the long-range-corrected (LC) functionals CAM-B3LYP and ωB97XD for the calculation the OH BDEs of phenol (**25**) and thirteen small phenolic compounds (**26-38**) (see Figure 24 for structures) representing various ortho-, para-, and meta-substituted phenols were compared. Firstly, the BDEs of the phenolic parent and radical compounds were calculated using a full basis B3LYP method, as described by Wright and colleagues.[234] Structure geometries were optimised and vibrational frequencies determined using the AM1 method. Frequencies were scaled by a factor of 0.973 to obtain the zero-point energy and the vibrational contribution to the enthalpy. The enthalpy of the parent molecule is then corrected for translational, rotational, vibrational, and PV-work terms within Gaussian 09 to obtain the thermal correction to the enthalpy, which includes the zero-point energy.[234]

For parent structures, an intermediate step involving a single point calculation with B3LYP/6-31G(d) was carried out at the AM1 optimised geometry to speed up convergence in the next step. Finally, a B3LYP/6-311+G(2d,2p) calculation was done using orbitals from the previous step. For radical structures, the intermediate and final single point calculations are carried out using restricted open-shell (RO)B3LYP. The total enthalpy (at 298 K) is calculated as the sum of the thermal correction to the enthalpy from AM1 calculation and the electronic energy from the final single point calculation. An enthalpy of -0.49764 au for the H-atom is used in all calculations for the reasons explained by DiLabio and co-workers.[387] The BDE is calculated as the enthalpy difference for the reaction ArOH → ArO· + H·, where ArOH is the parent phenol and ArO· is the corresponding phenoxyl radical. The BDE values obtained from this full basis method were benchmarked against BDEs calculated for the same structures using a locally-dense basis set (LDBS) B3LYP 6-311+G(2d,2p) method reported by Wright and colleagues.[234]

For the comparison of CAM-B3LYP and ωB97XD methods, a similar procedure to above was employed, with some additional variations, to gain more insight into the most suitable methods for optimisation and single point calculations of each LC

functional. For the geometry optimisation step, the phenolics were optimised with either the AM1 method or the 6-31+G(d,p) basis set. For the intermediate single point calculation only the 6-31+G(d,p) basis set was employed. For the final single point calculation either 6-311+G(d,p), 6-311+G(2d,2p) or 6-311+G(3df,2p) basis sets were used. This resulted in six methods, i.e. 6-311+G(d,p)//6-31+G(d,p), 6-311+G(d,p)//AM1, 6-311+G(2d,2p)//6-31+G(d,p), 6-311+G(2d,2p)//AM1, 6-311+G(3df,2p)//6-31+G(d,p), 6-311+G(3df,2p)//AM1, being assessed for each LC functional. Scale factors of 0.976 and 0.975 were used for CAM-B3LYP and ωB97XD,[388] respectively. The hydrogen atom energy was calculated separately for each method.

5.2.2 Calculation of the BDEs of 7-phloroeckol radical conformers by CAM-B3LYP

The conformational analysis of the 7-phloroeckol radical structures was carried out based on the outcomes of the previous comparative work of the LC functionals, which are discussed later in Section 6.3. The geometry of the neutral 7-phloroeckol structure (see Figure 25 for structure) was constructed and optimised with the semi-empirical AM1 method using Webmo (http://www.webmo.net/). Eight different 7-phloroeckol radical structures were created through the removal of a hydrogen atom from each of the individual hydroxyl sites. Confab, a conformation generator, was employed to carry out systematic conformational analysis on each of the eight phloroeckol radicals (**A-H**).[389] In an attempt to improve performance, accuracy has been favoured over approximations in this method. From the initial input structure, Confab generates multiple conformers using the torsion-driven approach from a set of predefined allowed torsion angles.[229] The confab algorithm is outlined in Figure 26 (adapted from[389]). The conformers were generated using a root-mean-square deviation (RMSD) diversity cut-off of 1.5 Å and energy cut-off of 50 kcal mol^{-1}. Confab uses the MMFF94 force-field to assess the energy. The lowest energy conformer found is used as a reference point for applying an energy cut-off during the conformer search.[389] Table 5 lists the conformers, and their respective values for the four torsion angles, that were within the RMSD and energy cut-offs for the eight 7-phloroeckol radicals. The geometry optimisations were carried out with AM1, an intermediate single point calculation was carried out on radical structures and their parent structures using (RO)CAM-B3LYP 6-31+G(d,p) and CAM-B3LYP 6-31+G(d,p), respectively. BDEs of the various conformers were calculated using the CAM-B3LYP 6-311+G(2d,2p) method for the parent structures and (RO)CAM-B3LYP 6-311+G(2d,2p) method for the radical structures.

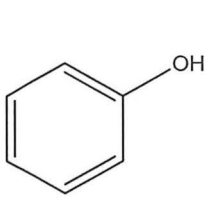

phenol **25**

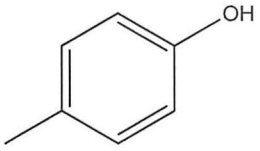

para-cresol **26**

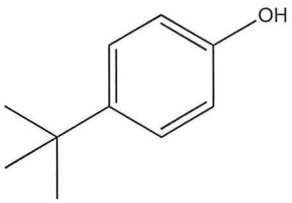

p-tert-butyl phenol **27**

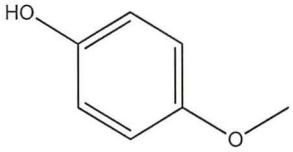

4-hydroxyanisole **28**

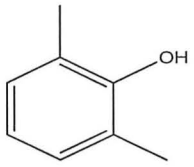

2,6-dimethylphenol **29**

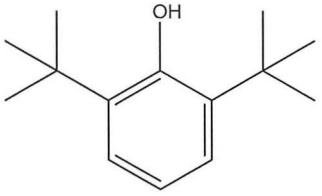

2.6-ditert-butylpheno **30**

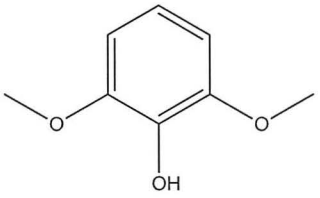

2,6-dimethoxy phenol **31**

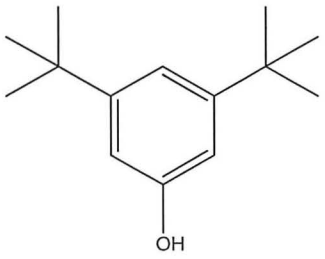

3,5-ditert-butyl phenc **32**

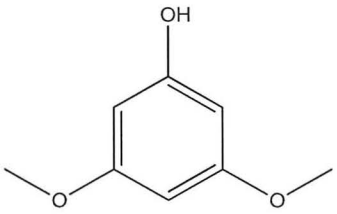

3,5-dimethoxy phenol **33**

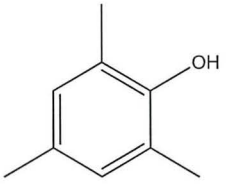

2,4,6-trimethyl phenol **34**

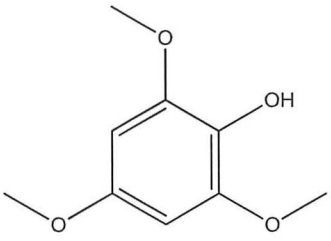

2,4,6-trimethoxy phenc **35**

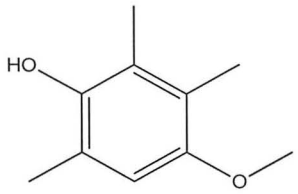

2,3,6-trimethyl 4-methoxy phenol **36**

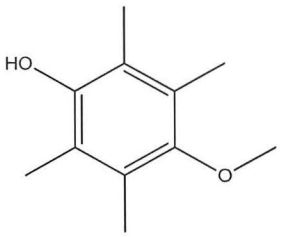

2,3,5,6-tetramethyl-4-methoxy phenol **37**

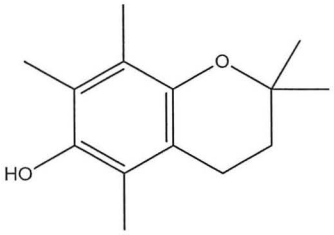

6-hydroxy-2,2,5,7,8-pentamethylchroman **38**

Figure 24: Structures of small phenolic compounds **25-38** investigated using two long-range corrected functionals.

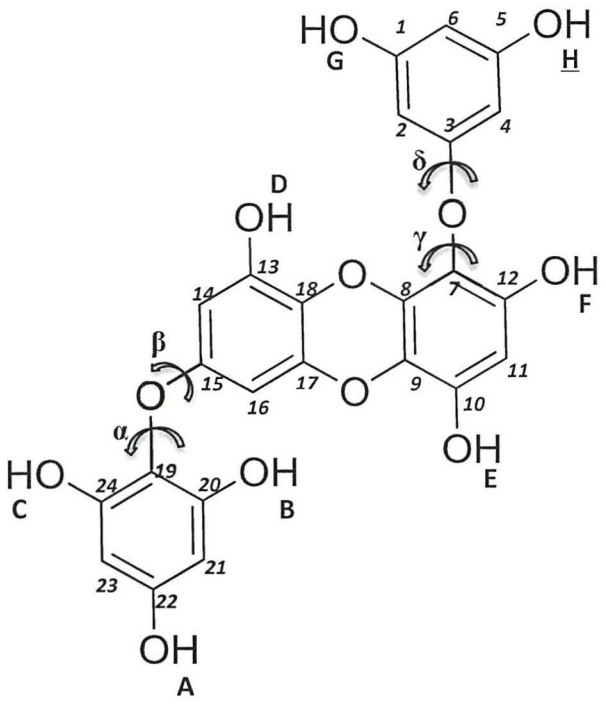

Figure 25: Structure of 7-phloroeckol, where torsion angle **α** is C20, C19, O, C15, torsion angle **β** is C19, O, C15, C16, torsion angle **δ** is C7, O, C3, C4 and torsion angle **γ** is C12, C7, O, C3. Letters **A-H** represent the 8 hydroxyl sites of potential H-abstraction.

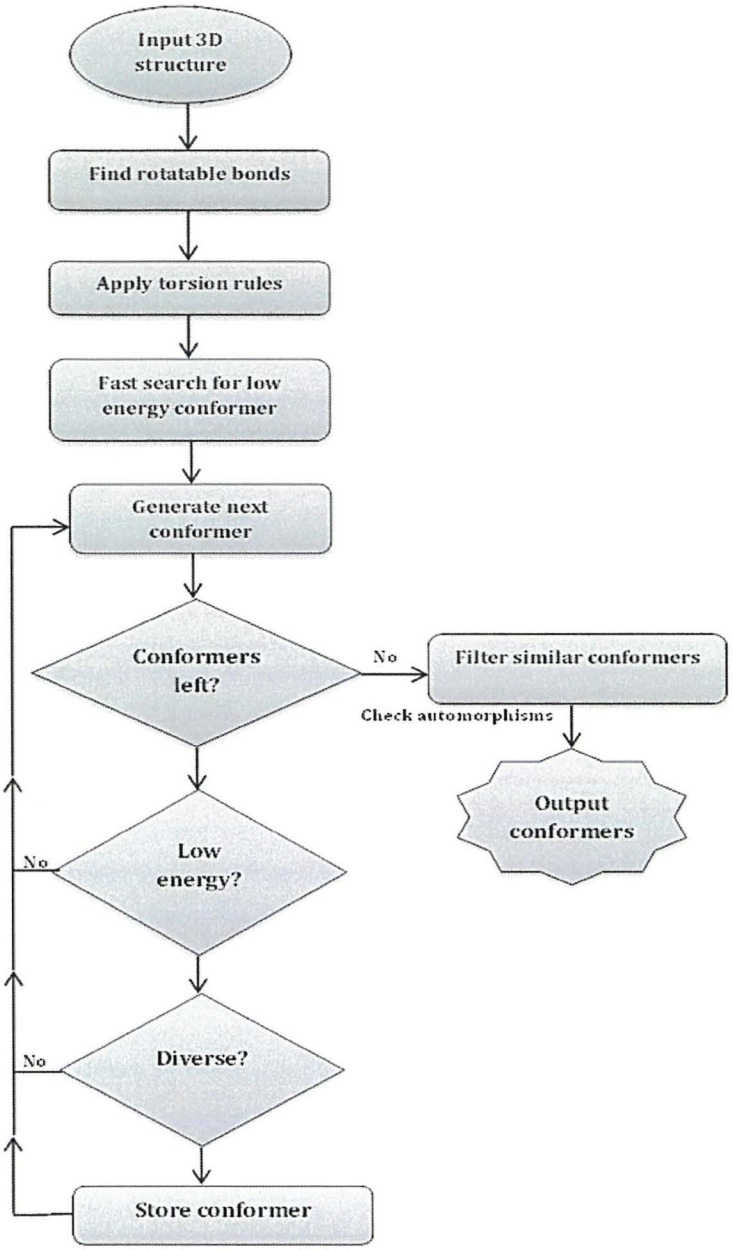

Figure 26: Flowchart of Confab algorithm. Adapted from[389]

Table 5: 7-Phloroeckol conformers and their torsion angles for angles α, β, γ and δ.

Conformer	Angle α	Angle β	Angle γ	Angle δ
A1	29.9988	33.9339	154.6464	-33.9019
A2	29.9988	33.9339	34.645	30.0001
A3	150.0014	153.934	-145.3544	-153.8995
A4	150.0014	153.934	-25.3556	-33.8976
A5	150.0031	-26.0657	-25.3556	-33.8976
B1	150.0028	152.038	154.1612	-33.528
B2	-30.0055	152.038	34.1626	-153.529
B3	150.0028	152.038	-25.8375	-33.5304
B4	29.9924	-147.961	-145.8407	-153.5335
B5	150.0008	-27.9652	-25.8375	-33.5304
B6	-29.9964	-27.9652	154.1612	-33.528
B7	29.9997	32.0357	-145.8407	-153.5335
C1	-29.9986	155.245	155.2256	-33.7537
C2	-29.9986	155.245	35.2247	-153.7519
C3	29.9984	35.2465	-24.7759	-33.7507
C4	30.0025	-144.7558	-24.7759	-33.7507
C5	-30.0023	-24.7552	155.2236	-33.7537
C6	29.9984	35.2465	-144.7732	-153.7506
C7	-30.0023	-25.7552	35.2247	-153.7509
C8	30.0025	-144.7558	-144.7732	-153.7506
D1	29.9984	35.2465	35.2247	-153.7519
D2	30.0025	-144.7558	155.2256	-33.7537
D3	150.001	155.245	-24.7759	-33.7507
D4	149.9996	-24.7552	155.2256	-33.7537
D5	29.9984	35.2465	-144.7732	-153.7506
E1	30.0025	-144.7558	155.2256	150.0014
E2	29.9985	35.2465	155.2256	-33.7537
E3	29.9984	35.2465	35.2247	-153.7519
E4	150.001	155.245	-24.7759	-33.7507
E5	149.9996	-24.7552	-24.7759	-33.7507
F1	30.0025	-144.7558	155.2256	-33.7537
F2	29.9984	35.2465	155.2256	-33.7537
F3	30.0025	-144.7558	35.2247	-153.7519
F4	29.9984	35.2465	35.2247	-153.7519
G1	29.9984	35.2465	35.2247	-153.7519
G2	30.0025	-144.7558	35.2247	-153.7519
G3	30.0028	-144.7588	155.2256	-33.7537
G4	149.9996	-24.7552	155.2256	-33.7537
G5	29.9984	35.2465	-144.7732	26.2437
G6	150.001	155.245	-24.7759	146.2495
G7	150.001	155.245	-144.7732	26.2437
H1	29.9984	35.2465	35.2247	-153.7519
H2	30.0025	-144.7558	35.2247	-153.7519
H3	30.0025	-144.7558	155.2256	-33.7537
H4	149.9996	-24.7552	155.2236	-33.7537
H5	150.001	155.245	-24.7759	146.2495
H6	29.9984	35.2465	-144.7732	26.2437
H7	150.001	155.245	-144.7732	26.2437

5.3 Results and Discussion

5.3.1 Comparison of LC-DFT functionals for the calculation of small phenolic compounds

Due to its inherent electron correlation, DFT has the advantage of being able to calculate geometries and relative energies in the same computational time required for HF calculations, but with similar accuracy to MP2 calculations.[208] Although theoretical studies on radical reactions are most often carried out using DFT, mainly due to its relatively lower computational cost,[390] it has been shown that the approximate exchange-correlation functionals used in DFT methods may be subject to significant error.[390-391] The basis for the substandard description of the intermolecular interactions in DFT lies in the approximations made in DFT functionals rather than in the density functional theory.[392] For example, the GGA approximation determines the exchange-correlation energy on the basis of the electron density and the reduced electron density gradient at a given grid point and, therefore, the total exchange correlation energy is also local. Overall, this results in the dispersion energy not being totally covered by the GGA functionals.[392] The improvement of DFT accuracy is constantly occurring through the modification of functionals based on experimental comparisons and intuition.[208] A renewed focus has been given to improving current DFT methods, particularly for the treatment of dispersive interactions and long-range correlation between/within non-covalently bonded molecules/atoms.[393-394] This assessment study was carried out to investigate how accurately the CAM-B3LYP and ωB97XD DFT functionals can calculate the BDEs for a set of small phenolic compounds. Furthermore, the impact of varying the geometry optimisation step and basis sets for the final single point calculations of these methods was also investigated. The experimental BDEs,[395] the LDBS B3LYP theoretical BDEs[234] and the full basis B3LYP theoretical BDEs, which were calculated in this work, for compounds **25-38** are displayed in table 6. The mean absolute deviations (MADs) of the theoretical BDEs of the group of phenolics relative to the experimental values were calculated and found to be 1.962 kcal mol^{-1} and 1.966 kcal mol^{-1} for the LDBS method and full basis method, respectively. This highlighted that there was good agreement between the two theoretical methods and, therefore, the full basis approach was employed as a benchmark to compare the performance of CAM-B3LYP and ωB97XD functionals for the same set of phenolics.

Table 6: Experimental, locally dense basis set (LDBS) B3LYP and full basis B3LYP bond dissociation enthalpies (BDEs).

	Bond Dissociation Enthalpies (BDEs) (kcal mol^{-1})		
ArOH	**Experimental**[395]	**LDBS**[234] **B3LYP/6-311+G(2d,2p)//AM1**	**Full Basis Set B3LYP/6-311+G(2d,2p)//AM1**
1	88.3 ± 0.8	87.05	87.04
2	86.2 ± 0.6	84.58	84.55
3	85.3 ± 0.5	84.76	84.91
4	82.81 ± 0.21	80.92	80.98
5	84.50 ± 0.38	82.88	82.69
6	82.80 ± 0.21	76.51	75.63
7	83.16 ± 0.15	82.44	82.44
8	86.62 ± 0.26	85.68	85.68
9	86.70 ± 0.3	86.00	86.67
10	82.73 ± 0.18	80.58	80.40
11	80.00 ± 0.12	78.07	78.36
12	79.20 ± 0.15	76.69	76.83
13	81.88 ± 0.20	79.04	79.12
14	78.25 ± 0.18	75.78	75.64
MAD		**1.962**	**1.966**

Table 6 shows that, for the most part, all the CAM-B3LYP approaches underestimate the BDEs of the phenolic structures relative to the experimental BDE values shown in table 4. Table 6 also shows that the CAM-B3LYP approaches that employ the basis set 6-31+G(d,p) for geometry optimisation rather than AM1 optimisation perform better for the calculation of the phenolic (**25-38**) BDEs as they result in comparatively lower deviations from the experimental BDEs. Interestingly, using either of the higher basis sets of 6-311+G(2d,2p) and 6-311+G(3df,2p) for the final single point calculation resulted in the same MADs from the experimental BDEs when equivalent optimisation was carried out (1.52 and 1.62 kcal mol^{-1} for 6-31+G(d,p) and AM1 optimisation, respectively). The similarity of these MAD values suggests that the underestimation of the BDE may be due to the CAM-B3LYP molecular energy calculation rather than the geometry optimisation methods. Furthermore, all four of these method combinations improved on the MAD of 1.966 kcal mol^{-1} observed for the initial B3LYP full basis set method (table 4). The difference in the BDE values of the phenolic structures **26-38** relative to phenol **25** are displayed in table 7. From this data it is apparent that the CAM-B3LYP 6-311+G(d,p)//6-31+G(d,p) shows the least amount of deviation, with

a MAD of 1.15 kcal mol^{-1}, from the experimental values in terms of calculating BDEs relative to phenol.

Table 7: CAM-B3LYP BDEs with three different basis sets, each optimised with AM1 or CAM-B3LYP/6-31+G(d,p). MAD values are relative to experimental BDE values in table 6.

	Bond Dissociation Enthalpies (kcal mol^{-1})					
ArOH	**CAM-B3LYP/6-311+G(d,p)// CAM-B3LYP/6-31+G(d,p)** (H atom = -0.498812779)	**CAM-B3LYP/6-311+G(d,p)// AM1** (H atom = -0.498812779)	**CAM-B3LYP/6-311+G(2d,2p)// CAM-B3LYP/6-31+G(d,p)** (H atom = -0.498812779)	**CAM-B3LYP/6-311+G(2d,2p)// AM1** (H atom = -0.498812779)	**CAM-B3LYP/6-311+G(3df,2p)// CAM-B3LYP/6-31+G(d,p)** (H atom = -0.498812779	**CAM-B3LYP/6-311+G(3df,2p)//AM1** (H atom = -0.498812779
1	87.04	86.80	87.72	87.49	87.84	87.61
2	84.77	84.54	85.46	85.22	85.57	85.34
3	85.07	84.78	85.77	85.48	85.89	85.60
4	81.07	80.76	81.64	81.32	81.68	81.37
5	82.20	81.91	82.89	82.60	82.98	82.68
6	78.71	78.27	79.26	78.82	79.38	78.94
7	82.25	82.75	82.39	82.89	82.26	82.76
8	85.33	85.09	86.01	85.77	86.13	85.89
9	86.59	86.37	87.23	87.02	87.42	87.21
10	80.16	79.85	80.84	80.54	80.90	80.60
11	78.31	78.71	78.36	78.76	78.21	78.61
12	75.09	74.49	75.82	75.22	75.70	75.10
13	79.06	78.75	79.80	79.49	79.80	79.50
14	75.30	75.52	75.94	76.17	75.97	76.20
MAD	**1.97**	**2.13**	**1.52**	**1.62**	**1.52**	**1.62**

Table 8: CAM-B3LYP BDEs relative to phenol using with three different basis sets, each optimised with AM1 and CAM-B3LYP/6-31+G(d,p). MAD values are relative to experimental relative BDE values.

	BDEs relative to phenol BDE(kcal mol^{-1})					
ArOH	**CAM-B3LYP/6-311+G(d,p)// CAM-B3LYP/6-31+G(d,p)**	**CAM-B3LYP/6-311+G(d,p)// AM1**	**CAM-B3LYP/6-311+G(2d,2p)// CAM-B3LYP/6-31+G(d,p)**	**CAM-B3LYP/6-311+G(2d,2p)// AM1**	**CAM-B3LYP/6-311+G(3df,2p)// CAM-B3LYP/6-31+G(d,p**	**CAM-B3LYP/6-311+G(3df,2p)//AM1**
1	87.04	86.80	87.72	87.49	87.84	87.61
2	-2.26	-2.26	-2.27	-2.26	-2.28	-2.27
3	-1.97	-2.02	-1.95	-2.01	-1.96	-2.01
4	-5.97	-6.04	-6.09	-6.16	-6.16	-6.23
5	-4.84	-4.90	-4.83	-4.89	-4.87	-4.92
6	-8.33	-8.53	-8.46	-8.67	-8.47	-8.67
7	-4.79	-4.05	-5.33	-4.59	-5.58	-4.84
8	-1.70	-1.72	-1.71	-1.72	-1.71	-1.72
9	-0.45	-0.43	-0.49	-0.47	-0.43	-0.40
10	-6.88	-6.95	-6.88	-6.95	-6.94	-7.01
11	-8.73	-8.10	-9.36	-8.73	-9.63	-9.00
12	-11.95	-12.31	-11.90	-12.26	-12.15	-12.51
13	-7.98	-8.05	-7.92	-7.99	-8.04	-8.11
14	-11.74	-11.28	-11.78	-11.32	-11.87	-11.41
MAD	**1.15**	**1.21**	**1.19**	**1.20**	**1.29**	**1.26**

The LC-DFT functional ωB97XD has previously shown to be the most reliable method for describing hydrogen-bond interaction compared to other DFT functionals B3LYP DFT-D, M06, and M06-2X,[396] and was found to provide similar stability trends of hydrogen-bonded complexes as that of MP2 method, which is considered one of the most reliable ways to describe hydrogen bonding.[392] For the calculation of the small phenolic BDEs with the ωB97XD functional (table 9), it was apparent the basis set employed for the single point calculation significantly affected the values obtained. Single point calculations using ωB97XD 6-311+G(d,p) basis set resulted in a large overestimation of the BDEs (MADs of 9.87 and 9.74 kcal mol^{-1} for 6-31+G(d,p) and AM1 geometry optimisations, respectively), whereas calculations using the 6-311+G(3df,2p) basis set resulted in a large under estimation of the BDE values (MADs of 11.53 and 11.65 kcal $^{-1}$ for 6-31+G(d,p) and AM1 geometry optimisations, respectively), relative to the experimental values. Of the three ωB97XD approaches the ωB97XD/6-311+G(2d,2p) method performed the best as, regardless of the geometry optimisation method employed, smaller deviations from experimental values (MADs of 1.64 and 1.73 kcal mol^{-1} for 6-31+G(d,p) and AM1 optimisations, respectively) were observed for this method, relative to the B3LYP full basis set. The difference in the BDE values of the phenolic structures **26-38** relative to phenol **25** for the ωB97XD methods are displayed in table 10. From this it is apparent that the ωB97XD 6-311+G(d,p)//AM1 shows the least amount of deviation, with a MAD of 1.10 kcal mol^{-1}, from the experimental values in terms of calculating the BDEs of the small phenolic structures relative to phenol. This MAD value is also lower than the most accurate CAM-B3LYP method for calculating relative BDE values. The ωB97XD 6-311+G(d,p) and ωB97XD 6-311+G(3df,2p) displayed significantly higher relative MAD values.

From the comparative study, it can be concluded that in terms of calculating absolute BDEs for phenol structures the CAM-B3LYP/6-311+G(2d,2p) or CAM-B3LYP/6-311+G(3df,2p) single point methods using 6-31+G(d,p) optimised geometries seem to be the most accurate. However, in relation to calculating BDEs values relative to phenol, the ωB97XD 6-311+G(2d,2p)//6-31+G(d,p) and ωB97XD 6-311+G(2d,2p)//AM1 methods appear to be the most suitable. It is also clear that both the LDBS and full basis set B3LYP/6-311+G(2d,2p)//AM1 methods underestimate the BDEs of the various small phenolics in comparison to the experimental values for the all structures. However, the use

of CAM-B3LYP CAM-B3LYP/6-311+G(2d,2p), CAM-B3LYP/6-311+G(3df,2p), or ωB97XD/6-311+G(2d,2p) in conjunction with either AM1 or 6-31+G(d,p) for geometry optimisation can reduce the extent of these deviations.

Table 9: ωB97XD BDEs with three different basis sets, each optimised with AM1 and ωB97XD /6-31+G(d,p). MAD values are relative to experimental BDE values in table 6.

	Bond Dissociation Enthalpies (kcal mol^{-1})					
ArOH	**ωB97XD /6-311+G(d,p)// ωB97XD /6-31+G(d,p)** (H atom = -0.502668339)	**ωB97XD /6-311+G(d,p)// AM1** (H atom = -0.502668339)	**ωB97XD /6-311+G(2d,2p)// ωB97XD /6-31+G(d,p)** (H atom = -0.502668339)	**ωB97XD /6-311+G(2d,2p)// AM1** (H atom = -0.502668339)	**ωB97XD /6-311+G(3df,2p)// ωB97XD /6-31+G(d,p** (H atom = -0.502668339)	**ωB97XD /6-311+G(3df,2p)//AM1** (H atom = -0.502668339)
1	93.93	93.79	87.44	87.31	81.21	81.08
2	92.80	92.67	85.21	85.07	78.55	78.42
3	95.85	95.74	85.45	85.34	77.39	77.27
4	90.44	90.24	81.32	81.12	71.79	71.59
5	91.48	91.29	82.78	82.58	75.81	75.61
6	94.25	93.38	79.99	79.11	70.36	69.49
7	93.49	93.95	81.67	82.14	68.77	69.24
8	100.28	100.08	85.87	85.68	76.04	75.85
9	98.70	98.57	87.03	86.90	74.30	74.17
10	90.61	90.39	80.76	80.55	73.40	73.19
11	91.97	92.43	77.54	78.00	61.39	61.86
12	88.30	87.76	76.02	75.48	65.53	64.98
13	92.84	92.66	79.56	79.38	68.88	68.69
14	91.64	91.92	75.83	76.11	63.65	63.93
MAD	**9.87**	**9.74**	**1.64**	**1.73**	**11.53**	**11.65**

Table 10: ωB97XD BDEs relative to phenol using with three different basis sets, each optimised with AM1 and ωB97XD /6-31+G(d,p). MAD values are relative to experimental relative BDE values.

	BDEs relative to phenol BDE(kcal mol^{-1})					
ArOH	**ωB97XD /6-311+G(d,p)// ωB97XD /6-31+G(d,p)**	**ωB97XD /6-311+G(d,p)// AM1**	**ωB97XD /6-311+G(2d,2p)// ωB97XD /6-31+G(d,p)**	**ωB97XD /6-311+G(2d,2p)// AM1**	**ωB97XD /6-311+G(3df,2p)// ωB97XD /6-31+G(d,p)**	**ωB97XD /6-311+G(3df,2p)//AM1**
1	93.93	93.79	87.44	87.31	81.21	81.08
2	-1.13	-1.13	-2.23	-2.24	-2.66	-2.67
3	1.92	1.94	-1.99	-1.97	-3.83	-3.81
4	-3.49	-3.56	-6.13	-6.19	-9.42	-9.49
5	-2.45	-2.51	-4.66	-4.73	-5.41	-5.47
6	0.32	-0.42	-7.45	-8.19	-10.85	-11.59
7	-0.44	0.16	-5.77	-5.17	-12.44	-11.84
8	6.35	6.29	-1.57	-1.63	-5.17	-5.23
9	4.77	4.77	-0.41	-0.41	-6.92	-6.91
10	-3.32	-3.40	-6.68	-6.76	-7.81	-7.89
11	-1.96	-1.36	-9.90	-9.30	-19.82	-19.22
12	-5.63	-6.04	-11.42	-11.83	-15.69	-16.10
13	-1.08	-1.14	-7.88	-7.93	-12.34	-12.39
14	-2.29	-1.87	-11.61	-11.19	-17.56	-17.15
MAD	**4.56**	**4.58**	**1.12**	**1.10**	**4.78**	**4.77**

5.3.2 Comparison of the theoretical BDEs of the 7-phloroeckol radical conformers calculated by CAM-B3LYP

An understanding of the conformational, electronic and geometrical nature of polyphenols is important to realise the relationship between phenolic structure and antioxidant activity. The use of QM conformational analysis is essential as a means to characterise the antioxidant capacity of polyphenols and their different conformers, as the behaviour of hydroxyl groups is strongly influenced by both the neighbouring groups and the geometry.[397] Although from the literature review and chapters 2-3 of this work it is evident that experimental research into bioactive marine and macroalgal polyphenols is widespread, the use of *in silico* methods, in particular QM, to investigate SARs of marine phenols or polyphenols is limited. Phlorotannins in particular have been well-reported as potent antioxidant compounds and their potential use in functional foods is a focus of research. Therefore, it would be beneficial to add knowledge and provide a theoretical benchmark regarding the SARs of antioxidant phlorotannins to the existing experimental research in this area in order to provide a wider representation of the potential of phlorotannins to be applied as functional components.

Numerous studies have employed different QM techniques to investigate the SARs of antioxidant plant polyphenols, with the B3LYP functional often being the functional of choice.[47, 397] Mikulski and Molski performed QM calculations in the gas phase and water medium using DFT in an attempt to explain the equilibrium SARs of resveratrol metabolites and peanut polyphenols.[47] In this study B3LYP 6-311++G(d,p) was employed for geometry optimisation of *trans*-resveratrol, five *trans*-resveratrol-*O*-sulphates and three peanut stilbenoids; namely archidin-1, archidin-2 and archidin-3. A conformational energy map was generated in gas phase, through the discrete rotation of selected torsional angles in the trans-stilbene moiety of the structures in 10° increments. The most stable structures obtained were optimised and their BDE calculated at the B3LYP 6-311++G(d,p) level. The BDE of the 4'-OH bond was found to be the lowest in all of the structures investigated both in gas phase and water. Notably, the BDE of the 3-OH and 5-OH bonds were almost identical due to their symmetrical location on the trans-stilbene moiety.[47] QM studies investigating the marine phenols for potential antioxidant activity are scarce, although

one study by Belcastro *et al.*[398] did assess the molecular properties of seven marine phenols known as 'acremonins'. The B3LYP/6-311++(d,p) method was used to calculate the BDEs of the marine compounds in both gas phase and solvent. This group concluded that the most efficient hydrogen donors systems are characterised by the ortho formation of the phenolic functionality and that the radicals produced are strongly stabilized by several resonance structures that allow the odd electron to be localised over the whole molecule.[398]

It is widely considered that the location of hydroxyl groups, as opposed to their number, in a polyphenol determines the level of its antioxidant activity. In a particular study to highlight this involving the phlorotannin monomer phloroglucinol, it was shown that increasing the number of hydroxyl groups in the meta position, C(1,3,5), as in phloroglucinol, does not show any significant change in the BDEs when compared to that of hydroxyl group in C(1) as in phenol.[399] The study also concluded that it seemed increasing the number of hydroxyl groups in the *ortho*-position promotes the formation of intramolecular hydrogen bonds.[399] Intramolecular hydrogen bonds allow phenolic groups to easily give up a hydrogen atom, promoting electron delocalisation in the resulting radical, and, therefore, result in decreased the BDEs.[399-400] Furthermore, it was shown that phloroglucinol afforded rate constants and activation energies in all solvents similar to those found for resorcinol, which has 2 *meta*-positioned hydroxyl groups. This result indicates that the arrangement of hydroxyl groups in the meta position does not contribute to the radical scavenging activity of phenols, irrespective of the number of hydroxyl groups.[381] Rossi *et al.*[401] demonstrated that, for piceatannol and resveratrol reactions with the hydroxyl radical, *para*-hydrogen atom transfer is generally more efficient than meta and that *meta*-hydrogen atoms were also not useful for scavenging $O_2 \cdot^-$.

In general, the goal of the Confab conformer generation tool is to build a reliable set of representative conformers that reasonably sample a molecule's energy landscape, without generating highly unlikely structures.[402] Confab uses a systematic approach, whereby regular, random sampling of each of the dimensions of the search space is carried out. This involves augmenting the torsion angles of all rotatable bonds by a predefined amount and only the conformers within a specified energy threshold of the lowest energy conformer are retained.[402] The DFT functional CAM-B3LYP with the basis set 6-311+G(2d,2p) was employed to analyse the BDEs of various 7-

phloroeckol radical conformers generated by Confab. Although the structures optimised with 6-31+G(d,p) had the lowest MAD values of 1.52 kcal mol^{-1} it was decided to employ the computationally cheaper AM1 method, with a MAD of 1.62 kcal mol^{-1} for geometry optimisation. Firstly, the BDE of the phlorotannin monomer of phloroglucinol (1,3,5,-trihydroxybenzene) was calculated using this method and a BDE of 89.39 kcal mol^{-1} was observed. The experimental BDE of phloroglucinol has been reported to be 371.4 kJ mol^{-1}, or 88.71 kcal mol^{-1}.[403] In the same study a theoretical BDEs of 347.1 and 374.4 kJ mol^{-1}, or 82.90 and 89.42 kcal mol^{-1}, respectively, were calculated with functionals MPW1PW91 (Barone's Modified Perdew-Wang 1991 exchange functional and Perdew and Wang's 1991 correlation functional)/aug-cc-pVDZ and CBS-4M (Complete Basis Set (CBS) method 4M), respectively.[403] Thavasi *et. al.*[399] observed a BDE of 354 kJ mol^{-1}, or 84.55 kcal mol^{-1}, for phloroglucinol using B3LYP/6-311G++(3df, 3pd). A BDE of 87.7 kcal mol^{-1} was observed when calculated with B3LYP/6-311++(d,p).[404] Therefore, when comparing the accuracy of the CAM-B3LYP method employed to these previously employed theoretical methods, it is apparent that CAM-B3LYP is the most accurate with a deviation of 0.68 kcal mol^{-1} from the experimental BDE values as opposed to a deviations of 0.70 for CBS-4M,[403] 1.01,[404] 4.16[399] and 5.81[403] kcal mol^{-1} for the other referenced methods.

The exact mechanism(s) by which phlorotannins exert their antioxidant effects are poorly understood and may be as a result of a mixture of direct free radical scavenging, sequestration of potential oxidants and/or altering cell signalling. No previous work has investigated the BDE of a phlorotannin, with the exception of the monomer phloroglucinol. Therefore, the data yielded from this study cannot be compared to other theoretical or experimental studies. This work will investigate the effect of structural conformation and H-atom abstraction site on the O-H BDE of 7-phloroeckol.

The structures of the radical conformers after the single point calculations can be observed in Appendix 3. The range of BDEs observed, as seen in table 11, for the various 7-phloroeckol radical structures was 80.59-95.45 kcal mol^{-1}. It is evident from the BDE values that, of all the conformers analysed, the F2, F3 and F4 conformers

have the greatest propensity to donate a hydrogen atom with BDEs of 81.21, 80.59 and 80.71 kcal mol^{-1}, respectively. The conformer F3 is shown in Figure 26. Therefore, it appears that H-abstraction from the **F** hydroxyl site would be most favoured by 7-phloroeckol in the presence of a free radical. The order of the BDEs, from lowest to highest, of different abstraction sites of the 7-phloroeckol conformers in terms of their average values is **F** (82.07 kcal mol^{-1}) < **E** (84.85 kcal mol^{-1}) < **D** (85.30) < **B** (85.99 kcal mol^{-1}) < **A** (86.85 kcal mol^{-1}) < **H** (88.67 kcal mol^{-1}) < **G** (89.09 kcal mol^{-1}) < **C** (92.80 kcal mol^{-1}). As a general rule, the stability order of radicals is a direct consequence of the number of resonance forms that give rise to the particular hybrid.[405-406] The radicals maintain a planar conformation along the middle dibenzodioxin structure, which ensures energetically favourable delocalisation of unpaired electron through this backbone. Furthermore, planar conformation of neutral compounds can promote favourable interaction with a free radical during the antioxidative process *in vivo*.[47] Therefore, the low BDEs of sites **F**, **E** and **D** may be attributed to their location on the dibenzodioxin moiety. In addition, it seems the abstraction sites **G** and **H**, which are symmetrical to each other, display similar BDEs. This effect of symmetry has been observed previously with the trans-stilbene moiety.[47]

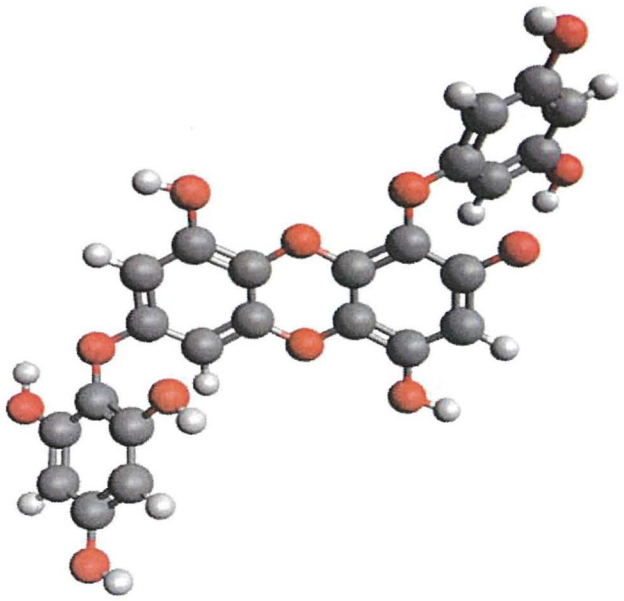

Figure 27: 7-phloroeckol F3 radical conformer

As discussed earlier, it is generally accepted that it is not the number of hydroxyl groups a polyphenol possesses that is necessary for efficient free radical scavenging activity, but their location in preferably the meta position, and to a lesser extent the para position. It could therefore be assumed that phlorotannins as polymers of phloroglucinol would not be effective free radical scavengers. However, the average BDEs of the **A**, **B**, **D**, **E** and **F** conformers exhibit BDEs lower than that calculated for phloroglucinol (88.65 kcal mol^{-1}), therefore highlighting that other factors may dominate the effect of *meta*-positioned hydroxyl groups in phlorotannin polymers. For instance, the presence of multiple aromatic rings in conjunction may be the favourable characteristic of 7-phloroeckol contributing to extensive electron delocalisation and, thus, to the lowering of its hydroxyl BDE in relation to phloroglucinol. Vennat *et. al.*[407] demonstrated that procyanidin tetramers exhibit greater antioxidant activity against peroxynitrite- and superoxide- mediated oxidation than trimers, and that heptamers and hexamers demonstrate significantly greater superoxide scavenging properties than trimers and tetramers.

LC DFT functionals are the most relevant in terms of investigating polyphenolic antioxidant SARs as they attempt to accurately treat dispersive interactions and long-range correlation found in non-covalent interactions, while at the same time limiting the potential computational expense. Therefore, in this chapter, two LC DFT functionals, namely CAM-B3LYP and ωB97XD, were compared to investigate their performance in calculating the BDEs of various small phenolic structures. From this it was concluded that the CAM-B3LYP/6-311+G(2d,2p) or CAM-B3LYP/6-311+G(3df,2p) single point methods using 6-31+G(d,p) optimised geometries seem to be the most accurate for calculating absolute BDEs, whereas, the ωB97XD 6-311+G(2d,2p)//6-31+G(d,p) and ωB97XD 6-311+G(2d,2p)//AM1 methods appeared to be the most suitable for calculating small phenolic BDEs relative to phenol

Table 11: 7-Phloroeckol conformers and their respective CAM-B3LYP/6-311+G(2d,2p) radical energies, relative energies within H-abstraction sites, BDEs, and relative deviation from phloroglucinol BDE (88.65 kcal mol^{-1})

Conformer	*E* radical (au)	Δ*E* (kcal mol^{-1})	BDE (kcal mol^{-1})	ΔBDE (kcal mol^{-1})
A1	-1825.95090314	0.261	**87.01**	-1.64
A2	-1825.95087584	0.278	**87.08**	-1.57
A3	-1825.95131861	0.000	**86.95**	-1.70
A4	-1825.95116753	0.095	**86.12**	-2.53
A5	-1825.95079379	0.329	**87.08**	-1.57
B1	-1825.95307422	0.068	**87.57**	-1.08
B2	-1825.95296432	0.137	**84.85**	-3.80
B3	-1825.95298471	0.124	**87.51**	-1.14
B4	-1825.95318298	0.000	**84.76**	-3.89
B5	-1825.94938820	2.381	**86.91**	-1.74
B6	-1825.95262018	0.353	**85.09**	-3.56
B7	-1825.95209099	0.685	**85.22**	-3.43
C1	-1825.93994375	0.003	**95.45**	6.80
C2	-1825.93994272	0.003	**93.07**	4.42
C3	-1825.93979501	0.096	**93.12**	4.47
C4	-1825.93966863	0.175	**92.68**	4.03
C5	-1825.93994807	0.000	**89.17**	0.52
C6	-1825.93946116	0.306	**93.09**	4.44
C7	-1825.93947933	0.294	**93.05**	4.40
C8	1825.93980018	0.093	**92.43**	3.78
D1	-1825.95478314	0.686	**84.11**	-4.54
D2	-1825.95216027	2.331	**85.18**	-3.47
D3	-1825.95324218	1.653	**88.54**	-0.11
D4	-1825.95587573	0.000	**83.38**	-5.27
E1	-1825.95991015	0.000	**84.88**	-3.77
E2	-1825.95975477	0.098	**84.32**	-4.33
E3	-1825.95954021	0.232	**85.00**	-3.65
E4	-1825.95980739	0.064	**84.98**	-3.67
E5	-1825.95944183	0.294	**85.08**	-3.57
F1	-1825.95972425	0.575	**85.75**	-2.90
F2	-1825.95951423	0.706	**81.21**	-7.44
F3	-1825.96064011	0.000	**80.59**	-8.06
F4	-1825.96030339	0.211	**80.71**	-7.94
G1	-1825.94818438	0.090	**88.24**	-0.41
G2	-1825.94800902	0.200	**87.91**	-0.74
G3	-1825.94444500	2.437	**90.25**	1.60
G4	-1825.94531579	1.890	**89.66**	1.01
G5	-1825.94463878	2.315	**89.95**	1.30
G6	-1825.94832834	0.000	**87.85**	-0.80
G7	-1825.94493891	2.127	**89.80**	1.15
H1	-1825.94423633	2.567	**90.15**	1.50
H2	-1825.94501660	2.078	**89.77**	1.12
H3	-1825.94804308	0.179	**87.29**	-1.36
H4	-1825.94803725	0.182	**87.21**	-1.44
H5	-1825.94449250	2.407	**90.21**	1.56
H6	-1825.94754467	0.491	**88.12**	-0.53
H7	-1825.94832766	0.000	**87.92**	-0.73

No experimental or theoretical data on the BDEs of 7-phloroeckol or any other phlorotannin have been reported previously. In this work, it was observed that the CAM-B3LYP/6-311+G(2d,2p)//AM1 approach was more accurate than previously employed QM methods for the calculation of the phloroglucinol BDE. The calculation of the theoretical BDE values of 7-phloroeckol radical conformers, indicated that in conditions promoting a HAT antioxidant mechanism that H-abstraction would occur from the **F** hydroxyl site, located in the dibenzodioxin moiety. However, to gain more insight into the SAR of 7-phloroeckol it would be useful to investigate whether or not HAT is the preferred antioxidant mechanism over SET-PT or SPLET through the calculation of other indicators of antioxidant activity, such as ionisation potential and proton affinity.[48] Furthermore, other factors must also be taken into consideration when assessing the relative importance of the different antioxidant mechanisms, such as the reactivity of the radical species and changes in electron densities of both the polyphenol and radical species over the reaction coordinate.[48, 408]

As the first report investigating phlorotannin BDEs, this study provides a good benchmark for future studies in which comparison among phlorotannin structures could be carried out. For instance, the effect of the presence/absence of aryl-aryl, di-aryl ether or dibenzodioxin linkages in phlorotannins may be worthy of further QM investigation using LC DFT functionals. It is evident that QM techniques are useful to quantify the enthalpies associated with antioxidant mechanisms, therefore they may serve as predictive tools for assessing the extent of potential antioxidant activity of macroalgal phlorotannins.

Future work

In terms of their future application as products that can be administered or consumed as part of pharmaceutical drugs, preservatives or functional foods, phlorotannin compounds will inevitably need to be combined with excipients or other functional components that will impact on their bioactivity. Additionally, considering from this work it was shown that bioactive peptides also occur within macroalgae, there may be an opportunity for these two bioactives to be incorporated into functional delivery systems together. In this thesis, brown algal phlorotannin enriched-fractions and peptides have both shown to have *in vitro* antioxidant and antihypertensive activities. Therefore, the integration of brown algal phlorotannin and peptide components together into functional foods may provide a means for assisting in the treatment of hypertension. It would be important, however, to first consider how these two types of components may interact with each other and how these interactions could potentially affect their overall bioactivity, as the occurrence of protein-polyphenol interactions in well documented.[171, 409-410] Thus, a prior understanding of their interactions and how these may affect their bioactivities would be beneficial.

In order to gain an understanding of the underlying characteristics involved in directing the interactions between phlorotannins and peptides, analysis of the system covering wide spatial and temporal ranges is required. Molecular dynamics (MD) has the ability to simulate the movements of atoms in complex molecular systems and its introduction has reduced the amount of time and expense involved in describing interactions of molecular systems by offering an alternative to the traditional crystallographic studies.[411] As a result, MD studies have become very valuable in observing how complex systems operate. It is anticipated that molecular dynamics simulations may have a significant impact on how the bioactivity of novel drugs is determined, by improving the ability to choose and design better molecules at all discovery stages, such as lead optimisation, and, therefore, may transform the current drug discovery process.[242] Following the successful profiling of the antioxidant phlorotannins polymers in chapter 3 and identification of various bioactive peptides from *Ascophyllum nodosum* in chapter 4, the prospect of modeling a macroalgal phlorotannin and peptide to observe binding patterns, and therefore hypothesise

potential effects on their activity, seemed worthwhile. Whilst a preliminary attempt has been made to initiate this work over the course of this PhD, there is much more that can be added. The initial MD approach taken is outlined in Appendix 4.

Conclusion

On the whole, the research in this thesis will contribute practical knowledge to areas of marine chemistry where knowledge is limited, such as the extraction optimisation, bioactivity, separation and profiling of phlorotannins; the extraction, separation and identification of bioactive peptides from a brown macroalga; and the potential use of quantum mechanics to investigate the potential radical scavenging capability of phlorotannin conformers.

Initially, two extraction methods, namely SLE and PLE, were compared for their efficiency in the extraction of antioxidant polyphenols from three brown macroalgae, *Ascophyllum nodosum*, *Pelvetia canaliculata* and *Fucus spiralis*, and a green macroalga, *Ulva intestinalis*. It was found that the conventional SLE was the more effective method for the generation of antioxidant extracts from the brown macroalgae than PLE where food-friendly solvents are involved and, thus, SLE should be considered to be more industrially relevant.

An efficient, inexpensive process for the enrichment of polyphenols from brown macroalgal SLE extracts was devised using molecular weight cut-off (MWCO) membranes. The analysis of the low molecular weight portion of enriched fractions using QTof-MS supported the supposition that the polyphenols present in these brown macroalgal extracts were phlorotannin polymers.

The use of a rapid UPLC-MS method provided reproducible metabolite profiles of purified macroalgal purified extracts and was identified as a useful tool to discriminate between the phlorotannin profiles of different species. This is the first report of phlorotannins of greater than 10 phloroglucinol units and their isomers being separated by any form of liquid chromatography. The identification of UPLC-MS as an effective technique for the profiling of phlorotannins may be useful to industry in terms of monitoring the standardization of extract compositions.

The use of SEC with Sephadex LH-20 proved to be effective for the separation of phlorotannins from *F. spiralis* and *A. nodosum* based on molecular weight. However, despite the high degree of separation, the complexity within individual fractions remained quite high due to the high degree of phlorotannin isomerisation. Therefore, the purification of phlorotannins from these macroalgal

species to a level where the characterization of individual structures could be carried out was not attained.

Although, the occurrence of phlorotannins in brown macroalgae has been well researched, the identification of bioactive peptides has been neglected. Peptide fractions isolated from an *A. nodosum* trypsin digest using flash chromatography displayed *in vitro* antioxidant, renin-inhibitory and ACE-inhibitory bioactives. Nine novel peptides identified in these fractions were synthesized, with two peptides exhibiting positive renin enzyme inhibition and another displaying positive antioxidant activity. This is the first report of bioactive peptides from *A. nodosum*, however further research into protein isolation from brown macroalgae is required to identify species with high amounts of protein and also to assess external factors that may affect protein production, such as seasonality.

Some of the macroalgal phlorotannins and BPs profiled in this work have exhibited in vitro antioxidant and antihypertensive activities. However, because the assays used to determine these activities measure chemical reactions in isolation, they may not truly reflect the extent of their potential activity in vivo where many other factors, such as ADME conditions, can either negatively or positively affect their bioavailability. For that reason in order to more accurately assess the value of the identified bioactive macroalgal components to the food and/or pharmaceutical industries further in vivo and intervention studies need to be carried out.

The quantum mechanics work showed that the determination of phenolic BDEs the CAM-B3LYP/6-311+G(2d,2p) or CAM-B3LYP/6-311+G(3df,2p) single point methods using 6-31+G(d,p) optimised geometries seem to be the more accurate than using the same basis sets with the functional ωB97XD. Computational chemistry may act as a support to natural products experiment, through the provision of data on the molecular properties of individual components and also on potential binding interactions between mixtures of bioactive components. DFT was employed in chapter 5 to theoretically determine the radical scavenging potential of various 7-phloroeckol conformers through the calculation of their O-H BDEs. This work served as a good example of how LC-DFT can be employed to theoretically investigate the radical scavenging potential of phlorotannins and to decipher the most favourable conformer in terms of antioxidant potential. Through the investigation of more

electronic properties, in addition to BDE, more information in this regard could be attained and, also, by assessing various phlorotannin structures a greater understanding of the molecular requirements for antioxidant activity among these structures may be achieved. Furthermore, a molecular dynamics simulation approach was proposed for the investigation of binding interactions between a selected macroalgal phlorotannin and a bioactive peptide from *Ascophyllum nodosum*.

References

1. FAO *The State of World Fisheries and Aquaculture - 2004 (SOFIA)*; 2004; p 153.
2. Bocanegra, A.; Bastida, S.; Benedi, J.; Rodenas, S.; Sanchez-Muniz, F. J., Characteristics and nutritional and cardiovascular-health properties of seaweeds. *J. Med. Food* **2009,** *12* (2), 236-258.
3. Connan, S.; Goulard, F.; Stiger, V.; Deslandes, E.; Ar Gall, E., Interspecific and temporal variation in phlorotannin levels in an assemblage of brown algae. *Bot. Mar.* **2004,** *47* (5), 410-416.
4. Plaza, M.; Cifuentes, A.; Ibáñez, E., In the search of new functional food ingredients from algae. *Trends Food Sci. Technol.* **2008,** *19* (1), 31-39.
5. Smit, A. J., Medicinal and pharmaceutical uses of seaweed natural products: A review. *J. Appl. Phycol.* **2004,** *16* (4), 245-262.
6. Rupérez, P.; Ahrazem, O.; Leal, J. A., Potential antioxidant capacity of sulfated polysaccharides from the edible marine brown seaweed *Fucus vesiculosus*. *J. Agric. Food Chem.* **2002,** *50* (4), 840-845.
7. Tierney, M. S.; Croft, A. K.; Hayes, M., A review of antihypertensive and antioxidant activities in macroalgae. *Bot. Mar.* **2010,** *53*, 387-408.
8. Plouguerné, E.; Le Lann, K.; Connan, S.; Jechoux, G.; Deslandes, E.; Stiger-Pouvreau, V., Spatial and seasonal variation in density, reproductive status, length and phenolic content of the invasive brown macroalga *Sargassum muticum* (Yendo) Fensholt along the coast of Western Brittany (France). *Aquat. Bot.* **2006,** *85* (4), 337-344.
9. Matlock, D. B.; Ginsburg, D. W.; Paul, V. J., Spatial variability in secondary metabolite production by the tropical red alga *Portieria hornemannii*. In *Sixteenth International Seaweed Symposium*, Kain, J. M.; Brown, M. T.; Lahaye, M., Eds. Springer Netherlands: 1999; Vol. 137, pp 267-273.
10. Apostolidis, E.; Karayannakidis, P. D.; Kwon, Y.-I.; Lee, C. M.; Seeram, N. P., Seasonal variation of phenolic antioxidant-mediated α-glucosidase inhibition of *Ascophyllum nodosum*. *Plant Foods Hum. Nutr.* **2011,** *66* (4), 313-319.
11. Halpin, H. A.; Morales-Sua´rez-Varela, M. M.; Martin-Moreno, J. M., Chronic disease prevention and the new public health. *Public Health Rev.* **2010,** *32*, 120-154.
12. Jones, P. J., Clinical nutrition: 7. Functional foods — more than just nutrition. *Can. Med. Assoc. J.* **2002,** *166* (12), 1555-1563.
13. Garcia-Casal, M. N.; Ramirez, J.; Leets, I.; Pereira, A. C.; Quiroga, M. F., Antioxidant capacity, polyphenol content and iron bioavailability from algae (*Ulva* sp., *Sargassum* sp. and *Porphyra* sp.) in human subjects. *Br. J. Nutr.* **2009,** *101* (01), 79-85.
14. Nwosu, F.; Morris, J.; Lund, V. A.; Stewart, D.; Ross, H. A.; McDougall, G. J., Anti-proliferative and potential anti-diabetic effects of phenolic-rich extracts from edible marine algae. *Food Chem.* **2010,** *126* (3), 1006-1012.
15. Kim, A. R.; Shin, T.-S.; Lee, M.-S.; Park, J.-Y.; Park, K.-E.; Yoon, N.-Y.; Kim, J.-S.; Choi, J.-S.; Jang, B.-C.; Byun, D.-S.; Park, N.-K.; Kim, H.-R., Isolation and Identification of Phlorotannins from *Ecklonia stolonifera* with Antioxidant and Anti-inflammatory Properties. *J. Agric. Food Chem.* **2009,** *57* (9), 3483-3489.

16. Sato, M.; Hosokawa, T.; Yamaguchi, T.; Nakano, T.; Muramoto, K.; Kahara, T.; Funayama, K.; Kobayashi, A.; Nakano, T., Angiotensin I-Converting Enzyme Inhibitory Peptides Derived from Wakame (*Undaria pinnatifida*) and Their Antihypertensive Effect in Spontaneously Hypertensive Rats. *J. Agric. Food Chem.* **2002,** *50* (21), 6245-6252.
17. Maeda, H.; Hosokawa, M.; Sashima, T.; Funayama, K.; Miyashita, K., Fucoxanthin from edible seaweed, *Undaria pinnatifida*, shows antiobesity effect through UCP1 expression in white adipose tissues. *Biochem. Biophys. Res. Commun.* **2005,** *332* (2), 392-397.
18. Diplock, A. T.; Aggett, P. J.; Ashwell, M.; Bornet, F.; Fern, E. B.; Roberfroid, M. B., Scientific concepts of functional foods in Europe: consensus document. *Br. J. Nutr.* **1999,** *81*, s1–s27.
19. Herrero, M.; Cifuentes, A.; Ibañez, E., Sub- and supercritical fluid extraction of functional ingredients from different natural sources: Plants, food-by-products, algae and microalgae: A review. *Food Chem.* **2006,** *98* (1), 136-148.
20. Prabhasankar, P.; Ganesan, P.; Bhaskar, N., Influence of Indian Brown Seaweed (*Sargassum marginatum*) as an Ingredient on Quality, Biofunctional, and Microstructure Characteristics of Pasta. *Food Sci. Technol. Int.* **2009,** *15* (5), 471-479.
21. López-López, I.; Cofrades, S.; Ruiz-Capillas, C.; Jiménez-Colmenero, F., Design and nutritional properties of potential functional frankfurters based on lipid formulation, added seaweed and low salt content. *Meat Science* **2009,** *83* (2), 255-262.
22. Kapetanovic, I. M., Computer-aided drug design and discovery (CADDD): *in silico*-chemico-biological approach. *Chem-Biol. Interact.* **2008,** *171* (2), 165-176.
23. Croft, A. K.; Groenewald, W.; Tierney, M. S., Marine Bioactive Compounds: Sources, Characterization and Applications. In *Marine Bioactive Compounds: Sources, Characterization and Applications*, Hayes, M., Ed. Springer: New York, 2012; pp 173-206.
24. von Korff, M.; Rufener, C.; Stritt, M.; Freyss, J.; Bär, R.; Sander, T., Integration of distributed computing into the drug discovery process. *Expert Opinion on Drug Discovery* **2011,** *6* (2), 103-1107.
25. Guiry, M. D. Irish seaweed biomass. http://www.seaweed.ie/uses_ireland/irishbiomass.php (accessed June, 2013).
26. BioMara, The importance of seaweed across the ages, . http://www.biomara.org/understanding-seaweed/the-importance-of-seaweed-across-the-ages (accessed July 2013).
27. Morrissey, J.; Kraan, S.; Guiry, M. D. *A guide to commercially important seaweeds on the Irish coast*; Bord Iascaigh Mhara/Irish Sea Fisheries Board: Dun Laoghaire, Co. Dublin, 2001; p 67.
28. Werner, A.; Kraan, S., Review of the potential mechanisation of kelp harvesting in Ireland. *Mar. Environ. Health Ser.* **2004,** *17*, 1-52.
29. Bruton, T.; Lyons, H.; Lerat, Y.; Stanley, M.; Rasmussen, M. B. *A review of the potential of marine algae as a source of biofuel in Ireland*; Sustainable Energy Ireland: 2009; pp 1-88.
30. Hession, C.; Guiry, M. D.; McGarvey, S.; Joyce, J., Mapping and assessment of the seaweed resources (*Ascophyllum nodosum*, *Laminaria* spp.) off the west coast of Ireland. *Mar Resour Ser (Dublin)* **1998,** *5*, 1-89.
31. Lordan, S.; Smyth, T. J.; Soler-Vila, A.; Stanton, C.; Ross, R. P., The α-amylase and α-glucosidase inhibitory effects of Irish seaweed extracts. *Food Chem.* **2013,** *141* (3), 2170-2176.

32. Cox, S.; Abu-Ghannam, N.; Gupta, S., An Assessment of the Antioxidant and Antimicrobial Activity of Six Species of Edible Irish Seaweeds. *Int. Food Res. J.* **2010,** *17*, 205-220.
33. Tierney, M. S.; Smyth, T. J.; Rai, D. K.; Soler-Vila, A.; Croft, A. K.; Brunton, N., Enrichment of polyphenol contents and antioxidant activities of Irish brown macroalgae using food-friendly techniques based on polarity and molecular size. *Food Chem.* **2013**.
34. Walsh, M.; Watson, L. *A market analysis towards the further development of seaweed aquaculture in Ireland. Part 1.*; Bord Iascaigh Mhara: 2011.
35. Freeman, B. A.; Crapo, J. D., Biology of disease: free radicals and tissue injury. *Laboratory investigation; a journal of technical methods and pathology* **1982,** *47* (5), 412-26.
36. Griendling, K. K.; Sorescu, D.; Lassègue, B.; Ushio-Fukai, M., Modulation of Protein Kinase Activity and Gene Expression by Reactive Oxygen Species and Their Role in Vascular Physiology and Pathophysiology. *Atertio. Thromb. Vasc. Biol.* **2000,** *20*, 2175-2183.
37. Chiarugi, P.; Cirri, P., Redox regulation of protein tyrosine phosphatases during receptor tyrosine kinase signal transduction. *Trends Biochem. Sci.* **2003,** *28* (9), 509–514.
38. Cosentino, F.; Barker, J. E.; Brand, M. P.; Heales, S. J.; Werner, E. R.; Tippins, J. R.; West, N.; Channon, K. M.; Volpe, M.; Lüscher, T. F., Reactive oxygen species mediate endothelium-dependent relaxations in tetrahydrobiopterin-deficient mice. *Atertio. Thromb. Vasc. Biol.* **2001,** *21* (4), 496-502.
39. Rao, G. N.; Berk, B. C., Active oxygen species stimulate vascular smooth muscle cell growth and proto-oncogene expression. *Circul. Res.* **1992,** *70* (3), 593-9.
40. Sesti, F.; Liu, S.; Cai, S.-Q., Oxidation of potassium channels by ROS: a general mechanism of aging and neurodegeneration? *Trends Cell Biol.* **2010,** *20* (1), 45-51.
41. Lodovici, M.; Bigagli, E., Oxidative stress and air pollution exposure. *Journal of Toxicology* **2011,** *2011* (Article ID 487074).
42. Sahlin, K.; Shabalina, I. G.; Mattsson, C. M.; Bakkman, L.; Fernström, M.; Rozhdestvenskaya, Z.; Enqvist, J. K.; Nedergaard, J.; Ekblom, B.; Tonkonogi, M., Ultraendurance exercise increases the production of reactive oxygen species in isolated mitochondria from human skeletal muscle. *J. Appl. Physiol.* **2010,** *108* (4), 780-787.
43. Javeshghani, D.; Schiffrin, E. L.; Sairam, M. R.; Touyz, R. M., Potentiation of vascular oxidative stress and nitric oxide-mediated endothelial dysfunction by high-fat diet in a mouse model of estrogen deficiency and hyperandrogenemia. *Journal of the American Society of Hypertension* **2009,** *3* (5), 295-305.
44. Touyz, R. M.; Schiffrin, E. L., Reactive oxygen species in vascular biology: implications in hypertension. *Histochem. Cell Biol.* **2004,** *122* (4), 339-352.
45. Zhu, Q.; Zhang, X.-M.; Fry, A. J., Bond dissociation energies of antioxidants. *Polym. Degradation Stab.* **1997,** *57* (1), 43-50.
46. Basu, T. K.; Temple, N. J.; Garg, M. L., *Antioxidants in human health and disease*. CABI publishing: 1999; p 1-14.
47. Mikulski, D.; Molski, M., A quantum chemical study on the antioxidant activity of bioactive polyphenols from peanut (*Arachis hypogaea*) and the major metabolites of trans-resveratrol. *Comp. Theor. Chem.* **2012,** *981*, 38-46.

48. Marković, Z.; Milenković, D.; Đorović, J.; Marković, J. M. D.; Stepanić, V.; Lučić, B.; Amić, D., PM6 and DFT study of free radical scavenging activity of morin. *Food Chem.* **2012,** *134* (4), 1754–1760.
49. Litwinienko, G.; Ingold, K. U., Abnormal Solvent Effects on Hydrogen Atom Abstraction. 2. Resolution of the Curcumin Antioxidant Controversy. The Role of Sequential Proton Loss Electron Transfer. *J. Org. Chem.* **2004,** *69 (18)* (18), 5888–5896.
50. Dhalla, N. S.; Elmoselhi, A. B.; Hata, T.; Makino, N., Status of myocardial antioxidants in ischemia–reperfusion injury. *Cardiovasc. Res.* **2000,** *47* (3), 446-456.
51. El-Gendy, K. S.; Aly, N. M.; Mahmoud, F. H.; Kenawy, A.; El-Sebae, A. K. H., The role of vitamin C as antioxidant in protection of oxidative stress induced by imidacloprid. *Food Chem. Toxicol.* **2010,** *48* (1), 215-221.
52. Brigelius-Flohe, R.; Traber, M. G., Vitamin E: function and metabolism. *FASEB J.* **1999,** *13* (10), 1145-1155.
53. Aldini, G.; Yeum, K.-J.; Carini, M.; Krinsky, N. I.; Russell, R. M., (−)-Epigallocatechin-(3)-gallate prevents oxidative damage in both the aqueous and lipid compartments of human plasma. *Biochem. Biophys. Res. Commun.* **2003,** *302* (2), 409-414.
54. Bhuvaneswari, V.; Velmurugan, B.; Nagini, S., Lycopene modulates circulatory antioxidants during hamster buccal pouch carcinogenesis. *Nutrition Research* **2001,** *21* (11), 1447-1453.
55. Huang, D.; Ou, B.; Prior, R. L., The Chemistry behind Antioxidant Capacity Assays. *J. Agric. Food Chem.* **2005,** *53* (6), 1841-1856.
56. Schroeter, H.; Boyd, C.; Spencer, J. P. E.; Williams, R. J.; Cadenas, E.; Rice-Evans, C., MAPK signaling in neurodegeneration: influences of flavonoids and of nitric oxide. *Neurobiol. Aging* **2002,** *23* (5), 861-880.
57. Adamson, G. E.; Lazarus, S. A.; Mitchell, A. E.; Prior, R. L.; Cao, G.; Jacobs, P. H.; Kremers, B. G.; Hammerstone, J. F.; Rucker, R. B.; Ritter, K. A.; Schmitz, H. H., HPLC Method for the Quantification of Procyanidins in Cocoa and Chocolate Samples and Correlation to Total Antioxidant Capacity. *J. Agric. Food Chem.* **1999,** *47*, 4184-4188.
58. Prior, R. L.; Wu, X.; Schaich, K., Standardized methods for the determination of antioxidant capacity and phenolics in foods and dietary supplements. *J. Agric. Food Chem* **2005,** *53* (53), 10.
59. Stratil, P.; Klejdus, B.; Kubáň, V., Determination of total content of phenolic compounds and their antioxidant activity in vegetables evaluation of spectrophotometric methods. *J. Agric. Food Chem.* **2006,** *54* (3), 607-616.
60. Moch, R. W., Pathology of BHA- and BHT-induced lesions. *Food Chem. Toxicol.* **1986,** *24* (10–11), 1167-1169.
61. Williams, G. M.; Wang, C. X.; Iatropoulos, M. J., Toxicity studies of butylated hydroxyanisole and butylated hydroxytoluene. II. Chronic feeding studies. *Food Chem. Toxicol.* **1990,** *28* (12), 799-806.
62. Luther, M.; Parry, J.; Moore, J.; Meng, J.; Zhang, Y.; Cheng, Z.; Yu, L., Inhibitory effect of Chardonnay and black raspberry seed extracts on lipid oxidation in fish oil and their radical scavenging and antimicrobial properties. *Food Chem.* **2007,** *104* (3), 1065-1073.
63. Fan, W.; Chi, Y.; Zhang, S., The use of a tea polyphenol dip to extend the shelf life of silver carp (*Hypophthalmicthys molitrix*) during storage in ice. *Food Chem.* **2008,** *108* (1), 148-153.

64. Sun-Waterhouse, D.; Chen, J.; Chuah, C.; Wibisono, R.; Melton, L. D.; Laing, W.; Ferguson, L. R.; Skinner, M. A., Kiwifruit-based polyphenols and related antioxidants for functional foods: kiwifruit extract-enhanced gluten-free bread. *Int. J. Food Sci. Nutr.* **2009,** *60* (s7), 251-264.
65. Roldán, E.; Sánchez-Moreno, C.; de Ancos, B.; Cano, M. P., Characterisation of onion (*Allium cepa* L.) by-products as food ingredients with antioxidant and antibrowning properties. *Food Chem.* **2008,** *108* (3), 907-916.
66. Chen, Z.-Y.; Peng, C.; Jiao, R.; Wong, Y. M.; Yang, N.; Huang, Y., Anti-hypertensive nutraceuticals and functional foods. *J. Agric. Food Chem.* **2009,** *57* (11), 4485–4499.
67. Oparil, S.; Zaman, A.; Calhoun, A., Pathogenesis of Hypertension. *Ann. Intern. Med.* **2003,** *139*, 761-776.
68. Ribeiro-Oliveira, A., Jr.; Nogueira, A. I.; Pereira, R. M.; Boas, W. W. V.; Santos, R. A. S.; Silva, A. C. S., The renin–angiotensin system and diabetes: An update. *Vascular Health and Risk Manangement* **2008,** *4* (4), 787-803.
69. Unger, T., The role of the renin-angiotensin system in the development of cardiovascular disease. *Am. J. Cardiol.* **2002,** *89* (2), 3-9.
70. Kopkan, L.; Cervenka, L., Renal interactions of renin-angiotensin system, nitric oxide and superoxide anion: implications in the pathophysiology of salt-sensitivity and hypertension. *Physiol. Res.* **2009,** *58 Suppl 2*, S55-67.
71. Ondetti, M. A.; Rubin, B.; Cushman, D. W., Design of specific inhibitors of angiotensin-converting enzyme: new class of orally active antihypertensive agents. *Science* **1977,** *196* (4288), 441-444.
72. Pfeffer, M. A.; Braunwald, E.; Moyé, L. A.; Basta, L.; Brown, E. J.; Cuddy, T. E.; Davis, B. R.; Geltman, E. M.; Goldman, S.; Flaker, G. C.; Klein, M.; Lamas, G. A.; Packer, M.; Rouleau, J.; Rouleau, J. L.; Rutherford, J.; Wertheimer, J. H.; Hawkins, C. M., Effect of captopril on mortality and morbidity in patients with left ventriculardysfunction after myocardial infarction. *New Engl. J. Med.* **1992,** *327* (10), 669-677.
73. SOLVD, i., Effect of enalapril on survival in patients with reduced left ventricular ejection fractions and congestive heart failure. *New Engl. J. Med.* **1991,** *325* (5), 293-302.
74. Ibrahim, M. M., RAS inhibition in hypertension. *J. Hum. Hypertens.* **2006,** *20* (2), 101-108.
75. Segura Campos, M. R.; Chel Guerrero, L. A.; Betancur Ancona, D. A., Angiotensin-I converting enzyme inhibitory and antioxidant activities of peptide fractions extracted by ultrafiltration of cowpea *Vigna unguiculata* hydrolysates. *J. Sci. Food Agric.* **2010,** *90* (14), 2512-2518.
76. Miguel, M.; Alonso, M. J.; Salaices, M.; Aleixandre, A.; López-Fandiño, R., Antihypertensive, ACE-inhibitory and vasodilator properties of an egg white hydrolysate: Effect of a simulated intestinal digestion. *Food Chem.* **2007,** *104* (1), 163–168.
77. Deng, Y. F.; Aluko, R. E.; Jin, Q.; Zhang, Y.; Yuan, L. J., Inhibitory activities of baicalin against renin and angiotensin-converting enzyme. *Pharm. Biol.* **2012,** *50* (4), 401-406.
78. Himaya, S. W. A.; Ngo, D.-H.; Ryu, B.; Kim, S.-K., An active peptide purified from gastrointestinal enzyme hydrolysate of Pacific cod skin gelatin attenuates angiotensin-1 converting enzyme (ACE) activity and cellular oxidative stress. *Food Chem.* **2012,** *132* (4), 1872-1882.

79. Ko, S.-C.; Kang, N.; Kim, E.-A.; Kang, M. C.; Lee, S.-H.; Kang, S.-M.; Lee, J.-B.; Jeon, B.-T.; Kim, S.-K.; Park, S.-J.; Park, P.-J.; Jung, W.-K.; Kim, D.; Jeon, Y.-J., A novel angiotensin I-converting enzyme (ACE) inhibitory peptide from a marine *Chlorella ellipsoidea* and its antihypertensive effect in spontaneously hypertensive rats. *Process Biochem.* **2012,** *47* (12), 2005-2011.
80. Suetsuna, K.; Nakano, T., Identification of an antihypertensive peptide from peptic digest of wakame (*Undaria pinnatifida*). *The Journal of Nutritional Biochemistry* **2000,** *11* (9), 450-454.
81. Fujita, H.; Yoshikawa, M., LKPNM: a prodrug-type ACE-inhibitory peptide derived from fish protein. *Immunopharmacology* **1999,** *44*, 123-127.
82. Takano, D. T., Anti-hypertensive activity of fermented dairy products containing biogenic peptides. *Antonie Van Leeuwenhoek* **2002,** *82* (1-4), 333-340.
83. Grossman, E., Does increased oxidative stress cause hypertension? *Diabetes Care* **2008,** *31* (2), S185-S189.
84. Sugamura, K.; Keaney, J. J. F., Reactive oxygen species in cardiovascular disease. *Free Radical Biol. Med.* **2011,** *51* (5), 978-992.
85. Cai, H.; Harrison, D. G., Endothelial Dysfunction in Cardiovascular Diseases: The Role of Oxidant Stress. *Circul. Res.* **2000,** *87*, 840-844.
86. Harrison, D. G., Cellular and Molecular Mechanisms of Endothelial Cell Dysfunction. *J. Clin. Invest.* **1997,** *100* (9), 2153-2157.
87. Chen, X.; Touyz, R. M.; Park, J. B.; Schiffrin, E. L., Antioxidant Effects of Vitamins C and E Are Associated With Altered Activation of Vascular NADPH Oxidase and Superoxide Dismutase in Stroke-Prone SHR. *Hypertension* **2001,** *38*, 606-611.
88. Zhou, A.; Carrell, R. W.; Murphy, M. P.; Wei, Z.; Yan, Y.; Stanley, P. L. D.; Stein, P. E.; Pipkin, F. B.; Read, R. J., A redox switch in angiotensinogen modulates angiotensin release. *Nature* **2010,** *468*, 108-111.
89. Targett, N. M.; Boettcher, A. A.; Targett, T. E.; Vrolijk, N. H., Tropical marine herbivore assimilation of phenolic-rich plants. *Oecologia* **1995,** *103* (2), 170-179.
90. Schoenwaelder, M. E. A.; Clayton, M. N., The secretion of phenolic compounds following fertilization in *Acrocarpia paniculata* (Fucales, Phaeophyta). *Phycologia* **1998,** *37* (1), 40-46.
91. Arnold, T. M.; Targett, N. M., Marine Tannins: The Importance of a Mechanistic Framework for Predicting Ecological Roles. *J. Chem. Ecol.* **2002,** *28* (10), 1919-1934.
92. Vreeland, V.; Laetsch, W. M., Role of alginate self-associating subunits in the assembly of *Fucus* embryo cell walls. In *Self assembling architecture*, J.E, V., Ed. Alan R. Liss: New York, 1988; pp 77-96.
93. Svensson, C.; Pavia, H.; Toth, G., Do plant density, nutrient availability, and herbivore grazing interact to affect phlorotannin plasticity in the brown seaweed *Ascophyllum nodosum*. *Mar. Biol.* **2007,** *151* (6), 2177-2181.
94. Kubanek, J.; Lester, S. E.; Fenical, W.; Hay, M. E., Ambiguous role of phlorotannins as chemical defenses in the brown alga *Fucus vesiculosus*. *Mar. Ecol. Prog. Ser.* **2004,** *277*, 79-93.
95. Deal, M. S.; Hay, M. E.; Wilson, D.; Fenical, W., Galactolipids rather than phlorotannins as herbivore deterrents in the brown seaweed *Fucus vesiculosus*. *Oecologia* **2003,** *136* (1), 107-114.
96. Koivikko, R. Brown algal phlorotannins: Improving and applying chemical methods. University of Turku, Turku, 2008.

97. Li, Y.-X.; Wijesekara, I.; Li, Y.; Kim, S.-K., Phlorotannins as bioactive agents from brown algae. *Process Biochem.* **2011,** *46* (12), 2219-2224.
98. Kamiya, M.; Nishio, T.; Yokoyama, A.; Yatsuya, K.; Nishigaki, T.; Yoshikawa, S.; Ohki, K., Seasonal variation of phlorotannin in sargassacean species from the coast of the Sea of Japan. *Phycol. Res.* **2010,** *58* (1), 53-61.
99. Ragan, M. A.; Glombitza, K. W., Phlorotannins, brown algal polyphenols. *Prog. Phycol. Res.* **1986,** *4*, 129-241.
100. Audibert, L. F., M.: Blanc, N.: Hauchard, D.: Ar Gall, E., Phenolic compounds in the brown seaweed *Ascophyllum nodosum*: distribution and radical-scavenging activities. *Phytochem. Anal.* **2010,** *21*, 399-405.
101. Julia, K.; Sarah, E. L.; William, F.; Mark, E. H., Ambiguous role of phlorotannins as chemical defenses in the brown alga *Fucus vesiculosus*. *Mar. Ecol. Prog. Ser.* **2004,** *277*, 79-93.
102. Breton, F.; Cerantola, S.; Ar Gall, E., Distribution and radical scavenging activity of phenols in *Ascophyllum nodosum* (Phaeophyceae). *J. Exp. Mar. Biol. Ecol.* **2011,** *399* (2), 167-172.
103. Audibert, L.; Fauchon, M.; Blanc, N.; Hauchard, D.; Ar Gall, E., Phenolic compounds in the brown seaweed *Ascophyllum nodosum*: distribution and radical-scavenging activities. *Phytochem. Anal.* **2010,** *21* (5), 399-405.
104. Le Lann, K.; Ferret, C.; VanMee, E.; Spagnol, C.; Lhuillery, M.; Payri, C.; Stiger-Pouvreau, V., Total phenolic, size-fractionated phenolics and fucoxanthin content of tropical Sargassaceae (Fucales, Phaeophyceae) from the South Pacific Ocean: Spatial and specific variability. *Phycol. Res.* **2012,** *60* (1), 37-50.
105. Guinea, M.; Franco, V.; Araujo-Bazán, L.; Rodríguez-Martín, I.; González, S., In vivo UVB-photoprotective activity of extracts from commercial marine macroalgae. *Food Chem. Toxicol.* **2012,** *50* (3–4), 1109-1117.
106. Shibata, T.; Ishimaru, K.; Kawaguchi, S.; Yoshikawa, H.; Hama, Y., Antioxidant activities of phlorotannins isolated from Japanese Laminariaceae. *J. Appl. Phycol.* **2008,** *20* (5), 705-711.
107. Nagayama, K.; Iwamura, Y.; Shibata, T.; Hirayama, I.; Nakamura, T., Bactericidal activity of phlorotannins from the brown alga *Ecklonia kurome*. *J. Antimicrob. Chemother.* **2002,** *50* (6), 889-890.
108. Garcia-Casal, M. N.; Ramirez, J.; Leets, I.; Pereira, A. C.; Quiroga, M. F., Antioxidant capacity, polyphenol content and iron bioavailability from algae (*Ulva* sp., *Sargassum* sp. and *Porphyra* sp.) in human subjects. *Br. J. Nutr.* **2009,** *101* (01), 79-85.
109. Nakai, M.; Kageyama, N.; Nakahara, K.; Miki, W., Phlorotannins as Radical Scavengers from the Extract of *Sargassum ringgoldianum*. *Mar. Biotechnol.* **2006,** *8* (4), 409-414.
110. Li, Y.; Qian, Z.-J.; Ryu, B.; Lee, S.-H.; Kim, M.-M.; Kim, S.-K., Chemical components and its antioxidant properties in vitro: An edible marine brown alga, *Ecklonia cava*. *Bioorg. Med. Chem.* **2009,** *17* (5), 1963-1973.
111. Cerantola, S.; Breton, F.; Ar Gall, E.; Deslandes, E., Co-occurrence and antioxidant activities of fucol and fucophlorethol classes of polymeric phenols in *Fucus spiralis*. *Bot. Mar.* **2006,** *49* (4), 347-351.
112. Jung, H.; Hyun, S.; Kim, H.; Choi, J., Angiotensin-converting enzyme I inhibitory activity of phlorotannins from *Ecklonia stolonifera*. *Fish. Sci.* **2006,** *72* (6), 1292-1299.
113. Spencer, J. P., Metabolism of tea flavonoids in the gastrointestinal tract. *J. Nutr.* **2003,** *133* (10), 3255s-3261s.

114. Bergmann, H.; Triebel, S.; Kahle, K.; Richlin, E., *The metabolic fate of apple polyphenols in humans*. 2014; Vol. 6.
115. Stahl, W.; van den Berg, H.; Arthur, J.; Bast, A.; Dainty, J.; Faulks, R. M.; Gartner, C.; Haenen, G.; Hollman, P.; Holst, B.; Kelly, F. J.; Polidori, M. C.; Rice-Evans, C.; Southon, S.; van Vliet, T.; Vina-Ribes, J.; Williamson, G.; Astley, S. B., Bioavailability and metabolism. *Mol. Aspects Med.* **2002,** *23* (1-3), 39-100.
116. D'Archivio, M.; Filesi, C.; Di Benedetto, R.; Gargiulo, R.; Giovannini, C.; Masella, R., Polyphenols, dietary sources and bioavailability. *Ann. Ist. Super. Sanita* **2007,** *43* (4), 348-61.
117. Romier, B.; Schneider, Y. J.; Larondelle, Y.; During, A., Dietary polyphenols can modulate the intestinal inflammatory response. *Nutr. Rev.* **2009,** *67* (7), 363-78.
118. Romero, J. C.; Reckelhoff, J. F., State-of-the-Art lecture. Role of angiotensin and oxidative stress in essential hypertension. *Hypertension* **1999,** *34* (4 Pt 2), 943-9.
119. Touyz, R. M.; Schiffrin, E. L., Reactive oxygen species in vascular biology: implications in hypertension. *Histochem. Cell Biol.* **2004,** *122* (4), 339-352.
120. Grassi, D.; Lippi, C.; Necozione, S.; Desideri, G.; Ferri, C., Short-term administration of dark chocolate is followed by a significant increase in insulin sensitivity and a decrease in blood pressure in healthy persons. *Am. J. Clin. Nutr.* **2005,** *81* (3), 611-4.
121. Mackenzie, G. G.; Carrasquedo, F.; Delfino, J. M.; Keen, C. L.; Fraga, C. G.; Oteiza, P. I., Epicatechin, catechin, and dimeric procyanidins inhibit PMA-induced NF-kappaB activation at multiple steps in Jurkat T cells. *FASEB J.* **2004,** *18* (1), 167-9.
122. Actis-Goretta, L.; Ottaviani, J. I.; Keen, C. L.; Fraga, C. G., Inhibition of angiotensin converting enzyme (ACE) activity by flavan-3-ols and procyanidins. *FEBS Lett.* **2003,** *555* (3), 597-600.
123. Stern, J. L.; Hagerman, A. E.; Steinberg, P. D.; Mason, P. K., Phlorotannin-protein interactions. *J. Chem. Ecol.* **1996,** *22* (10), 1877-1899.
124. Shibata, T.; Yamaguchi, K.; Nagayama, K.; Kawaguchi, S.; Nakamura, T., Inhibitory activity of brown algal phlorotannins against glycosidases from the viscera of the turban shell *Turbo cornutus*. *Eur. J. Phycol.* **2002,** *37* (4), 493-500.
125. Wijesinghe, W. A. J. P.; Ko, S.-C.; Jeon, Y.-J., Effect of phlorotannins isolated from *Ecklonia cava* on angiotensin I-converting enzyme (ACE) inhibitory activity. *Nutr. Res. Pract.* **2011,** *5* (2), 93-100.
126. Liu, J. C.; Hsu, F. L.; Tsai, J. C.; Chan, P.; Liu, J. Y.; Thomas, G. N.; Tomlinson, B.; Lo, M. Y.; Lin, J. Y., Antihypertensive effects of tannins isolated from traditional Chinese herbs as non-specific inhibitors of angiontensin converting enzyme. *Life Sci.* **2003,** *73* (12), 1543-1555.
127. Munin, A.; Edwards-Lévy, F., Encapsulation of natural polyphenolic compounds; A review. *Pharmaceutics* **2011,** *3* (4), 793-829.
128. Hartmann, R.; Meisel, H., Food-derived peptides with biological activity: from research to food applications. *Curr. Opin. Biotechnol.* **2007,** *18* (2), 163-169.
129. Gu, R.-Z.; Li, C.-Y.; Liu, W.-Y.; Yi, W.-X.; Cai, M.-Y., Angiotensin I-converting enzyme inhibitory activity of low-molecular-weight peptides from Atlantic salmon (*Salmo salar* L.) skin. *Food Res. Int.* **2011,** *44* (5), 1536-1540.
130. Alemán, A.; Giménez, B.; Pérez-Santin, E.; Gómez-Guillén, M. C.; Montero, P., Contribution of Leu and Hyp residues to antioxidant and ACE-inhibitory activities of peptide sequences isolated from squid gelatin hydrolysate. *Food Chem.* **2011,** *125* (2), 334-341.

131. Udenigwe, C. C.; Aluko, R. E., Food protein-derived bioactive peptides: Production, processing, and potential health benefits. *J. Food Sci.* **2011,** *77* (1), R11-R24.
132. Hernández-Ledesma, B.; Amigo, L.; Ramos, M.; Recio, I., Angiotensin converting enzyme inhibitory activity in commercial fermented products. Formation of peptides under simulated gastrointestinal digestion. *J. Agric. Food Chem.* **2004,** *52* (6), 1504-1510.
133. Qin, L.; Zhu, B.-W.; Zhou, D.-Y.; Wu, H.-T.; Tan, H.; Yang, J.-F.; Li, D.-M.; Dong, X.-P.; Murata, Y., Preparation and antioxidant activity of enzymatic hydrolysates from purple sea urchin (*Strongylocentrotus nudus*) gonad. *LWT - Food Sci. Technol.* **2011,** *44* (4), 1113-1118.
134. Firdaous, L.; Dhulster, P.; Amiot, J.; Gaudreau, A.; Lecouturier, D.; Kapel, R.; Lutin, F.; Vezina, L.-P.; Bazinet, L., Concentration and selective separation of bioactive peptides from an alfalfa white protein hydrolysate by electrodialysis with ultrafiltration membranes. *J. Membr. Sci.* **2009,** *329* (1-2), 60-67.
135. Wang, Y. K.; He, H. L.; Wang, G. F.; Wu, H.; Zhou, B. C.; Chen, X. L.; Zhang, Y. Z., Oyster (*Crassostrea gigas*) hydrolysates produced on a plant scale have antitumor activity and immunostimulating effects in BALB/c Mice. *Mar. Drugs* **2010,** *8* (2), 255-268.
136. Samaranayaka, A. G. P.; Li-Chan, E. C. Y., Food-derived peptidic antioxidants: A review of their production, assessment and, and potential applications. *J. Functional Foods* **2011,** *3* (4), 229-254.
137. Chen, H.-M.; Muramoto, K.; Yamauchi, F.; Nokihara, K., Antioxidant activity of designed peptides based on the antioxidative peptide isolated from digests of a soybean protein. *J. Agric. Food Chem.* **1996,** *44* (9), 2619-2623.
138. Torres-Fuentes, C.; Alaiz, M.; Vioque, J., Iron-chelating activity of chickpea protein hydrolysate peptides. *Food Chem.* **2012,** *134* (3), 1585-1588.
139. Peña-Ramos, E. A.; Xiong, Y. L.; Arteaga, G. E., Fractionation and characterisation for antioxidant activity of hydrolysed whey protein. *J. Sci. Food Agric.* **2004,** *84* (14), 1908-1918.
140. Kamau, S. M.; Lu, R.-R., The Effect of Enzymes and Hydrolysis Conditions on Degree of Hydrolysis and DPPH Radical Scavenging Activity of Whey Protein Hydrolysates. *Curr. Res. Dairy Sci.* **2011,** *3*, 25-35.
141. Saito, K.; Jin, D.-H.; Ogawa, T.; Muramoto, K.; Hatakeyama, E.; Yasuhara, T.; Nokihara, K., Antioxidative Properties of Tripeptide Libraries Prepared by the Combinatorial Chemistry. *J. Agric. Food Chem.* **2003,** *51* (12), 3668-3674.
142. Hernandez-Ledesma, B.; Amigo, L.; Recio, I.; Bartolome, B., ACE-Inhibitory and Radical-Scavenging Activity of Peptides Derived from β-Lactoglobulin f(19-25). Interactions with Ascorbic Acid. *J. Agric. Food Chem.* **2007,** *55* (9), 3392-3397.
143. Rajapakse, N.; Mendis, E.; Jung, W.-K.; Je, J.-Y.; Kim, S.-K., Purification of a radical scavenging peptide from fermented mussel sauce and its antioxidant properties. *Food Res. Int.* **2005,** *38* (2), 175-182.
144. Chen, H.-M.; Muramoto, K.; Yamauchi, F.; Fujimoto, K.; Nokihara, K., Antioxidative Properties of Histidine-Containing Peptides Designed from Peptide Fragments Found in the Digests of a Soybean Protein. *J. Agric. Food Chem.* **1998,** *46* (1), 49-53.
145. Kohl, S.; Behrens, M.; Dunkel, A.; Hofmann, T.; Meyerhof, W., Amino Acids and Peptides Activate at Least Five Members of the Human Bitter Taste Receptor Family. *J. Agric. Food Chem.* **2012,** *61* (1), 53-60.

146. Favaro-Trindade, C. S.; Santana, A. S.; Monterrey-Quintero, E. S.; Trindade, M. A.; Netto, F. M., The use of spray drying technology to reduce bitter taste of casein hydrolysate. *Food Hydrocolloids* **2010,** *24* (4), 336-340.
147. Barbosa, C. M. S.; Morais, H. A.; Delvivo, F. M.; Mansur, H. S.; De Oliveira, M. C.; Silvestre, M. P. C., Papain hydrolysates of casein: molecular weight profile and encapsulation in lipospheres. *J. Sci. Food Agric.* **2004,** *84* (14), 1891-1900.
148. Vermeirssen, V.; Camp, J. V.; Verstraete, W., Bioavailability of angiotensin I converting enzyme inhibitory peptides. *Br. J. Nutr.* **2004,** *92* (3), 357-366.
149. Ko, S.-C.; Kim, D. G.; Han, C.-H.; Lee, Y. J.; Lee, J.-K.; Byun, H.-G.; Lee, S.-C.; Park, S.-J.; Lee, D.-H.; Jeon, Y.-J., Nitric oxide-mediated vasorelaxation effects of anti-angiotensin I-converting enzyme (ACE) peptide from *Styela clava* flesh tissue and its anti-hypertensive effect in spontaneously hypertensive rats. *Food Chem.* **2012,** *134* (2), 1141-1145.
150. Fitzgerald, C.; Mora-Soler, L.; Gallagher, E.; O'Connor, P.; Prieto, J.; Soler-Vila, A.; Hayes, M., Isolation and characterization of bioactive pro-peptides with in vitro renin inhibitory activities from the macroalga *Palmaria palmata*. *J. Agric. Food Chem.* **2012,** *60* (30), 7421–7427.
151. Ibañez, E.; Herrero, M.; Mendiola, J. A.; Castro-Puyana, M., Extraction and characterization of bioactive compounds with health benefits from marine resources: Macro and micro algae, cyanobacteria, and invertebrates. In *Marine Bioactive Compounds: Sources, Characterization and Applications*, Hayes, M., Ed. Springer US: 2012; pp 55-98.
152. Romdhane, M.; Gourdon, C., Investigation in solid–liquid extraction: influence of ultrasound. *Chem. Eng. J.* **2002,** *87* (1), 11-19.
153. Pinelo, M.; Fabbro, P. D.; Manzocco, L.; Nuñez, M. J.; Nicoli, M. C., Optimization of continuous phenol extraction from *Vitis vinifera* byproducts. *Food Chem.* **2005,** *92* (1), 109-117.
154. Azizah, A. H.; Nik Ruslawati, N. M.; Swee Tee, T., Extraction and characterization of antioxidant from cocoa by-products. *Food Chem.* **1999,** *64* (2), 199-202.
155. Baydar, N. G.; Özkan, G.; Sağdiç, O., Total phenolic contents and antibacterial activities of grape (*Vitis vinifera* L.) extracts. *Food Control* **2004,** *15* (5), 335-339.
156. Wijngaard, H. H.; Brunton, N., The optimisation of solid–liquid extraction of antioxidants from apple pomace by response surface methodology. *J. Food Eng.* **2010,** *96* (1), 134-140.
157. Heinrich, M.; Barnes, J.; Gibbons, S.; Williamson, E., *Fundamentals of Pharmacognosy and Phytotherapy*. Churchhill Livingstone: 2004.
158. Kaufmann, B.; Christen, P., Recent extraction techniques for natural products: microwave-assisted extraction and pressurised solvent extraction. *Phytochem. Anal.* **2002,** *13* (2), 105-113.
159. Chemat, F.; Vian, M. A.; Cravotto, G., Green extraction of natural products: concept and principles. *Int. J. Mol. Sci.* **2012,** *13* (7), 8615-8627.
160. Olivas, R. M.; Camara, C., Sample preparation. In *Handbook of elemental speciation: Techniques and methodology*, Cornelis, R.; Caruso, J. A.; Crews, H.; Heumann, K. G., Eds. Wiley & Son: 2003.
161. Zaibunnisa, A. H.; Norashikin, S.; Mamot, S.; Osman, H., An experimental design approach for the extraction of volatile compounds from turmeric leaves (*Curcuma domestica*) using pressurized liquid extraction (PLE). *LWT-Food Sci. Technol.* **2009,** *42*, 233-238.

162. Plaza, M.; Santoyo, S.; Jaime, L.; Garcia-Blairsy Reina, G.; Herrero, M.; Senorans, F. J.; Ibanez, E., Screening for bioactive compounds from algae. *J. Pharm. Biomed. Anal.* **2010,** *51*, 450-455.
163. Antunes, P.; Viana, P.; Vinhas, T.; Capelo, J. L.; Rivera, J.; Gaspar, E. M. S. M., Optimization of pressurized liquid extraction (PLE) of dioxin-furans and dioxin-like PCBs from environmental samples. *Talanta* **2008,** *75* (4), 916-925.
164. Zhang, B.; Pan, X.; Cobb, G. P.; Anderson, T. A., Use of pressurized liquid extraction (PLE)/gas chromatography–electron capture detection (GC–ECD) for the determination of biodegradation intermediates of hexahydro-1,3,5-trinitro-1,3,5-triazine (RDX) in soils. *Journal of Chromatography B* **2005,** *824* (1–2), 277-282.
165. López, A.; Rico, M.; Rivero, A.; Suárez de Tangil, M., The effects of solvents on the phenolic contents and antioxidant activity of *Stypocaulon scoparium* algae extracts. *Food Chem.* **2011,** *125* (3), 1104-1109.
166. Onofrejová, L.; Vašíčková, J.; Klejdus, B.; Stratil, P.; Mišurcová, L.; Kráčmar, S.; Kopecký, J.; Vacek, J., Bioactive phenols in algae: The application of pressurized-liquid and solid-phase extraction techniques. *J. Pharm. Biomed. Anal.* **2010,** *51* (2), 464-470.
167. Hickey, R. M., Extraction and characterization of bioactive carbohydrates with health benefits from marine resources: macro- and microalgae, cyanobacteria, and invertebrates. In *Marine Bioactive Compounds*, Hayes, M., Ed. Springer US: 2012; pp 159-172.
168. Rostagno, M. A.; Palma, M.; Barroso, C. G., Ultrasound-assisted extraction of soy isoflavones. *J. Chromatogr.* **2003,** *1012* (2), 119-128.
169. Mason, T. J.; Paniwnyk, L.; Lorimer, J. P., The uses of ultrasound in food technology. *Ultrason. Sonochem.* **1996,** *3* (3), S253-S260.
170. Trombley, J. D.; Loegel, T. N.; Danielson, N. D.; Hagerman, A. E., Capillary electrophoresis methods for the determination of covalent polyphenol–protein complexes. *Anal. Bioanal. Chem.* **2011,** *401* (5), 1527-1533.
171. Richard, T.; Lefeuvre, D.; Descendit, A.; Quideau, S.; Monti, J. P., Recognition characters in peptide–polyphenol complex formation. *Biochimica et Biophysica Acta (BBA) - General Subjects* **2006,** *1760* (6), 951-958.
172. Puri, M.; Sharma, D.; Barrow, C. J., Enzyme-assisted extraction of bioactives from plants. *Trends Biotechnol.* **2012,** *30* (1), 37-44.
173. Gardossi, L.; Poulsen, P. B.; Ballesteros, A.; Hult, K.; Švedas, V. K.; Vasić-Rački, Đ.; Carrea, G.; Magnusson, A.; Schmid, A.; Wohlgemuth, R.; Halling, P. J., Guidelines for reporting of biocatalytic reactions. *Trends Biotechnol.* **2010,** *28* (4), 171-180.
174. Pihlanto, A.; Mäkinen, S., Antihypertensive properties of plant protein derived peptides. In *Bioactive Food Peptides in Health and Disease*, Hernandez-Ledesma, B.; Hsieh, C.-C., Eds. InTech: 2013; p 266.
175. Wijesinghe, W. A. J. P.; Jeon, Y.-J., Enzyme-assistant extraction (EAE) of bioactive components: A useful approach for recovery of industrially important metabolites from seaweeds: A review. *Fitoterapia* **2012,** *83* (1), 6–12.
176. Thomas, N. V.; Kim, S.-K., Potential pharmacological applications of polyphenolic derivatives from marine brown algae. *Environ. Toxicol. Pharmacol.* **2011,** *32* (3), 325–335.
177. Gupta, S.; Abu-Ghannam, N., Recent developments in the application of seaweeds or seaweed extracts as a means for enhancing the safety and quality attributes of foods. *Innovative Food Science & Emerging Technologies* **2011,** *12* (4), 600-609.

178. Wang, T.; Jónsdóttir, R.; Liu, H.; Gu, L.; Kristinsson, H. G.; Raghavan, S.; Ólafsdóttir, G., Antioxidant capacities of phlorotannins extracted from the brown algae *Fucus vesiculosus*. *J. Agric. Food Chem.* **2012,** *60* (23), 5874-5883.
179. Kang, S.-M.; Heo, S.-J.; Kim, K.-N.; Lee, S.-H.; Jeon, Y.-J., Isolation and identification of new compound, 2,7"-phloroglucinol-6,6'-bieckol from brown algae, *Ecklonia cava* and its antioxidant effect. *J. Funct. Foods* **2012,** *4* (1), 158-166.
180. Zubia, M.; Payri, C.; Deslandes, E., Alginate, mannitol, phenolic compounds and biological activities of two range-extending brown algae, *Sargassum mangarevense* and *Turbinaria ornata* (Phaeophyta: Fucales), from Tahiti (French Polynesia). *J. Appl. Phycol.* **2008,** *20* (6), 1033-1043.
181. Mian, A. J.; Percival, E., Carbohydrates of the brown seaweeds *Himanthalia lorea*, *Bifurcaria bifurcata*, and *Padina pavonia*: Part I. Extraction and Fractionation. *Carbohydr. Res.* **1973,** *26* (1), 133-146.
182. Liu, H.; Gu, L., Phlorotannins from Brown Algae (*Fucus vesiculosus*) Inhibited the Formation of Advanced Glycation Endproducts by Scavenging Reactive Carbonyls. *J. Agric. Food Chem.* **2012,** *60* (5), 1326-1334.
183. Jerez, M.; Touriño, S.; Sineiro, J.; Torres, J. L.; Núñez, M. J., Procyanidins from pine bark: Relationships between structure, composition and antiradical activity. *Food Chem.* **2007,** *104* (2), 518–527.
184. Spencer, P.; Sivakumaran, S.; Fraser, K.; Foo, L. Y.; Lane, G. A.; Edwards, P. J. B.; Meagher, L. P., Isolation and characterisation of procyanidins from *Rumex obtusifolius*. *Phytochem. Anal.* **2007,** *18* (3), 193-203.
185. Heo, S.-J.; Jeon, Y.-J., Evaluation of diphlorethohydroxycarmalol isolated from *Ishige okamurae* for radical scavenging activity and its protective effect against H2O2-induced cell damage. *Process Biochem.* **2009,** *44* (4), 412-418.
186. Weber, P.; Hamburger, M.; Schafroth, N.; Potterat, O., Flash chromatography on cartridges for the separation of plant extracts: Rules for the selection of chromatographic conditions and comparison with medium pressure liquid chromatography. *Fitoterapia* **2011,** *82* (2), 155-161.
187. Still, W. C.; Kahn, M.; Mitra, A., Rapid chromatographic technique for preparative separations with moderate resolution. *J. Org. Chem.* **1978,** *43* (14), 2923-2925.
188. Lawton, L. A.; McElhiney, J.; Edwards, C., Purification of closely eluting hydrophobic microcystins (peptide cyanotoxins) by normal-phase and reversed-phase flash chromatography. *J. Chromatogr.* **1999,** *848* (1–2), 515-522.
189. Li, Y.; Lee, S.-H.; Le, Q.-T.; Kim, M.-M.; Kim, S.-K., Anti-allergic effects of phlorotannins on histamine release via binding inhibition between IgE and FcεRI. *J. Agric. Food Chem.* **2008,** *56* (24), 12073-12080.
190. Kubanek, J.; Jensen, P. R.; Keifer, P. A.; Sullards, M. C.; Collins, D. O.; Fenical, W., Seaweed resistance to microbial attack: A targeted chemical defense against marine fungi. *Proceedings of the National Academy of Sciences* **2003,** *100* (12), 6916-6921.
191. Bianco, É. M.; Rogers, R.; Teixeira, V. L.; Pereira, R. C., Antifoulant diterpenes produced by the brown seaweed *Canistrocarpus cervicornis*. *J. Appl. Phycol.* **2009,** *21* (3), 341-346.
192. Isaza Martínez, J. H.; Torres Castañeda, H. G., Preparation and Chromatographic Analysis of Phlorotannins. *J. Chromatogr. Sci.* **2013,** *51*(8), 825-38.
193. Koivikko, R.; Loponen, J.; Pihlaja, K.; Jormalainen, V., High-performance liquid chromatographic analysis of phlorotannins from the brown alga Fucus Vesiculosus. *Phytochem. Anal.* **2007,** *18* (4), 326-332.

194. Steevensz, A. J.; MacKinnon, S. L.; Hankinson, R.; Craft, C.; Connan, S.; Stengel, D. B.; Melanson, J. E., Profiling phlorotannins in brown macroalgae by liquid chromatography–high resolution mass spectrometry. *Phytochem. Anal.* **2012,** *3* (5), 547-553.
195. Steevensz, A. J.; MacKinnon, S. L.; Hankinson, R.; Craft, C.; Connan, S.; Stengel, D. B.; Melanson, J. E., Profiling Phlorotannins in Brown Macroalgae by Liquid Chromatography–High Resolution Mass Spectrometry. *Phytochem. Anal.* **2012**, *23*(5), 547-553.
196. Novakova, L.; Matysova, L.; Solich, P., Advantages of application of UPLC in pharmaceutical analysis. *Talanta* **2006,** *68* (3), 908-918.
197. Hemström, P.; Irgum, K., Hydrophilic interaction chromatography. *J. Sep. Sci.* **2006,** *29* (12), 1784-1821.
198. Yanagida, A.; Murao, H.; Ohnishi-Kameyama, M.; Yamakawa, Y.; Shoji, A.; Tagashira, M.; Kanda, T.; Shindo, H.; Shibusawa, Y., Retention behavior of oligomeric proanthocyanidins in hydrophilic interaction chromatography. *J. Chromatogr.* **2007,** *1143* (1-2), 153-161.
199. Ragan, M. A.; Glombitza, K. W., Phlorotannins, brown algal polyphenols. In *Progress in Phycological Research*, Round, F. E.; Chapman, D. J., Eds. Elsevier Biomedical Press: Bristol, 1986; Vol. 4, p 481.
200. Wright, J. S.; Johnson, E. R.; DiLabio, G. A., Predicting the activity of phenolic antioxidants: theoretical method, analysis of substituent effects, and application to major families of antioxidants. *J. Am. Chem. Soc.* **2001,** *123* (6), 1173-83.
201. Litwinienko, G.; Ingold, K. U., Solvent Effects on the Rates and Mechanisms of Reaction of Phenols with Free Radicals. *Acc. Chem. Res.* **2007,** *40* (3), 222-230.
202. Musialik, M.; Kuzmicz, R.; Pawłowski, T. S.; Litwinienko, G., Acidity of Hydroxyl Groups: An Overlooked Influence on Antiradical Properties of Flavonoids. *J. Org. Chem.* **2009,** *74* (7), 2699-2709.
203. Klein, E.; Lukeš, V., Study of gas-phase O-H bond dissociation enthalpies and ionization potentials of substituted phenols - Applicability of *ab initio* and DFT/B3LYP methods. *Chemical Physics* **2006,** *330* (3), 515-526.
204. Russo, N.; Toscano, M.; Uccella, N., Semiempirical molecular modeling into quercetin reactive site: Structural, conformational, and electronic features. *J. Agric. Food Chem.* **2000,** *48* (8), 3232-3237.
205. Moalin, M.; van Strijdonck, G. P. F.; Beckers, M.; Hagemen, G. J.; Borm, P. J.; Bast, A.; Haenen, G. R. M. M., A planar conformation and the hydroxyl groups in the B and C rings play a pivotal role in the antioxidant capacity of quercetin and quercetin derivatives. *Molecules* **2011,** *16* (11), 9636-9650.
206. Heim, K. E.; Tagliaferro, A. R.; Bobilya, D. J., Flavonoid antioxidants: chemistry, metabolism and structure-activity relationships. *J. Nutr. Biochem* **2002,** *13*, 572–584.
207. Leopoldini, M.; Russo, N.; Toscano, M., A comparative study of the antioxidant power of flavonoid catechin and its planar analogue. *J. Agric. Food Chem.* **2007,** *55*, 7944–7949.
208. Lewars, E., *Computational Chemistry: Introduction to the theory and applications of molecular and quantum mechanics*. Kluwer Academic Publ.: Boston/Dordrecht/London, 2003; p 664.
209. Lynch, B. J.; Truhlar, D. G., How well can hybrid density functional methods predict transition state geometries and barrier heights? *J. Phys. Chem. A* **2001,** *105* (13), 2936-2941.

210. Silverstein, D. W.; Jensen, L., Assessment of the accuracy of long-range corrected functionals for describing the electronic and optical properties of silver clusters. *J. Chem. Phys.* **2010,** *132* (19), 194302.
211. Jacquemin, D.; Perpete, E. A.; Scalmani, G.; Frisch, M. J.; Kobayashi, R.; Adamo, C., Assessment of the efficiency of long-range corrected functionals for some properties of large compounds. *J. Chem. Phys.* **2007,** *126* (14), 144105.
212. Johnson, E. R.; DiLabio, G. A., Structure and binding energies in van der Waals dimers: Comparison between density functional theory and correlated ab initio methods. *Chem. Phys. Lett.* **2006,** *419*, 333–339.
213. Klimeš, J.; Michaelides, A., Perspective: Advances and challenges in treating van der Waals dispersion forces in density functional theory. *J. Chem. Phys.* **2012,** *137* (12), 120901-120913.
214. Kolandaivel, P.; Uma Maheswari, D.; Senthilkumar, L., The study of performance of DFT functional for van der Waals interactions. *Comp. Theor. Chem.* **2013,** *1004*, 56-60.
215. Pahari, B.; Chakraborty, S.; Chaudhuri, S.; Sengupta, B.; Sengupta, P. K., Binding and antioxidant properties of therapeutically important plant flavonoids in biomembranes: Insights from spectroscopic and quantum chemical studies. *Chem. Phys. Lipids* **2012,** *165* (4), 488-496.
216. Trouillas, P.; Marsal, P.; Siri, D.; Lazzaroni, R.; Duroux, J.-L., A DFT study of the reactivity of OH groups in quercetin and taxifolin antioxidants: The specificity of the 3-OH site. *Food Chem.* **2006,** *97* (4), 679–688.
217. Amat, A.; Angelis, F. D.; Sgamellotti, A.; Fantacci, S., Theoretical investigation of the structural and electronic properties of luteolin, apigenin and their deprotonated species. *J. Mol. Struc.: THEOCHEM* **2008,** *868* (1-3), 12-21.
218. Rice-Evans, C. A.; Miller, N. J.; Paganga, G., Structure-antioxidant activity relationships of flavonoids and phenolic acids. *Free Radical Biol. Med.* **1996,** *20* (7), 933-956.
219. Lavarda, F. C., Relation between Antioxidant Activity and Electronic Structure of Phenols. *Int. J. Quantum Chem.* **2003,** *95* (3), 219-223.
220. Mikulski, D.; Molski, M., Quantum-mechanical computations on the electronic structure of trans-resveratrol and trans-piceatannol: a theoretical study of the stacking interactions in trans-resveratrol dimers. *J. Mol. Model.* **2012,** *18* (7), 3255-3266.
221. Gill, P. M. W.; Johnson, B. G.; Pople, J. A.; Frisch, M. J., The performance of the Becke-Lee-Yang-Parr (B-LYP) density functional theory with various basis sets. *Chem. Phys. Lett.* **1992,** *197* (4, 5), 499–505.
222. Lucarini, M.; Pedulli, G. F.; Guerra, M., A critical evaluation of the factors determining the effect of intramolecular hydrogen bonding on the O-H bond dissociation enthalpy of catechol and flavonoid antioxidants. *Chemistry - A European Journal* **2004,** *10*, 933-939.
223. Justino, G. C.; Vieira, A. J. S. C., Antioxidant mechanisms of quercetin and myricetin in the gas phase and in solution - a comparison and validation of semi-empirical methods. *J. Mol. Model.* **2010,** *16* (5), 863-876.
224. Nam, P. C.; Chandra, A. K.; Nguyen, M. T., Performance of an integrated approach for prediction of bond dissociation enthalpies of phenols extracted from ginger and tea. *Chem. Phys. Lett.* **2013,** *555*, 44-50.
225. Zhao, Y.; Schultz, N. E.; Truhlar, D. G., Exchange-correlation functional with broad accuracy for metallic and nonmetallic compounds, kinetics, and noncovalent interactions. *J. Chem. Phys.* **2005,** *123* (16), 161103-160117.

226. Mendoza-Wilson, A. M.; Santacruz-Ortega, H.; Balandrán-Quintana, R. R., Relationship between structure, properties, and the radical scavenging activity of morin. *J. Mol. Struct.* **2011,** *995*, 134-141.
227. Panhwar, Q. K.; Memon, S.; Bhanger, M. I., Synthesis, characterization, spectroscopic and antioxidation studies of Cu(II)–morin complex. *J. Mol. Struct.* **2010,** *967* (1-3), 47-53.
228. Amić, D.; Lučić, B., Reliability of bond dissociation enthalpy calculated by the PM6 method and experimental TEAC values in antiradical QSAR of flavonoids. *Bioorg. Med. Chem.* **2010,** *18* (1), 28-35.
229. Chai, J. D.; Head-Gordon, M., Long-range corrected hybrid density functionals with damped atom-atom dispersion corrections. *Phys. Chem. Chem. Phys.* **2008,** *10* (44), 6615-6620.
230. Tawada, Y.; Tsuneda, T.; Yanagisawa, S.; Yanai, T.; Hirao, K., A long-range-corrected time-dependent density functional theory. *J. Chem. Phys.* **2004,** *120* (18), 8425–8433.
231. Yanai, T.; Tew, D. P.; Handy, N. C., A new hybrid exchange-correlation functional using the Coulomb-attenuating method (CAM-B3LYP). *Chem. Phys. Lett.* **2004,** *393* (1-3), 51-57.
232. Chai, J.-D.; Head-Gordon, M., Long-range corrected hybrid density functionals with damped atom-atom dispersion corrections. *Phys. Chem. Chem. Phys.* **2008,** *10* (44), 6615-6620.
233. Grimme, S., Semiempirical GGA-type density functional constructed with a long-range dispersion correction. *J. Comput. Chem.* **2006,** *27* (15), 1787-1799.
234. Wright, J. S.; Johnson, E. R.; DiLabio, G. A., Predicting the activity of phenolic antioxidants: Theoretical method, analysis of substituent effects, and application to major families of antioxidants. *J. Am. Chem. Soc.* **2001,** *123*, 1173-1183.
235. DiLabio, G. A., Using locally dense basis sets for the determination of molecular properties. *J. Phys. Chem. A* **1999,** *103* (51), 11414-11424.
236. Wright, J. S., Predicting the antioxidant activity of curcumin and curcuminoids. *J.Mol. Struc.: THEOCHEM* **2002,** *591* (1–3), 207-217.
237. Li, M.-J.; Liu, L.; Fu, Y.; Guo, Q.-X., Accurate bond dissociation enthalpies of popular antioxidants predicted by the ONIOM-G3B3 method. *J. Mol. Struc.: THEOCHEM* **2007,** *815* (1-3), 1-9.
238. Svensson, M.; Humbel, S.; Froese, R. D. J.; Matsubara, T.; Sieber, S.; Morokuma, K., ONIOM: A Multilayered Integrated MO + MM Method for Geometry Optimizations and Single Point Energy Predictions. A Test for Diels−Alder Reactions and Pt(P(t-Bu)3)2 + H2 Oxidative Addition. *J. Phys. Chem.* **1996,** *100* (50), 19357–19363.
239. Vivas, N.; Laguerre, M.; De Boissel, I. P.; De Gaijlejac, N. V.; Nonier, M. F., Conformational interpretation of vescalagin and castalagin physicochemical properties. *J. Agric. Food Chem.* **2004,** *52* (7).
240. Paton, R. S.; Goodman, J. M., Hydrogen bonding and π-stacking: How reliable are force fields? A critical evaluation of force field descriptions of nonbonded interactions. *J. Chem. Inf. Model.* **2009,** *49* (4), 944-955.
241. Gundertofte, K.; Liljefors, T.; Norrby, P.; Pettersson, I., A Comparison of Conformational Energies Calculated by Several Molecular Mechanics Methods. *J. Comput. Chem.* **1996,** *17* (4), 429-449.
242. Borhani, D. W.; Shaw, D. E., The future of molecular dynamics simulations in drug discovery. *J. Comput.-Aided Mol. Des.* **2012,** *26* (1), 15-26.

243. Wang, J.; Wolf, R. M.; Caldwell, J. W.; Kollman, P. A.; Case, D. A., Development and testing of a general amber force field. *J. Comput. Chem.* **2004,** *25* (9), 1157-1174.
244. Van der Spoel, D.; Lindahl, E.; Hess, B.; van Buuren, A. R.; Apol, E.; Meulenhoff, P. J.; Tieleman, D. P.; Sijbers, A. L. T. M.; Feenstra, K. A.; van Drunen, R.; Berendsen, H. J. C., Gromacs User Manual version 4.5.6. www.gromacs.org **2010.**
245. Berhanu, W. M.; Masunov, A. E., Natural polyphenols as inhibitors of amyloid aggregation. Molecular dynamics study of GNNQQNY heptapeptide decamer. *Biophys. Chem.* **2010,** *149* (1-2), 12-21.
246. Bras, N. F.; Goncalves, R.; Mateus, N.; Fernandes, P. A.; Ramos, M. J.; de Freitas, V., Inhibition of pancreatic elastase by polyphenolic compounds. *J. Agric. Food Chem.* **2010,** *58* (19), 10668-10676.
247. Saragusti, A. C.; Ortega, M. G.; Cabrera, J. L.; Estrin, D. A.; Marti, M. A.; Chiabrando, G. A., Inhibitory effect of quercetin on matrix metalloproteinase 9 activity Molecular mechanism and structure-activity relationship of the flavonoid-enzyme interaction. *Eur. J. Pharmacol.* **2010,** *644* (1-3), 138-145.
248. Liu, F.-F.; Dong, X.-Y.; He, L.; Middelberg, A. P. J.; Sun, Y., Molecular Insight into Conformational Transition of Amyloid β-Peptide 42 Inhibited by (-)-Epigallocatechin-3-gallate Probed by Molecular Simulations. *J. Phys. Chem. B* **2011,** *115* (41), 11879-11887.
249. Goncalves, R.; Mateus, N.; Pianet, I.; Laguerre, M.; de Freitas, V., Mechanisms of tannin-induced trypsin inhibition: a molecular approach. *Langmuir* **2011,** *27* (21), 13122-13129.
250. Jiang, P.; Li, W.; Shea, J. E.; Mu, Y., Resveratrol Inhibits the Formation of Multiple-Layered β-Sheet Oligomers of the Human Islet Amyloid Polypeptide Segment 22–27. *Biophys. J.* **2011** *100* (6), 1550–1558.
251. Tsitsanoua, K. E.; Joseph M. Hayes; Maria Keramioti; Michalis Mamais; Oikonomakos, N. G.; Kato, A.; Leonidas, D. D.; Zographos, S. E., Sourcing the affinity of flavonoids for the glycogen phosphorylase inhibitor site via crystallography, kinetics and QM/MM-PBSA binding studies: Comparison of chrysin and flavopiridol. *Food Chem. Toxicol.* **2012,** *61*, 14-27.
252. Meersman, F.; Dobson, C. M., Probing the pressure–temperature stability of amyloid fibrils provides new insights into their molecular properties. *BBA - Proteins and Proteomics* **2006,** *1764* (3), 452–460.
253. Cornell, W. D.; Cieplak, P.; Bayly, C. I.; Gould, I. R.; Merz Jr., K. M.; Ferguson, D. M.; Spellmeyer, D. C.; Fox, T.; Caldwell, J. W.; Kollman, P. A., A Second Generation Force Field for the Simulation of Proteins, Nucleic Acids, and Organic Molecules. *J. Am. Chem. Soc.* **1995,** *117* (19), 5179-5197.
254. Lee, M. R.; Duan, Y.; Kollman, P. A., Use of MM-PB/SA in estimating the free energies of proteins: application to native, intermediates, and unfolded villin headpiece. *Proteins Struct. Funct. Bioinformat.* **2000,** *39* (4), 309–316.
255. Hornak, V.; Abel, R.; Okur, A.; Strockbine, B.; Roitberg, A.; Simmerling, C., Comparison of multiple amber force fields and development of improved protein backbone parameters. *Proteins Struct. Funct. Bioinformat.* **2006,** *65* (3), 712–725.
256. Pirard, B.; Matter, H., Matrix metalloproteinase target family landscape: a chemometrical approach to ligand selectivity based on protein binding site analysis. *J. Med. Chem.* **2006,** *49* (1), 51-69.
257. Lemkul, J. A.; Bevan, D. R., Destabilizing Alzheimer's Aβ42 Protofibrils with Morin: Mechanistic Insights from Molecular Dynamics Simulations. *Biochemistry* **2010,** *49* (18), 3935-3946.

258. Lemkul, J. A.; Allen, W. J.; Bevan, D. R., Practical Considerations for Building GROMOS-Compatible Small-Molecule Topologies. *J. Chem. Inf. Model.* **2010,** *50* (12), 2221-2235.
259. Oostenbrink, C.; Villa, A.; Mark, A. E.; van Gunsteren, W. F., A biomolecular force field based on the free enthalpy of hydration and solvation: the GROMOS force-field parameter sets 53A5 and 53A6. *J. Comput. Chem.* **2004,** *25* (13), 1656-76.
260. Horta, B. A. C.; Fuchs, P. F. J.; van Gunsteren, W. F.; Hunenberger, P. H., New Interaction Parameters for Oxygen Compounds in the GROMOS Force Field: Improved Pure-Liquid and Solvation Properties for Alcohols, Ethers, Aldehydes, Ketones, Carboxylic Acids, and Esters. *J. Chem. Theory Comput.* **2011,** *7* (4), 1016-1031.
261. Medeiros, D. d. J.; Cortopassi, W. A.; França, T. C. C.; Pimentel, A. S., ITP Adjuster 1.0: A New Utility Program to Adjust Charges in the Topology Files Generated by the PRODRG Server. *J. Chem.* **2013,** *2013* (803151), 1-6.
262. Goncalves, R.; Soares, S.; Mateus, N.; De Freitas, V., Inhibition of Trypsin by Condensed Tannins and Wine. *J. Agric. Food Chem.* **2007,** *55* (18), 7596-7601.
263. Sengupta, B.; Chakraborty, S.; Crawford, M.; Taylor, J. M.; Blackmon, L. E.; Biswas, P. K.; Kramer, W. H., Characterization of diadzein–hemoglobin binding using optical spectroscopy and molecular dynamics simulations. *Int. J. Biol. Macromol.* **2012,** *51* (3), 250–258.
264. Sirk, T. W.; Brown, E. F.; Friedman, M.; Sum, A. K., Molecular binding of catechins to biomembranes: Relationship to biological activity. *J. Agric. Food Chem.* **2009,** *57* (15), 6720-6728.
265. Sirk, T. W.; Friedman, M.; Brown, E. F., Molecular binding of black tea theaflavins to biological membranes: Relationship to bioactivities. *J. Agric. Food Chem.* **2011,** *59* (8), 3780-3787.
266. Jorgensen, W. L.; Maxwell, D. S.; Tirado-Rives, J., Development and Testing of the OPLS All-Atom Force Field on Conformational Energetics and Properties of Organic Liquids. *J. Am. Chem. Soc.* **1996,** *118* (45), 11225-11236.
267. Dupradeau, F.-Y.; Pigache, A.; Zaffran, T.; Savineau, C.; Lelong, R.; Grivel, N.; Lelong, D.; Rosanski, W.; Cieplak, P., The R.E.D. tools: advances in RESP and ESP charge derivation and force field library building. *Phys. Chem. Chem. Phys.* **2010,** *12* (28), 7821-7839.
268. Mishra, R.; Sellin, D.; Radovan, D.; Gohlke, A.; Winter, R., Inhibiting islet amyloid polypeptide fibril formation by the red wine compound resveratrol. *ChemBioChem* **2009,** *10* (3), 445-449.
269. Verma, S.; Singh, A.; Mishra, A., Quercetin and taxifolin completely break MDM2–p53 association: molecular dynamics simulation study. *Med. Chem. Res.* **2012,** *Accepted Oct 2012; DOI:10.1007/s00044-012-0274-9.*
270. Sousa, M. C.; Braga, R. C.; Cintra, B. A. S.; De Oliveira, V.; Andrade, C. H., In silico metabolism studies of dietary flavonoids by CYP1A2 and CYP2C9. *Food Res. Int.* **2013,** *50* (1), 102–110.
271. Patel, S.; Brooks III, C. L., Fluctuating charge force fields: Recent developments and applications from small moleculas to macromolecular biological systems. *Mol. Simulat.* **2006,** *32*, 231-249.
272. Gleeson, M. P.; Hannongbua, S.; Gleeson, D., QM methods in structure based design: utility in probing protein-ligand interactions. *J. Mol. Graph. Model.* **2010,** *29* (4), 507-517.

273. Kaukonen, M.; Söderhjelm, P.; Heimdal, J.; Ryde, U., QM/MM–PBSA Method To Estimate Free Energies for Reactions in Proteins. *J. Phys. Chem. B* **2008,** *112* (39), 12537-12548.
274. Je, J.-Y.; Park, P.-J.; Kim, E.-K.; Park, J.-S.; Yoon, H.-D.; Kim, K.-R.; Ahn, C.-B., Antioxidant activity of enzymatic extracts from the brown seaweed *Undaria pinnatifida* by electron spin resonance spectroscopy. *LWT - Food Sci. Technol.* **2009,** *42* (4), 874-878.
275. Wang, L.; Weller, C. L., Recent advances in extraction of nutraceuticals from plants. *Trends Food Sci. Technol.* **2006,** *17* (6), 300-312.
276. Wang, T.; Jónsdóttir, R.; Ólafsdóttir, G., Total phenolic compounds, radical scavenging and metal chelation of extracts from Icelandic seaweeds. *Food Chem.* **2009,** *116* (1), 240-248.
277. Wang, T.; Jónsdóttir, R.; Kristinsson, H. G.; Hreggvidsson, G. O.; Jónsson, J. Ó.; Thorkelsson, G.; Ólafsdóttir, G., Enzyme-enhanced extraction of antioxidant ingredients from red algae *Palmaria palmata*. *LWT - Food Sci. Technol.* **2010,** *43* (9), 1387-1393.
278. Richter, B. E.; Jones, B. A.; Ezzell, J. L.; Porter, N. L., Accelerated Solvent Extraction: A Technique for Sample Preparation. *Anal. Chem.* **1996,** *68* (6), 1033-1039.
279. Huie, C. W., A review of modern sample-preparation techniques for the extraction and analysis of medicinal plants. *Anal. Bioanal. Chem.* **2002,** *373* (1-2), 23-30.
280. Zubia, M.; Fabre, M. S.; Kerjean, V.; Lann, K. L.; Stiger-Pouvreau, V.; Fauchon, M.; Deslandes, E., Antioxidant and antitumoural activities of some Phaeophyta from Brittany coasts. *Food Chem.* **2009,** *116* (3), 693-701.
281. Karacabeya, E.; Mazzaa, G., Optimisation of antioxidant activity of grape cane extracts using response surface methodology. *Food Chem.* **2010,** *119* (1), 343–348.
282. Mussatto, S. I.; Ballesteros, L. F.; Martins, S.; Teixeira, J. A., Extraction of antioxidant phenolic compounds from spent coffee grounds. *Separ. Purif. Technol.* **2011,** *83*, 173–179.
283. Cassano, A.; Conidi, C.; Drioli, E., Physico-chemical parameters of cactus pear (*Opuntia ficus-indica*) juice clarified by microfiltration and ultrafiltration processes. *Desalination* **2010,** *250* (3), 1101-1104.
284. Mello, B.; Petrus, J. C. C.; Hubinger, M. D., Concentration of flavonoids and phenolic compounds in aqueous and ethanolic propolis extracts through nanofiltration. *J. Food Eng.* **2010,** *96* (4), 533-539.
285. Lee, M. H.; Lee, K. B.; Oh, S. M.; Lee, B. H.; Chee, H. Y., Antifungal Activities of Dieckol Isolated from the Marine Brown Alga *Ecklonia cava* against *Trichophyton rubrum*. *Journal of the Korean Society for Applied Biological Chemistry* **2010,** *53* (4), 504-507.
286. Heo, S.-J.; Park, E.-J.; Lee, K.-W.; Jeon, Y.-J., Antioxidant activities of enzymatic extracts from brown seaweeds. *Bioresour. Technol.* **2005,** *96* (14), 1613-1623.
287. Mejárea, M.; Bülow, L., Metal-binding proteins and peptides in bioremediation and phytoremediation of heavy metals. *Trends Biotechnol.* **2001,** *19* (2), 67-73.
288. Inui, T.; Wang, Y.; Pro, S. M.; Franzblau, S. G.; Pauli, G. F., Unbiased evaluation of bioactive secondary metabolites in complex matrices. *Fitoterapia* **2012,** *83* (7), 1218–1225.

289. Piretti, M. V.; Doghieri, P., Separation of peracetylated flavanoid and flavonoid polyphenols by normal-phase high-performance liquid chromatography on a cyano-silica column and their determination. *J. Chromatogr. A* **1990,** *514*, 334-342.
290. Takahata, Y.; Ohnishi-Kameyama, M.; Furuta, S.; Takahash, M.; Suda, I., Highly Polymerized Procyanidins in Brown Soybean Seed Coat with a High Radical-Scavenging Activity. *J. Agric. Food Chem.* **2001,** *49* (12), 5843–5847.
291. Sun, B.; Belchior, G. P.; Ricardo-da-Silva, J. M.; Spranger, M. I., Isolation and purification of dimeric and trimeric procyanidins from grape seeds. *J. Chromatogr.A* **1999,** *841* (1), 115–121.
292. Ollanketo, M.; Peltoketo, A.; Hartonen, K.; Hiltunen, R.; Riekkola, M.-L., Extraction of sage (*Salvia officinalis*) by pressurized hot water and conventional methods: antioxidant activity of the extracts. *Eur. Food Res. Technol.* **2002,** *215* (2), 158-163.
293. Brand-Williams, W.; Cuvelier, M. E.; Berset, C., Use of a free radical method to evaluate antioxidant activity. *LWT - Food Sci. Technol.* **1995,** *28* (1), 25-30.
294. Lam, L. H.; Shimamura, T.; Sakaguchi, K.; Noguchi, K.; Ishiyama, M.; Fujimura, Y.; Ukeda, H., Assay of angiotensin I-converting enzyme-inhibiting activity based on the detection of 3-hydroxybutyric acid. *Anal. Biochem.* **2007,** *364* (2), 104-111.
295. Tierney, M. S.; Smyth, T. J.; Rai, D. K.; Soler-Vila, A.; Croft, A. K.; Brunton, N., Enrichment of polyphenol contents and antioxidant activities of Irish brown macroalgae using food-friendly techniques based on polarity and molecular size. *Food Chem.* **2013,** *139* (1-4), 753–761.
296. Grebenstein, N.; Frank, J., Rapid baseline-separation of all eight tocopherols and tocotrienols by reversed-phase liquid-chromatography with a solid-core pentafluorophenyl column and their sensitive quantification in plasma and liver. *J. Chromatogr., A* **2012,** *1243*, 39-46.
297. Taylor, A. W.; Barofsky, E.; Kennedy, J. A.; Deinzer, M. L., Hop (*Humulus lupulus* L.) Proanthocyanidins Characterized by Mass Spectrometry, Acid Catalysis, and Gel Permeation Chromatography. *J. Agric. Food Chem.* **2003,** *51* (14), 4101–4110.
298. Steevensz, A. J.; MacKinnon, S. L.; Hankinson, R.; Craft, C.; Connan, S.; Stengel, D. B.; Melanson, J. E., Profiling phlorotannins in brown macroalgae by liquid chromatography–high resolution mass spectrometry. *Phytochem. Anal.* **2012,** *23* (5), 547-553.
299. Audibert, L.; Fauchon, M.; Blanc, N.; Hauchard, D.; Ar Gall, E., Phenolic compounds in the brown seaweed *Ascophyllum nodosum*: distribution and radical-scavenging activities. *Phytochem. Anal.* **2010,** *21*, 399-405.
300. Parys, S.; Kehraus, S.; Krick, A.; Glombitza, K.-W.; Carmeli, S.; Klimo, K.; Gerhäuser, C.; König, G. M., In vitro chemopreventive potential of fucophlorethols from the brown alga *Fucus vesiculosus* L. by anti-oxidant activity and inhibition of selected cytochrome P450 enzymes. *Phytochemistry (Elsevier)* **2010,** *71* (2-3), 221-229.
301. Sailler, B.; Glombitza, K.-W., Phlorethols and fucophlorethols from the brown alga *Cystophora retroflexa*. *Phytochemistry (Elsevier)* **1999,** *50* (5), 869–881.
302. Glombitza, K. W.; Pauli, K., Fucols and phlorethols from the brown alga *Scytothamnus australis* hook. et Harv. (Chnoosporaceae). *Bot. Mar.* **2003,** *46* (3), 315-320.
303. CHEMnetBASE, The Chapman & Hall / CRC Combined Chemical Dictionary (CCD). Taylor & Francis Group.

304. Turner, A. J.; Hooper, N. M., The angiotensin converting enzyme gene family: genomics and pharmacology. *Trends Pharmacol. Sci.* **2002,** *23* (4), 177-183.
305. Tsai, J.-S.; Chen, J.-L.; Pan, B. S., ACE-inhibitory peptides identified from the muscle protein hydrolysate of hard clam (*Meretrix lusoria*). *Process Biochem.* **2008,** *43* (7), 743–747.
306. Parys, S.; Kehraus, S.; Pete, R.; Küpper, F. C.; Glombitza, K.-W.; König, G. M., Seasonal variation of polyphenolics in Ascophyllum nodosum (Phaeophyceae). *European Journal of Phycology* **2009,** *44* (3), 331-338.
307. Qu, W.; Ma, H.; Pan, Z.; Luo, L.; Wang, Z.; He, R., Preparation and antihypertensive activity of peptides from *Porphyra yezoensis*. *Food Chem.* **2010,** *123* (1), 14-20.
308. Fitzgerald, C.; Mora-Soler, L.; Gallagher, E.; O'Connor, P.; Prieto, J.; Soler-Vila, A.; Hayes, M., Isolation and characterization of bioactive pro-peptides with in vitro renin inhibitory activities from the macroalga *Palmaria palmata*. *J. Agric. Food Chem.* **2012,** *60*, 7421−7427.
309. Unger, T., The role of the renin-angiotensin system in the development of cardiovascular disease. *Am. J. Cardio.* **2002,** *89* (2, Supplement 1), 3-9.
310. Rajagopalan, S.; Kurz, S.; Münzel, T.; Tarpey, M.; Freeman, B. A.; Griendling, K. K.; Harrison, D. G., Angiotensin II–mediated hypertension in the rat increases vascular superoxide production via membrane NADH/NADPH oxidase activation. Contribution to alterations of vasomotor tone. *J. Clin. Investig.* **1996,** *97* (8), 1916–1923.
311. He, R.; Malomo, S. A.; Alashi, A.; Girgih, A. T.; Ju, X.; Aluko, R. E., Purification and hypotensive activity of rapeseed protein-derived renin and angiotensin converting enzyme inhibitory peptides. *J. Funct. Foods* (0).
312. Najafian, L.; Babji, A. S., A review of fish-derived antioxidant and antimicrobial peptides: Their production, assessment, and applications. *Peptides* **2012,** *33* (1), 178-185.
313. He, H.-L.; Liu, D.; Ma, C.-B., Review on the angiotensin-I-converting enzyme (ACE) inhibitor peptides from marine proteins. *Appl. Biochem. Biotechnol.* **2013,** *169* (3), 738-749.
314. Stengel, D. B.; Connan, S.; Popper, Z. A., Algal chemodiversity and bioactivity: sources of natural variability and implications for commercial application. *Biotechnol. Adv.* **2011,** *29* (5), 483-501.
315. McDermid, K. J.; Stuercke, B., Nutritional composition of edible Hawaiian seaweeds. *J. Appl. Phycol.* **2003,** *15* (6), 513-524.
316. Hernández-Carmona, G.; Carrillo-Domínguez, S.; Arvizu-Higuera, D. L.; Rodríguez-Montesinos, Y. E.; Murillo-Álvarez, J. I.; Muñoz-Ochoa, M.; Castillo-Domínguez, R. M., Monthly variation in the chemical composition of *Eisenia arborea* J.E. Areschoug. *J. Appl. Phycol.* **2009,** *21* (5), 607-616.
317. Dawczynski, C.; Schubert, R.; Jahreis, G., Amino acids, fatty acids, and dietary fibre in edible seaweed products. *Food Chem.* **2007,** *103* (3), 891–899.
318. Harnedy, P. A.; Fitzgerald, R. J., Bioactive proteins, peptides, and amino acids from macroalgae. *J. Phycol.* **2011,** *47* (2), 218–232.
319. Cian, R. E.; Martínez-Augustin, O.; Drago, S. R., Bioactive properties of peptides obtained by enzymatic hydrolysis from protein byproducts of *Porphyra columbina*. *Food Res. Int.* **2012,** *49* (1), 364-372.
320. Pihlanto-Leppälä, A., Bioactive peptides derived from bovine whey proteins: opioid and ACE-inhibitory peptides. *Trends Food Sci. Technol.* **2000,** *11* (9-10).

321. Wu, H.; He, H.-L.; Chen, X.-L.; Sun, C.-Y.; Zhang, Y.-Z.; Zhou, B.-C., Purification and identification of novel angiotensin-I-converting enzyme inhibitory peptides from shark meat hydrolysate. *Process Biochem.* **2008,** *43* (4), 457-461.
322. Suetsuna, K.; Nakano, T., Identification of an antihypertensive peptide from peptic digest of wakame (*Undaria pinnatifida*). *J. Nutr. Biochem.* **2000,** *11* (9), 450-454.
323. Wong, K. H.; Cheung, P. C. K., Nutritional evaluation of some subtropical red and green seaweeds Part II. In vitro protein digestibility and amino acid profiles of protein concentrates. *Food Chem.* **2001,** *72* (1), 11-17.
324. Shirsath, S. R.; Sonawane, S. H.; Gogate, P. R., Intensification of extraction of natural products using ultrasonic irradiations—A review of current status. *Chemical Engineering and Processing: Process Intensification* **2012,** *53*, 10-23.
325. Boja, E. S.; Fales, H. M., Overalkylation of a protein digest with iodoacetamide. *Anal. Chem.* **2001,** *73* (15), 3576–3582.
326. Rai, D. K.; Landin, B.; Griffiths, W. J.; Alvelius, G.; Green, B. N., Characterization of the elusive disulfide bridge forming human Hb variant: Hb Ta-Li β83 (EF7)Gly 3 Cys by electrospray mass spectrometry. *J. Am. Soc. Mass Spectrom.* **2002,** *13* (2), 187-191.
327. Ko, S.-C.; Lee, J.-K.; Byun, H.-G.; Lee, S.-C.; Jeo, Y.-J., Purification and characterization of angiotensin I-converting enzyme inhibitory peptide from enzymatic hydrolysates of *Styela clava* flesh tissue. *Process Biochem.* **2012,** *47* (1), 34-40.
328. Duan, J.; Sun, L.; Liang, Z.; Zhang, J.; Wang, H.; Zhang, L.; Zhang, W.; Zhang, Y., Rapid protein digestion and identification using monolithic enzymatic microreactor coupled with nano-liquid chromatography-electrospray ionization mass spectrometry. *J. Chromatogr.* **2006,** *1106* (1–2), 165-174.
329. Huang, E. C.; Henion, J. D., LC/MS and LC/MS/MS Determination of protein tryptic digests. *J. Am. Soc. Mass Spectrom.* **1990,** *1* (2), 158-165.
330. Lowry, O. H.; Rosebrough, N. J.; Farr, A. L.; Randall, R. J., Protein measurement with the folin phenol reagent. *J. Biol. Chem.* **1951,** *193*, 265-275.
331. Smith, P. K.; Krohn, R. I.; Hermanson, G. T.; Mallia, A. K.; Gartner, F. H.; Provenzano, M. D.; Fujimoto, E. K.; Goeke, N. M.; Olson, B. J.; Klenk, D. C., Measurement of protein using bicinchoninic acid. *Anal. Biochem.* **1985,** *150* (1), 76-85.
332. Stratil, P.; Klejdus, B.; Kuban, V., Determination of total content of phenolic compounds and their antioxidant activity in vegetables evaluation of spectrophotometric methods. *J. Agric. Food Chem.* **2006,** *54* (3), 607-616.
333. Munda, I. M., Differences in amino acid composition of estuarine and marine fucoids. *Aquat. Bot.* **1977,** *3*, 273–280.
334. Hotchkiss, S. *Investigation of the flavouring and taste components of Irish seaweeds*; Marine Institute: 2010.
335. Indergaard, M.; Minsaas, J., Animal and human nutrition. In *Seaweed Resources in Europe: Uses and Potential*, Guiry, M. D.; Blunden, G., Eds. John Wiley & Sons: Chichester, 1991; pp 21-64.
336. Munda, I. M., Distribution and use of some economically important seaweeds in Iceland. *Hydrobiologia* **1987,** *151/152*, 257-260.
337. Marinho-Soriano, E.; Fonseca, P. C.; Carneiro, M. A. A.; Moreira, W. S. C., Seasonal variation in the chemical composition of two tropical seaweeds. *Bioresour. Technol.* **2006,** *97*, 2402–2406.

338. Samaranayaka, A. G. P.; Li-Chan, E. C. Y., Autolysis-assisted production of fish protein hydrolysates with antioxidant properties from Pacific hake (*Merluccius productus*). *Food Chem.* **2008,** *107* (768-776).
339. Issaq, H. J.; Conrads, T. P.; Janini, G. M.; Veenstra, T. D., Methods for fractionation, separation and profiling of proteins and peptides. *Electrophoresis* **2002,** *23*, 3048–3061.
340. Chen, H. M.; Muramoto, K.; Yamauchi, F.; Nokihara, K., Antioxidant activity of designed peptides based on the antioxidant peptide isolated from digests of a soybean protein. *J. Agric. Food Chem.* **1996,** *44*, 2619-2623.
341. Zhou, S.; Decker, E. A., Ability of amino acids, dipeptides, polyamines, and sulfhydryls to quench hexanal, a saturated aldehydic lipid oxidation product. *J. Agric. Food Chem.* **1999,** *47*, 1932-1936.
342. Chan, K. M.; Decker, E. A.; Feustman, D. C., Endogenous skeletal muscle antioxidants. *Crit. Rev. Food Sci. Nutr.* **1994,** *34* (4), 403-426.
343. Gobbetti, M.; Ferranti, P.; Smacchi, E.; Goffredi, F.; Addeo, F., Production of angiotensin-I-converting-enzyme-inhibitory peptides in fermented milks started by *Lactobacillus delbrueckii* subsp. *bulgaricus* SS1 and Lactococcus lactis subsp. cremoris FT4. *Appl. Environ. Microbiol.* **2000,** *66* (9), 3898–3904.
344. Workman, R. J.; McKown, M. M.; Gregerman, R. I., Renin. Inhibition by proteins and peptides. *Biochemistry* **1974,** *13* (15), 3029-3035.
345. He, R.; Malomo, S. A.; Alashi, A.; Girgih, A. T.; Ju, X.; Aluko, R. E., Purification and hypotensive activity of rapeseed protein-derived renin and angiotensin converting enzyme inhibitory peptides. *J. Funct. Foods* **2013,** *5*(2), 781–789.
346. Udenigwe, C. C.; Aluko, R. E., Multifunctional cationic peptide fractions from flaxseed protein hydrolysates. *Plant Foods Hum. Nutr.* **2012,** *67* (1), 1-9.
347. Ajibola, C. F.; Fashakin, J. B.; Fagbemi, T. N.; Aluko, R. E., Renin and angiotensin converting enzyme inhibition with antioxidant properties of African yam bean protein hydrolysate and reverse-phase HPLC-separated peptide fractions. *Food Res. Int.* *52* (2), 437–444.
348. Byun, H.-G.; Kim, S.-K., Structure and activity of angiotensin I converting enzyme inhibitory peptides derived from alaskan pollack skin. *J. Biochem. Mol. Biol.* **2002,** *35* (2), 239-243.
349. Kobayashi, Y.; Yamauchi, T.; Katsuda, T.; Yamaji, H.; Katoh, S., Angiotensin-I converting enzyme (ACE) inhibitory mechanism of tripeptides containing aromatic residues. *J. Biosci. Bioeng.* **2008,** *106* (3), 310-312.
350. Wu, J.; Aluko, R. E.; Nakai, S., Structural requirements of angiotensin I-converting enzyme inhibitory peptides: Quantitative structure-activity relationship modeling of peptides containing 4-10 amino acid residues. *QSAR Comb. Sci.* **2006,** *25* (10), 873 – 880.
351. Matsufuji, H.; Matsui, T.; Ohshige, S.; Kawasaki, T.; Osajima, K.; Osajima, Y., Antihypertensive effects of angiotensin fragments in SHR. *Biosci. Biotechnol. Biochem.* **1994,** *58* (8), 1398-1401.
352. Kawasaki, T.; Seki, E.; Osajima, K.; Yoshida, M.; Asada, K.; Matsui, T.; Osajima, Y., Antihypertensive effect of Valyl-Tyrosine, a short chain peptide derived from sardine muscle hydrolyzate, on mild hypertensive subjects. *J. Hum. Hypertens.* **200,** *14*, 519–523.
353. Fahmi, A.; Morimura, S.; Guo, H. C.; Shigematsu, T.; Kida, K.; Uemura, Y., Production of angiotensin I converting enzyme inhibitory peptides from sea bream scales. *Process Biochem.* **2004,** *39* (10), 1195-1200.

354. Wu, J.; Aluko, R. E.; Nakai, S., Structural requirements of angiotensin I-converting enzyme inhibitory peptides: Quantitative structure−activity relationship study of di- and tripeptides. *J. Agric. Food Chem.* **2006,** *54* (3), 732–738.
355. Webb, K. E., Jr., Intestinal absorption of protein hydrolysis products: a review. *J. Anim. Sci.* **1990,** *68* (9), 3011-3022.
356. Grossman, E., Does increased oxidative stress cause hypertension? *Diabetes Care* **2008,** *2*, S185-189.
357. Kunsch, C.; Medford, R. M., Oxidative Stress as a Regulator of Gene Expression in the Vasculature. *Circ. Res.* **1999,** *85*, 753-766.
358. Vaziri, N. D.; Wang, X. Q.; Oveisi, F.; Rad, B., Induction of oxidative stress by glutathione depletion causes severe hypertension in normal rats. *Hypertension* **2000,** *36* (1), 142-146.
359. Zalba, G.; Beaumont, F. J.; San Jose, G.; Fortuno, M. A.; Etayo, J. C.; Diez, J., Vascular NADH/NADPH oxidase is involved in enhanced superoxide production in spontaneously hypertensive rats. *Hypertension* **2000,** *35*, 1055-1061.
360. Marques, C.; Licks, F.; Zattoni, I.; Borges, B.; de Souza, L. E. R.; Marroni, C. A.; Marroni, N. P., Antioxidant properties of glutamine and its role in VEGF-Akt pathways in portal hypertension gastropathy. *World J. Gastroenterol.* **2012,** *19* (28), 4464–4474.
361. Khalil, M. I.; Moniruzzaman, M.; Boukraâ, L.; Benhanifia, M.; Islam, M. A.; Islam, M. N.; Sulaiman, S. A.; Gan, S. H., Physicochemical and antioxidant properties of algerian honey. *Molecules* **2012,** *17* (9), 11199-11215.
362. Sharp, G., *Ascophyllum nodosum* and its harvesting in Eastern Canada. In *Case study of seven commercial seaweeds resources*, Doty, M.; Caddy, J. F.; Santelices, B., Eds. Food and Agriculture Organization of the United Nations: Rome, 1987; Vol. 821, pp 3-46.
363. Pripp, A. H., Effect of peptides derived from food proteins on blood pressure: a meta-analysis of randomized controlled trials. *Food Nutr. Res.* **2008,** *52*.
364. Vermeirssen, V.; van der Bent, A.; Van Camp, J.; van Amerongen, A.; Verstraete, W., A quantitative in silico analysis calculates the angiotensin I converting enzyme (ACE) inhibitory activity in pea and whey protein digests. *Biochimie* **2004,** *86* (3), 231-239.
365. Zhou, M.; Du, K.; Ji, P.; Feng, W., Molecular mechanism of the interactions between inhibitory tripeptides and angiotensin-converting enzyme. *Biophys. Chem.* **2012,** *168–169*, 60-66.
366. Vafiadis, A. P.; Bakalbassis, E. G., A computational study of the structure-activity relationships of some p-hydroxybenzoic acid antioxidants. *J. Am. Oil Chem. Soc.* **2003,** *80* (12), 1217-1223.
367. Mendoza-Wilson, A. M.; Armenta-Vázquez, M. E.; Castro-Arredondo, S. I.; Espinosa-Plascencia, A.; Robles-Burgueño, M. d. R.; González-Ríos, H.; González-León, A.; Balandrán-Quintana, R. R., Potential of polyphenols from an aqueous extract of apple peel as inhibitors of free radicals: An experimental and computational study. *J. Mol. Struct.* **2013,** *1035* (0), 61-68.
368. Kim, H.; Jeong, K.; Jung, S., Molecular dynamics simulations on the coplanarity of quercetin backbone for the antioxidant activity of quercetin-3-monoglycoside *Bull. Korean Chem. Soc.* **2006,** *27* (2), 325-328.
369. Leopoldini, M.; Russo, N.; Toscano, M., The molecular basis of working mechanism of natural polyphenolic antioxidants. *Food Chem.* **2011,** *125* (2), 288-306.

370. Borges dos Santos, R. M.; Martinho Simões, J. A., Energetics of the O–H Bond in Phenol and Substituted Phenols: A Critical Evaluation of Literature Data. *Journal of Physical and Chemical Reference Data* **1998,** *27* (3), 707-740.
371. Denisov, E. T.; Khudyakov, I. V., Mechanisms of action and reactivities of the free radicals of inhibitors - Chemical Reviews (ACS Publications). *Chem. Rev.* **1987,** *87* (6), 1313-1357.
372. Zhang, J.; Xiong, Y.; Peng, B.; Gao, H.; Zhou, Z., Density functional study on the bioactivity of ellagic acid, its derivatives and metabolite. *Comp. Theor. Chem.* **2011,** *963* (1), 6-6.
373. Košinová, P.; Di Meo, F.; Anouar, E. H.; Duroux, J.-L.; Trouillas, P., H-atom acceptor capacity of free radicals used in antioxidant measurements. *Int. J. Quantum Chem.* **2011,** *111* (6), 1131-1142.
374. Wright, J. S.; Carpenter, D. J.; McKay, D. J.; Ingold, K. U., Theoretical Calculation of Substituent Effects on the O–H Bond Strength of Phenolic Antioxidants Related to Vitamin E. *J. Am. Chem. Soc.* **1997,** *119* (18), 4245–4252.
375. Yoon, N. Y.; Eom, T.-K.; Kim, M.-M.; Kim, S.-K., Inhibitory effect of phlorotannins isolated from *Ecklonia cava* on mushroom tyrosinase activity and melanin formation in mouse B16F10 melanoma cells. *J. Agric. Food Chem.* **2009,** *57* (10), 4124-4129.
376. Eom, S.-H.; Lee, M.-S.; Lee, E.-W.; Kim, Y.-M.; Kim, T. H., Pancreatic lipase inhibitory activity of phlorotannins isolated from *Eisenia bicyclis*. *Phytother. Res.* **2013,** *27* (1), 148-151.
377. Moon, H. E.; Islam, N.; Ahn, B. R.; Chowdhury, S. S.; Sohn, H. S.; Jung, H. A.; Choi, J. S., Protein tyrosine phosphatase 1B and α-glucosidase inhibitory phlorotannins from edible brown algae, *Ecklonia stolonifera* and *Eisenia bicyclis*. *Biosci., Biotechnol., Biochem.* **2011,** *75* (8), 1472-1480.
378. Mendoza-Wilson, A. M.; Armenta-Vázquez, M. E.; Castro-Arredondo, S. I.; Espinosa-Plascencia, A.; Robles-Burgueño, M. d. R.; González-Ríos, H.; González-León, A.; Balandrán-Quintana, R. R., Potential of polyphenols from an aqueous extract of apple peel as inhibitors of free radicals: An experimental and computational study. *J. Mol. Struct.* **2013,** *1035*, 61-68.
379. Lewars, E., *Computational Chemistry: Introduction to the theory and applications of molecular and quantum mechanics*. Kluwer Academic Publ.: Boston/Dordrecht/London, 2003; p 484.
380. Kohn, W.; Becke, A. D.; Parr, R. G., Density functional theory of electronic structure. *J. Phys. Chem.* **1996,** *100* (31), 12974-12980.
381. Velmurugan, T. Modelling of reaction between antioxidants and free radicals. National University of Singapore, 2007.
382. Morgado, C.; Vincent, M. A.; Hillier, I. H.; Shan, X., Can the DFT-D method describe the full range of noncovalent interactions found in large biomolecules? *Phys. Chem. Chem. Phys.* **2007,** *9* (4), 448-451.
383. Grimme, S., Accurate description of van der Waals complexes by density functional theory including empirical corrections. *J. Comput. Chem.* **2004,** *25* (12), 1463-1473.
384. Tawada, Y.; Tsuneda, T.; Yanagisawa, S.; Yanai, T.; Hirao, K., A long-range-corrected time-dependent density functional theory. *J. Chem. Phys.* **2004,** *120* (18), 8425-8433.
385. Becke, A. D., Density-functional thermochemistry. V. Systematic optimization of exchange-correlation functionals. *J. Chem. Phys.* **1997,** *107* (20), 8554-8561.

386. Frisch, M. J.; Trucks, G. W.; Schlegel, H. B.; Scuseria, G. E.; Robb, M. A.; Cheeseman, J. R.; Scalmani, G.; Barone, V.; Mennucci, B.; Petersson, G. A.; Nakatsuji, H.; Caricato, M.; Li, X.; Hratchian, H. P.; Izmaylov, A. F.; Bloino, J.; Zheng, G.; Sonnenberg, J. L.; Hada, M.; Ehara, M.; Toyota, K.; Fukuda, R.; Hasegawa, J.; Ishida, M.; Nakajima, T.; Honda, Y.; Kitao, O.; Nakai, H.; Vreven, T.; Montgomery, J., J. A.;; Peralta, J. E. O., F.; ; Bearpark, M.; Heyd, J. J.; Brothers, E.; Kudin, K. N.; Staroverov, V. N.; Kobayashi, R.; Normand, J.; Raghavachari, K.; Rendell, A.; Burant, J. C.; Iyengar, S. S.; Tomasi, J.; Cossi, M.; Rega, N.; Millam, J. M.; Klene, M.; Knox, J. E.; Cross, J. B.; Bakken, V.; Adamo, C.; Jaramillo, J.; Gomperts, R.; Stratmann, R. E.; Yazyev, O.; Austin, A. J.; Cammi, R.; Pomelli, C.; Ochterski, J. W.; Martin, R. L.; Morokuma, K.; Zakrzewski, V. G.; Voth, G. A.; Salvador, P.; Dannenberg, J. J.; Dapprich, S.; Daniels, A. D.; Farkas, Ö.; Foresman, J. B.; Ortiz, J. V.; Cioslowski, J.; Fox, D. J. *Gaussian 09, Revision A.1*, 09; Gaussian, Inc., Wallingford CT: Gaussian, Inc., Wallingford CT, 2009.

387. DiLabio, G. A.; Pratt, D. A.; LoFaro, A. D.; Wright, J. S., Theoretical Study of X–H Bond Energetics (X = C, N, O, S): Application to Substituent Effects, Gas Phase Acidities, and Redox Potentials. *J. Phys. Chem. A* **1999,** *103* (11), 1653-1661.

388. Alecu, I. M.; Zheng, J.; Zhao, Y.; Truhlar, D. G., Computational thermochemistry: Scale factor databases and scale factors for vibrational frequencies obtained from electronic model chemistries. *J. Chem. Theory Comput.* **2010,** *6* (9), 2872-2887.

389. O'Boyle, N.; Vandermeersch, T.; Flynn, C.; Maguire, A.; Hutchison, G., Confab - Systematic generation of diverse low-energy conformers. *J. Cheminform.* **2011,** *3* (1), 8.

390. Izgorodina, E. I.; Brittain, D. R.; Hodgson, J. L.; Krenske, E. H.; Lin, C. Y.; Namazian, M.; Coote, M. L., Should contemporary density functional theory methods be used to study the thermodynamics of radical reactions? *J. Phys. Chem. A* **2007,** *111* (42), 10754-68.

391. Izgorodina, E. I.; Coote, M. L., Reliable low-cost theoretical procedures for studying addition-fragmentation in RAFT polymerization. *J. Phys. Chem. A* **2006,** *110* (7), 2486-92.

392. Riley, K. E.; Pitoňák, M.; Jurečka, P.; Hobza, P., Stabilization and structure calculations for noncovalent interactions in extended molecular systems based on wave function and density functional theories. *Chem. Rev.* **2010,** *110* (9), 5023-5063.

393. Johnson, E. R.; Mackie, I. D.; DiLabio, G. A., Dispersion interactions in density-functional theory. *J. Phys. Org. Chem.* **2009,** *22* (12), 1127-1135.

394. Schwabe, T.; Grimme, S., Double-hybrid density functionals with long-range dispersion corrections: higher accuracy and extended applicability. *Phys. Chem. Chem. Phys.* **2007,** *9* (26), 3397-3406.

395. Lucarini, M.; Pedulli, G. F.; Cipollone, M., Bond Dissociation Enthalpy of alpha-Tocopherol and Other Phenolic Antioxidants. *J. Org. Chem.* **1994,** *59* (17), 5063-5070.

396. Pal, S.; Kundu, T. K., Stability Analysis and frontier orbital study of different glycol and water complex. *ISRN Phys. Chem.* **2013,** *2013*, 16.

397. Xue, Y.; Zheng, Y.; An, L.; Zhang, L.; Qian, Y.; Yu, D.; Gong, X.; Liu, Y., A theoretical study of the structure–radical scavenging activity of hydroxychalcones. *Compu. Theo. Chem.* **2012,** *982* (0), 74-83.

398. Belcastro, M.; Marino, T.; Russo, N.; Toscano, M., Structural and electronic characterization of antioxidants from marine organisms. *Theo. Chem. Acc.* **2006,** *115* (5), 361-369.

399. Thavasi, V.; Leong, L. P.; Bettens, R. P. A., Investigation of the influence of hydroxy groups on the radical scavenging ability of polyphenols. *J. Phys. Chem. A* **2006,** *110* (14), 4918-4923.
400. Andrade-Filho, T.; Martins, H.; Del Nero, J., Theoretical investigation of the electronic absorption spectrum of Piceatannol in methanolic solution. *Theor. Chem. Accounts* **2008,** *121* (3-4), 147-153.
401. Rossi, M.; Caruso, F.; Opazo, C.; Salciccioli, J., Crystal and molecular structure of piceatannol; Scavenging features of resveratrol and piceatannol on hydroxyl and peroxyl radicals and docking with transthyretin. *J. Agric. Food Chem.* **2008,** *56* (22), 10557-10566.
402. Ebejer, J.-P.; Morris, G. M.; Deane, C. M., Freely available conformer generation methods: How good are they? *J. Chem. Inf. Model.* **2012,** *52* (5), 1146-1158.
403. Correia, C. F.; Guedes, R. C.; Borges dos Santos, R. M.; Costa Cabral, B. J.; Martinho Simoes, J. A., O-H Bond dissociation enthalpies in hydroxyphenols. A time-resolved photoacoustic calorimetry and quantum chemistry study. *Phys. Chem. Chem. Phys.* **2004,** *6* (9), 2109-2118.
404. Hoelz, L. V. B.; Horta, B. A. C.; Araújo, J. Q.; Albuquerque, M. G.; de Alencastro, R. B.; da Silva, J. F. M., Quantitative structure-activity relationships of antioxidant phenolic compounds *J. Chem. Pharm. Res.* **2010,** *2* (5), 291-306.
405. Leopoldini, M.; Marino, T.; Russo, N.; Toscano, M., Density functional computations of the energetic and spectroscopic parameters of quercetin and its radicals in the gas phase and in solvent. *Theor. Chem. Acc.* **2004,** *111* (2-6), 210-216.
406. Leopoldini, M.; Russo, N.; Toscano, M., Gas and liquid phase acidity of natural antioxidants. *J. Agric. Food Chem.* **2006,** *54* (8), 3078-3085.
407. Vennat, B.; Bos, M.-A.; Pourrat, A.; Bastide, P., Procyanidins from tormentil: fractionation and study of the anti-radical activity towards superoxide anion. *Biol. Pharm. Bull.* **1994,** *17*, 1613–1615.
408. Estévez, L.; Mosquera, R. A., Molecular structure and antioxidant properties of delphinidin. *J. Phys. Chem. A* **2008,** *112* (42), 10614-10623.
409. Richard, T.; Vitrac, X.; Merillon, J. M.; Monti, J. P., Role of peptide primary sequence in polyphenol-protein recognition: An example with neurotensin. *BBA, General Subjects* **2005,** *1726* (3), 238-243.
410. Hara, K.; Ohara, M.; Hayashi, I.; Hino, T.; Nishimura, R.; Iwasaki, Y.; Ogawa, T.; Ohyama, Y.; Sugiyama, M.; Amano, H., The green tea polyphenol (−)-epigallocatechin gallate precipitates salivary proteins including alpha-amylase: biochemical implications for oral health. *Eur. J. Oral Sci.* **2012,** *120* (2), 132-139.
411. Durrant, J. D.; McCammon, J. A., Molecular dynamics simulations and drug discovery. *BMC Biol.* **2011,** *9:* (71).
412. Hanwell, M. D.; Curtis, D. E.; Lonie, D. C.; Vandermeersch, T.; Zurek, E.; Hutchison, G. R., Avogadro: An advanced semantic chemical editor, visualization, and analysis platform. *J. Cheminform.* **2012,** *4*, 17.
413. Ray, B. D. *Topolbuild version 1.3*, 2009.
414. Kang, S.-M.; Heo, S.-J.; Kim, K.-N.; Lee, S.-H.; Yang, H.-M.; Kim, A.-D.; Jeon, Y.-J., Molecular docking studies of a phlorotannin, dieckol isolated from *Ecklonia cava* with tyrosinase inhibitory activity. *Bioorg. Med. Chem.* **2012,** *20* (1), 311-316.
415. Jung, H. A.; Oh, S. H.; Choi, J. S., Molecular docking studies of phlorotannins from *Eisenia bicyclis* with BACE1 inhibitory activity. *Bioorg. Med. Chem. Lett.* **2010,** *20* (11), 3211-3215.

Appendices

Appendix 1: Reverse phase flash chromatograms of LMW fractions from water extracts of (a) *Ascophyllum nodosum*, (b) *Fucus spiralis* and (c) *Pelvetia canaliculata*; and of ethanol water extracts of (d) *Ascophyllum nodosum*, (e) *Fucus spiralis* and (f) *Pelvetia canaliculata*. In all cases the first peak corresponds to the polar fraction, assumed to be prominently sugars, and the second peak is the less polar peak, assumed to be enriched with phlorotannins.

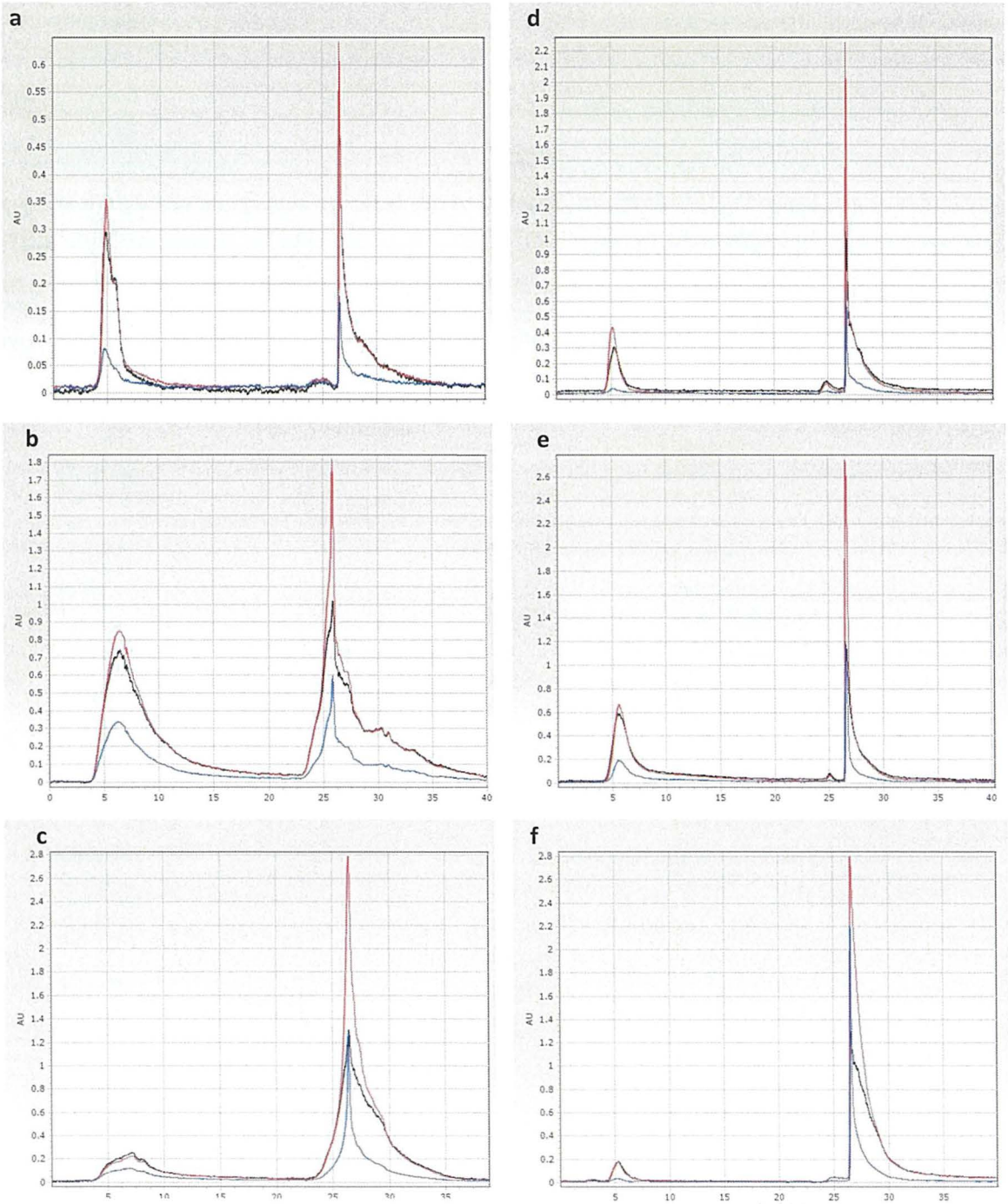

Appendix 2: ^{1}H NMR spectra for phlorotannin-enriched reverse-phase flash fractions from (a) *A. nodosum*, (b) *P. canaliculata* and (c) *F. spiralis*

a

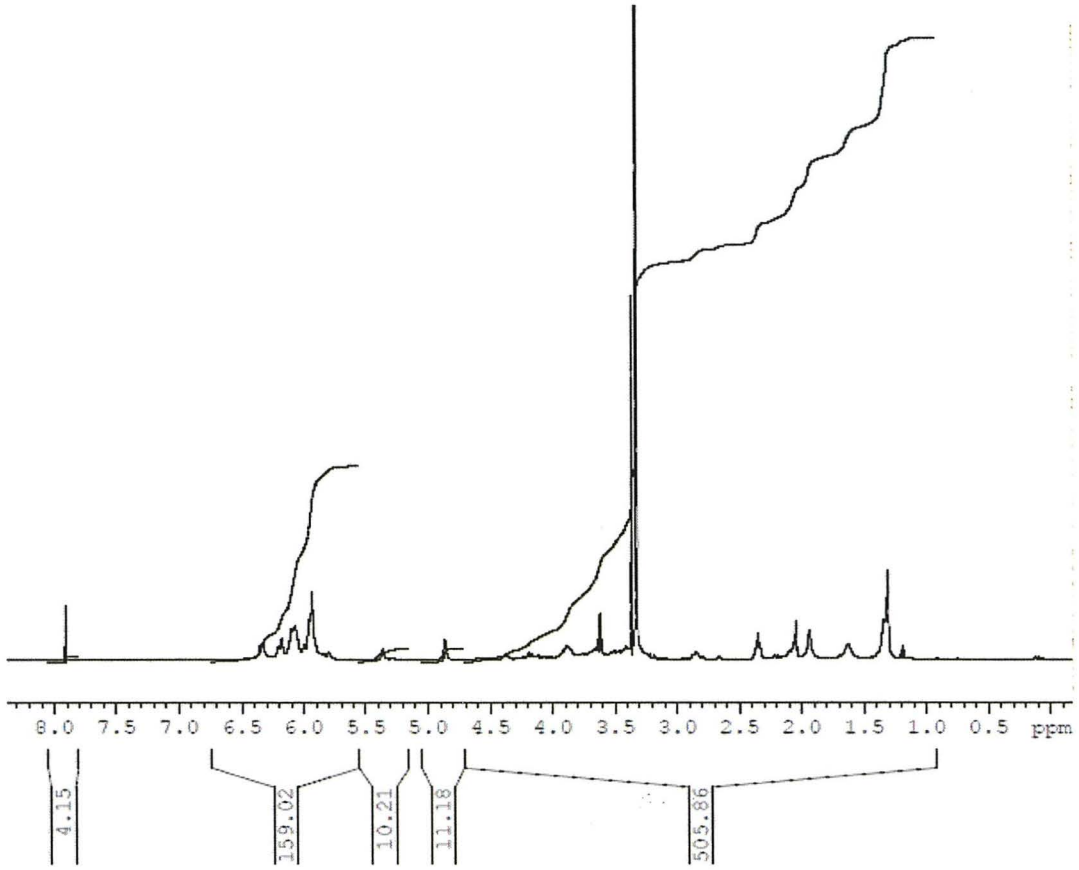

b

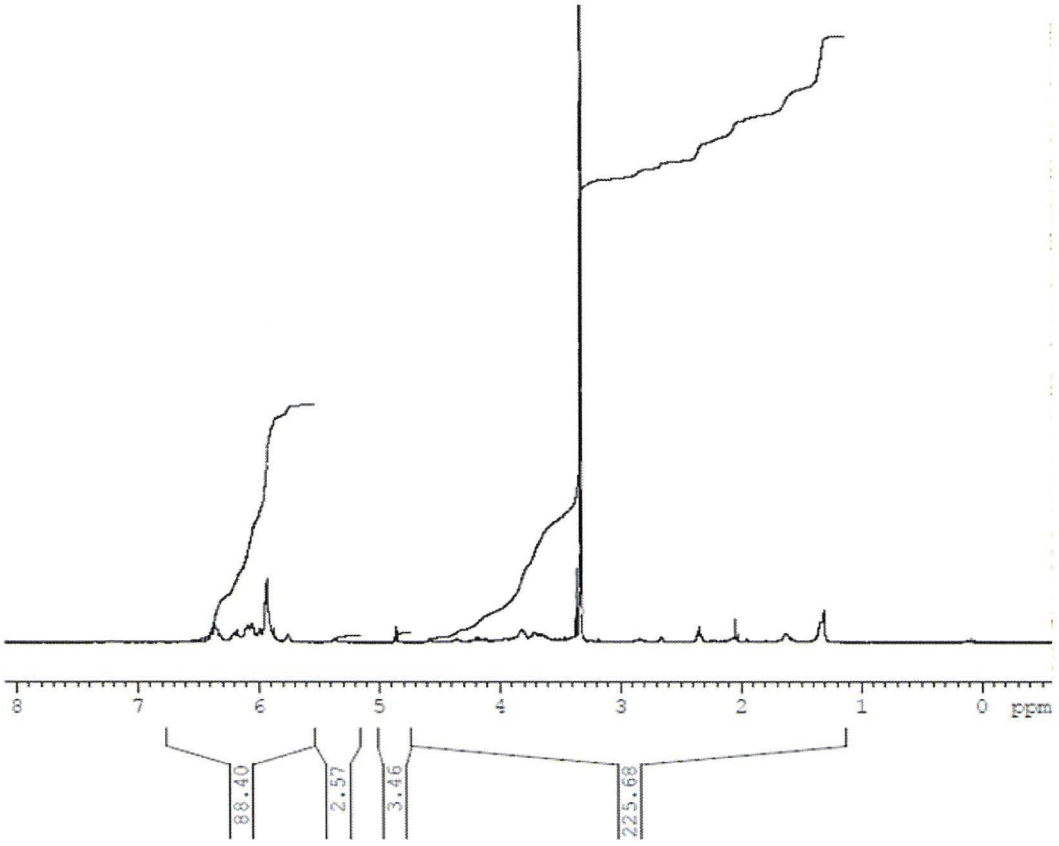

c

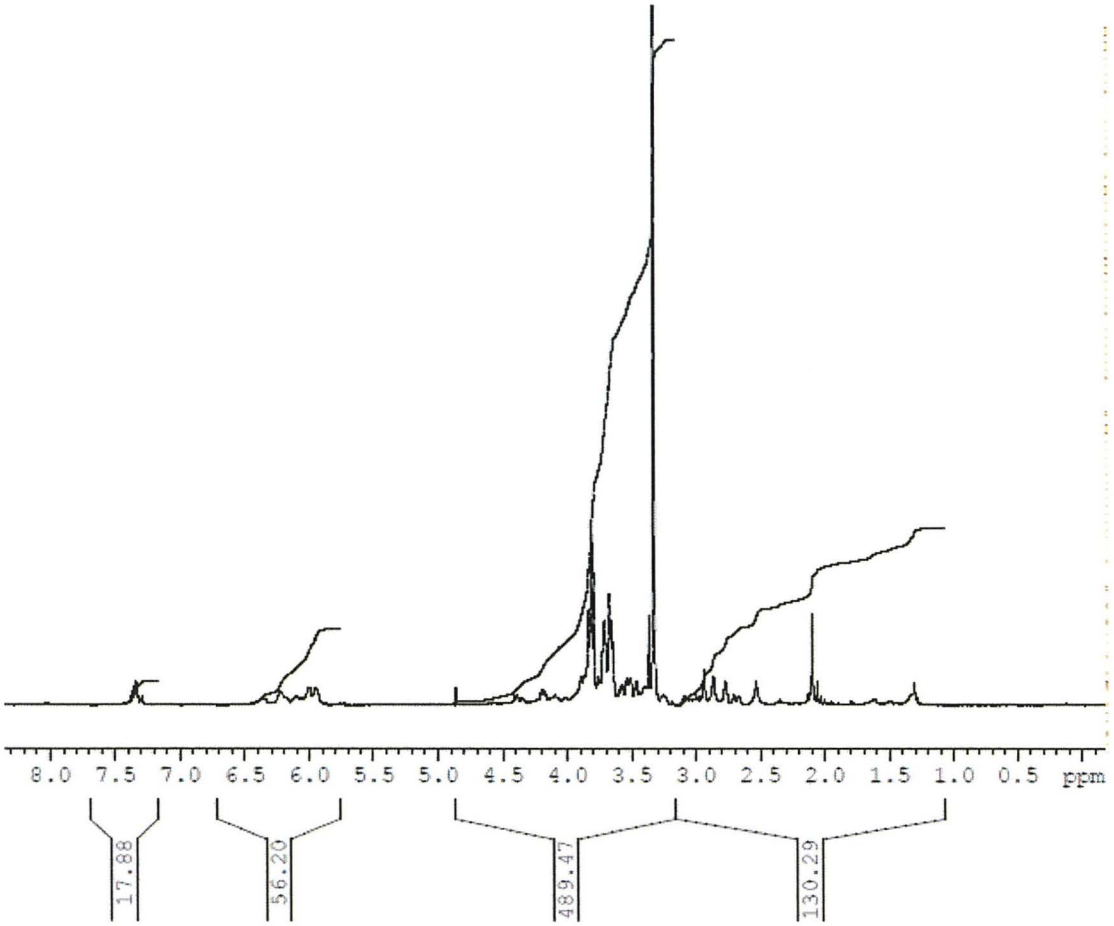
8.0 7.5 7.0 6.5 6.0 5.5 5.0 4.5 4.0 3.5 3.0 2.5 2.0 1.5 1.0 0.5 ppm
17.88
56.20
489.47
130.29

Appendix 3: Conformer structures of 7-phloroeckol radicals **A-H** investigated

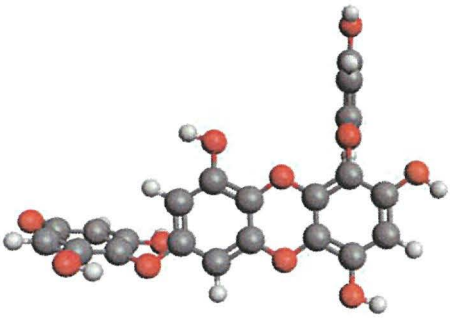

A1

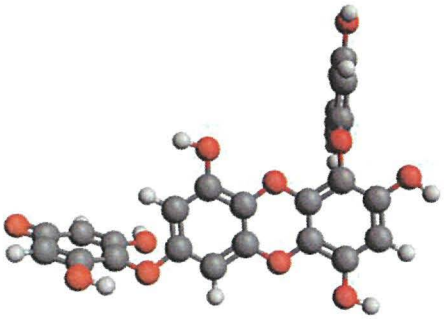

A2

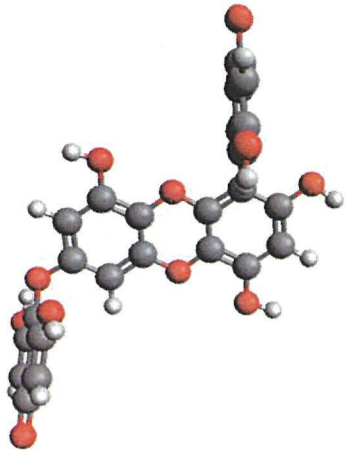

A3

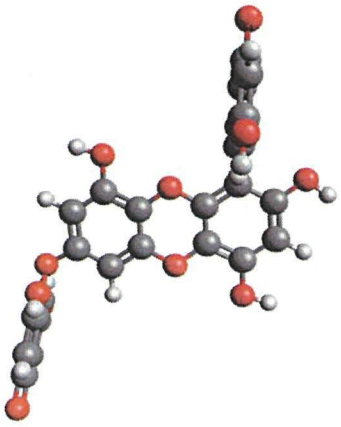

A4

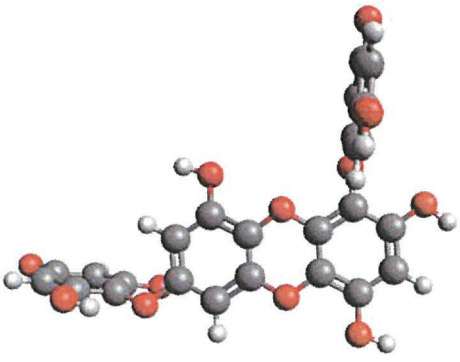

A5

Appendix 3: Conformer structures of 7-phloroeckol radicals **A-H** investigated

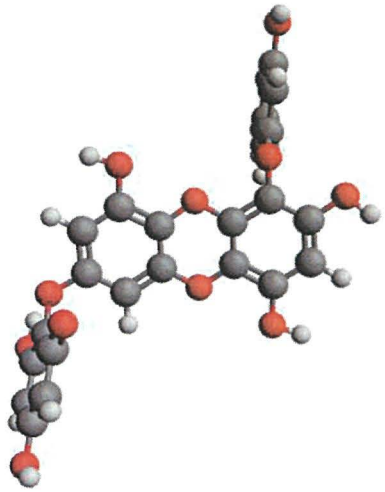

B1

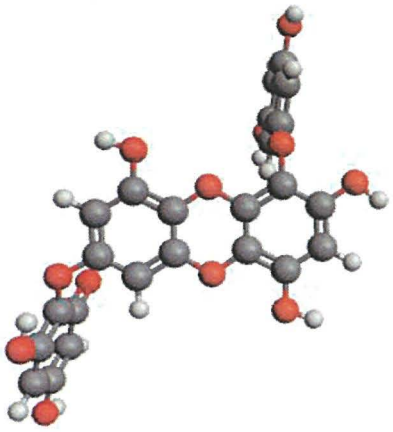

B2

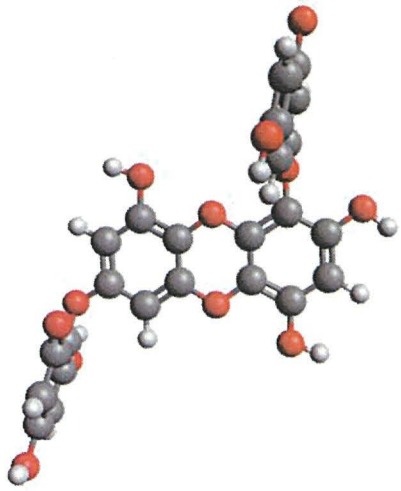

B3

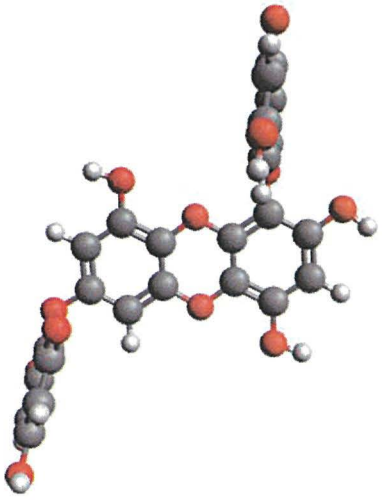

B4

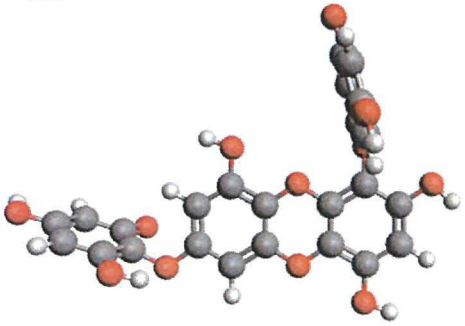

B5

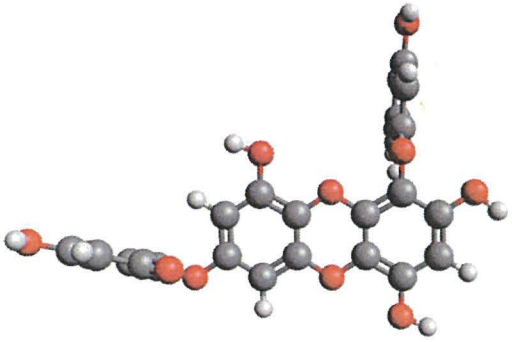

B6

Appendix 3: Conformer structures of 7-phloroeckol radicals **A-H** investigated

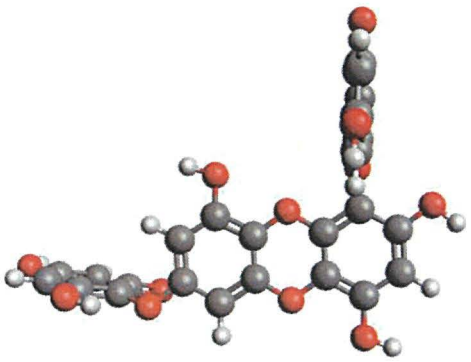

B7

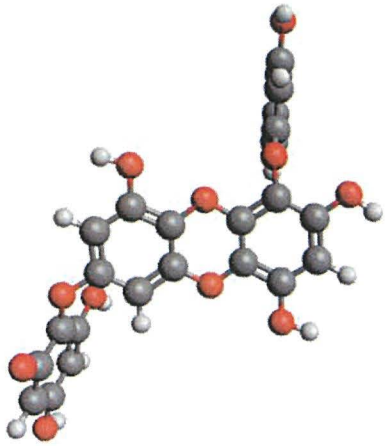

C1

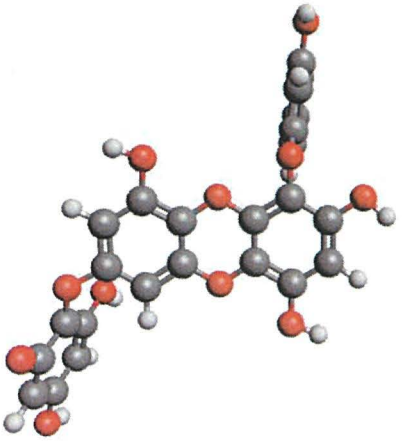

C2

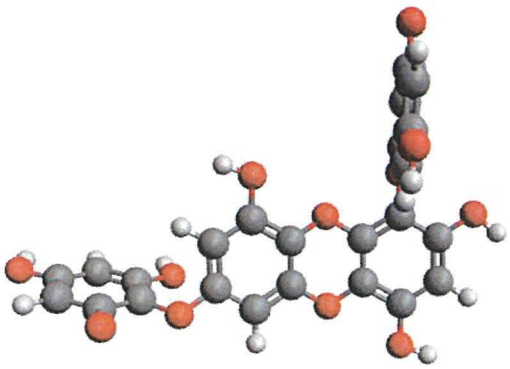

C3

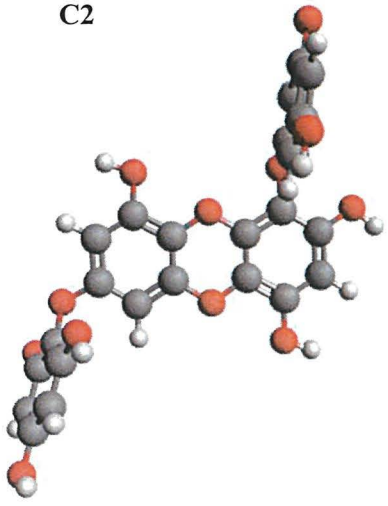

C4

Appendix 3: Conformer structures of 7-phloroeckol radicals **A-H** investigated

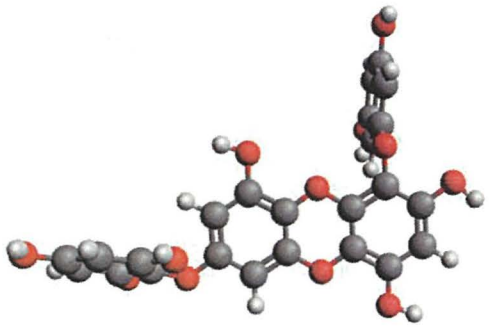

C5

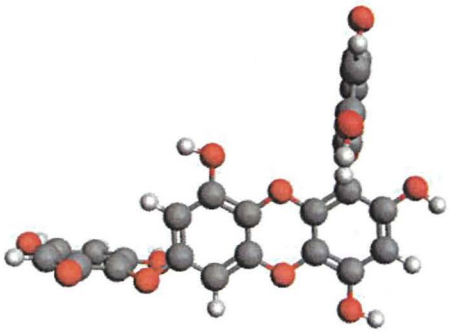

C6

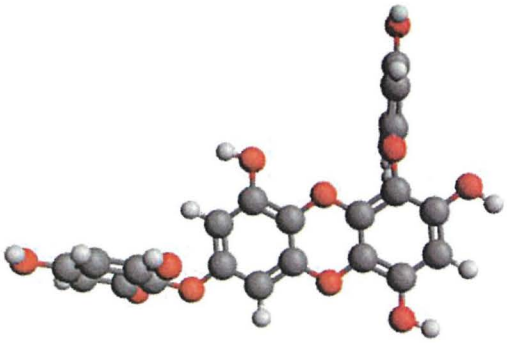

C7

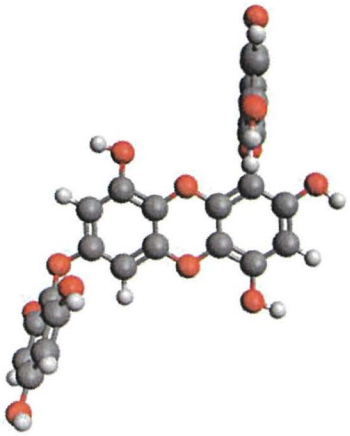

C8

Appendix 3: Conformer structures of 7-phloroeckol radicals **A-H** investigated

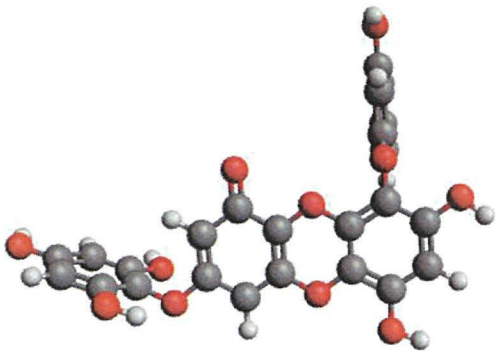

D1

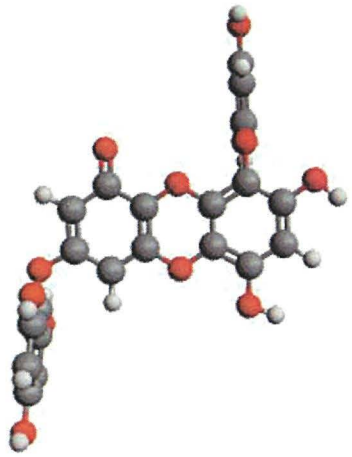

D2

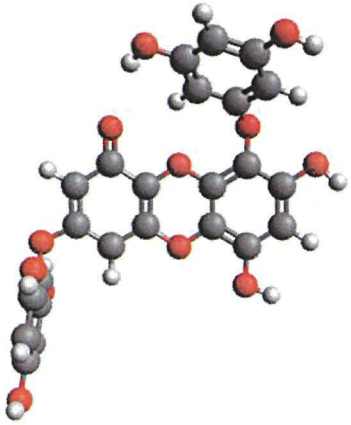

D3

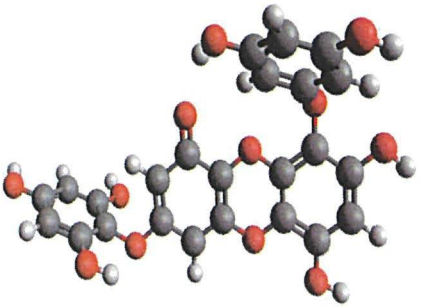

D4

Appendix 3: Conformer structures of 7-phloroeckol radicals **A-H** investigated

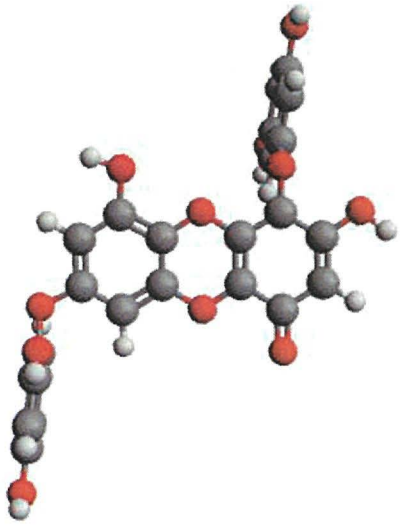

E1

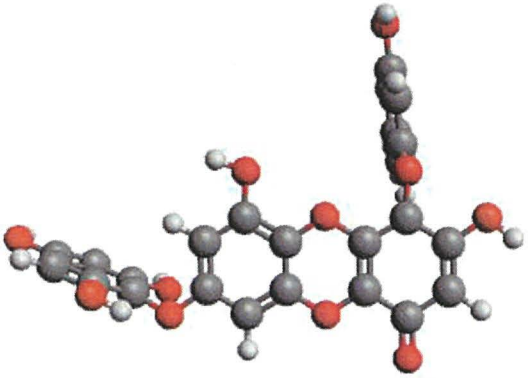

E2

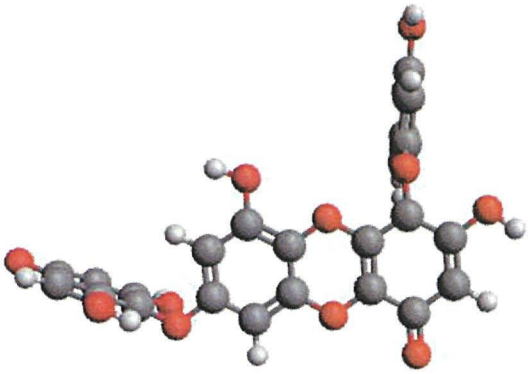

E3

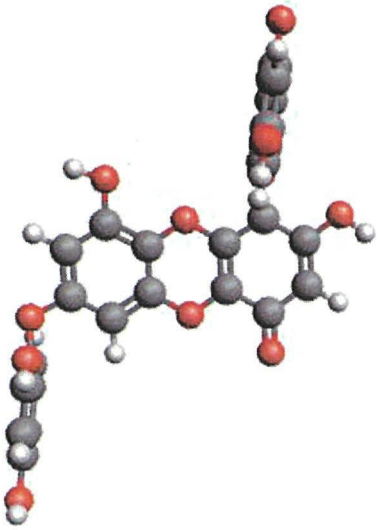

E4

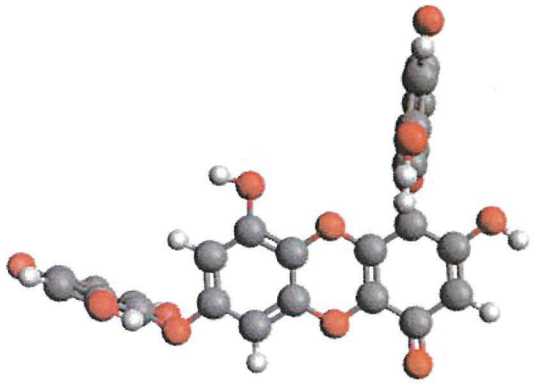

E5

Appendix 3: Conformer structures of 7-phloroeckol radicals **A-H** investigated

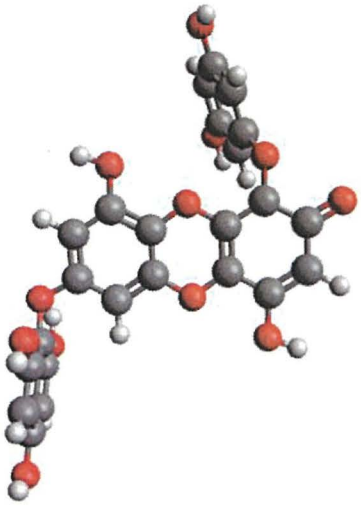

F1

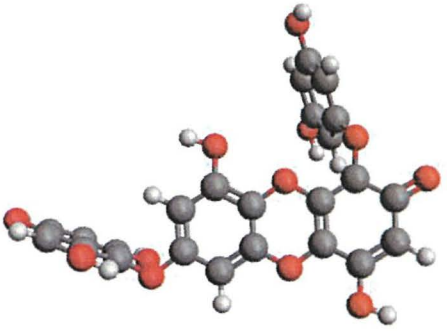

F2

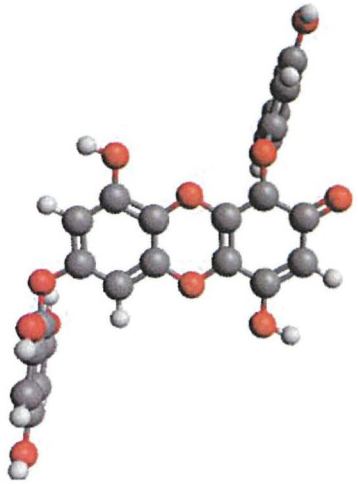

F3

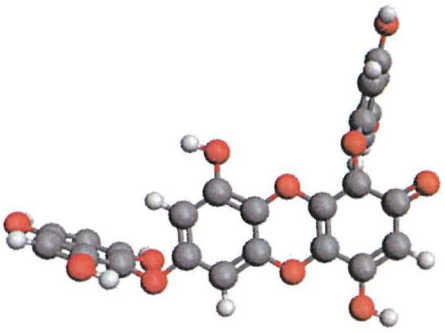

F4

Appendix 3: Conformer structures of 7-phloroeckol radicals **A-H** investigated

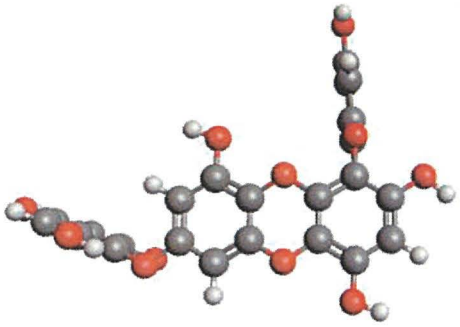

G1

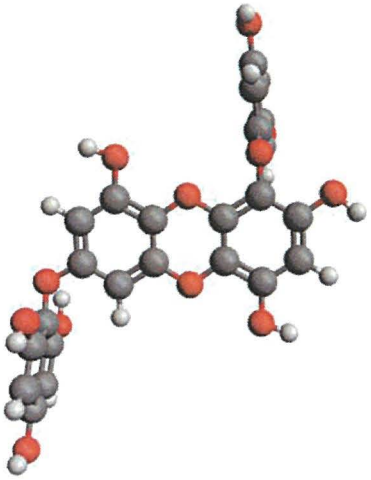

G2

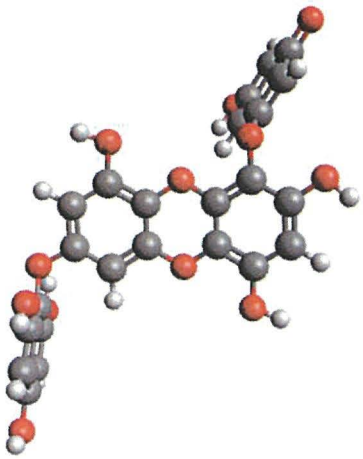

G3

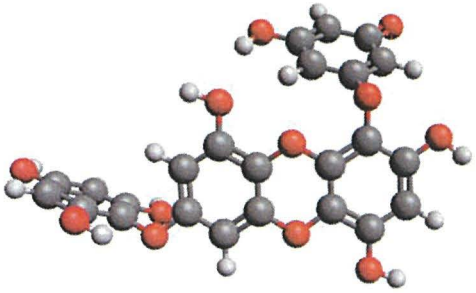

G4

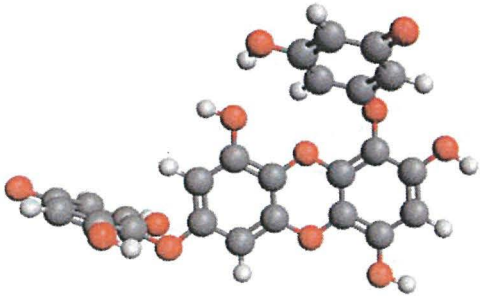

G5

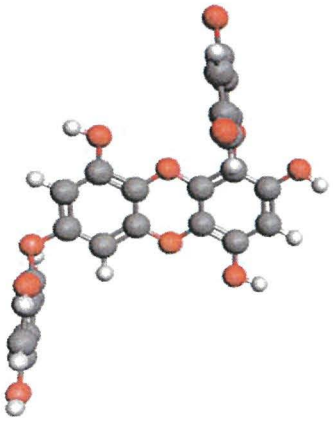

G6

Appendix 3: Conformer structures of 7-phloroeckol radicals **A-H** investigated

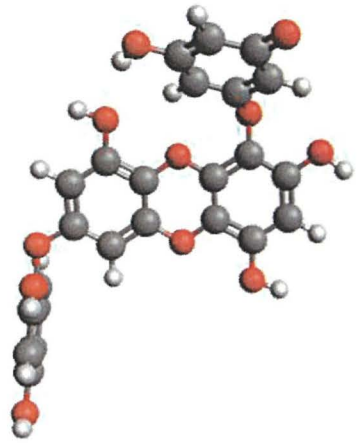

G7

Appendix 3: Conformer structures of 7-phloroeckol radicals **A-H** investigated

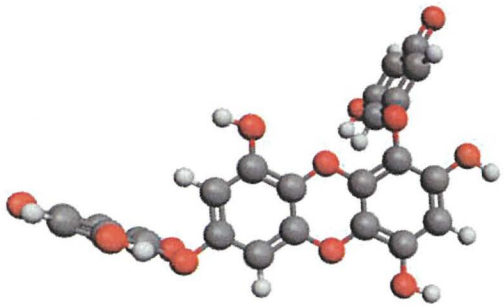

H1

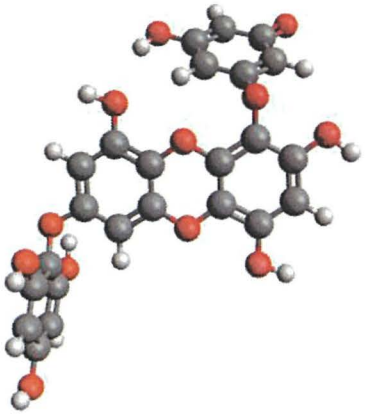

H2

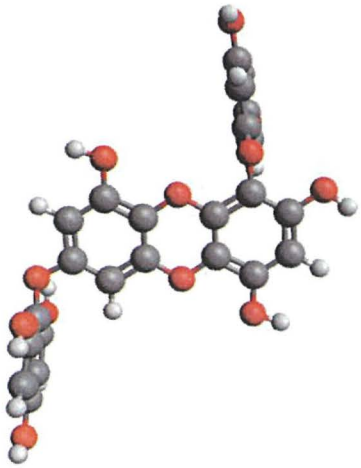

H3

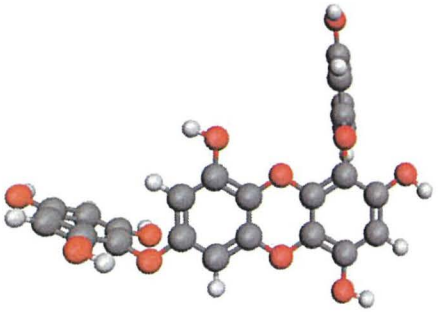

H4

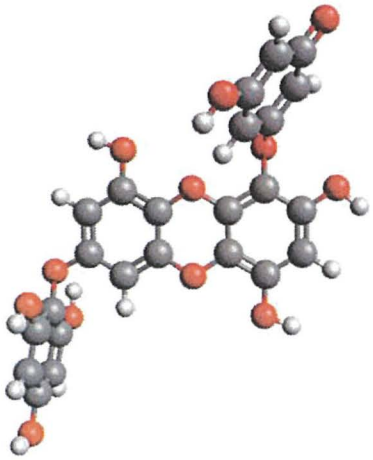

H5

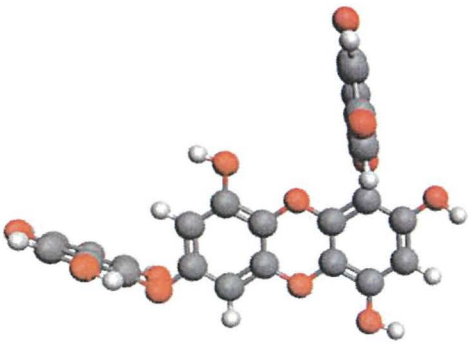

H6

Appendix 3: Conformer structures of 7-phloroeckol radicals **A-H** investigated

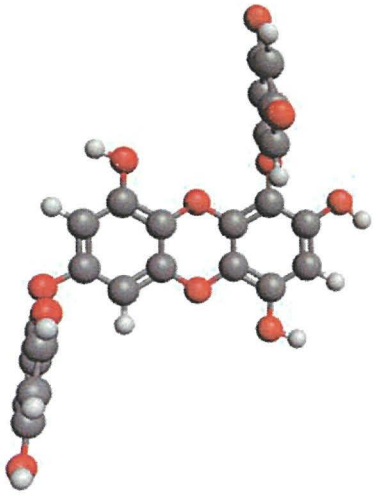

H7

Appendix 4: Phlorotannin-peptide MD simulation approach

An initial approach was undertaken for carrying out a MD simulation of the phlorotannin fucotriphlorethol with the peptide QPK isolated from *Ascophyllum nodosum*. The following is a summary of the approach taken in this work. In both cases the force-field optimized potential for liquid simulations (OPLS) was employed as it has also shown to be a practical option for the parameterisation of polyphenols and carrying out MD simulations involving phenolic interactions with proteins.[263]

Structure preparation, energy minimisation and equilibration of QPK

Initially, the structure of QPK was built and optimised in the open source program Avogadro.[412] The conformer generator program Confab was then employed to find the lowest energy conformer of QPK. After the conversion, using pdb2gmx, of the QPK structure file into a suitable format for further use in Gromacs, the QPK peptide was added to a solvated simulation box (explicit solvent model TIP4P) and energy minimisation of the system was carried out to find a local potential energy minimum near the starting structure. Following this, a series of equilibration steps, which allow the solvent to relax around the peptide, using the NPT ensemble, where temperature and pressure are kept constant, were carried out with the timestep increasing from 0.0001 to 0.001 fs. The temperature of the equilibration steps was increased from 0-300 K in increments of 50 K. The Berendsen algorithm was employed for the equilibration as it is the most robust to the volume changes that might be expected during equilibration. Equilibration is used to evade excessive distortion of the protein when performing the production simulation. The following is an image of the equilibrated solvated peptide simulation box. Also, the relevant gromacs and trajectory files (view in VMD software) and video of the simulation movement is as attached as electronic supplementary material.

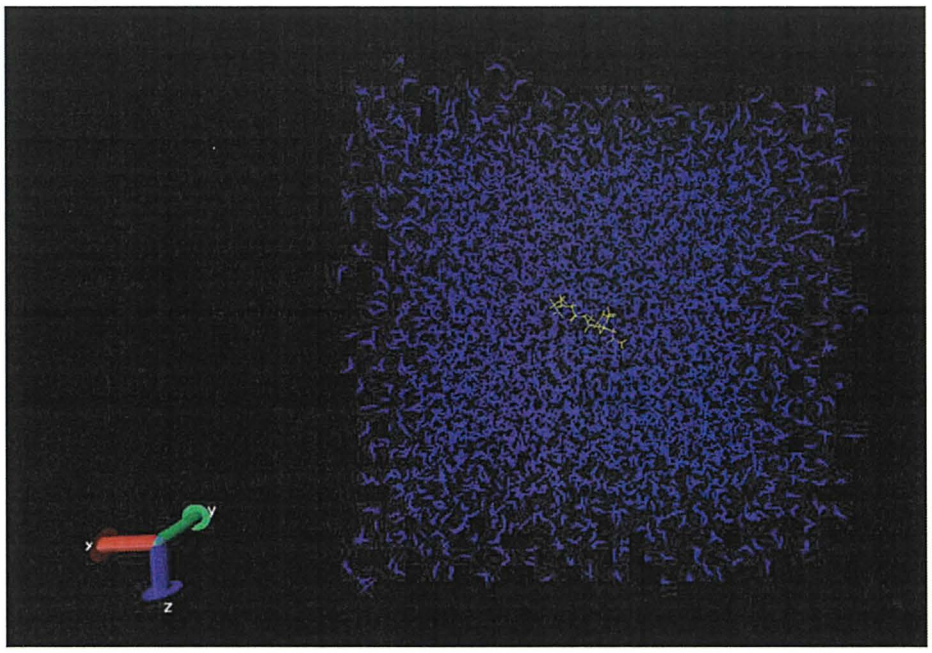

Equilibrated solvated peptide simulation box

Structure preparation, energy minimisation and equilibration of fucotriphlorethol

Initially, fucotriphlorethol structure was optimised at the AM1 and HF6-31G(d) levels of theory. The program Topolbuild 1.3 with OPLS_AA forcefield was employed to generate the gromacs and topology files from the optimised phlorotannin structure file.[413] New parameters relevant to the phlorotannin structure were added to the relevant residue topology file in Gromacs. The phlorotannin structure was then energy minimised and equilibrated similar to the peptide earlier. The following is an image of the equilibrated solvated fucotriphlorethol simulation box. Also, the relevant gromacs and trajectory files (view in VMD software) and video of the simulation movement is as attached as electronic supplementary material.

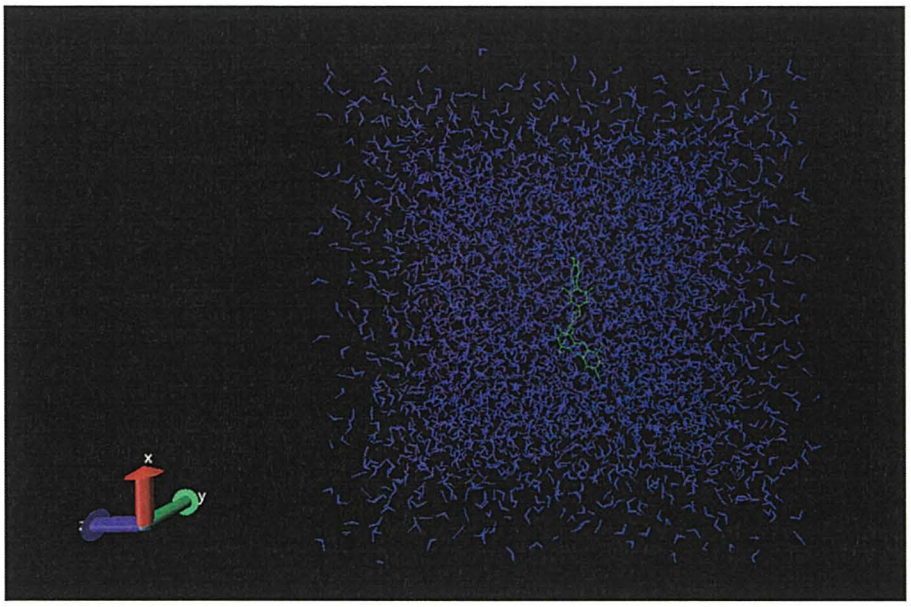

Equilibrated solvated fucotriphlorethol simulation box

Future steps

The next steps to be carried out would be to combine the peptide and phlorotannin structures into a single simulation solvent box and to carry out both an equilibration and a production simulation with the bioactive compounds together. Following is an image of the minimised solvated QPK and fucotriphlorethol simulation box. Also, the relevant gromacs and trajectory files (view in VMD software) and video of the simulation movement are attached as electronic supplementary material. The production run generally differs from the equilibration in that position restraints and pressure coupling would be turned off and the run would be significantly longer. Following the production run, binding free energies would need to be determined using a post-processing method to assess the level and type of interaction between the phlorotannin and peptide.

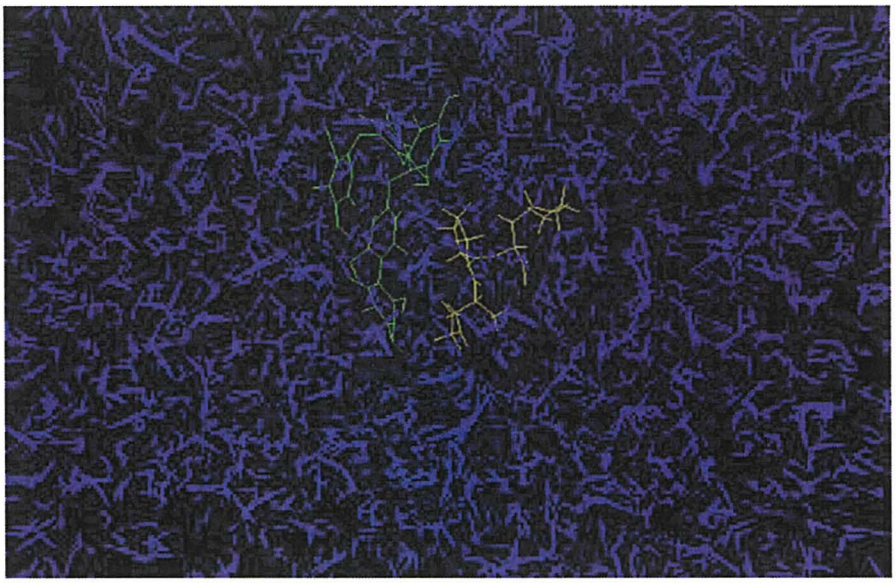

Minimised solvated QPK and fucotriphlorethol simulation box

Molecular modeling techniques have previously been employed as a means to investigate the bioactivities of phlorotannins and, thus, can be used to provide an insight into potential health promoting applications of phlorotannins. For example, the phlorotannin dieckol, which was isolated from the brown alga *Ecklonia cava*, was examined for its potential tyrosinase inhibitory effects, which is an indicator of melanin synthesis inhibition.[414] The results from a molecular docking experiment suggested that dieckol had the potential to be further developed as a cosmetic agent for use in dermatological disorders associated with melanin.[414] Jung *et. al.*[415] used molecular docking to confirm observed *in vitro* BACE1 inhibitory activities of phlorotannins from *Eisenia bicyclis* and to propose guidelines for phlorotannins as BACE1 inhibitors in drug discovery for the potential treatment of Alzheimers. Therefore, there is evidence to show that molecular modeling can support experimental data and at the same time provide detailed binding pattern information that comprises the basis for predicting phlorotannin bioactivity. The outlined approach above for carrying out molecular modeling of bioactive phlorotannins and peptides may provide the foundation for the future modeling of such compounds to gain knowledge on how they may interact as ingredients in future health promoting products, such as functional foods